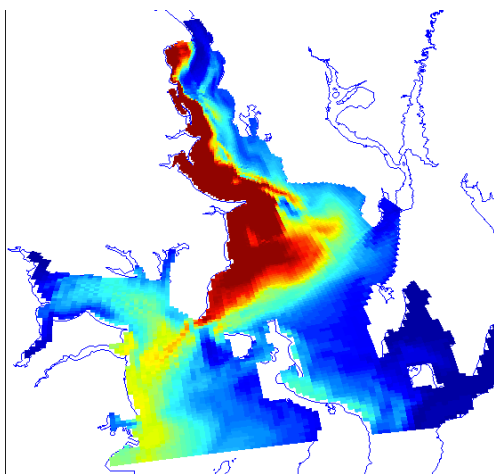


A Seekonk-Narragansett Bay (SNB) ROMS Model applied to coupled circulation-ecosystem processes: A 2010 Seasonal Study



Report to the Narragansett Bay Commission
March 5, 2018

Report prepared by:
Chris Kincaid
Professor of Oceanography
Graduate School of Oceanography
University of Rhode Island
Narragansett, RI 02882

1.0 Introduction

The Narragansett Bay (NB) ecosystem represents an essential resource for the State of Rhode Island, in terms of commercial and recreational fishing, marine trades, tourism, property values, state identity and Rhode Islanders' overall quality of life. RI coastal waters are stressed by factors such as bacteria, invasive species, warming waters, low oxygen conditions and threats due to suspension and transport of chemicals of emerging concern (CECs) residing in riverine sediments. Many regions of the Bay suffer from chronic low oxygen, most notably the Seekonk and Providence Rivers and Greenwich Bay (Brush, 2002; Deacutis et al., 2006; Saarman et al, 2008; Deacutis 2008). Hypoxia mitigation strategies developed since the August 2003 fish kill in Greenwich Bay (RI) target nitrogen as the primary driver of phytoplankton blooms and subsequent bacterial decay leading to low oxygen conditions (Greenwich Bay Special Area Management Plan, 2005). Management strategies focus on reducing nitrogen from point sources (e.g., major waste water treatment facilities (WWTFs)). Testing the merits of present and potential management strategies requires a combination of better spatially and temporally detailed data sets and improved modeling tools capable of representing both hydrodynamic and ecosystem processes. Policy decisions should be based upon such a coupled systems approach.

We present results from a newly developed version of the Narragansett Bay ROMS (SNB-ROMS) that builds from extensive existing circulation data throughout NB and Regional Ocean Modeling System (ROMS) development efforts supported by the Narragansett Bay Commission (NBC) (Kincaid, 2001a-c; Bergondo and Kincaid, 2005; Kincaid, 2012a,b) (Figure 1). Prior observational work (described below) includes underway (Figure 2) and time series current meter data in the Providence (Figure 3, 4) and Seekonk Rivers. A prior modeling study using ROMS made use of these data in characterizing circulation and chemical transport but did not include the Seekonk River. Two important components of this work include: a) the incorporation of a high resolution representation of the Seekonk River up to Slater Dam into the SNB-ROMS model and b) the application of a widely used ecosystem model that utilizes a simplified coupling between four basic fields: nutrients (N), phytoplankton (P), zooplankton (Z) and detritus (D). This is referred to as an NPZD model. The specific version used in ROMS is the NPZD-Franks model (Franks et al., 1986; Franks, 2002). Benefits of this version are that this simplified treatment minimizes the number of unconstrained biological parameters while also tracking all ecosystems components as coupled Eulerian fields on the same hydrodynamic grid.

A goal of this project is to develop capacity within models for simulating input and transport of nitrogen that is coupled to phytoplankton and zooplankton growth/transport in the Bay. Results are used to characterize the interplay between ecosystem processes and 4-D circulation/transport. A major portion of this work is testing the efficacy of various nutrient point source management strategies by simulating a range of WWTF permit release levels and comparing relative improvements in nutrient and phytoplankton

levels throughout the estuary. Results show that increases and decreases in spatially averaged phytoplankton concentrations driven by WWTF nitrogen reductions are similar in size or smaller than changes due to other model parameters: varying wind conditions, parameter choices for phytoplankton/zooplankton growth rates and light extinction and conditions in Greenwich Bay. Models show phytoplankton levels for the chosen 2010 bloom event are only reduced by significant levels in the case when nitrogen levels from WWTFs are reduced from 15 mg L^{-1} to 5 mg L^{-1} . Phytoplankton reductions in the simulated bloom produced by lowering WWTF release levels from 5 to 3 mg L^{-1} and from 3 mg L^{-1} to 0 mg L^{-1} are small, smaller in fact than those produced by changes in prevailing winds or by altering the model ecosystem parameters within realistic ranges.

Two distinct types of model simulations have been developed and completed for this report. The first set of preliminary runs test the stability of the new Seekonk River high resolution grid. This includes a continuous simulation from January 2010 through April 2010. This time period in 2010 coincides with a detailed tilt current meter (TCM) experiment on the Edgewood Shoals (Figure 3, 4). Starting from this point, an extensive series of model runs have been performed to provide a sensitivity test for the primary parameters of the NPZD sub-module in SNB-ROMS and to define important aspects of coupled circulation/ecosystem processes within Narragansett Bay. All NPZD simulations using SNB-ROMS begin from April 20, 2010 and run for two months, into late June, 2010. Results show the NPZD sub-model reproduces the first-order structure of the down-bay nutrient gradient, in an average sense based on years of Bay observations, and in close agreement with buoy records and NBC data from this time period.

2.0 Prior Work

A combination of current meter observations (Figures 2-4) and ROMS modeling (Figures 1, 5-7) has led to an improved understanding of Narragansett Bay circulation (Rosenberger, 2001; Kincaid, 2001a-c; Kincaid et al., 2003; Bergondo, 2004; Kincaid, 2006; Bergondo and Kincaid, 2007; Kincaid and Bergondo, 2005; Kincaid et al, 2008; Rogers, 2008; Kremer et al., 2010; Pfeiffer-Herbert, 2012; Kincaid 2012a,b; Pfeiffer-Herbert et al., 2015). The Bay has been shown to circulate predominantly in a counterclockwise direction, with residual (or net non-tidal) flow up the East Passage and down, or out, the West Passage of the estuary (Kincaid et al, 2008). Residual circulation, northward in the East Passage and southward in the West Passage, has been shown to stall given northward blowing winds and to strengthen under southward blowing wind conditions (Pfeiffer-Herbert et al, 2015). These persistent residual circulation patterns tend to carry water entering at any point (latitude) along the eastern side of the East Passage well northward into the system, as far as the Mt Hope Bay, the Providence River (PR) or around the north end of Prudence Island and into the upper West Passage. It is important to note that this background style of flow in the Bay can be upset and altered by prevailing winds and runoff patterns.

The focus of this report is on work within the upper Bay, specifically looking at the relationship between nutrient inputs from rivers and WWTFs, nutrient transport through the Providence River into upper Narragansett Bay and the evolution of phytoplankton primary productivity and zooplankton populations. The project builds off of a number of

prior studies which used different observational methods to gather both spatially detailed and temporally detailed circulation data. A series of underway acoustic Doppler current meter (ADCP) measurements by the NBC in 2001 (Kincaid, 2001a-c) show the Providence River is characterized by a strong residual outflow along the western edge of the shipping channel and a strong residual inflow of deeper water along the eastern side of the shipping channel (Figure 2a). These data show the weaker, often reversed flow of water in the shallow regions adjacent to the shipping channel. The most notable of these counter-rotating gyres, or eddies, occupies the shallow region of the Edgewood Shoals, west and south of Fields Point and west of the local trend of the shipping channel. Another is within Bristol Harbor (Kincaid, 2012b). NBC funded bottom mounted ADCPs placed in the Providence River shipping channel and within the Port Edgewood channel that extends through the western section of the Edgewood Shoals support this basic picture of flow in this region of the estuary and reveal time characteristics of these flows (Kincaid and Bergondo, 2005). Two-layer flow in the shipping channel (surface out and deep in) is seen to be a very stable feature (Figure 2a). Moreover, data show a very persistent layered flow structure on the shoals, where the mid to lower portion of the water column moves as part of a northward moving limb of a clockwise gyre on the shoal. The upper water column is strongly influenced by winds, moving in phase, and aligned with, prevailing winds (Kincaid and Bergondo, 2005). A distributed network of low cost current meters, called tilt current meters (or TCMs), were deployed in 2010 in the Providence River (Figure 3) (Kincaid, 2012a) to reveal enhanced spatial-temporal detail of the Edgewood Shoals gyre, where residual flow rates are only 1-2 cm/s, suggesting significant water retention in this region (Figure 4, 6, 7).

While data provide an essential constraint on local circulation, it is the combination of these data with modeling results that enable us to build toward accurate predictive tools for managing the estuary. A benefit of model development in the upper Narragansett Bay is the extensive data available for comparisons. When modeled and observed hydrodynamic behavior compare well it improves the hydrodynamic foundation on which the ecological model rests. A number of studies have considered how well ROMS simulations do in matching both flow and hydrographic data collected in the Bay (Rogers, 2008; Kremer et al., 2010; Balt, 2014). The first set of ROMS models, supported in part by NBC, were focused on the upper Bay, with a grid that extended from North Prudence Island to the Seekonk River (Figure 1) (Bergondo, 2004). This model had a number of limitations. One was that the model boundary was deemed to be too close to the area of interest, or the area that was the focus of the modeling study (e.g. the Providence River) (Mendahlson, 2007). A second issue was this model domain did not allow for studying the interaction of the northern rivers (Blackstone, Ten Mile and Seekonk) with the WWTF inputs. The most important issue, however, was that instantaneous (or tidal) flows and sub-tidal flows did not match the current meter observations in key areas such as the Edgewood Shoals (Figure 2b, 5a). Due to limits on computational resources, these models used relatively coarse grid resolution within the Providence River, which in turn led to flow solutions that were unable to produce features like the clockwise circulating gyre on Edgewood Shoals (Figure 4 vs. Figure 5). Instead solutions suggested efficient southward flow and flushing in these shallow regions. Underway and moored ADCP data, along with detailed tilt current meter data all show a clear, robust and persistent

clockwise gyre on Edgewood Shoals, essentially 180 degrees out of phase with these early, low resolution ROMS model predictions (Bergondo, 2004). These early ROMS models are also counter to results from physical lab models developed in the GFD lab of the Australian National University which simulate channel/shoal geometry similar in scale to the Edgewood Shoals. Lab models agree with diverse data sets showing a robust clockwise flow on a broad shoal adjacent to a channel.

The cycle of generating data-model comparisons in the Providence River showed that an improved version of ROMS needed to be developed. As part of a collaborative effort, a newer, high resolution version was developed with a combination of NBC and NOAA funding (Figure 1, 5b, 8a). The new version of ROMS for the Bay balanced reviewer comments from an outside consulting company (Mendahlson, 2007) calling for the ocean boundary to be further removed to the south from the region of interest while also maintaining finer grid resolution in key regions of the Providence River. The trade-off was between total number of grid boxes (resolution vs. total area covered by the grid) given limitations in computational speed (e.g., too many grid boxes means slow simulations). The strategy was to locate the open ocean boundary at the mouth of Narragansett Bay where information on exchange could be supplied by a larger, regional scale model (Rogers, 2008; Pfeiffer-Herbert, 2012), and to use the curvilinear grid capability of ROMS to transition from coarser spacing near the mouth to finer spacing near the head of the estuary (Figure 8a). With ~50 m horizontal grid spacing (vs. > 150 m spacing in prior models), the newer ROMS model was able to reproduce key aspects of the circulation, including the clockwise gyre on the Edgewood Shoals (Figures 4, 5b, 6, 7). This version of ROMS was compared with unprecedented levels of spatially-temporally detailed current meter data within the Providence River (Figure 3). This is shown through both qualitative and quantitative methods. A well accepted parameter for quantitatively assessing model accuracy is the Willmott skill (Warner et al, 2005; Willmott, 1981), or

$$\text{Skill} = 1 - \frac{\sum |X_{\text{model}} - X_{\text{data}}|^2}{\sum (|X_{\text{model}} - X_{\text{data}}| + |X_{\text{data}} - \text{mean}(X_{\text{data}})|)^2} \quad (1)$$

, where X represents a time series of either data or ROMS generated values for water velocity, temperature or salinity. A skill of 1.0 would result from a perfect match between data and model fields. Willmott model skill values for instantaneous data-model records (e.g., including tidal responses) are typically >0.9 for surface elevations, water currents and hydrographic parameters (salinity, temperature) (Balt, 2014). Skills calculated on ROMS derived surface elevation variations versus data at Newport, Quonset, Conimicut Point and Providence tide gauge stations have been found to be >0.95 in a number of ROMS studies (Rogers, 2008; Balt; 2014; Kincaid, 2012a). In all cases, the model skill values for instantaneous fields were extremely strong.

However, it is the residual, or tidally-averaged, flow patterns that are most important for controlling long-term biogeochemical transport and flushing processes. They are challenging to match well because they are significantly lower energy than instantaneous or tidal variations. A recent dye circulation study with the higher resolution SNB-

ROMS model shows that the model does well at simulating residual flows recorded by TCMs, even given the extreme discharges from the 2010 sampling period. Willmott skills of >0.8 are calculated for periods before, during and after the 2010 flood (Kincaid, 2012a). Remarkably, ROMS matches both the amplitude and time-evolution of the flood-induced flows along the shoal-channel interface and within the interior of Edgewood Shoals (Table 1, Figures 6, 7). The process of calibrating the ROMS model with data from these TCMs greatly improves the usefulness of the models in quantitatively mapping relationships between flow, flushing and transport in the estuary.

Once compared with circulation data, the SNB-ROMS model was used to study dye transport/dispersion for distinct dye fields representing each major river and primary WWTF releasing to Narragansett Bay for the spring-summer 2010 period (Kincaid, 2012a). Dye inputs were scaled to actual nutrient levels for source, and were used to document transport/flushing pathways for each source, given a range of environmental forcing conditions. While these use oversimplified assumptions that nutrient concentrations (dye concentration) are conservative (e.g., no drawdown due to phytoplankton productivity), they reveal important patterns, including which sources contribute most to the productivity in sub-regions exhibiting chronically low oxygen levels. Results from these simulations show 3-D circulation leads to often unexpected patterns: 1) deep northward transport carries Taunton River dye well into the Providence River, 2) Edgewood Shoals is supplied with nutrients primarily from the Blackstone and Pawtuxet Rivers, 3) the Pawtuxet River chemical plume bifurcates into distinct regions, a surface plume that advects south along the western Providence River, an intermediate depth plume that moves onto Edgewood Shoals, and a deep plume that moves northward in the shipping channel (Kincaid, 2012a). A series of idealized process runs show most conditions result in northern dye sources moving past Greenwich Bay, while sea breeze winds can lead to episodic pumping of these dyes into Greenwich Bay. Finally, a comparison simulation is done where the 2010 flood runoff pulse is removed from the river forcing. Comparing runs with and without the flood allows the persistence of flood dye mass to be documented. Dye from the 2010 flood lasted the longest in Greenwich Bay (e.g., seen ~ 40 days after the flood). Results are also used to test different WWTF release strategies for dye concentration, showing that reductions from 8 mg L^{-1} nitrogen to 5 mg L^{-1} and then 3 mg L^{-1} are largely insignificant throughout much of lower Providence River and upper Narragansett Bay. Models suggest such changes will be imperceptible to Greenwich Bay waters. It is important to note, however, that these simple dye runs represent nitrogen input and transport as a conservative species, which is not being influenced by ecosystem/biological processes. These results were meant to lay the foundation for subsequent, more complicated ecosystem models such as those presented here.

3.0 Methods

To simulate coastal circulation patterns, we use the three-dimensional (3-D) Regional Ocean Modeling System (ROMS) hydrodynamic model (Shchepetkin and McWilliams, 2003; 2005). ROMS is a split-explicit, free-surface, primitive equation model with curvilinear and terrain-following coordinates. Using the curvilinear capabilities of the grid, the original ROMS model for NB utilized a computational grid for the full extent of

Narragansett Bay which focused resolution towards the northern end of the estuary (Figure 8a). Horizontal spacing of grids varied from 300m in the south, near the Bay mouth, to roughly 30m in the vicinity of Fields Point, RI (Figure 9b). Fifteen vertical (or sigma) layers in the model resulted in a vertical resolution that varied locally with the water depth (e.g., water depth divided by 15 vertical levels). The use of sigma coordinates in ROMS allows for modeling circulation in the presence of varying bathymetry.

A major new component of the project reported here has been to add the Seekonk River. In all prior Narragansett Bay ROMS models, including cases done for NBC (Kincaid, 2012a) and in NOAA-CHRP models for Narragansett Bay (Kremer et al., 2010), the Seekonk River was represented in a highly simplified fashion (Figure 8b). A quasi-rectangular volume was put in place of the Seekonk River, representing the total volume of the sub-system, but making no effort to recreate actual bathymetry or coastline. In these new models reported here, a new grid has been developed which closely replicates key features of Seekonk River shape and bathymetry (Figures 8c, 9a). The new Seekonk River portion of SNB-ROMS allows for improved representation of major rivers (Blackstone, Ten Mile) and the Bucklin Point WWTF (Figure 10a) and for simulating basic Seekonk River processes (Figures 9, 10). The focus of this report is on the development of an ecosystem model for Narragansett Bay, however a few details of the differences and similarities between the SNB-ROMS and prior ROMS versions for NB are provided below.

Simulations using the SNB-ROMS model are run for 2010 environmental conditions using freshwater discharge applied at primary river sites (Blackstone, Pawtuxet, Ten Mile, Woonasquatucket, Moshassuck, Palmer, Hunt/Green, two Greenwich Bay rivers and the Taunton). To better understand the relationship between transport of northern riverine/WWTF nutrient sources either bypassing or entering into Greenwich Bay, riverine sources are also included in Greenwich Bay, and south of Greenwich Bay. These include Harding Brook, Muskerchug River and the Greenwich Cove WWTF, and the Hunt River. Winds and atmospheric air-sea flux conditions are applied at the surface and conditions on water velocity, temperature and salinity applied along the open ocean boundary of the model (e.g., the mouth of Narragansett Bay). A nesting procedure is used to apply conditions at the mouth of the estuary. Values for water velocity, temperature and salinity are applied along this boundary from information supplied from the coarser, but spatially larger coupled Rhode Island Sound (RIS) ROMS model (Figure 1) (Rogers, 2008; Pfeiffer-Herbert, 2012). This RIS-ROMS version is, in turn, forced at its open boundaries by information provided from the ROMS-ESPRESSO model of the Mid-Atlantic Bight (<http://www.myroms.org/espresso/>). As recommended by Janekovic and Powell (2012), separate applications of tidal forcing were applied around the RIS ROMS boundary using tidal harmonics from the ADCIRC model of the U. S. East Coast (Mukai et al., 2002; <http://www.unc.edu/ims/ccats/tides/tides.htm>). The inclusion of input from the ESPRESSO model has improved the accuracy of this RIS model in terms of providing boundary conditions that match the tidal and non-tidal characteristics of flows at the mouth of Narragansett Bay (Pfeiffer-Herbert, 2012) and match the tidal records from buoys within the Bay, such as records from within the Providence River

(e.g., data in Figure 11).

These recent SNB-ROMS simulations build from Kincaid (2012a) by focusing on 2010. Models are spun up from January, 2010, beginning from simplified initial conditions on salt (S) and temperature (T) (Figure 12). These are generated by applying simple linear (horizontal/vertical) gradients onto the ROMS grid. Wind forcing for the RIS-ROMS providing boundary conditions to SNB-ROMS is applied from meteorological data from the Buzzards Bay monitoring station (www.ndbc.noaa.gov/station=buzm3). Wind forcing for the SNB-ROMS grid covering Narragansett Bay is constructed by taking an average of wind speed and direction at four real-time physical oceanographic real-time system sites (PORTS) (<http://tidesandcurrents.noaa.gov/ports.html>), including Fall River (MA), Providence (RI), Quonset Point (RI) and Newport (RI) (Figure 13). A similar process is used for determining air temperature and pressure values. Radiative surface heat flux and relative humidity data used in forcing ROMS were obtained from the North American Regional Reanalysis data set (<http://www.emc.ncep.noaa.gov/mmb/rrean/>). Precipitation data were gathered from T.F. Green International Airport (Station ID GHCND:USW00014765, <http://www.ncdc.noaa.gov/cdo-web/search>).

Model runs use information on runoff obtained from the United States Geological Survey records (<http://waterdata.usgs.gov/nwis/dv>). In the development of SNB-ROMS for Narragansett Bay, an analysis has been done to correct river discharge values by determining the extent of un-gauged drainage areas, below the last gauging station and correcting published data values by a scale factor (Kremer et al., 2010). Corrected runoff values applied through the Blackstone River are shown in Figure 14. For rivers without gauged data, an estimate is developed by multiplying time series for gauged rivers by the ratio of drainage areas (gauged time series x (un-gauged drainage area/gauged drainage area)).

Nitrogen Transport Patterns in the SNB-ROMS:

At the foundation of ecosystem models is the input, transport and mixing of nitrogen through estuaries. Building from prior efforts (Kincaid, 2012b), we use nitrogen inputs calculated within a total maximum daily load (TMDL) model for the Blackstone River supplied for 2010-2011 by P. Reese (UMass Water Resources Group) (Figures 15-18). For the 2010 flood simulation cases we utilize information from the computer simulation program called “The Hydrologic Simulation Program – FORTRAN” or “HSPF” developed by University of Massachusetts Water Resources Research Center (P. Rees, Director, Massachusetts Water Resources Research Center, Univ. of Massachusetts; rees@ecs.umass.edu) with funding from the Upper Blackstone Water Pollution Abatement District (UBWPAD) (Patterson, 2007). The HPSF program forms the basis of the Blackstone River Water Quality Model (BRWQ), which was developed to assess the effectiveness of future pollution control strategies on downstream river quality, in line with the goals of this work. The Blackstone River Water Quality model has been run to predict time-varying nutrient concentrations for water entering the Bay through the Blackstone River for 2010. The BRWQ model predicts not only the total nutrient concentration, but also the percent contribution from each of three sources: 1) the Upper Blackstone WWTF, 2) non-point sources and 3) other point sources (Figures 15-17).

Nutrient concentration is higher during low flow periods and lower (diluted) during high flow periods (Figure 18). An empirical model is used to extend the BRWQ derived relationship between river discharge and river nutrient concentration in generating time series for all other river sources based on their measured discharges (Figure 18). This basic pattern of higher (lower) concentration given lower (higher) discharge values from the Blackstone River is also seen in the Taunton River, Ten Mile River and Moshassuck River. This extrapolation method then is better suited to these rivers. However, data suggest the Pawtuxet, Woonasquatucket and Palmer Rivers do not exhibit this flow versus concentration relationship, instead following a more scattered, less coherent trend. Given our extrapolation method, nutrient concentrations for these rivers are likely high (low) for periods of low (high) runoff. In our models we test ecosystem models ranging from May-July, and so largely avoid discharge extremes where the nutrient model extrapolations are less accurate for these rivers. While the Palmer and Woonasquatucket Rivers are very minor contributors, and so the influence of river nutrient errors is expected to be small, we likely under estimate the nutrient inputs from the Pawtuxet River using our extrapolation method. Future observations and simulations should be done to improve how the Pawtuxet River is included in the ecosystem model, particularly given the importance of this source on ecosystem dynamics of the Edgewood Shoals. Data on volume and nutrient discharges from Fields Point and Bucklin Point WWTFs are supplied for this period from NBC. Discharges for additional WWTFs (East Providence, Greenwich Bay, and Fall River) are produced by scaling time series values by ratios of mean discharges for each plant.

Ecosystem Model:

The ecosystem model chosen for this study is an NPZD-type, which limits the number of model parameters, many of which are marginally constrained by observations. While many ecosystem models include multiple phytoplankton types and zooplankton species, the NPZD Franks model that exists within ROMS includes only coupling between nitrogen and just one component each of phytoplankton and zooplankton. The NPZD model solves the coupled system of equations for total nitrogen (N), phytoplankton (P), zooplankton (Z) and detritus (D) all represented as milli-Moles/ m³ in the simulations. Phytoplankton concentration grows by consuming N, controlled by the N uptake rate (V_m). Phytoplankton biomass is reduced by a mortality coefficient (loss to the detrital pool) or by a loss term representing zooplankton grazing, in turn controlled by zooplankton grazing rate (Z_g). Zooplankton concentrations, therefore, increase by grazing of available P and are reduced through a mortality rate term. Mortality of P and Z are conserved by conversion to the detritus field, which is in turn converted or recycled back into the nutrient (N) field. In addition to various source/sink relationships, each eco-field (N, P, Z, D) is advected with the ROMS circulation fields, and diffused by turbulent (eddy) mixing. The additional components to the equations solved for P, Z and N fields, beyond advection and eddy diffusion, are as follows:

$$\frac{dP}{dt} = UP - mP - I_i Z \quad (1)$$

$$\frac{dZ}{dt} = (1 - \gamma)I_i Z - gZ \quad (2)$$

$$\frac{dN}{dt} = -\frac{V_m N P}{k_s + N} + mP + gZ + \gamma I_i Z \quad (3)$$

$$I_i = R_m(1 - e^{-\Lambda P}) \quad (4)$$

$$U = \frac{V_m N}{k_s + N} \frac{\alpha I}{\sqrt{V_m^2 + \alpha^2 I^2}} \quad (5)$$

$$I = I_o e^{k_L Z} \quad (6)$$

Here g , γ , k_s , m , and V_m are zooplankton death rate, unassimilated grazing fraction, nutrient uptake half saturation constant, phytoplankton mortality rate and maximum phytoplankton uptake rate. An Izlev grazing formulation is employed (equation 4) where I_i is the ingestion rate, R_m is maximum ingestion rate and Λ is the rate at which saturation is achieved. Phytoplankton growth U (as term UP in (1)) has two terms in (5), the first is the standard growth term controlled by V_m , N and half saturation constant, k_s . The second term in (5) is a light limiting term, described in (6). Light I is reduced exponentially with depth z from a background constant level I_o . As with other ecosystem models, a range in expected light extinction parameters is tested in this range of simulations (Edwards, 2001; del Barrio et al., 2014). Values vary between 0.55 d^{-1} to 0.75 d^{-1} based on estimates reported for Narragansett Bay (Smayda and Borkman, 2008). Detritus is formed through phytoplankton and zooplankton mortality and egestion and remineralized into nitrogen. Ecological simulations are initialized with low concentrations for N , P , Z , D . River nutrient fluxes are included as discussed above, and not varied between SNB-ROMS model simulations. Models do allow for different nutrient concentrations being released from the WWTFs, which can be used in characterizing the benefit (on phytoplankton biomass levels) derived from past and planned WWTF nitrogen permit levels. Simulations systematically compare how a full suite of model parameters and both actual and idealized environmental forcing variables combine with 4 different WWTF release concentrations (15 mg L^{-1} , 5 mg L^{-1} , 3 mg L^{-1} and 0 mg L^{-1}) to modulate coupled nutrient, phytoplankton, zooplankton and detrital fields. Phytoplankton and zooplankton concentrations are set to zero for river inflow, as is commonly done in coastal/estuarine ecosystems based on the assumption that freshwater species do not survive in salt water. However, there are some indications that there may be levels of phytoplankton entering in the rivers that survive. This is an area that should be pursued with observations that can better inform ecosystem parameters used in SNB-ROMS river forcing files.

There are many flavors of ecosystem models. Many use relatively few ecological grid boxes and highly simplified, highly averaged circulation/exchange estimates between eco-boxes. The benefit of this model type is the ability to cover long periods of simulated time and perform detailed sensitivity study of many biological parameters. Our effort lies at the opposite end of the spectrum. We build from extensive detailed data

sets on small-scale to mid-scale dynamics throughout the Bay, but particularly within key regions of the Providence River, within a coupled modeling framework that represents fine details of the circulation. The clear benefit is the ability to define relationships between physics and ecosystem response. The downside is the computational expense in terms of time to run, say, month long simulations. Our strategy is to select a specific event, on the scale of a month, and to run a parameter sensitivity test, employing large numbers of simulations that cover just this focused time period.

The time period chosen for this initial study builds from prior ROMS modeling/data validation studies while beginning to explore existing ecological data/trends with the new SNB-ROMS ecosystem simulations. Observations from buoys and cruises in NB show that ecological parameters of nitrogen, phytoplankton and oxygen are highly time variable and exhibit extreme spatial patchiness (Smayda and Borkman, 2008). A few, fairly robust patterns have been identified including the strong nutrient trend that exists along the salinity gradient from high values in the north (Seekonk River, upper Providence River) to lower values in the mid-Bay, a region loosely defined as between the mouth the Providence River at Conimicut Point and the northern end of Prudence Island (Figure 19). There is commonly a 50% reduction that occurs along this latitudinal gradient, from the head of the Providence River at India Point (IP) to its mouth at Conimicut Point (CP) expressed as a nitrogen ratio $N_g = N_{CP}/N_{IP} \sim 0.5$ (Smayda and Borkman, 2008; Oviatt, 2008) (Figure 19). Observations show a different latitudinal distribution in phytoplankton biomass (often represented with a proxy of Chlorophyll concentration). The tendency is for peak phytoplankton levels in the mid-Bay with a significant reduction in phytoplankton concentrations to the south. Interestingly, the mid-Bay phytoplankton levels are often higher than values recorded to the north, where nutrient levels are highest (Smayda and Borkman, 2008). Smayda and Borkman (2008) suggest that the northern rivers are nutrient saturated and light limited, whereas the mid-Bay has light, but is nutrient limited. A review of NU-shuttle data shows that the general region around Conimicut Point often shows peak chlorophyll levels, in agreement with Smayda and Borkman, (2008). Oviatt (2008) reports that a 1997-1998 survey showed that chlorophyll levels increase northward to the mid-Bay and then remained fairly level through the high nitrogen regions of the Providence and Seekonk Rivers. However, recent data sets (NBC, Figure 20) show chlorophyll levels decreasing by a factor of 2 from the Seekonk River down to Conimicut Point, along the lines of the nitrogen gradient. Chlorophyll trends through the northern rivers appear to be variable. Significant effort has been put into documenting trends in oxygen levels throughout the Bay since the 2003 fish kill event in Greenwich Bay (GB) (Codiga et al., 2009). Results show a number of general patterns. One striking trend in the data is that GB produces significantly more low dissolved oxygen (DO) events per summer than other regions of Upper Narragansett Bay (UNB) and PR. Events evolve in different ways, from gradual downward trends (order 20-30 days) to those with ~ 1 week onset periods (e.g. Phillipsdale buoy station (PP), July 2006; 2007).

A goal of this work is develop, test and apply a fully coupled version of SNB-ROMS hydrodynamics with an NPZD-Franks ecosystem model. This involves first conducting a parameter sensitivity test on the most important NPZD parameters and then using the

model to begin identifying repeatable, underlying processes. We begin with a focus on 2010 (Figures 21-23) to build from prior data-model comparison tests and chemical transport simulations using the ROMS model (Kincaid, 2012). Figures 21 and 22 show how cyclical chlorophyll data are at many of the buoy sites. A common periodicity is ~2 cycles per month. Data also show that GB tends to have the highest chlorophyll levels for much of the summer period (Figure 21). This is in agreement with the analysis of buoy data by Codiga et al., 2009 for low oxygen event deficit duration, where GB greatly exceeds stations at North Prudence and Conimicut Point during years 2003-2006. Observations from a combination of the Narragansett Bay Fixed Site Monitoring Network buoys (NBFSMN), a series of NU-shuttle cruises and from NBC periodic surveys show there are two large phytoplankton bloom events in the spring-summer period of 2010. The NBC data (Figure 23) highlight the two dominant blooms for this summer period, one near June 16, 2010 and the other around August 18, 2010. These combined data sets show two very important trends: 1) that GB has the largest values and 2) that during the early summer bloom the region near Edgewood Shoals exhibits the highest chlorophyll levels, but during the August bloom the largest values are recorded in the Seekonk River. Figure 24 shows that a trend toward low levels of bottom oxygen begins around days 167-169 (6/16-6/18), or just after the chlorophyll peak and continues to day 179 (6/28) when there is a sudden reset, roughly correlated with a reduction in water stratification, as shown in Figure 24b by changes in the vertical salinity gradient, or the difference between near-bottom and near-surface salinity. This period of destratification and re-oxygenation coincides with 20-30 knot wind event and accompanied by a sudden drop in air temperature (NOAA-PORTS: tidesandcurrents.noaa.gov/met.html?bdate=20100619&edate=20100701&units=standard&timezone=GMT&id=8452944&interval=6). After this re-oxygenation event there is another gradual downward trend in bottom oxygen culminating on day 200 (7/20). One additional feature of the June bloom is that it appears to start within GB and to progress northward (Figure 25). A steady, linear increase in chlorophyll concentration within GB is observed to precede the onset of a bloom on Ohio Ledge, between Warwick Neck and Conimicut Point, by ~5-7 days. We choose to focus initial development and testing of the NPZD ROMS model for this period of early summer 2010 (Figures 21-25).

4.0 Results:

New Seekonk River Model: Chemical Dye Pathways

We begin by showing results from nitrogen (N) input/transport where N is a conservative tracer. A much more thorough treatment of N-dye dispersion for 2010 conditions and idealized conditions is given in Kincaid (2012b). Here we present a brief overview of dispersion trends given the hydrodynamic coupling of the Seekonk River to the Providence River. This first step is to check circulation patterns. Time series velocity information from TCM locations within the new grid were compared with model output from the ROMS 2010 simulations without the Seekonk which were statistically validated against 2010 TCM data (Kincaid, 2012b; Table 1). Results show the new SNB-ROMS does very well at recreating the prior modeled flow patterns on the Edgewood Shoals (Figure 26), both in terms of tidal flows and longer term, sub-tidal trends. With the circulation being well-represented in the SNB-ROMS, the addition of a highly resolved Seekonk River that is fully coupled to the Providence River adds a new dimension to the

chemical transport models of UNB. Results are shown from the spin up phase of the SNB-ROMS modeling, from January through April 2010 when nutrient fields are tracked as conservative fields (e.g., NPZD model not engaged). Results show a number of interesting, characteristic trends, including that the constriction at India Point Park appears to act as a choke valve for material leaving and entering the Seekonk. Figure 27 highlights near-surface WWTF nutrient fields from the Blackstone River. High concentrations are confined to within the Seekonk while narrow, dilute chemical plumes extend to Fields Pt./Edgewood Shoals. The down-bay dispersion of higher concentration chemical (nutrient) plumes from Blackstone non-point source (NPS) inputs are shown in Figures 28-29. Concentrations are much higher through the Edgewood region. As documented in Kincaid (2012b) mid-Bay contours of this NPS Blackstone plume reveal repeatable trends in mid-Bay pathways. Prevailing winds are important in determining if plumes from northern sources move into upper East versus West Passages (Figure 29). Northeastward blowing winds favor the former. Additional fresh water nutrient sources in the SNB-ROMS model are from Bucklin Point and the Ten Mile (new to these models). Figure 30 shows these are less concentrated during this winter period than Blackstone NPS, and also tend to follow typical pattern of high concentrations held within the Seekonk, with narrow, much diluted plume sections extending towards Fields Point.

Down bay chemical transport of northern sources is one aspect of the new SNB-ROMS models. Alternatively, results with the SNB-ROMS show transport patterns for chemical plumes entering the Seekonk River from the south. Figures 31-32 are contours highlighting the northward transport of Taunton River nutrient fields to the Fox Point Hurricane Barrier and the mouth of the Seekonk River. Similarly, Pawtuxet River nutrient fields are seen to accumulate within the shallows of the Providence River (as in Kincaid, 2012b), but are also readily transferred to the mouth of the Seekonk River. From this point, narrow lenses of lower concentration material from these southern chemical sources are shown to periodically entrain deep into the Seekonk (Figures 32b, 33b). In agreement with the prior ROMS dye study (Kincaid, 2012), Fields Point WWTF nutrient plumes tend to be transported efficiently southward, showing limited northward entrainment into the Seekonk River (Figure 34).

Ecosystem Models:

Results are presented from an extensive set of coupled hydrodynamics-NPZD simulations using the new SNB-ROMS (with the Seekonk River included) covering the time period April 20 to June 28, 2010. Spatial-temporal patterns in phytoplankton blooms are characterized for a wide range in ecological parameters (Table 2). Key parameters tested here are phytoplankton (V_m) and zooplankton (Z_g) growth rates, light extinction coefficient (K_L) and nitrogen release levels for the WWTFs. A small number of cases tested parameters that had a smaller influence on the solutions, including the phytoplankton mortality rate and the nutrient half saturation constant. Results are highlighted using mapview, color contour plots of ecosystem fields to show spatial structure versus depth (e.g., Figures 35-37) and using time series plots at key locations (Figure 38). An additional representation of model results uses a common technique of plotting N and P (chlorophyll) versus latitude.

4.1: A starting case: WWTF 355; V_m 2.5, K_L 0.75, Z_g 0.6

We begin by describing results for a starting set of NPZ parameters, which are high phytoplankton growth, limited light penetration and small zooplankton grazing (table 2: WWTF release levels of 355 mM m^{-3} (5 mg L^{-1}), $V_m=2.5 \text{ day}^{-1}$, $K_L=0.75 \text{ m}^{-1}$, $Z_g=0.6 \text{ day}^{-1}$). Contour plots show the progression of N through the rivers and down bay. As seen in prior models, the highest N levels enter through the northern sources and are advected southward as a coherent chemical plume. The dispersion patterns for this plume, however, are distinct from prior dye studies (Kincaid, 2012a; Figures 29-36) in that nitrogen is actively converting into other ecosystem parameters. Despite being depleted by phytoplankton, dispersion of this nitrogen plume follows basic transport/dispersion pathways that are consistent with prior chemical dye simulations. As in the dye cases, Figures 35 and 36 show the N plume flowing from the north to be confined to the eastern mid-Bay/East Passage when winds are northward (Figure 13) and to the western mid-Bay/West Passage when winds are southward (Figure 13). Another common result of the NPZD models, consistent with conservative dye models (Kincaid, 2012a) is that nutrients tend to accumulate in the near-bottom water within the shallow edges of the Providence River (Figure 37b) and Ohio Ledge (Figure 37c).

Despite the similarities with the conservative dye transport simulations, the SNB-ROMS NPZD model provides an important tool for simulating basic ecosystem processes in Narragansett Bay. The advection, diffusion and loss of nutrients to phytoplankton growth consistently produce a latitudinal (Seekonk to Conimicut Point) N distribution (Figure 39a) that matches data trends (Figure 19). On day 161, prior to the onset of Bay-wide bloom there is a ~ 80 to $\sim 25 \text{ mM m}^{-3}$ reduction in total N from the Seekonk River mouth at India Point (IP) to the Providence River mouth at Conimicut Point (CP). A common description of nutrient distributions in the upper Bay involves the nutrient gradient from the head of the Providence River to the mouth. We define a nitrogen gradient N_g defined as the nitrogen concentration at the mouth normalized by the concentration at the head (India Point), or $N_g=N_{CP}/N_{IP}$, which is ~ 0.3 . This is consistent with N_g ratios for 2010, and years 2007-2011 (Figure 19). After 2011 the N_g ratio increases to 0.4, reflecting a drop in maximum N and a smaller N_g value. North of India Point, at Phillipsdale in the Seekonk River, the N concentration is higher, or $\sim 140 \text{ mM m}^{-3}$ (Figure 39a). Averaged values on day 170 (7/19), after the bay-wide phytoplankton bloom show different latitudinal distributions depending on nutrient uptake rate, or V_m (Figure 39b). A value of 1.5 day^{-1} generates very little growth and the N-trend remains unchanged. Alternatively, a higher uptake rate of $V_m=2.5 \text{ day}^{-1}$ generates significant growth, reduced N through the Providence River and a severe $N_g \sim 0.1$.

Details of the June 2010 upper Bay blooms for these three uptake rates are summarized in Figures 40-42. On day 160 (6/9) phytoplankton growth begins at a mid-latitude, within Greenwich Bay (Figure 40a). The bloom peaks near day 163 (6/12) at a mid-latitude range (Figure 40b) from North Prudence to Conimicut Point, or the Ohio Ledge region (Figure 38). By day 166 the peak phytoplankton biomass is located to the north, in the vicinity of Edgewood Shoals (Figure 40c). The wave in peak P-biomass continues to progress northward (Figure 41), essentially breaking upon the head of the Seekonk River

on day 173 (6/22). The sensitivity of uptake rate on the solutions can be seen in comparisons between cases with $V_m=2 \text{ day}^{-1}$ and $V_m=2.5 \text{ day}^{-1}$. A reduction in uptake rate to $V_m=2 \text{ day}^{-1}$ generates a bloom that has 50% (red vs. green in Figure 40a), 15% (Figure 40b) and 20% (Figure 40c) of the $V_m=2.5 \text{ day}^{-1}$ phytoplankton concentration at different times and locations through the mid-Bay. There is also a reduction in northward progression rate of the peak of the phytoplankton versus latitude curve for the lower $V_m=2 \text{ day}^{-1}$. For example, the pulse in biomass reaches Edgewood on days 166 (Figure 40c) and 173 (Figure 41c) for $V_m=2.5 \text{ day}^{-1}$ and $V_m=2 \text{ day}^{-1}$, respectively. For the lower V_m rate, the pulse doesn't reach the northern section of the Seekonk until ~day 178 (6/28) (Figure 42). Interestingly, the peak biomass levels for $V_m=2 \text{ day}^{-1}$ are 1/5th of the $V_m=2.5 \text{ day}^{-1}$ case through the mid-Bay, but reach equivalent levels of 70-100 mM m^{-3} within the upper Seekonk. Notably, the lowest uptake rate, $V_m=1.5 \text{ day}^{-1}$, that lies in the low to mid-range for estimates in estuaries like Narragansett Bay, produces no discernable bloom through much of the mid to upper Bay. For comparing the effects of advection versus biological growth, the black symbols in figures 39-42 are cases of passive chemical transport of the nutrient field, without any coupling to the other ecosystem fields (reflected in the zero values for P in Figures 40-42).

Prior plots of phytoplankton versus latitude are instructive, but do not represent much of the rich spatial-temporal detail of the SNB-ROMS NPZD model simulations. Two key outcomes of these plots are that blooms begin in the mid-Bay and progress northwards, and that the uptake rate controls the spatial-temporal pattern of the blooms. We use a series of time series plots within key locations (Figure 38) to bring out some additional aspects of bloom dynamics throughout the Bay. Figures 43-45 summarize the growth in phytoplankton with time moving from Greenwich Bay (Figure 43) to Ohio Ledge (Figure 44) and then up through the Providence and Seekonk Rivers (Figure 45). These plots are for a reference case with WWTFs releasing at 355 mM m^{-3} (5 mg L^{-1}) and values for light extinction and zooplankton grazing rate of 0.75 (m^{-1}) and 0.6 (day^{-1}). Three different nutrient uptake rates are considered ($V_m=1.5, 2$ and 2.5 day^{-1}). At stations located within innermost Greenwich Bay (GB) and near the mid-point buoy at Sally Rock, the two higher values produce the same bloom. Even the lowest value V_m produces a similar bloom by day 161, and an even larger bloom beyond day 161. Blooms from the two higher V_m cases track similarly in records near the GB mouth (site of prior ADCP deployments), while the low V_m case doesn't reach these biomass levels until later, > day 163. The strong oscillations at the time scale of the tidal flow suggest the low V_m bloom is patchy.

Moving outside of Greenwich Bay the influence of V_m is much stronger. The mid-Bay East Passage station and stations in the Providence and Seekonk Rivers show no bloom over these time scales for $V_m=1.5 \text{ day}^{-1}$. Only the West Passage station, just north of the GB mouth shows a bloom for this low value. Figures 44-45 show clearly how the timing of the bloom with the two larger V_m values progresses from south (mid-Bay) to north. In the East Passage regions of the mid-Bay, the biomass passes 10 mM m^{-3} on days 165 and 179 for V_m of 2.5 and 2, respectively.

A series of color contours are used to illustrate the patchiness and speed of the bloom growth for certain regions. Figure 46 shows phytoplankton levels in surface and bottom waters for this reference case early on day 164 (6/13). At this point the bloom growth hotspots are inner GB, the northern shore of the Taunton River, in shallow water along the western shore of Ohio Ledge and in the shallow edge regions of the lower Providence River. A part of the pattern in the near-bottom contours reflects changes in depth, where deep channel waters have low values. However, much of the area away from the channels has fairly uniform depth, and the bright red centers do reflect repeatable high productivity centers. By late in this day (Figure 47), the bloom has grown significantly in these areas and has spread from the Taunton River to Bristol Harbor, from Ohio Ledge into outer Greenwich Bay and further north within the Providence River. A day later (Figure 48), the bloom is quite strong and no longer patchy, covering a region from mid-Providence River to south of Ohio Ledge. Contour plots for subsequent days show the continued northward progression of the bloom into the upper Providence River and Seekonk River, while the bloom is diminished throughout the mid-Bay (Figure 49, 50). While it is difficult to see in still frames, movie animations of these near-surface and near-bottom phytoplankton concentrations show the red fields to move with tidal oscillations and a non-tidal residual motion northward from Edgewood and into the Seekonk River. The up-estuary tidal pumping of material is constricted at India Point (shown in Figure 50).

While there are number of parameters that can be adjusted, a result that is seen over most combinations of parameters within these models is that blooms seem to begin in shallower mid-Bay and lower Providence River locations and migrate northward. This could be an apparent northward motion due to delayed, in-situ growth of phytoplankton in the northern versus southern locations or due to an actual northward advection of phytoplankton (and zooplankton/detritus). This is consistent with return flow residual currents (running from the estuary mouth towards the head) that have been well-documented, particularly in the deeper and eastern portions of the Bay's main channels (Kincaid et al., 2003; Kincaid, 2006; Rogers, 2008; Pfeiffer-Herbert et al., 2015). The phytoplankton fields shown in Figures 49 and 50 indicate northward, up-estuary transport but the detrital pool that appears in tandem with a bloom also provides an interesting way to view in-situ versus advected processes. Figure 51 shows near-bottom detrital concentrations early in the bloom, day 162.7. A yellow line in Figure 51a marks a detrital front that can be seen in movie format to move out of Greenwich Bay and onto Ohio Ledge. Figure 51b highlights both in-situ and advected signals occurring. The detrital patch from Greenwich Bay (yellow line) has moved eastward at a ~ 3 cm/s residual flow rate. There is also a detrital patch evolving in the lower Providence River that is reflecting in-situ growth. Figures 52-54 are a series of contour fields of detritus levels during this event that combine in-situ growth on Ohio Ledge and in the Providence River and also northward advection. Up-estuary advection is occurring throughout, but the patterns are particularly apparent within the dredged Port Edge Channel across Edgewood Shoals and the main shipping channel between Fields Point and India Point (Figures 52, 53). Estimated residual transport rates for the latter are highlighted in Figure 54. The estimate of 8 cm/s is consistent with observations. A more direct measure of up versus down estuary of transport of ecosystem parameters (N, P and Z) is

shown in Figure 55. Here residual (non-tidal) transport fluxes are shown for a ROMS station located in the main shipping channel, east of Edgewood. Shown as the time varying product of residual flow and each parameter, the plots clearly show that surface water exhibits a net southward (down-estuary) export while mid-level to deeper water shows a net import of bloom products. While there is clearly in-situ production in the Providence River, the shipping channel also provides an efficient conduit connecting biochemical components of a bloom from Ohio Ledge to the Seekonk River.

4.2: The Influence of WWTF Release Levels

While the SNB-ROMS utilizes a simplified NPZD-Franks ecosystem representation, strengths of the model include: a) it is simple and does not include large numbers of parameters that are not known for the Bay, b) it has been well tested for years, and in many situations, and c) its simple nature allows for testing the relative importance of the key parameters. We use the SNB-ROMS NPZD model to test the impact on this simulated bay-wide June, 2010 bloom of variations in the nutrient release levels from all WWTFs represented in the model (Fields Point, Bucklin Point, Fall River, Greenwich Bay, East Providence). The reference model, summarized above, used a release concentration of 355 mM m^{-3} (or 5 mg L^{-1}) for total nitrogen. Figures 56-60 summarize the behavior of this bloom event given change in all WWTF releases including 1071, 213 and 0 mM m^{-3} (or 15, 3 and 0 mg L^{-1}). Model runs with the different WWTF release levels were begun from a start date of April 20, 2010, more than a month in advance of the bloom period. As above, we start with plots of nutrient and phytoplankton levels versus latitude through Narragansett Bay (locations summarized in Figure 38). Early in the event (Figure 56, day 163), there is the expected nutrient gradient from India Point to Conimicut Point. The Providence River head to mouth nutrient gradient is from roughly 100 mM m^{-3} to 30 mM m^{-3} , or $N_g \sim 0.3$. This linear trend in nutrient concentration that is commonly discussed for the Providence River is shown to be variable, not just with changing parameters, but also with time for a given parameter set due to the northward sweep of bloom events. The higher release level (1071 mM m^{-3} or 15 mg L^{-1}) is reflected in a nearly uniform upward shift in N concentration of $25\text{-}30 \text{ mM m}^{-3}$ throughout the Providence River. Within Greenwich Bay, and on Ohio Ledge total N concentrations are low, and the difference in simulated concentrations between the modeled release levels is less than 1% those seen in the upper Providence River. Interestingly, the differences generated by the smaller WWTF release levels (5 vs 3 mg L^{-1}) are minimal. Plotted trends for each of these release levels and for 0 mg L^{-1} coming from the WWTFs, are nearly identical.

Results showing very small net changes in nutrient levels within the Providence River for cases with nutrient concentrations within WWTF releases that vary between 5, 3 and 0 mg L^{-1} are in line with prior studies that treated N as a conservative dye (Kincaid, 2012b). However, a benefit of the SNB-ROMS NPZD model is the ability to propagate these permit level management strategies through to the other ecosystem fields, phytoplankton, zooplankton and detritus during the period of this June 2010 bloom. Figure 56b shows the modeled phytoplankton response versus latitude for day 163. At this point, where the bloom is initiating in the mid-Bay, there is a noticeable increase in phytoplankton biomass for the high WWTF release case of 1071 mM m^{-3} (or 15 mg L^{-1}).

Within Greenwich Bay, at the Ohio Ledge stations and at lower Providence River stations of Bullocks Reach and Conimicut Point there is a 1-1.5 mM m⁻³ enhancement in biomass, or a 25% increase from the lower release cases. At this early stage in the bloom (with the high value of $V_m=2.5 \text{ day}^{-1}$) there is a roughly 10% increase in biomass in the mid-Bay between the 0 and 3 mg L⁻¹ release cases and the 5 mg L⁻¹ release case. As the bloom progresses this pattern of noticeable difference in bloom magnitude between 15 mg L⁻¹ and all other releases, and smaller differences between the lower release cases, persists. Figures 57-58 show the northward progression of the peak in biomass, from mid-Bay up into the Seekonk River discussed above. The nitrogen levels during this period retain the pattern of decreasing from India Point to Conimicut Point, but with the high release exhibiting a trend that is well shifted upward from the other three cases (Figure 58a). On Edgewood Shoals the peak biomass on day 167 is 54 mM m⁻³, compared to a range of 38-41 mM m⁻³ for the releases of 5, 3 and 0 mg L⁻¹ (Figure 57b). It is interesting that Edgewood sits particularly high for phytoplankton relative to stations further north and south. These trends are more apparent on day 170 (Figure 58), where the P concentration on Edgewood hits 80 mM m⁻³, compared to an average 50 mM m⁻³ for the releases of 5, 3 and 0 mg L⁻¹.

Figures 59-60 summarize a similar set of simulations for different WWTF release levels but for the lower uptake rate of $V_m=2 \text{ day}^{-1}$. The same basic patterns and trends hold for this sequence. The high WWTF release level (15 mg L⁻¹) still produces a noticeable enhancement in phytoplankton biomass. The primary differences are that the spread P concentration between 5, 3 and 0 mg L⁻¹ releases gets smaller with the lower uptake rate, and the rate of northward progression of the bloom is shown to be significantly slower, cresting in the mid-Seekonk on day 179 (Figure 60b). The similarity in phytoplankton distributions between cases with $V_m=2.5 \text{ day}^{-1}$ and $V_m=2 \text{ day}^{-1}$, but just with a ~5 day delay, in values seen through the upper Providence River in Figure 58b versus Figure 60a. The pattern of relatively uniform phytoplankton level with latitude in Figure 60b is also consistent with similar trends seen in chlorophyll data (e.g., Figure 29).

4.3: The Influence of Zooplankton Grazing Rate

Figures 61-68 are plots of all four ecosystem variables, N, P, Z and D from key stations which summarize the sensitivity of solutions to the parameter describing zooplankton grazing rate (Z_g). All cases use a WWTF nitrogen release concentration of 355 mM⁻³ (5 mg L⁻¹), a light extinction coefficient (K_L) of 0.75 m⁻¹ and a relatively high value for nutrient uptake rate (V_m) of 2.5 day⁻¹. The distribution of phytoplankton with latitude (Figures 60, 61) shows the importance of grazing rate. The reference case with low grazing rate ($Z_g=0.6 \text{ day}^{-1}$) produce the largest blooms (and reductions in nutrients), along with rapid northward progressions. The time-variability introduced by rapid grazing is apparent in Figure 62, where by day 170 the zooplankton bloom produced with $Z_g=2.5 \text{ day}^{-1}$ has declined below levels produced with $Z_g=2.0 \text{ day}^{-1}$. Time series plots also show the damping effect of zooplankton grazing rate. In Figure 63c rapid grazing ($Z_g=2.5 \text{ day}^{-1}$) stalls the phytoplankton bloom before it can start, leading to rapid growth of the zooplankton population. This is followed by a gradual decline without a zooplankton food supply. Figures 66-68 show that increased grazing rates lead to progressively delayed phytoplankton biomass increases moving from Conimicut Point to the Seekonk

River. Rates of 0.6-1.5 result in very long wavelength blooms, in the order of 10 days (e.g., Figure 66 for Conimicut Point). A grazing rate of 2 produces a bloom at Conimicut Point that last 5-6 days. For the highest grazing rate, $Z_g=2.5 \text{ day}^{-1}$, there is no bloom produced.

4.4: The Influence of Light Extinction Coefficient

The other parameter that was varied in order to gauge its importance in controlling ecosystem processes was the light extinction coefficient, K_L . A number of estimates for K_L have been made for Narragansett Bay (Smayda and Borkman, 2008), with values ranging from roughly 0.5 to 0.8 m^{-1} . We test three K_L values: 0.55, 0.65 and 0.75, using a reference, elevated uptake rate of $V_m=2.5 \text{ day}^{-1}$ and a reduced grazing rate of $Z_g=0.6 \text{ day}^{-1}$. Figures 69-71 summarize phytoplankton (and detritus) variations with latitude, from the head of the Bay through the mid-Bay. On day 161 a bloom initiates in the mid-Bay for $K_L=0.55 \text{ m}^{-1}$, where nutrients are relatively low. A significantly stronger bloom (60 mM m^{-3}) has grown within the Providence River on day 165 (Figure 70) for the higher K_L . The intermediate $K_L=0.65 \text{ m}^{-1}$ produces a lower amplitude bloom ($\sim 40 \text{ mM m}^{-3}$). By day 170, blooms from K_L values of 0.55 and 0.65 have reached the mid Seekonk River (Figure 71). As with the sensitivity test for grazing rate, the range of K_L values does not produce noticeable differences in the ecosystem response within inner Greenwich Bay (Figure 72), the mouth of Greenwich Bay (Figure 73) or the West Passage outside of Greenwich Bay (Figure 74). In the latter case, a short-lived, enhanced bloom occurs for $K_L=0.55$ from day 160 to 162. Within the mid to upper Bay, away from the Greenwich Bay region, the range in K_L values leads to delays in phytoplankton growth rates of roughly 2 days for coefficients ranging between 0.55 to 0.75 m^{-1} (Figures 75-80). Figures 81-85 show time series plots that compare the relative importance of V_m values of 2.5 and 2 and K_L of 0.55-0.75. Lower K_L and higher V_m lead to larger, faster blooms. Higher K_L and lower V_m results in lower amplitude blooms that evolve more slowly than suggested by data from June, 2010 bloom event. For the lower uptake of $V_m=2.0 \text{ day}^{-1}$, a lower K_L , of 0.55, is needed to produce a bloom on the time scale of most Bay bloom events.

An interesting result revealed in this parameter sensitivity study is that very similar bloom characteristics can occur for different parameter combinations. Figure 83 shows such a case, where plots of phytoplankton concentration (and detritus) versus time show a close overlap. The combination of a higher uptake rate with lower light penetration (blue line in Figure 83a) overlaps almost exactly the trend for medium uptake rate, but with higher light penetration (red dashed line). It is remarkable that the balancing of these enhancers/reducers of productivity result in trends that have similar onset times, growth trends (slopes) and higher frequency oscillations.

5.0 Discussion

A summary of Narragansett Bay fixed site buoy data shows that Greenwich Bay suffers from more low DO events than all other stations (Codiga et al., 2009). For example, Greenwich Bay suffered from 5, 9 and 11 events (defined as DO below 2.9 mg L^{-1}), in years 2004, 2005 and 2006, respectively. This is opposed to 0, 1 and 4 events during

those same years at Bullocks Reach. The data suggest that Greenwich Bay experiences chronic bloom events, but only a relatively few of these coincide with bay-wide blooms. In 2010 there were only two bay-wide blooms (Figure 32), and a review of the available data for the June 2010 reveals an interesting spatial-temporal pattern for the bay-wide event during this month. Trends shown in Figures 34 and 87 reveal a time progression in the chlorophyll data from mid-Bay locations (early) to northern Providence River and Seekonk River (later). A strength of the SNB-ROMS NPZD models is the ability to test whether these simplified ecosystem simulations can recreate such a trend, and check what parameters are important in best matching data trends. Figures 85 and 86 show that most simulations recreate a northward age-progressive trend in the onset of blooms during the June 2010 period. Figure 86 compares timing of first onset of blooms in data (circles) versus models with a range of parameters. As discussed above, higher (lower) uptake rates lead to faster (slower) northward progressions. Deeper (shallower) light penetration also produces notably faster (slower) northward progressions. The closest match in Figure 86 to the observed progression for June, 2010 is for the case of $V_m=2.5 \text{ day}^{-1}$ and $K_L=0.55 \text{ m}^{-1}$.

Data and SNB-ROMS NPZD models are consistent with a conceptual model of blooms developing, either partly or entirely in the mid-Bay and subsequently moving northward (Figures 87). A question is how much of this is due to transport of phytoplankton biomass from mid-Bay to northern regions with lower P, but very high N levels. Alternatively, the progression is not due to transport, but simply delays in in-situ growth rates in the north versus mid-Bay locations. As a test, we ran a simulation where we zeroed out all GB nutrients ($N_{GB}=0$) and zeroed out nutrient inputs in the rivers/WWTF within GB (Figure 88). This was done for an output file from May 20, 2010, prior to the onset of any bloom. This modified file was then used as input for simulations beginning May 20 and running through June 28, 2010. If GB is not exerting an influence, then at stations in the north there should be no change in ecosystem fields for these $N_{GB}=0$ cases. Figures 89-91 show time series plots of P and D fields for stations in the West Passage (just north of GB), Conimicut Point and India Point, at the mouth of the Seekonk River. Eliminating production in Greenwich Bay ($N_{GB}=0$ cases) produces a reduction in biomass and detritus concentrations as far north as the Seekonk River for the reference case of low zooplankton grazing rate (red versus green lines). Interestingly, the effect of eliminating GB is more pronounced for the case of high zooplankton grazing (blue versus black lines in Figures 89-91). What is particularly striking is the influence is reversed. Without GB, there is a significantly larger northward detrital flux as far north as Phillipsdale. In all cases considered, the removal of GB from the bloom generation process is felt as far north as Seekonk River, on the time scales of the bloom event (e.g., 10 days). This is most dramatically shown in Figure 92, where turning off the wind (leaving Greenwich Bay turned on) produces a 50% reduction in bloom intensity as far north as Phillipsdale station. However, by far the largest effect seen on bloom intensity is the case where Greenwich Bay has been zeroed out leading up to the bloom. Even though this effect is far to the south, the bloom intensity is increased by a factor of 4 over the reference case (e.g. Greenwich Bay running normally, or not zeroed out). Figures 93 and 94 show how processes in Greenwich Bay and winds tending to transfer biological products northward

conspire to produce significantly larger impacts on overall bloom intensity in the northern rivers.

How is it that GB biomass can influence the northern regions? Figure 93 shows that with GB operating, a strong zooplankton bloom accompanies the phytoplankton bloom that progresses northward from Ohio Ledge into the Providence River. But without GB ecosystem processes, a zooplankton deficit occurs on Ohio Ledge, which allows unchecked growth phytoplankton fields moving northward into the high nutrient zone of the Providence River. By subtracting zooplankton concentration fields of the reference case (Greenwich Bay on, all forcing on) from the case with Greenwich Bay zeroed out, it is clear that without Greenwich Bay processes operating, there is a deficit of zooplankton on Ohio Ledge (Figure 95). This leads to significantly larger phytoplankton blooms within the upper Bay. Two sub-tidal flow and transport processes are identified that carry water and biological fields from the Greenwich Bay region to the mid Bay and up into the Providence/Seekonk Rivers. Figures 96-98 show conservative dye transport from sources entirely within Greenwich Bay that ends up on the eastern side of Ohio Ledge. These events are from the 2010 ROMS simulations (Kincaid, 2012a) and are in response to north/northeastward blowing winds (see Figure 13). The implications of rapid, high volume transport of GB dye mass to Ohio Ledge, particularly eastern Ohio Ledge, is that these are the primary source waters for the efficient subtidal northward flow entering the Providence River shipping channel. A second, lower volume but higher frequency mode of GB to Ohio Ledge transport is due to tidal pumping. Figures 99-100 show the tidal pumping of dye filaments from GB through the constriction just outside, and north of, the GB mouth. Model simulations are from a combination study involving ROMS and a current meter study of Greenwich Bay (Balt, 2014). These use dye patches within GB to characterize flushing rates. Results show that for intermediate to large amplitude tides there is a persistent pumping of GB-derived dye in a residual northward jet that hugs the western shore in this region. Dye makes it onto Ohio Ledge during flood, and is left there during the subsequent ebb. These results suggest that persistent biomass events observed routinely within GB have two pumping mechanisms for infusing phytoplankton into northern regions that are characterized by very high nutrient levels and limited consumers of this food supply. Such a coupled process could explain why GB experiences many blooms each summer while only a very few bay-wide blooms are recorded each summer, despite the constant presence of high nutrient levels throughout the Providence River and Ohio Ledge.

Even though our models do not directly simulate oxygen systematics, the NPZD formulation is powerful in its simplicity, not relying on too large a number of poorly constrained parameters. As the evolution of DO in the Bay depends critically on concentrations and distributions of phytoplankton biomass, these models show which parameter choices influence total phytoplankton biomass, and by extension DO. Comparisons between total, time-integrated phytoplankton for cases with different management strategies, parameter choices, physical factors and far-field impacts (e.g. Greenwich Bay bloom nucleation) show which factors produce the largest increase or decrease relative to a reference. Figure 101 shows such a plot summarizing the effect of different WWTF release levels for a bloom centered on the Edgewood Shoals region.

The only significant reduction in bloom intensity occurs between WWTF release levels of 15 mg L^{-1} and 5 mg L^{-1} , and only when the highest phytoplankton uptake rate is used ($V_m=2.5$). Additional WWTF release reductions from 5 to 3 and from 3 to 0 mg L^{-1} produce negligible reductions in integrated biomass. The differences between WWTF release levels are significantly smaller for cases with a lower phytoplankton uptake rate. Moreover, the maximum reductions in biomass intensity due to WWTF changes in these models are of the same order, or smaller, than changes predicted from other forcing factors (winds, Figure 102) and processes occurring in the nucleation zone of Greenwich Bay (Figure 103). Figure 104 summarizes the magnitudes of biomass differences between specific cases covering the range of model parameter choices, forcing functions and management strategies explored in these cases.

6.0 Conclusions

A new version of ROMS has been successfully developed that includes the dynamics and transport processes operating in the Seekonk River. This SNB-ROMS model has been run for 2010 conditions and compares favorably to prior ROMS simulations which have been statistically validated against current meter data on Edgewood Shoals. The SNB-ROMS shows interesting new aspects of chemical transport, which could not be simulated in prior versions. Simulations including the Seekonk River show the geographic constriction at India Point acts as a check valve for water/dye exchange. Dye leaving the Seekonk from the north and entering the Seekonk from the south is stalled at this location, leading to relatively sharp changes in dye concentration across this interface. Specific environmental conditions lead to pulses of exchange. This is less pronounced in surface outflow of dye from northern sources and more pronounced in deep northward flow of dye from southern sources. There is limited time series current meter data available for the Seekonk River. Observational work should be done to collect details of flow structures/patterns in the Seekonk that can be used to check/calibrate the modeled flow fields in this new part of the model.

In agreement with prior ROMS dye studies, the dominant source for down-bay dye transport is from non-point sources, relative to point source inputs to our models provided by from the Blackstone Watershed Model (UMass). Also consistent with prior models, the down-bay transport of northern sources varies considerably with prevailing winds. Northeastward winds confine the northern chemical plumes to the East Passage. All other winds (particularly southward winds) favor outflow of northern dye plumes into the West Passage.

We have produced a successful initial development and application of the NPZD Franks model within the SNB-ROMS model. These models have been run for April-June, 2010 time period, with a specific focus on the bay-wide June, 2010 phytoplankton bloom event. Model results show a number of interesting results. A major goal of this work is to test the efficacy of various nutrient point source management strategies by simulating a range of WWTF permit release levels and comparing relative improvements in nutrient and phytoplankton levels throughout the estuary. Results show that increases and decreases in spatially averaged phytoplankton concentrations driven by WWTF reductions are smaller than changes due to other model parameters: varying wind

conditions, parameter choices for phytoplankton/zooplankton growth rates and light extinction and conditions in Greenwich Bay. Model results indicate phytoplankton levels are only improved in cases with maximum, perhaps extreme, growth rates in cases when WWTF levels are reduced from 15 mg L^{-1} to 5 mg L^{-1} . Phytoplankton decreases resulting from the lowering of WWTF release nitrogen concentrations from 5 to 3 mg L^{-1} and from 3 mg L^{-1} to 0 mg L^{-1} are relatively small. It is worth noting that these managed reductions produce generally smaller changes in simulated bloom magnitudes than the natural effects that were considered in these models, such as altering prevailing wind conditions. For intermediate and lower growth rate parameter choices, all WWTF reduction scenarios (e.g., 15 to 5 mg L^{-1} , 5 to 3 mg L^{-1} and 3 to 0 mg L^{-1}) are shown to produce changes in spatially averaged phytoplankton biomass that are small relative to other tested factors of wind patterns, zooplankton growth rate and light extinction coefficient. A strength of models is the ability to isolate on the impact of specific factors in producing blooms. For cases with similar sets of parameters and forcing conditions, the simple model manipulation of eliminating Greenwich Bay from the equation had the single biggest influence on the strength of blooms for summer 2010 conditions. Perhaps more remarkable, the role of Greenwich Bay in these simulated blooms extends all the way north to the Seekonk and the entry point of the Blackstone River at Slater Dam.

An interesting process result is that modeled blooms tend to initiate in specific, repeatable hotspot locations: 1. northern shore of Mt. Hope Bay, 2. Eastern and western shores of Ohio Ledge, 3. Greenwich Bay, 4. Eastern and western shallow regions inside mouth of Providence River, 5. Edgewood Shoals. A sensitivity test shows that nitrogen uptake rate and light extinction coefficient are very important in controlling the magnitude of blooms, and the northern progression of blooms from mid-Bay to northern Bay regions. Zooplankton grazing rate is important for limiting the amplitude of blooms, and for matching the decay profile for these events. The best match to the observed June 2010 bloom progression from Greenwich Bay, to Ohio Ledge, Providence and Seekonk Rivers is for our highest uptake rate ($V_m=2.5 \text{ day}^{-1}$), deepest light penetration ($K_L=0.55 \text{ m}^{-1}$), and a small to medium zooplankton grazing rate ($Z_g=0.6-1.5 \text{ day}^{-1}$). A targeted model simulation eliminating GB from the bloom shows the connection from mid-Bay to northern Bay is present.

While these models are not perfect by any means, they do point to some basic insights for coupled physical-biochemical processes operating in the Bay. Up-bay residual flows that are well documented with spatial-temporal current meter data provide a conduit allowing essential components like phytoplankton, zooplankton and detritus to move northward over significant distances. Results suggest an alternate view of the north to south gradient of ecosystem factors must be balanced with a south to north view. Residual current transport conduits are capable of connecting productive zones in the shallow mid-Bay regions, where nutrient levels are somewhat lower (e.g., Greenwich Bay, Ohio Ledge, Mt. Hope Bay and Lower Providence River) to the most impacted water quality regions in the north (e.g., the Seekonk River). Models are particularly powerful at identifying frequent, but smaller and larger but less frequent up-bay transport mechanisms. Northeastward wind events and tidal pumping in spring tides are just two examples of these. Future work should involve combined ecosystem modeling with time

series observations of up-Bay fluxes of key parameters surrounding bloom events. Models could also systematically eliminate Ohio Ledge and Mt. Hope regions, in similar fashion to what was done with Greenwich Bay, to gauge the relative importance of these sites for providing up-Bay transport of biochemical products capable of influencing blooms in the north.

References:

- Balt, C, 2014. Subestuarine circulation and dispersion in Narragansett Bay, PhD dissertation, University of Rhode Island, 184 pages.
- Bergondo, D., 2004. Examining the processes controlling water column variability in Narragansett Bay: Time series data and numerical modeling," Ph.D. dissertation, University of Rhode Island.
- Bergondo, D., and C. Kincaid, 2007. Development and calibration of a model for tracking dispersion of waters from Narragansett Bay Commission facilities within the Providence River, Narragansett Bay Commission Final Report, 46 pages.
- Brush, M.J. 2002. Development of a numerical model for shallow marine ecosystems with application to Greenwich Bay, RI. Ph.D. dissertation, University of Rhode Island, Graduate School of Oceanography
- Codiga, D., H. Stoffel, C. Deacutis, S. Kiernan, C. Oviatt. 2009. Narragansett Bay hypoxic event characteristics: Inter-annual variability, geographic distribution, intermittency, and spatial synchronicity. *Estuaries and Coasts*. 32(4):621-641.
- Deacutis, C., D. Murray, W. Prell, E. Saarman, and L. Korhun. 2006. Natural and anthropogenic influences on the Mount Hope Bay ecosystem, *Northeastern Naturalist* 13(Special Issue 4):173–198.
- Deacutis, C., 2008. Evidence of ecological impacts from excess nutrients in upper Narragansett Bay," in *Science for Ecosystem-Based Management: Narragansett Bay in the 21st Century*, Desbonnet, A. and Costa-Pierce, B., Eds. Springer, pp. 349-381.
- Del Barrio, P., N. Ganju, A. Aretxabaleta, M. Hayn, A. Garcia and R. Howarth, Modeling future scenarios of light attenuation and potential seagrass success in eutrophic estuary, *Est. Coastal Shelf Sci*, 149, 13-23, 2014.
- Edwards, A., Adding detritus to a nutrient-phytoplankton-zooplankton model: a dynamical systems approach, *J. Plankton Res.*, Vol. 23, No4, 389-413, 2001
- Franks, P.J.S., Wroblewski, J.S., Flierl, G.R., 1986. Behavior of a simple plankton model with food-level acclimation by herbivores. *Marine Biology* 91, 121–129
- Franks, P.J.S., 2002. NPZ models of plankton dynamics: their construction, coupling to physics, and application. *Journal of Oceanography* 58 (379–387).
- Greenwich Bay Special Area Management Plan, Coastal Resources Management Council by the Coastal Resources Center/Sea Grant, University of Rhode Island, 498 pages, May, 2005
- Janeković, I., Powell, B., 2012. Analysis of Imposing Tidal Dynamics to Nested Numerical Models. *Continental Shelf Research*, 34, 30-40.
- Kincaid, C., The exchange of water through multiple entrances to the Mt. Hope Bay Estuary, *Northeast Naturalist*, 13(Special Issue 4): 117-144, 2006.
- Kincaid, C., R. Pockalny, and L. Huzzey, 2003. Spatial and temporal variability in flow at the mouth of Narragansett Bay, *Journal Geophysical Research*, doi:10/1029/2002JC001395.
- Kincaid C., and D. Bergondo, 2005, Development and Calibration of a Model for Tracking Dispersion of Waters from Narragansett Bay Commission Facilities within the Providence River & Narragansett Bay, Report submitted to the Narragansett Bay Commission, Prov., R.I., 27 pp.
- Kincaid, C., D. Bergondo, and K. Rosenburger, 2008. Water exchange between

- Narragansett Bay and Rhode Island Sound, in Science for Ecosystem-based Management, edited by A. Desbonnet and B. A. Costa-Pierce, chap. 10, Springer, 2008.
- Kincaid, C., 2001a. Results of Hydrographic Surveys on the Providence and Seekonk Rivers: Summer Period, Report submitted to the Narragansett Bay Commission, Prov., R.I., 45 pp.
- Kincaid, C., 2001b. Results of Hydrographic Surveys on the Providence and Seekonk Rivers: Fall Period, Report submitted to the Narragansett Bay Commission, Prov., R.I., 35 pp.
- Kincaid, C., 2001c. Results of Hydrographic Surveys on the Providence and Seekonk Rivers: Winter Period, Report submitted to the Narragansett Bay Commission, Prov., R.I., 27 pp.
- Kremer, J.N., J. Vaudrey, D. Ullman, D. Bergondo, N. LaSota, C. Kincaid, D. Codiga, and M.J. Brush, 2010. Simulating property exchange in estuarine ecosystem models at ecologically appropriate scales. *Ecological Modelling* 221:1080-1088.
- Kincaid, C., 2012a. Development of the Full Bay ROMS Hydrodynamic-Dye Transport Model for the Providence River: Comparisons with data from Spring 2010 tilt current meter network. Final Report Prepared for the Narragansett Bay Commission (Project 08A-114-01-00).
- Kincaid, C., 2012b. Results of tilt current meter time series measurements in the Bristol Harbor estuarine system during August, 2011, Report submitted to Save Bristol Harbor, Bristol (RI), 46 pages.
- Mendahlson, D., 2007. Review of the University of Rhode Island ROMS Hydrodynamic Model application to Narragansett Bay. Report prepared for the Narragansett Bay Commission by Applied Technology Management Inc., 5 pp.
- Mukai, A., Westerink, J., Luettich, R., and Mark, D., 2002. East coast 2001, a tidal constituent database for western North Atlantic, Gulf of Mexico, and Caribbean Sea, Report ERDC/CHL TR-02-24, Coastal Inlets Research Program, U.S. Army Corps of Engineers., Tech. Rep.
- Oviatt, C.A. 2008. Impacts of nutrients on Narragansett Bay productivity: A gradient approach. In: Desbonnet, A. and B.A. Costa-Pierce (eds.) Science for Ecosystem-based Management. Springer, N.Y. p. 519-539.
- Patterson, M, 2007. Evaluation of nutrients along the Blackstone River, Master of Science Thesis, Univ. of Massachusetts at Amherst, 2007.
- Pfeiffer-Herbert, A. S., 2012. Larval transport in an estuarine-shelf system: Interaction of circulation patterns and larval behavior, Ph.D. Thesis, Graduate School of Rhode Island, University of Rhode Island, 227pp.
- Pfeiffer-Herbert, A. S., C. Kincaid, D. Bergondo and R. Pockalny. Dynamics of wind-driven estuarine-shelf exchange in the Narragansett Bay estuary, *Continental Shelf Research*, vol 105, pp42-59, 2015.
- Rogers, J., 2008. Circulation and transport in upper Narragansett Bay, University of Rhode Island, Master Thesis, Kingston, RI, 107 pages
- Rosenberger, K., 2001. Circulation patterns in Rhode Island Sound: Constraints from a bottom mounted acoustic Doppler current profiler, M.S. Thesis in Oceanography, University of Rhode Island, Narragansett, RI, 226pp.
- Saarman, E., Prell, W., Murray, D., and Deacutis, C., 2008. Summer bottom water

- dissolved oxygen in upper Narragansett Bay, in Science for Ecosystem-Based Management: Narragansett Bay in the 21st Century, Desbonnet, A. and Costa-Pierce, B., Eds. Springer, pp. 325-348.
- Shchepetkin, A.F. and J.C. McWilliams, 2003: A Method for Computing Horizontal Pressure-Gradient Force in an Oceanic Model with a Non-Aligned Vertical Coordinate, *Journal of Geophysical Research*, 108,1-34.
- Shchepetkin, A. and McWilliams, J., 2005. The regional oceanic modeling system (ROMS): a split-explicit, free-surface, topography-following-coordinate oceanic model, *Ocean Modelling*, vol. 9, pp. 347-404.
- Smayda, T.J. & Borkman, D.G. 2008. Nutrient and Plankton Dynamics in Narragansett Bay. In: Desbonnet, A., B.A. Costa-Pierce [Ed.] Science for Ecosystem-based Management. Springer, New York, pp. 431-484.
- Warner, J., Geyer, W., and Lerczak, 2005. Numerical modeling of an estuary: a comprehensive skill assessment, *Journal of Geophysical Research*, vol. 110, p. C05001.
- Willmott, C. J., 1981. On the validation of models, *Phys. Geogr.*, 2, 184 – 194.

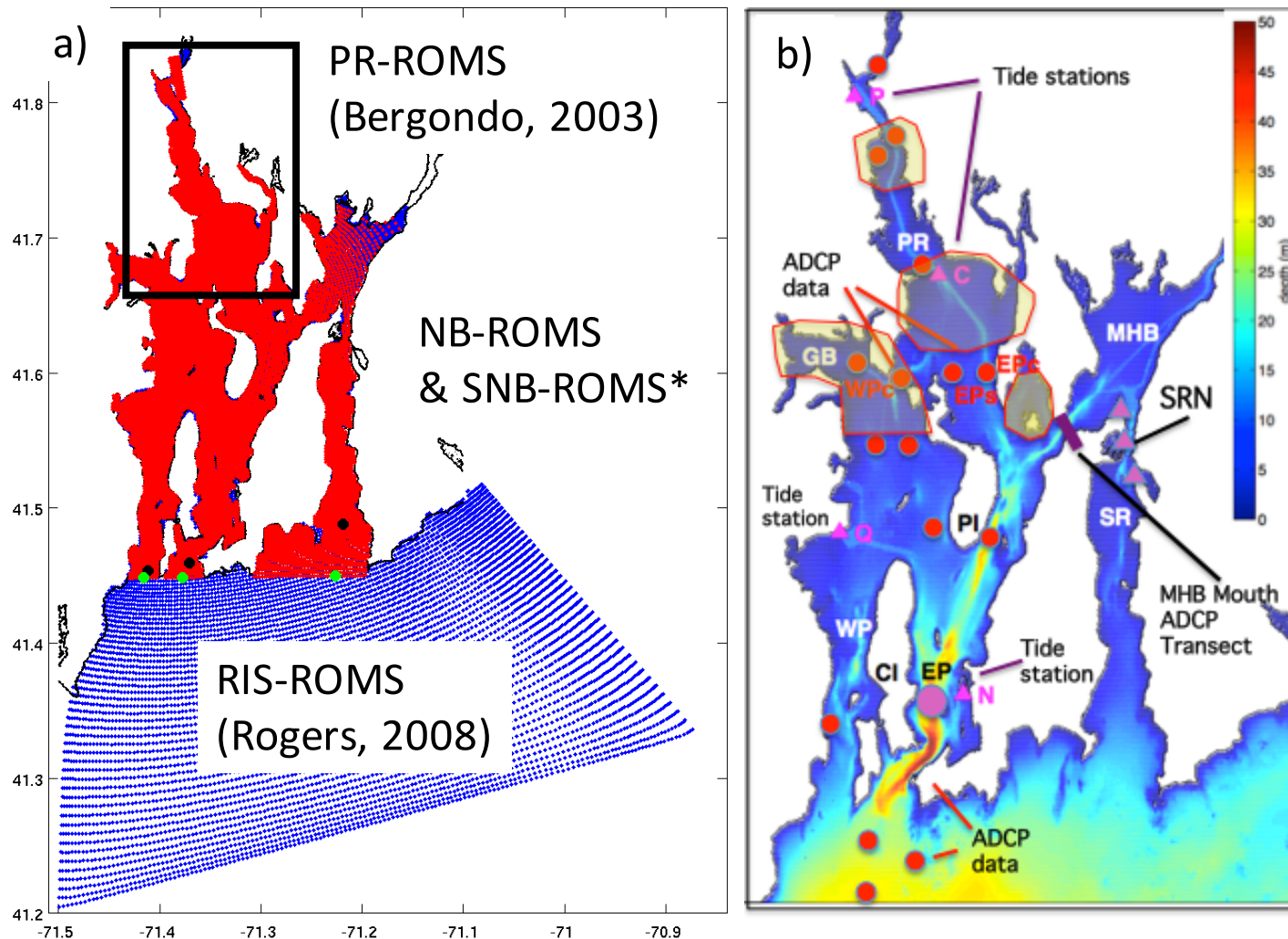


Figure 1. a) The Regional Ocean Modeling System (ROMS) hydrodynamic-transport model has been developed for Narragansett Bay and Rhode Island Sound (RIS) (Bergondo, 2003, Rogers, 2008). Bergondo (2003) used a coarse grid for upper Bay processes (black box). Rogers (2008) developed a ROMS grid extending from RIS up through the Seekonk River (blue grid), or the RIS-ROMS model. Both model grids have coarsely spaced grid boxes in the Providence River (>150 m horizontal spacing). A Full-Bay ROMS model (red region), has been developed with finer grid box spacing in the Providence River (<50 m). A new SNB-ROMS is used here that includes the Seekonk River. b) Map summarizing data for the Bay and key geographic features (EP=East Passage, WP=West Passage, GB=Greenwich Bay, PR=Prov. River, MHB=Mt. Hope Bay, SRN=Sakonnet River, SR=Sakonnet River, PI=Prudence Is.). Also shown are locations for existing hydrodynamic data for NB. ADCP=Acoustic Doppler Current Profiler. Shaded regions are Tilt Current Meter (TCM) deployments. Fixed buoy sites shown are N:Newport, Q:Quonset, C:Conimicut, P: Prov.

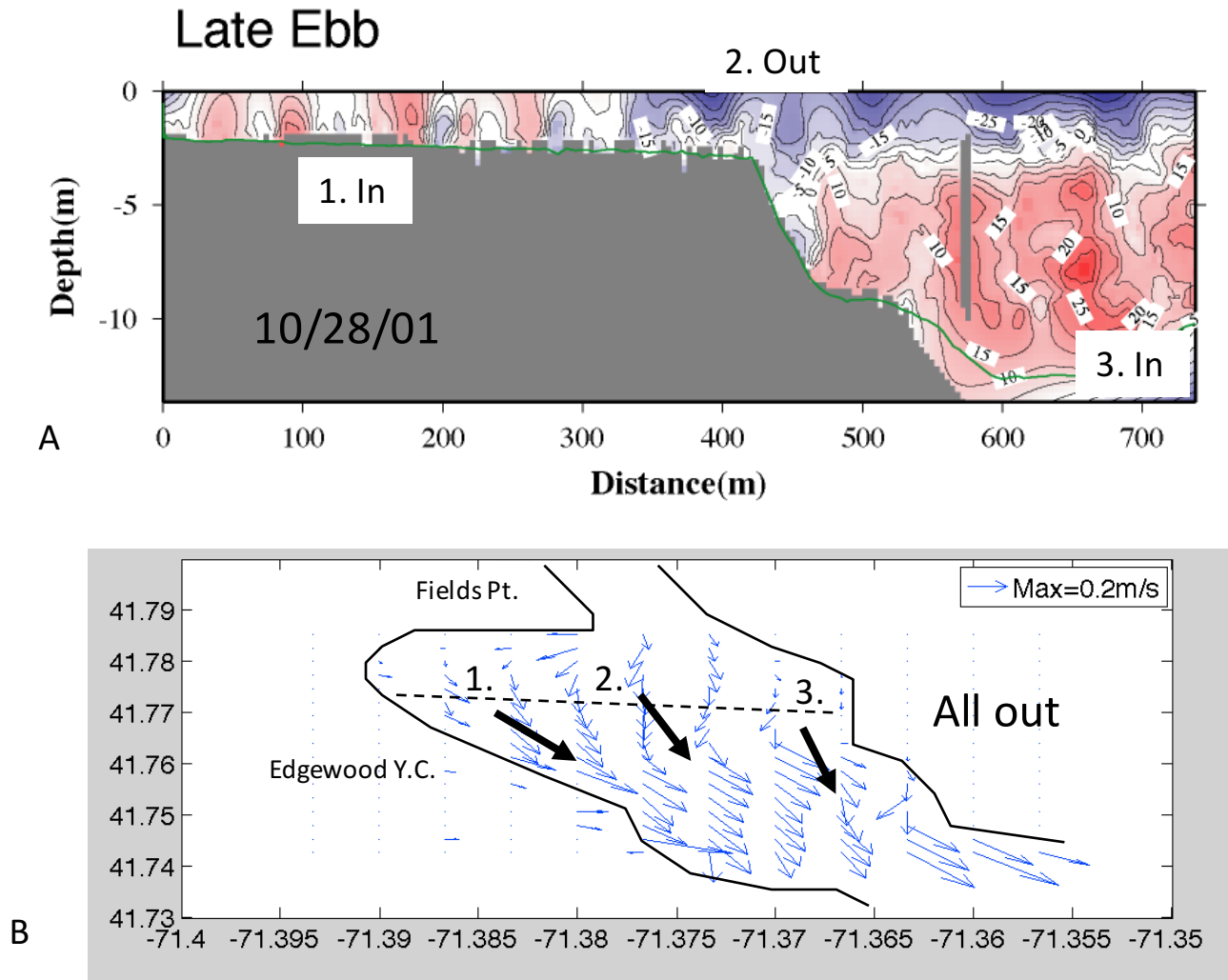


Figure 2. A. Underway ADCP data from the Edgewood Shoals region of the Providence River collected for NBC during 2001. Data highlight three characteristic, repeatable flow regimes within this section of Edgewood Shoals. Underway and moored ADCP data consistently show a pattern of surface outflow (2) and deep inflow (3) within the shipping channel, and a broad northward recirculation zone (1) on the western shoals (or shallows). B. Neither of the coarser grid models (PR-ROMS; NB-RIS ROMS) capture the level of flow heterogeneity seen in the ADCP data (A). Coarse models predict a sweeping outflow across the shoals. Such a discrepancy between models and data needed to be resolved to improve chemical transport studies (e.g., Figures 4-6),

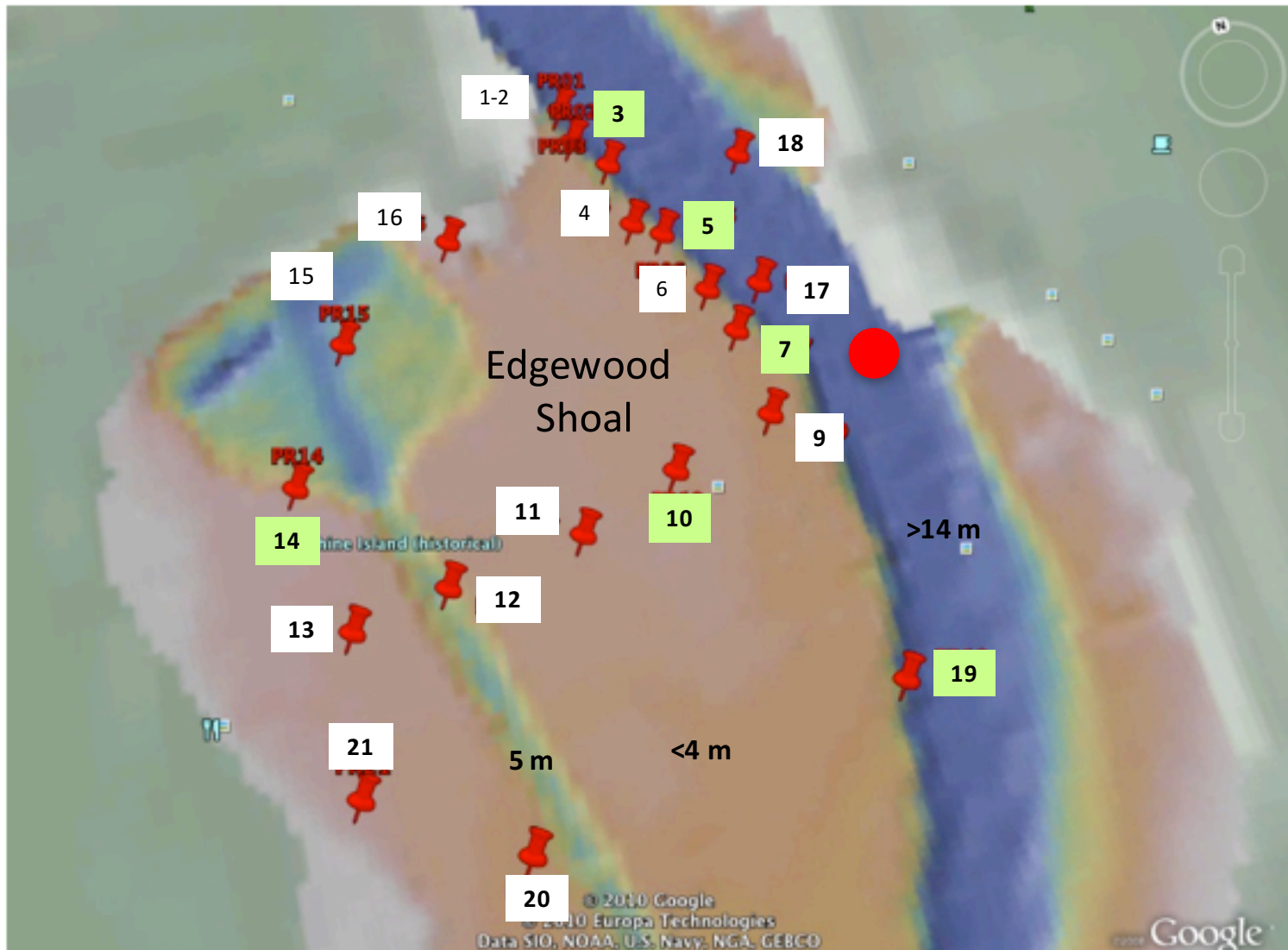


Figure 3. Map showing locations of the tilt current meters (TCMs) deployed in the Providence River during March 8 -May 1, 2010. Blue color shows the deep channel. TCMs at stations 1-9 lie along the eastern edge of the Shoal, at the boundary with the shipping channel. Stations 9-13 are distributed along a transect running from east to west across the shoal. Stations 14, 21 and 20 lie along the western shoal. NBC TCMs (green shaded) were used to fill in the array in key locations along the channel edge and on the Edgewood Shoals. The red circle is a station location for time series plot of eco-parameter fluxes, Figure 55.

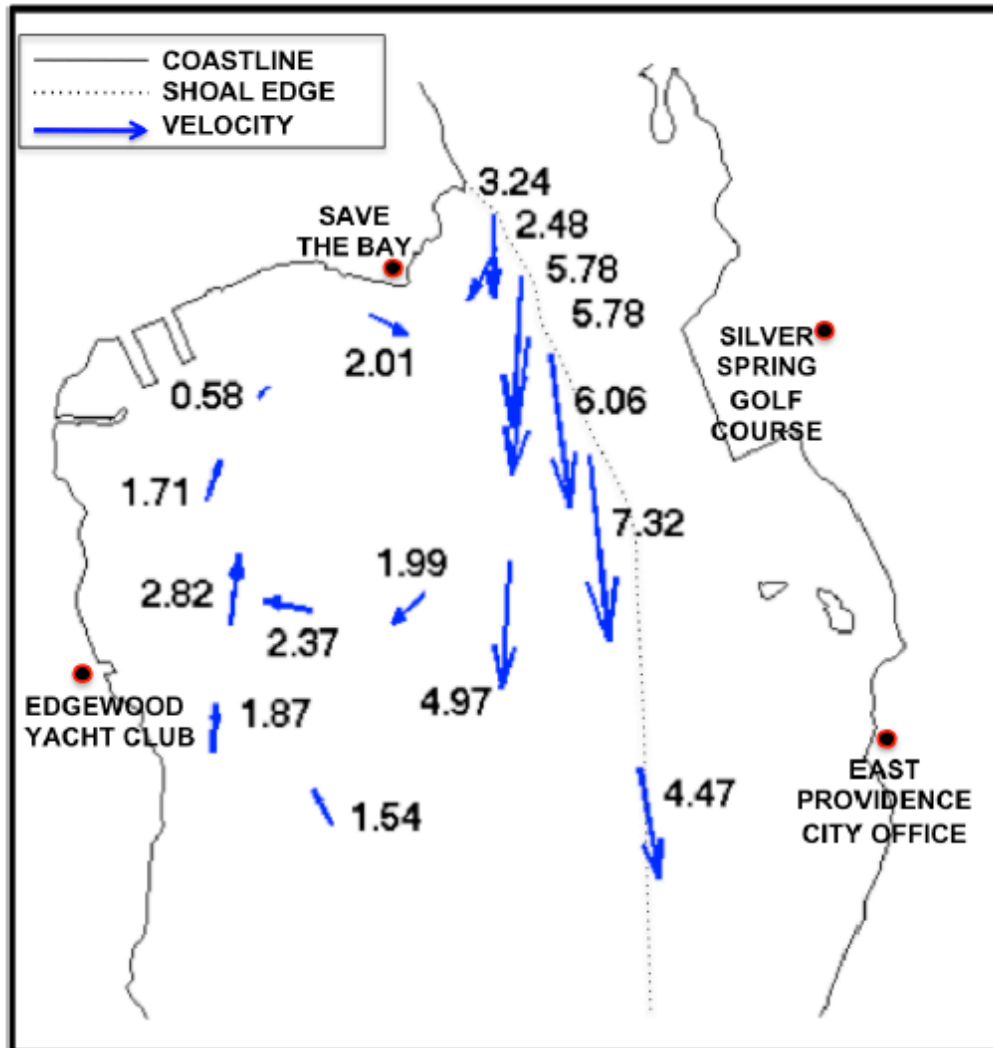
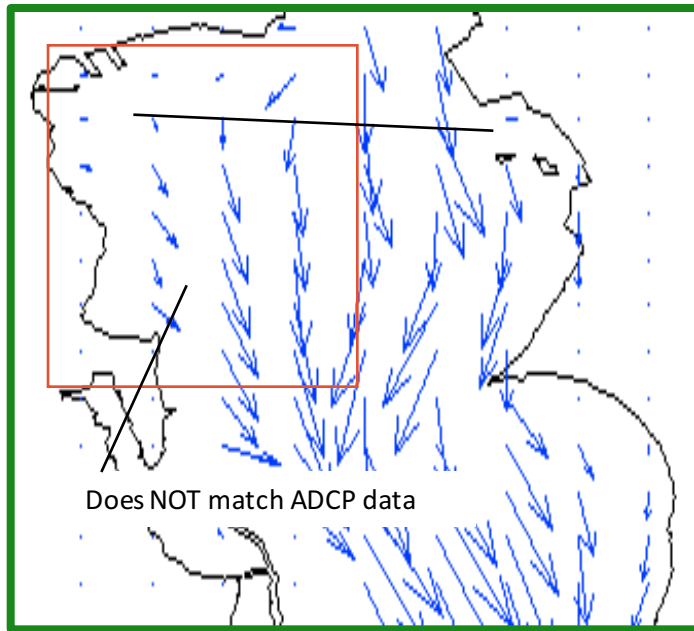
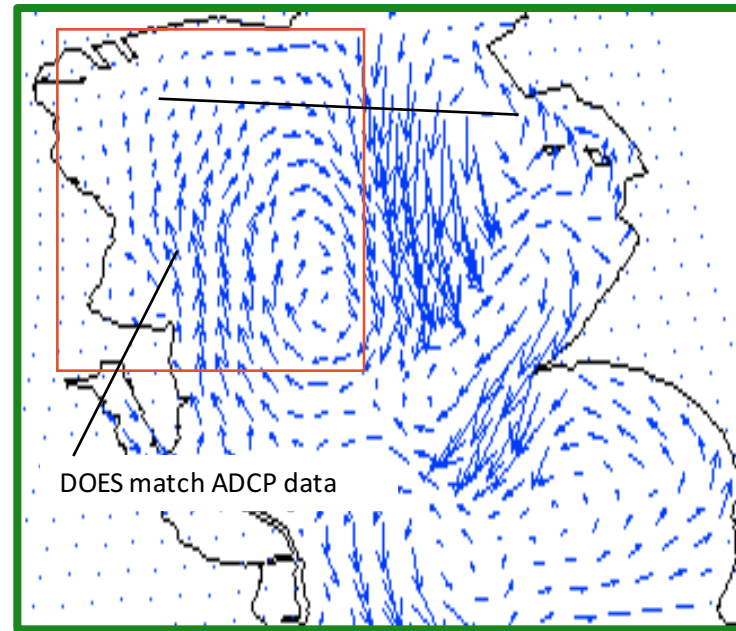


Figure 4. Map showing plots of velocity vectors at each TCM station. The arrows represent flow vectors for data that is averaged over the entire TCM deployment (locations of the tilt current meters (TCMs) deployed in the Providence River during Spring, 2010. Arrows show average directions. Flow speeds (cm/s) are listed by each arrow.



A ROMS: 150 m grid spacing



B ROMS: 35 m grid spacing

Figure 5. Mapview plots showing vertically averaged flow vectors for the Edgewood Shoals region (red box) of the Providence River highlight the importance of grid spacing on computational accuracy. The blue arrows indicate the direction and speed (length of arrow) for data at each grid node location within the ROMS model domain for similar 2006 forcing conditions, at similar ebb stages of the tide cycle. The plots are shown to compare how different the flow fields are for ROMS runs with coarse grid spacing (A) and fine grid spacing (B). In A, there is no flow field on the western shoals that matches data (e.g., Figure 2a,4). But in the fine grid model run (B), a very stable clockwise flow gyre produces a flow field that matches very closely with trends seen in ADCP data (Figure 4). The dark line shows location of ADCP data transect shown in Figure 2a.

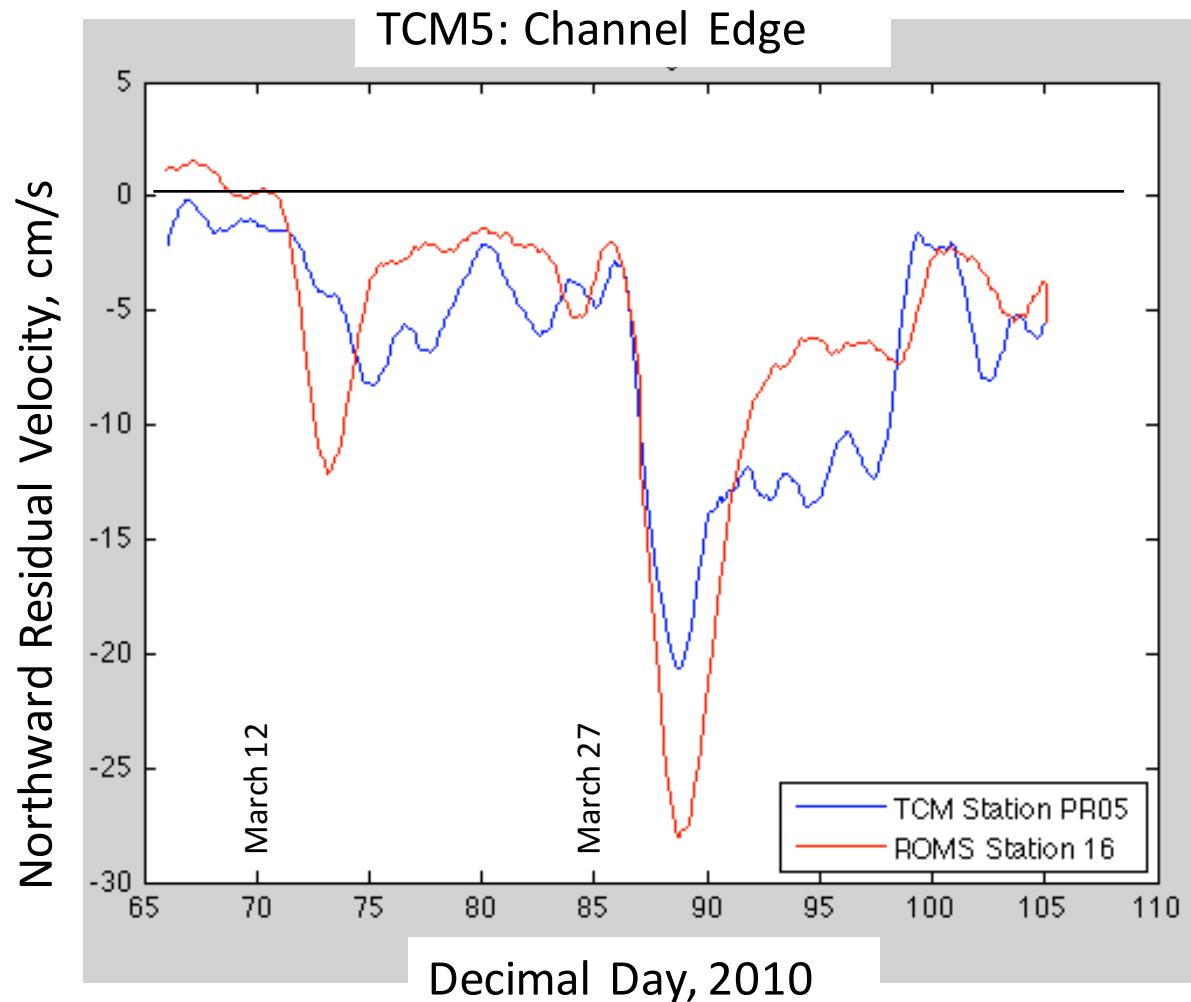


Figure 6. Plot that overlays the TCM record and ROMS simulation output for 2010 conditions at TCM station 5, at the northeastern boundary of the shoals and the shipping channel (Figure 3). The model output (red) does very well matching the residual, or non-tidal nature of TCM observations during the period before the large 2010 flood event (before day 85) and well after the great flood (>day 99). The ROMS prediction on flow is slightly larger than observed during the peak of the flood event, but smaller than observed values during recovery from the event (days 93-98).

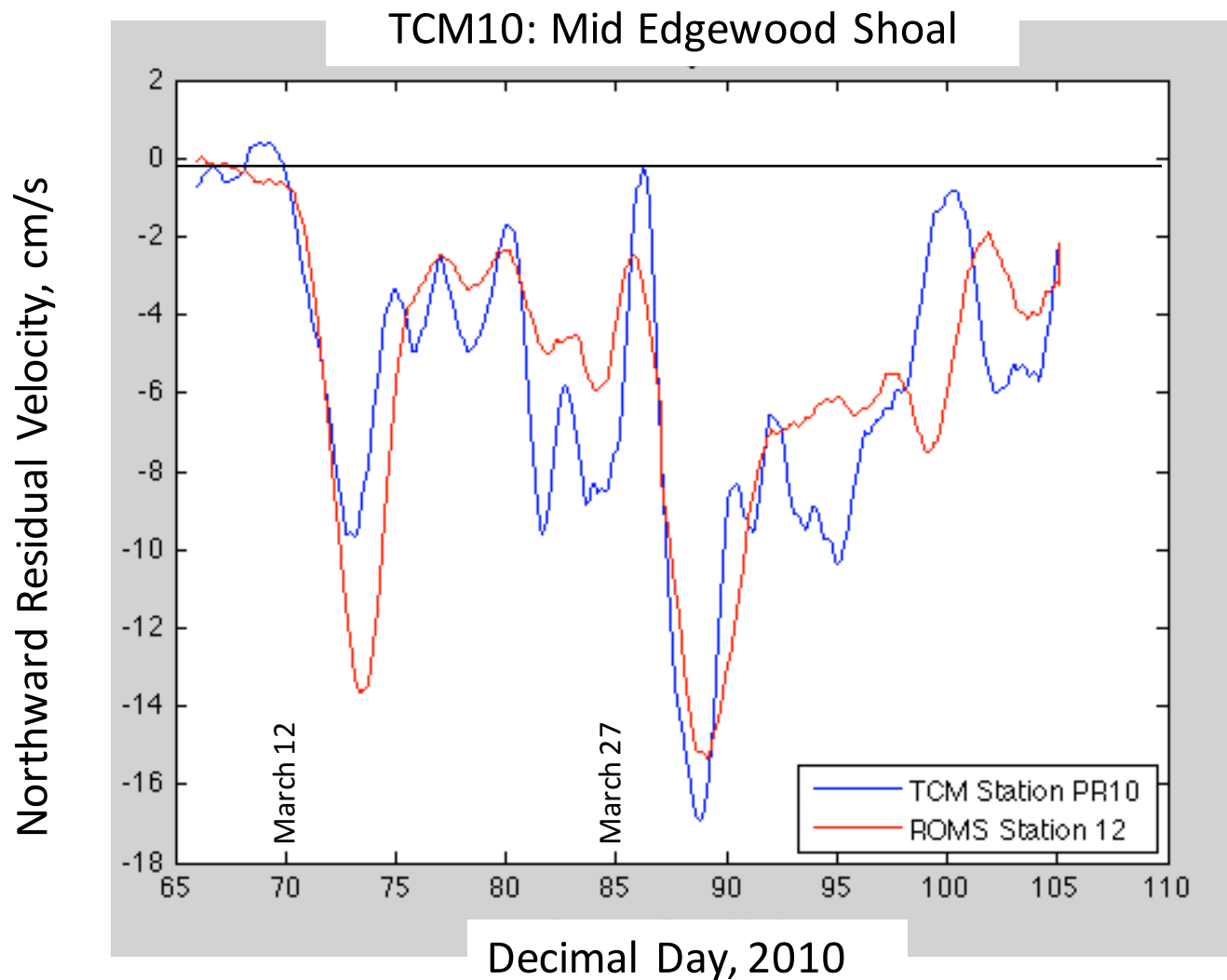


Figure 7. Many hydrodynamic models can readily recreate the instantaneous, or tidal, data records for estuaries. The residual, or non-tidal records are often very challenging to recreate. The Narragansett Bay ROMS does an excellent job of simulating non-tidal flow patterns. This is particularly apparent in the data-model comparison for TCM 10, where ROMS captures both the flood event and the decay of the flood in amplitude and timing. TCM 10 is west of the shoal-channel boundary, midway across the shoal.

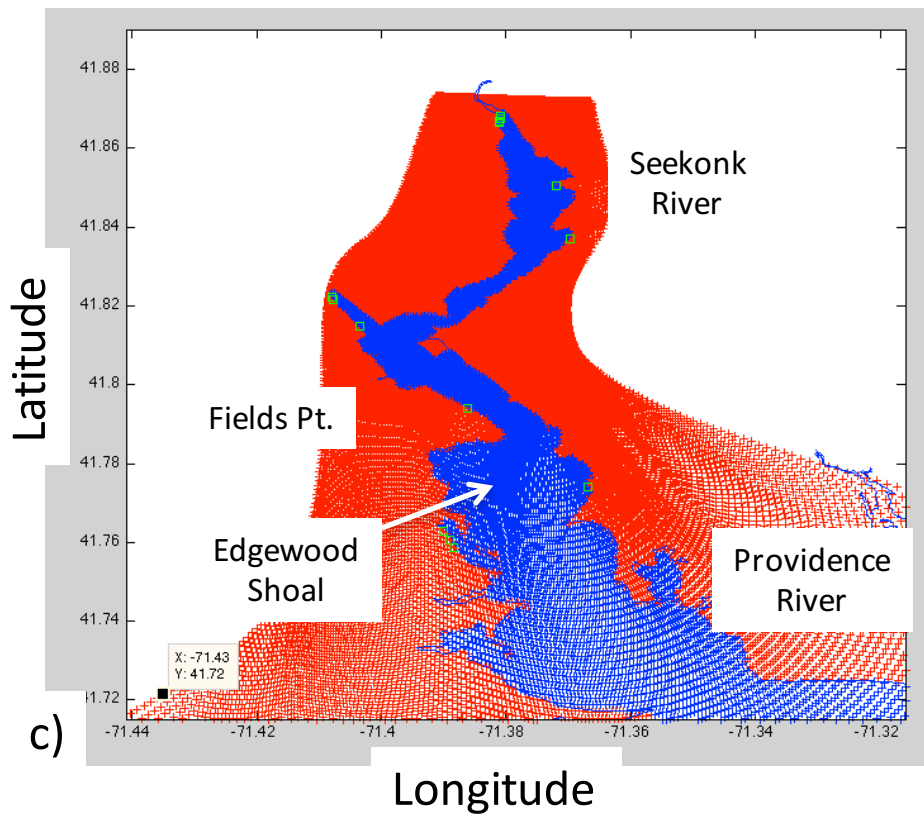
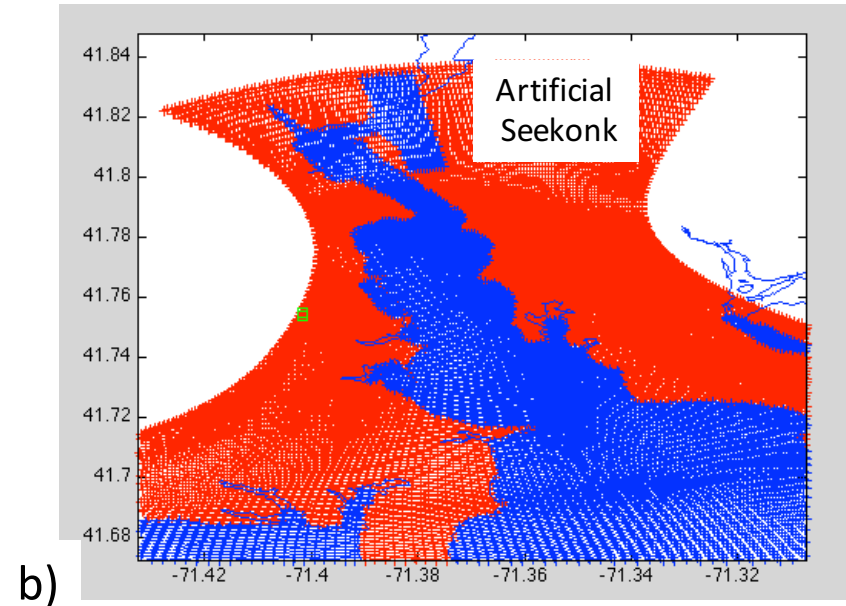
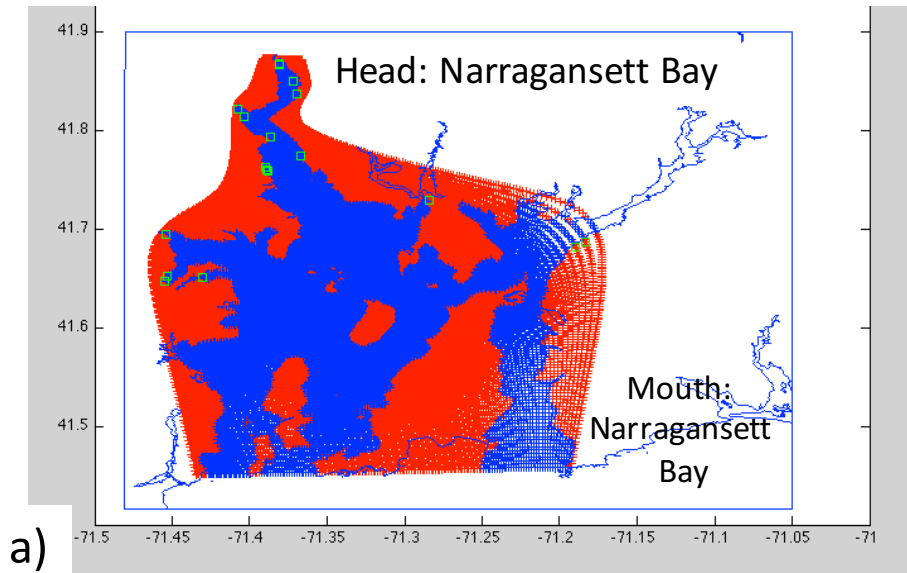


Figure 8. Mapview plots of grid nodes (blue) and land nodes (red). a) Both versions of the Narragansett Bay Commission (NBC) ROMS Full-bay models, without and now with the Seekonk River, employ a grid building strategy whereby nodes are compressed in east-west direction moving northward, from the mouth to the head. b) To avoid numerical instabilities, the original NBC Full-bay ROMS employed an artificial shaped water reservoir that represented the volume of the Seekonk, but not the shape. c) The new version of the NBC Full-bay ROMS includes the actual shape and volume of the Seekonk River

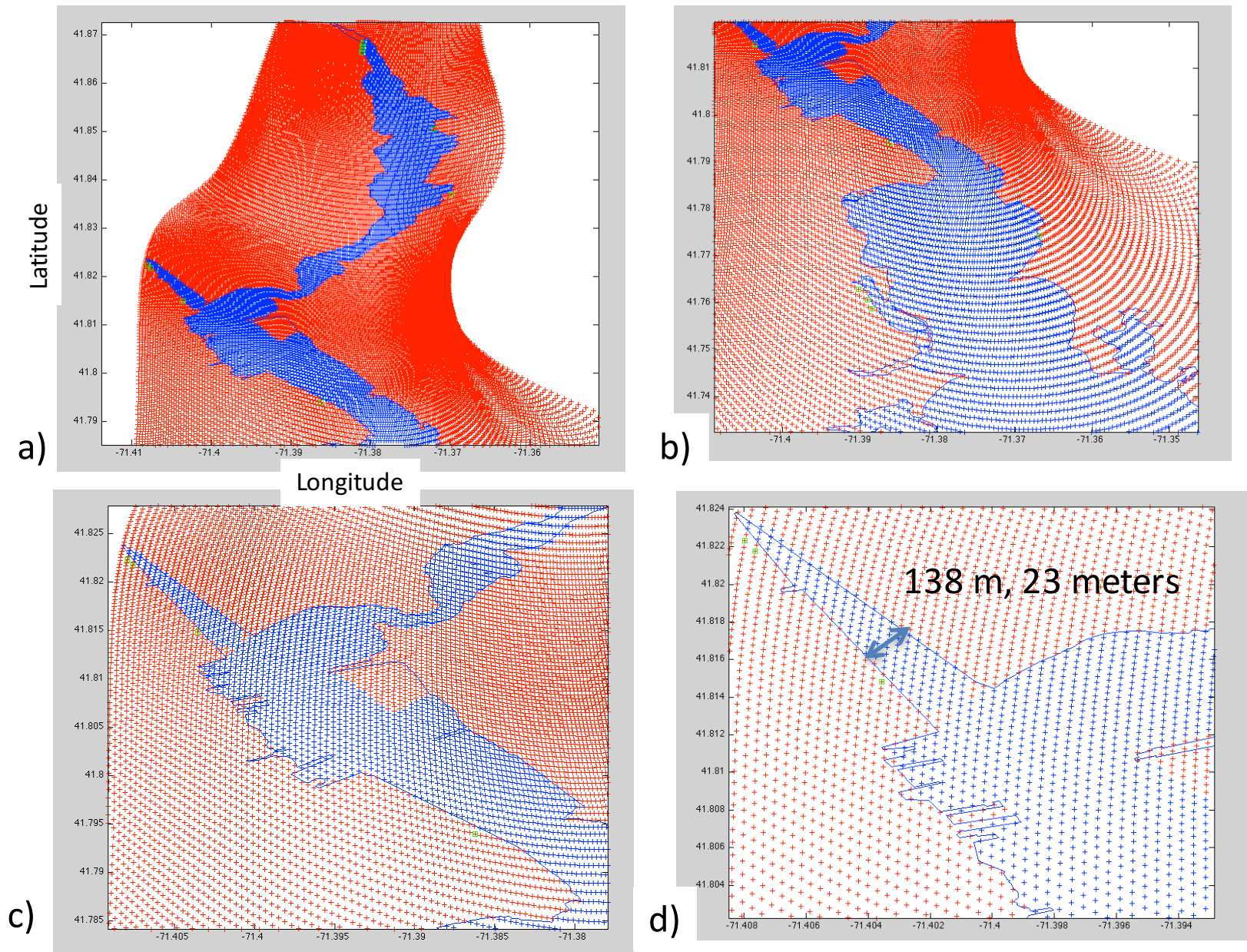


Figure 9. Mapview plots of grid nodes (blue) and land nodes (red) showing grid node spacing in strategic areas a) The Seekonk River, b) mid-reach of the Providence River, c) Fields Pt to the Hurricane Barrier and d) a close-up of the Hurricane Barrier and India Pt. Grid spacing is roughly 25-35 meters throughout these sensitive regions.

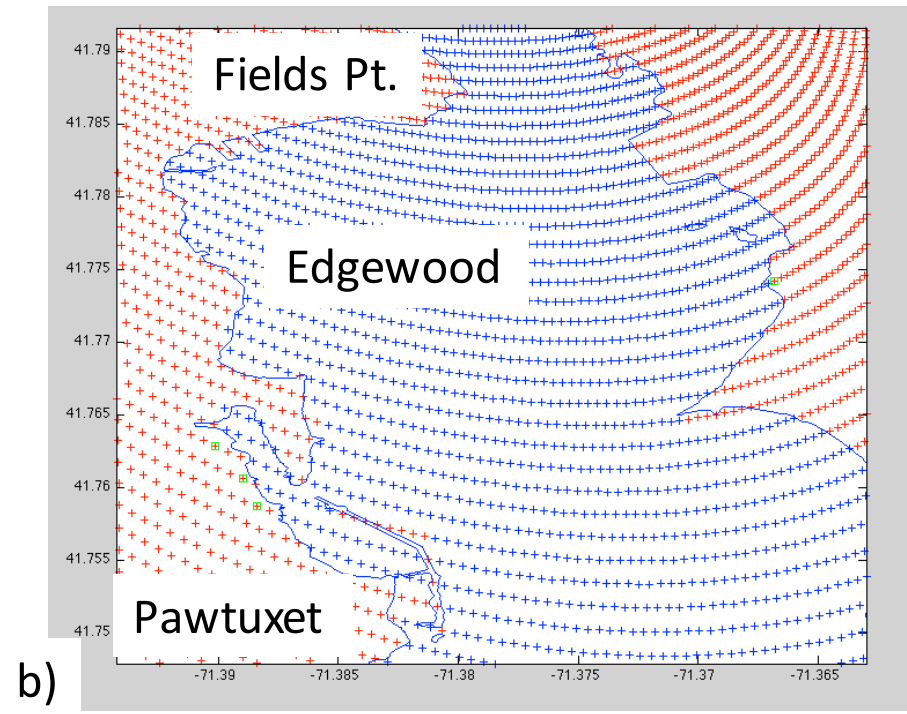
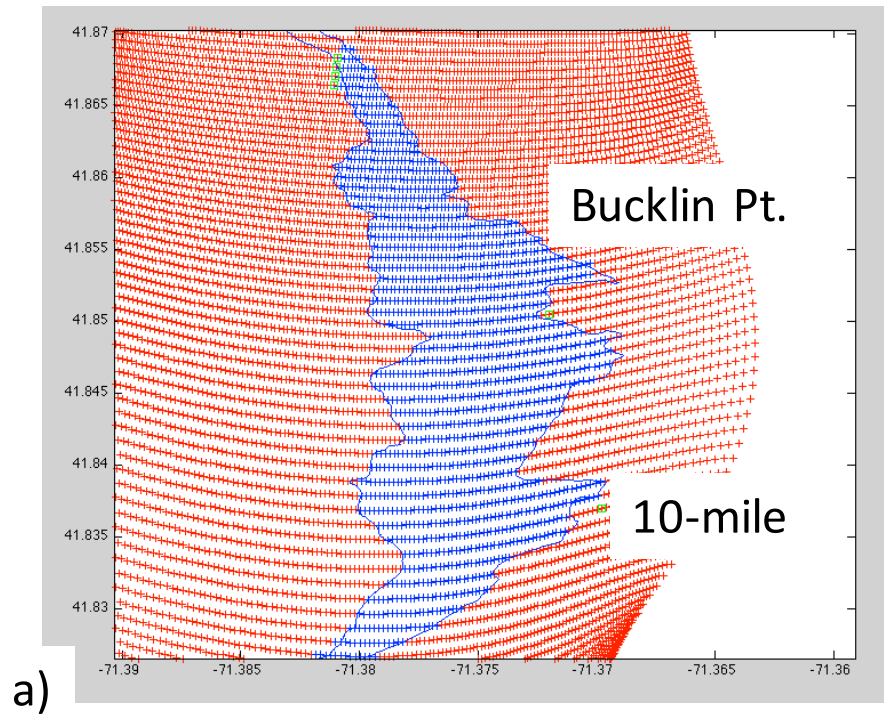


Figure 10. Mapview plots of grid nodes (blue) and land nodes (red) showing grid node spacing in strategic areas a) The Seekonk River, highlighting two important fresh water sources (Bucklin Pt. WWTF, 10 Mile River) and b) the Edgewood Shoals region of the Providence River. In both regions there are sufficient computational nodes in the horizontal directions to resolve eddy, or gyre style of circulation.

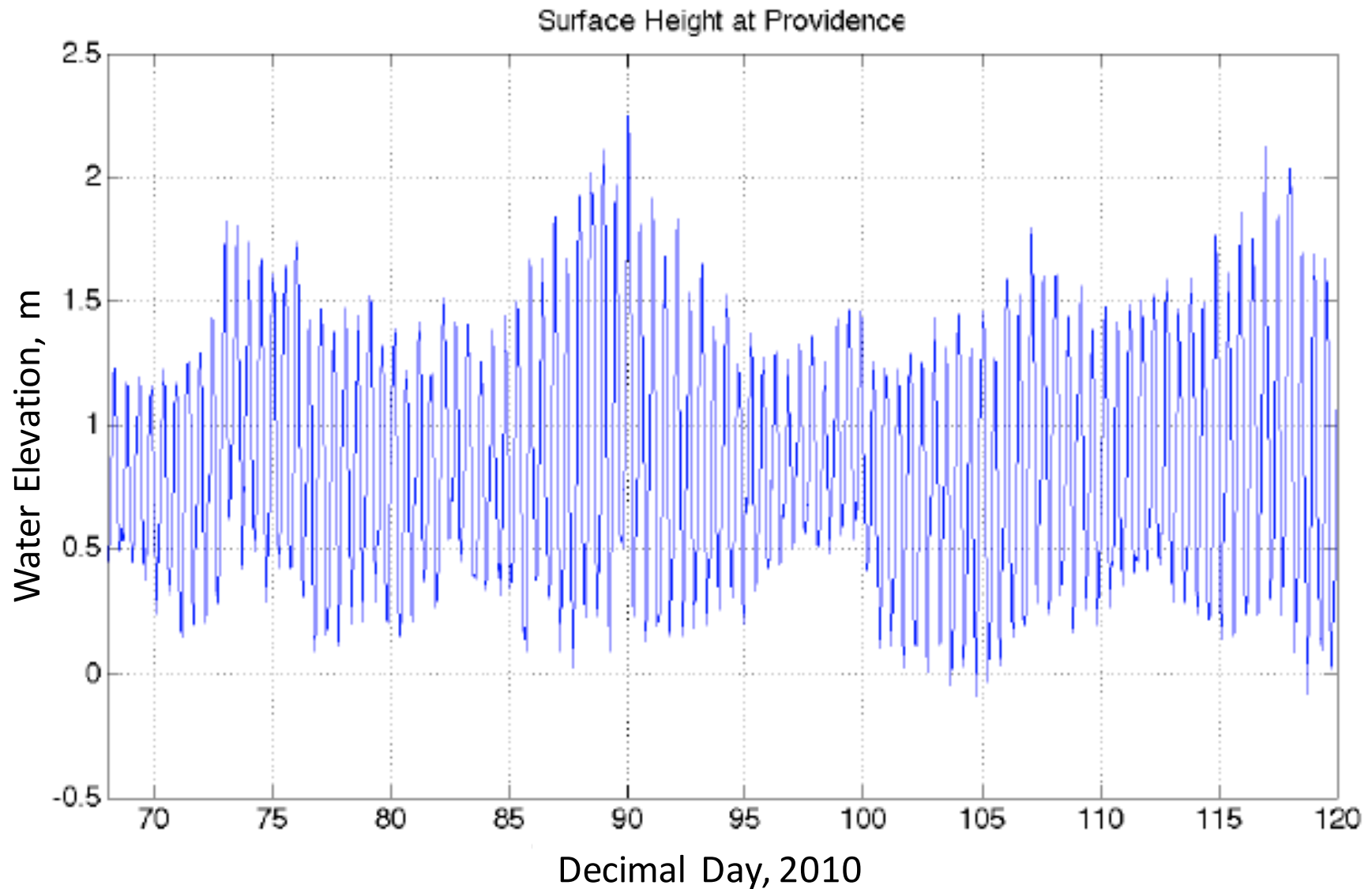


Figure 11. Plot of water elevation measured in Providence Harbor for the TCM deployment period in 2010. Plot highlights aspects of tidal record, the semi-diurnal oscillation in the tides (or water elevation) and the longer period variations through spring-neap cycles, that are used to drive and to test ROMS model simulations.

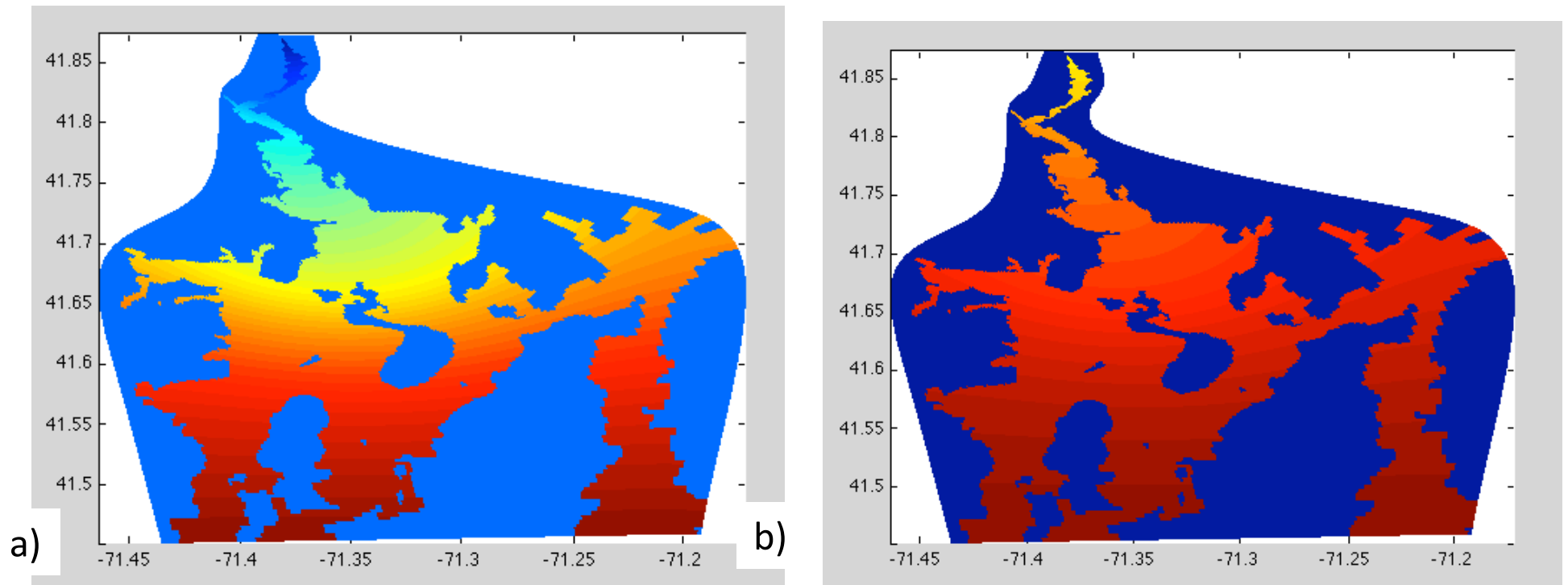


Figure 12. A series of test runs were performed for the new SNB-ROMS model to test the stability and characteristics of the solutions. Here are mapview plots of initial conditions for a) salinity (red=32 ppt; blue = 5 ppt) and b) temperature (red=3.2 C and blue = 0 C). The solutions begin in 2010 on decimal day 30 (January 31, 2010).

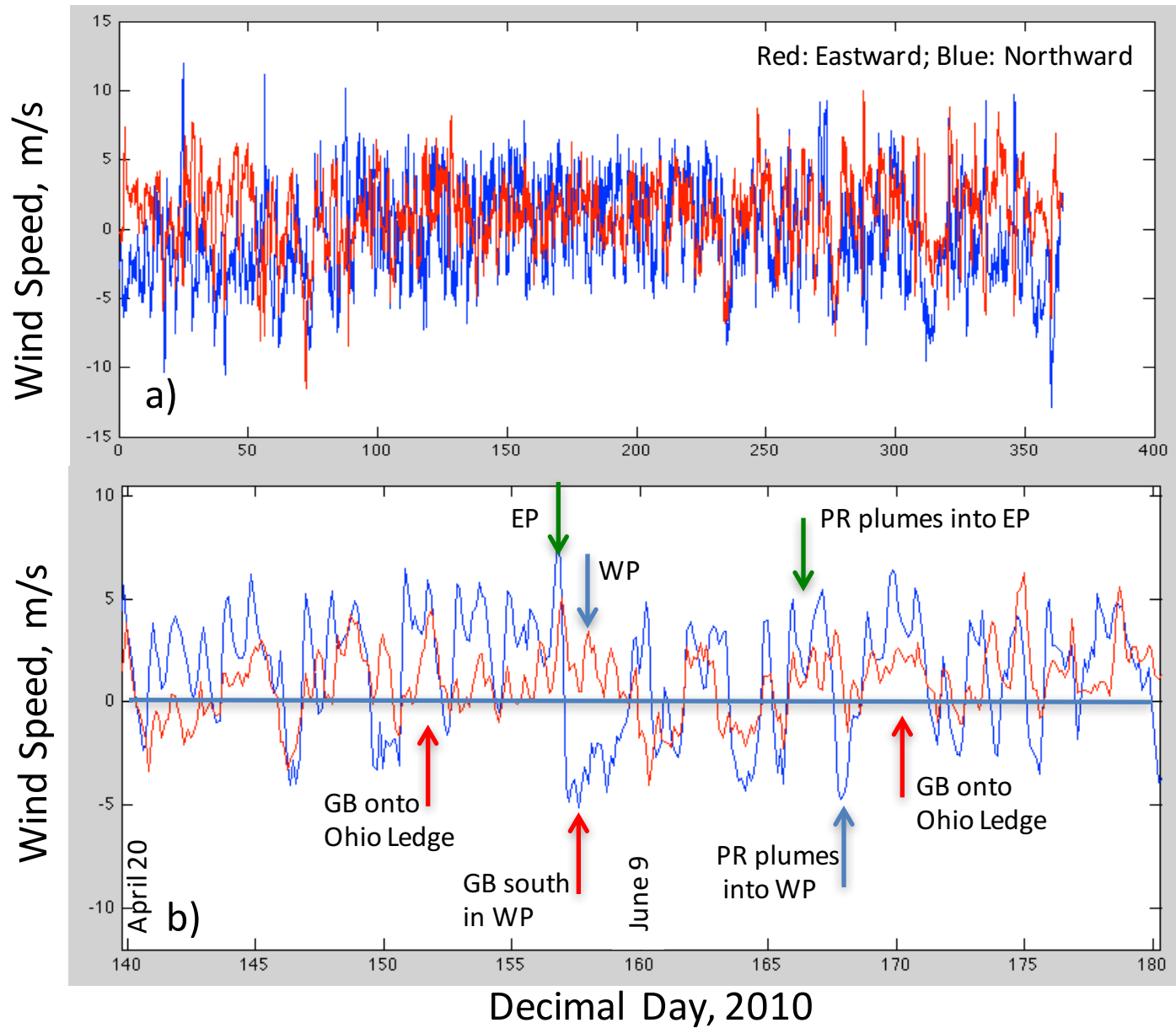


Figure 13. Plots of Providence winds (northward blowing = blue) and (eastward = red) for a) all of 2010 and b) a close-up of the 4/20-6/28 period of this study. Records show oscillations in wind magnitude occur on a roughly 5-10 day cycle or between southward and northward blowing wind events.

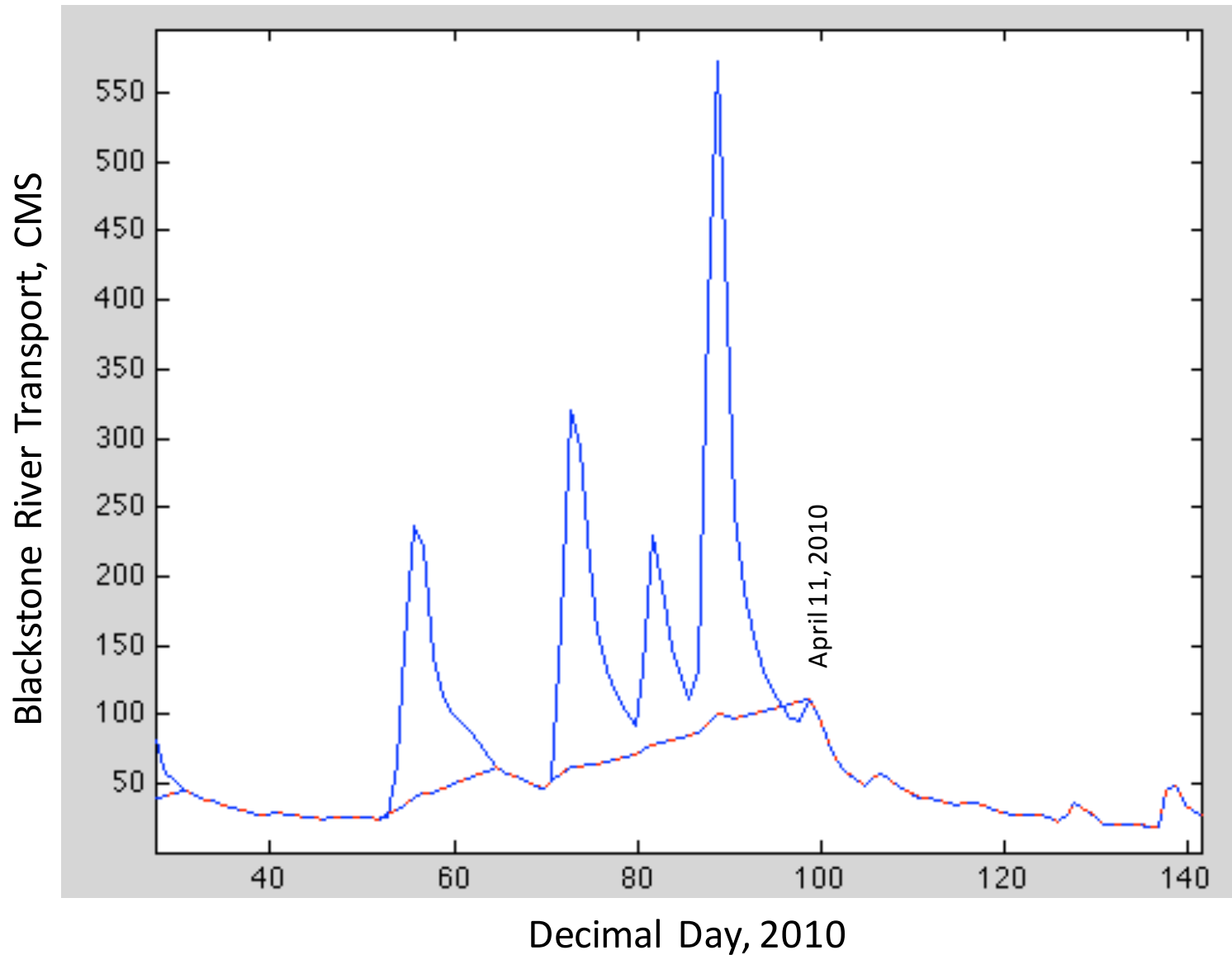


Figure 14. Plot of river transport (in cubic meters per second, CMS) for the Blackstone River for 2010 used in the model runs, shown as the blue line. Shown are the high amplitude runoff events associated with the floods of March-April 2010. A series of simulations were run using a reduced (non-flood) runoff out for the Blackstone (and other rivers) shown by the dashed line.

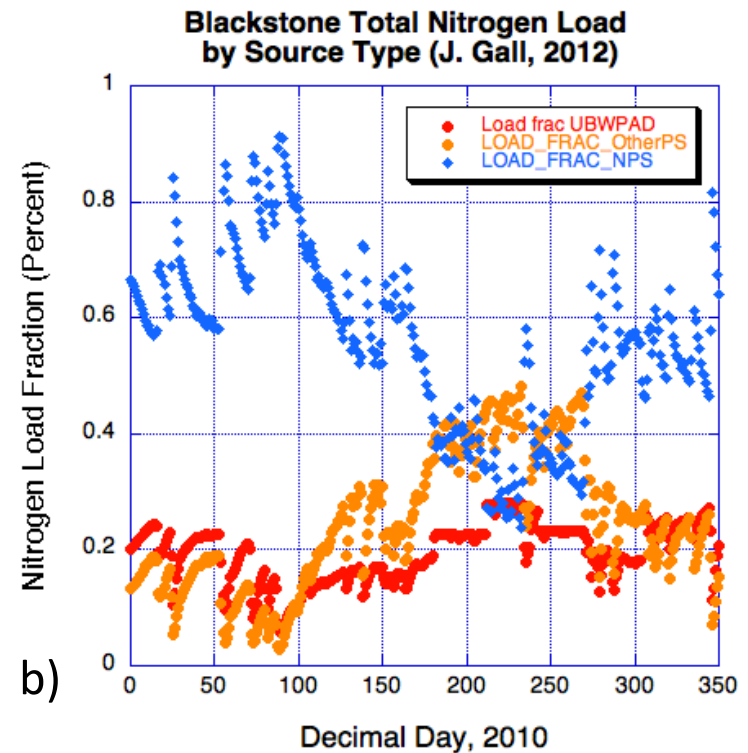
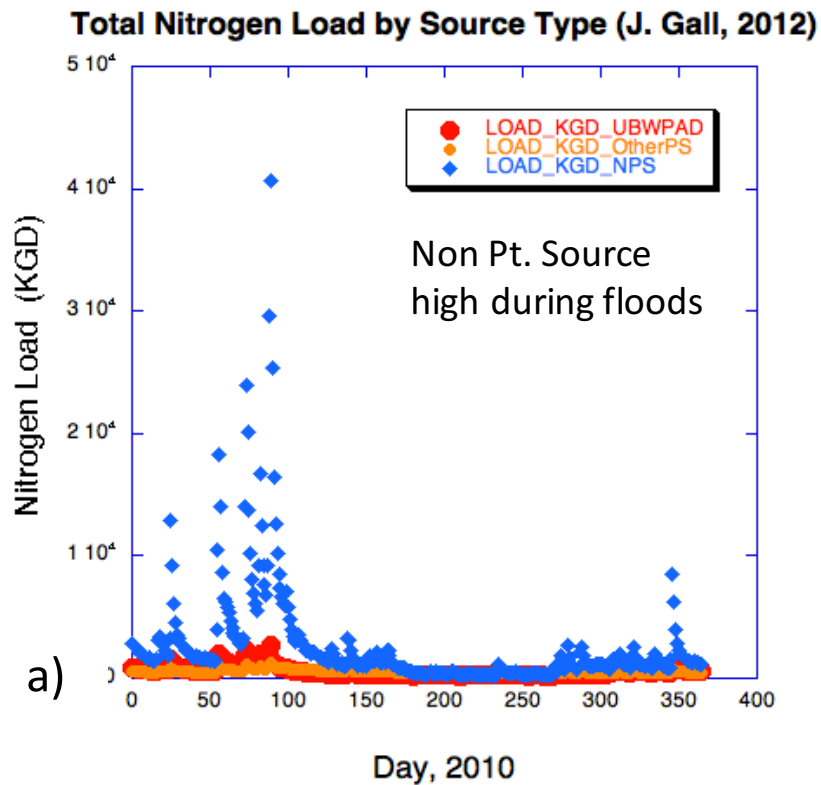


Figure 15. a) Plot of nitrogen loading to the Bay from the Blackstone River on a daily basis in 2010. Nitrogen input to the Bay varies with discharge magnitude, as do the percent contributions to the total nitrogen load from point sources versus non-point sources. Researchers at University of Massachusetts (Prof. P. Reese) have developed a TMDL model for the Blackstone River which outputs the magnitude of nutrient levels entering Narragansett Bay from point sources (given as the Upper Blackstone WWTF (red) and other point sources (orange)) and from all other non-point sources (blue). b) Plot of the percent fraction of each nutrient source entering the Bay through the Blackstone River as a function of day in 2010, predicted from UMass Blackstone TMDL Model (data provided by P. Reese, Univ. Mass.). During high runoff periods non-point sources (blue) contribute higher levels as a percent of total. During low flow, summer periods, the percent contribution from other point sources increases.

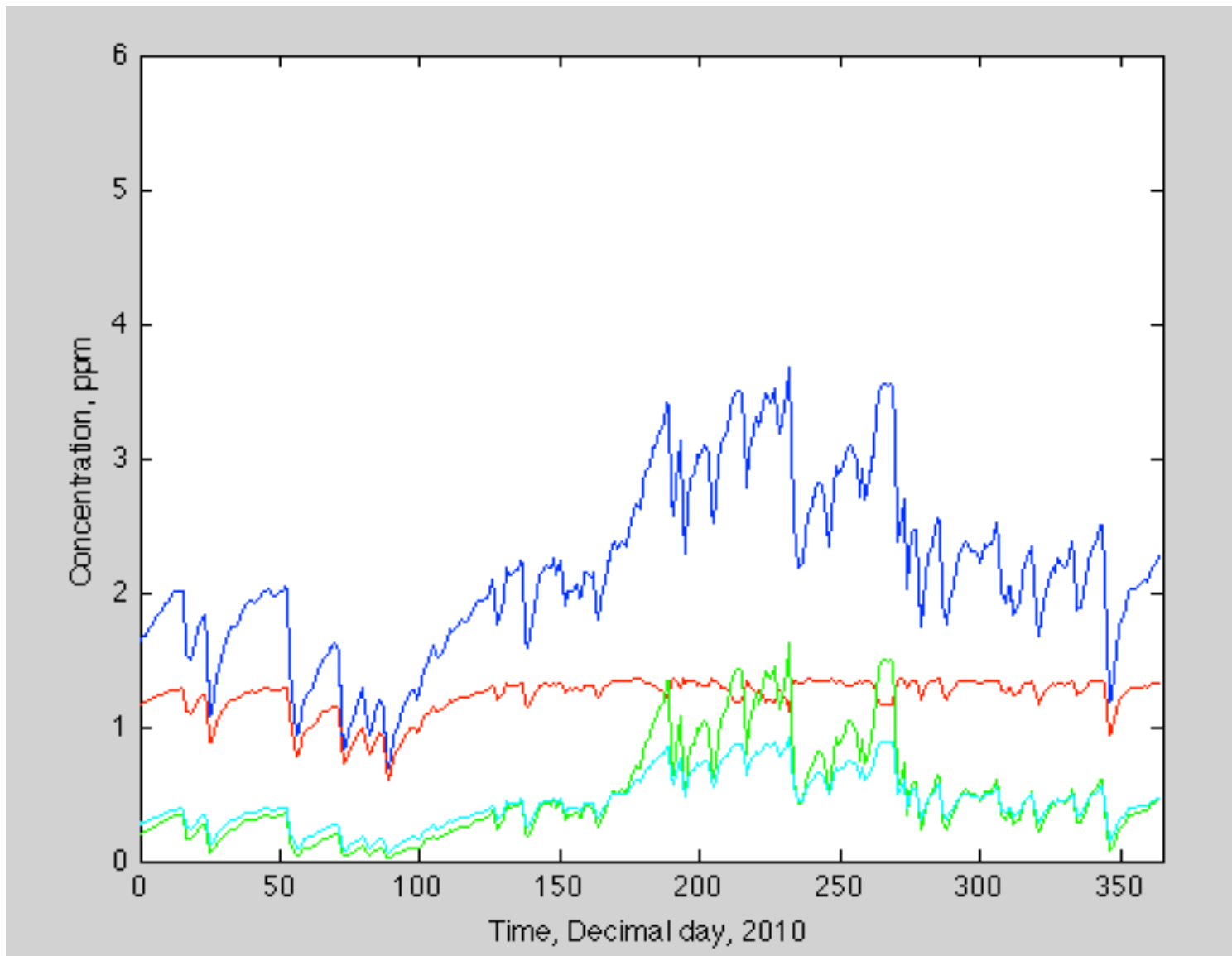


Figure 16. Plot of total nutrient concentrations (blue) in source waters for Blackstone River for the 2010 simulations, as supplied from non-point sources (red), other point sources (green) and the Upper Blackstone WWTF (cyan).

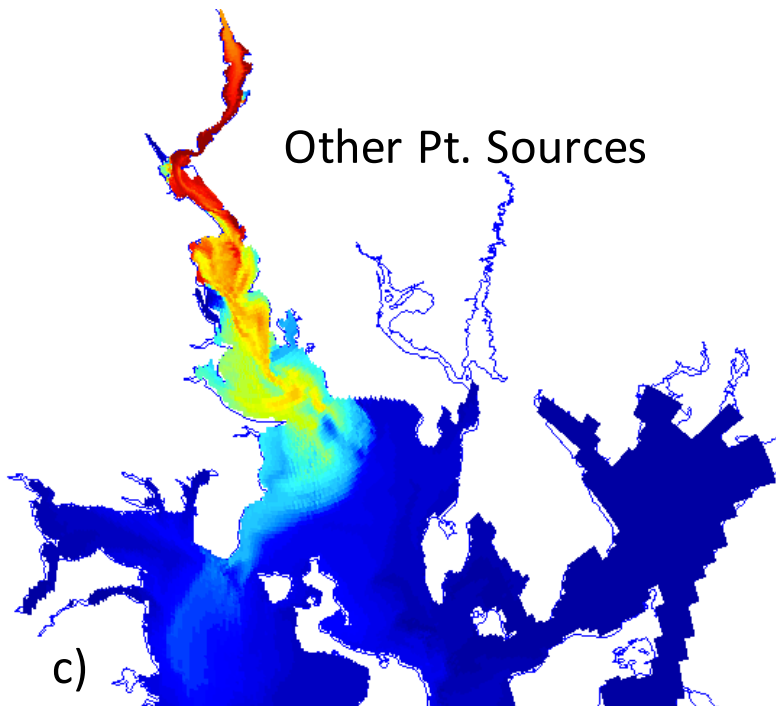
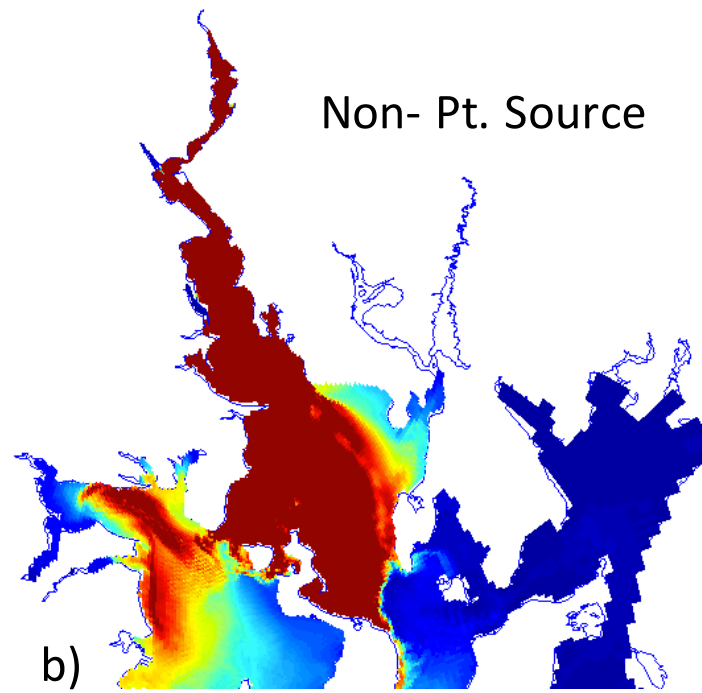
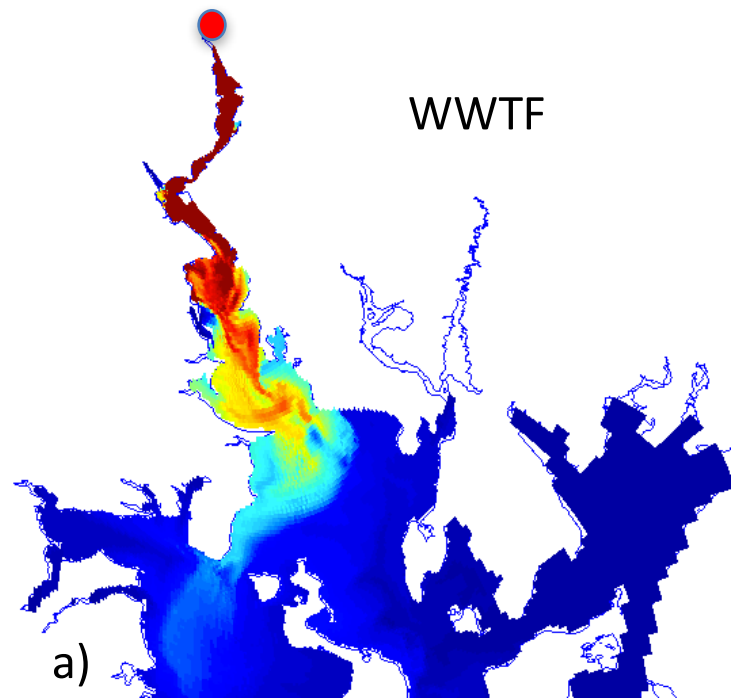


Figure 17. Contour images of near surface N (nutrients) for each type of source supplied by UMASS_TMDL (Figure 16). These show the relative magnitudes and transport pathways for this period (day 54; 2/23/10) between three sources: a) Nutrient source from Upper Blackstone WWTF, b) nutrients from non-point sources and c) nutrients from other point sources. The Blackstone River values are actual total nutrient concentrations supplied by U Mass (P. Reese) Blackstone TMDL Model. Red colors are set to 0.1 mg/L, which produces a saturation in the color scale, but shows down-bay dispersion patterns. Dye source location as red circle.

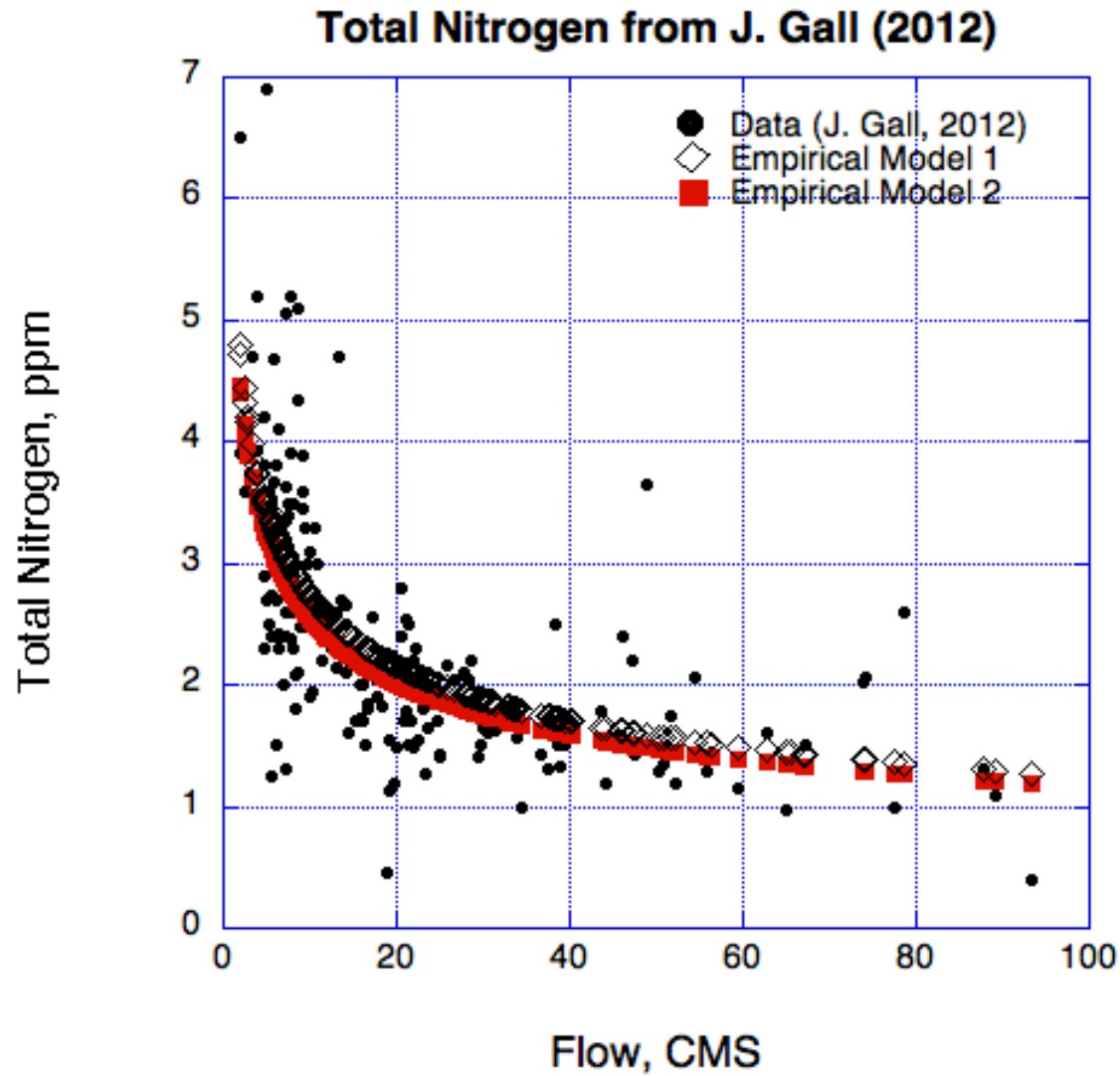


Figure 18. For the 2010 simulation cases, we use information supplied by the U. Mass. Blackstone River TMDL Model for the Blackstone River. For other rivers we estimate varying nutrient concentrations by developing an empirical model for nutrient concentration in the supply water versus discharge level. The empirical model utilizes information for 2010 from the U. Mass Group to calculate nutrient concentrations in unmeasured rivers in 2010 based on measured river transports (e.g., volume flux).

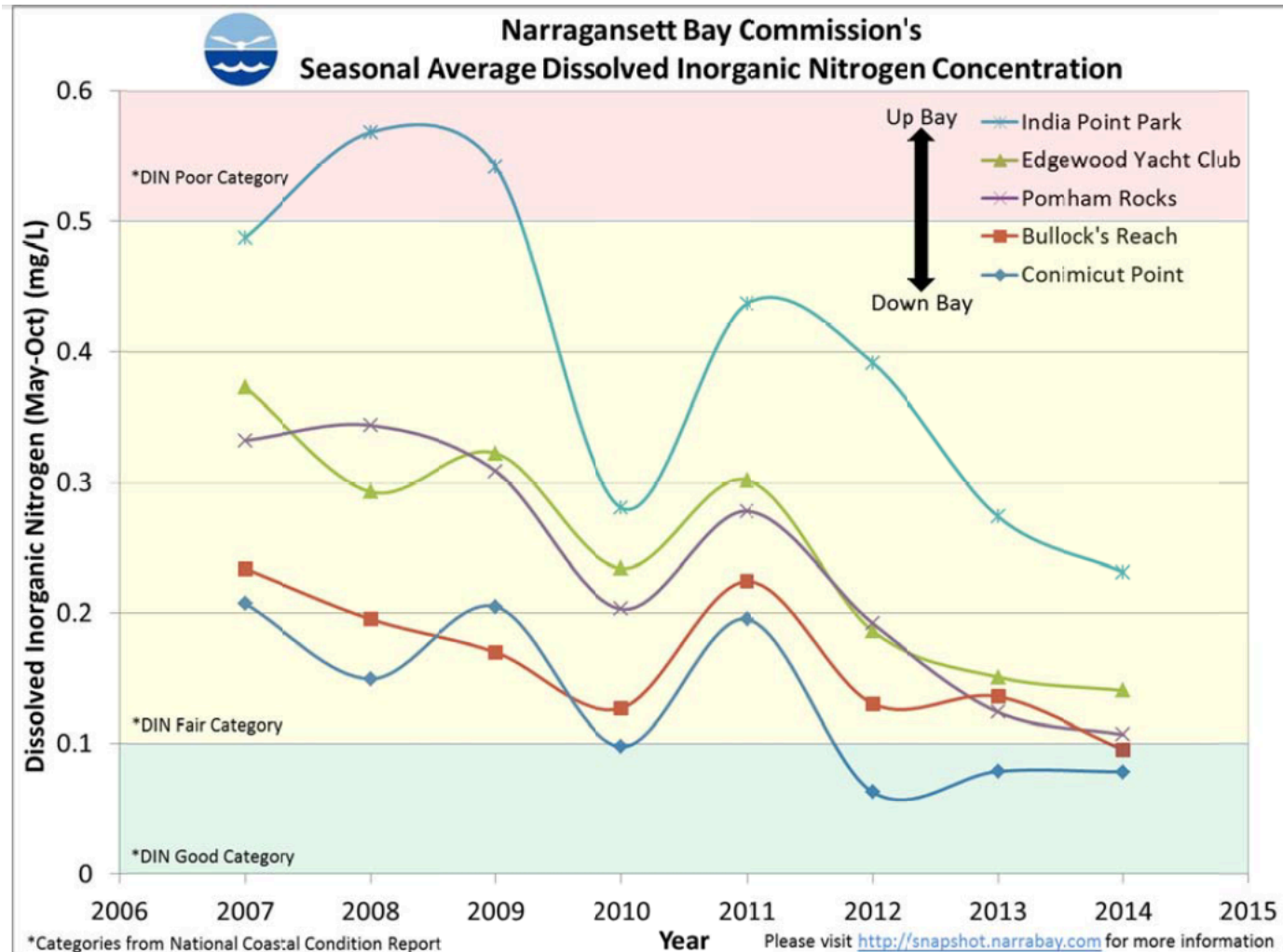


Figure 19. Plots of average dissolved inorganic nitrogen over a decade. Plot supplied by NBC, shows nitrogen trends with latitude, for multiple years. There is a very common, repeatable trend of nitrogen levels decreasing by ~40% from the mouth of the Seekonk to the mouth of the Providence River. This is in agreement with historical conditions (Smayda and Borkman, 2008). In addition, data show a declining trend in nitrogen levels at each station or latitude from 2006 to 2014.

NBC Bay Nutrient Sampling Stations
Summer 2010 Chlorophyll Concentrations (ug/L)

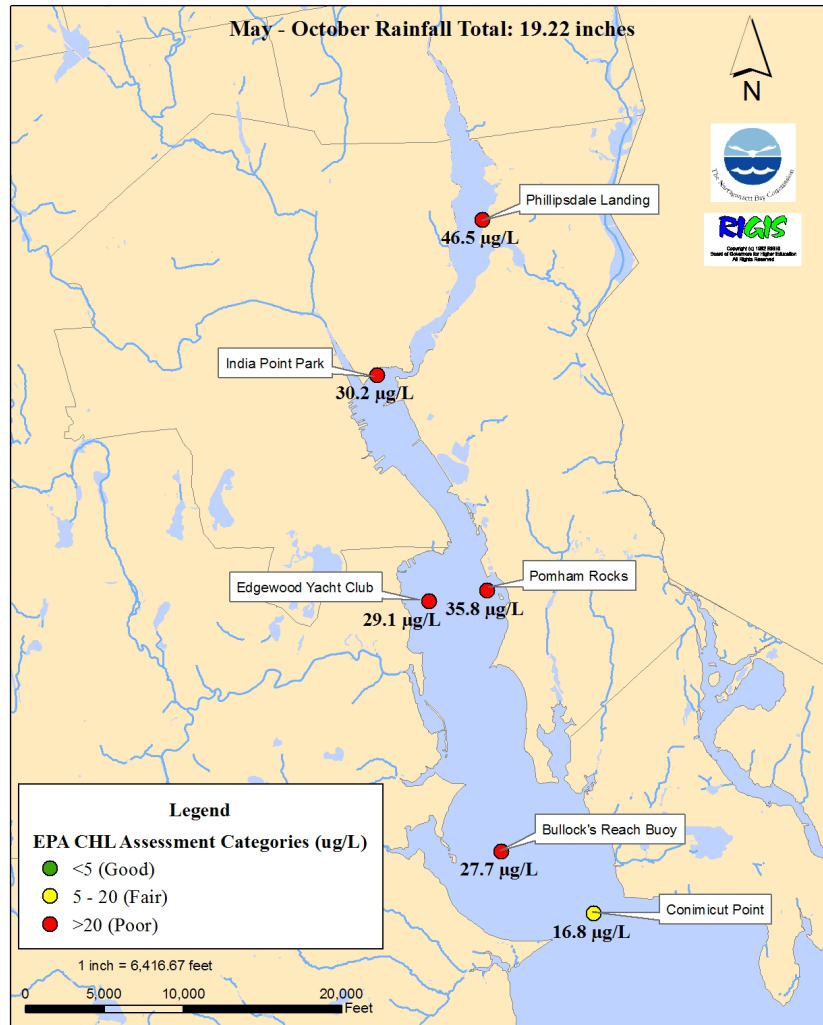


Figure 20. Supplied by NBC, showing chlorophyll concentration trends through the uppermost Bay for 2010. Similar to nitrogen, there is a roughly 35-40% reduction in chlorophyll levels moving from the Seekonk to the mouth of the Providence River.

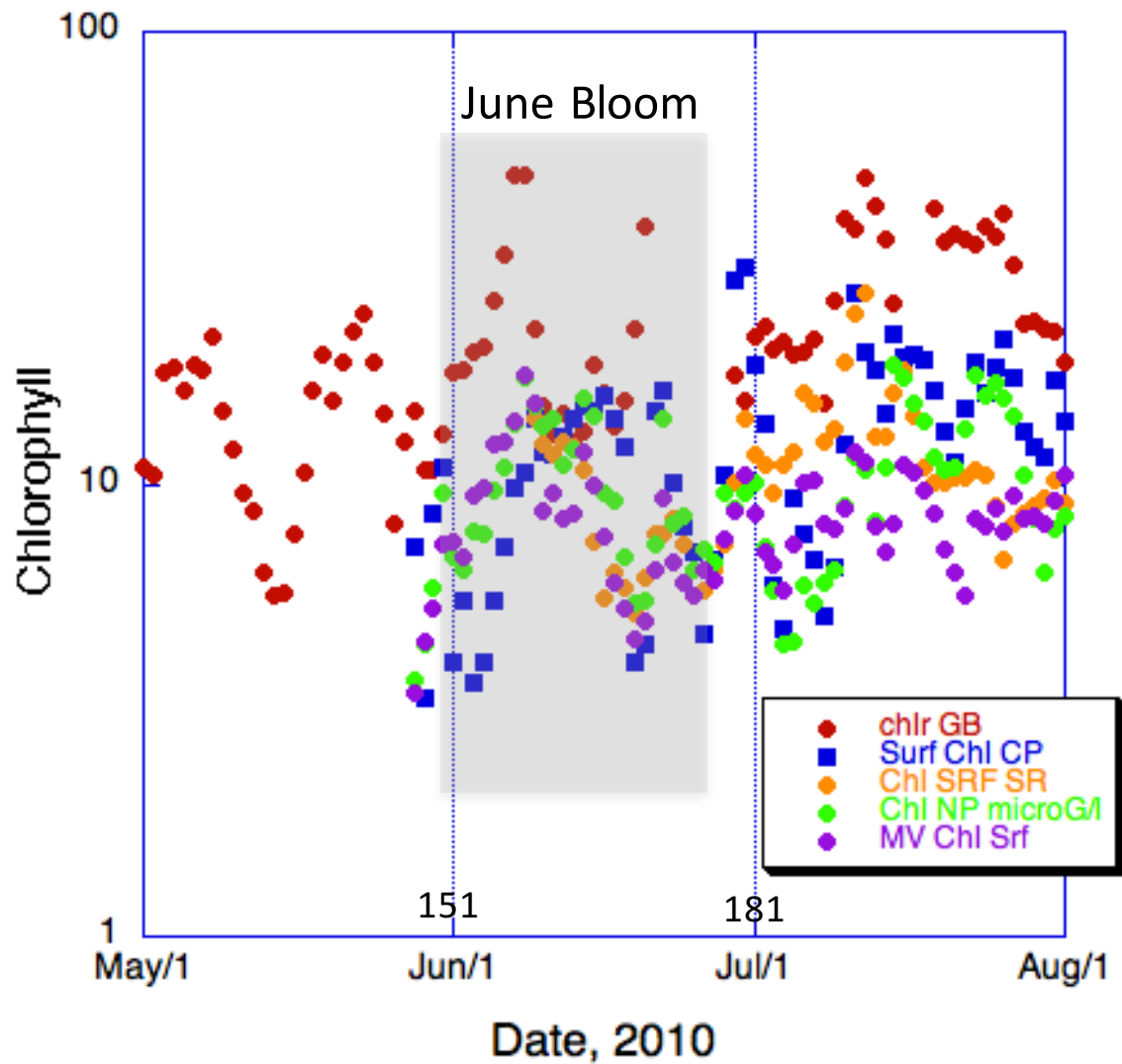


Figure 21. Chlorophyll data from the Narragansett Bay buoy network for summer 2010 (GB: Greenwich Bay innermost basin, CP: Conimicut Point, SR: Sally Rock, NP: North Prudence, MV: Mount View). Data show inner GB sites consistently high relative to other mid-Bay stations. We focus on a June production event.

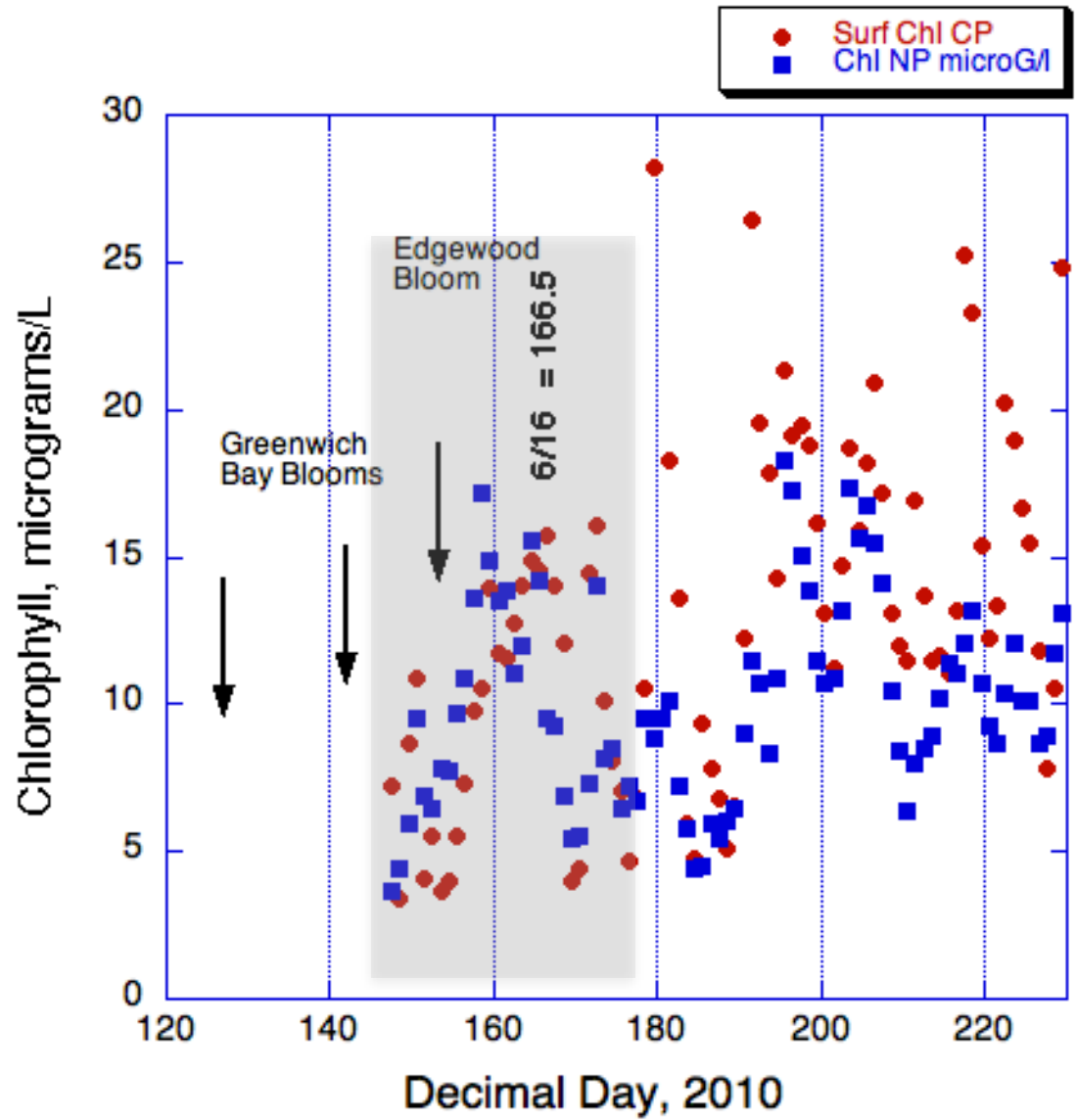


Figure 22. Chlorophyll data from the Narragansett Bay buoy network located at northern and southern edges of the Ohio Ledge-mid-Bay region for May-August 2010 (CP: Conimicut Point, NP: North Prudence). Timing of Greenwich Bay and Edgewood Shoals blooms are shown for reference.

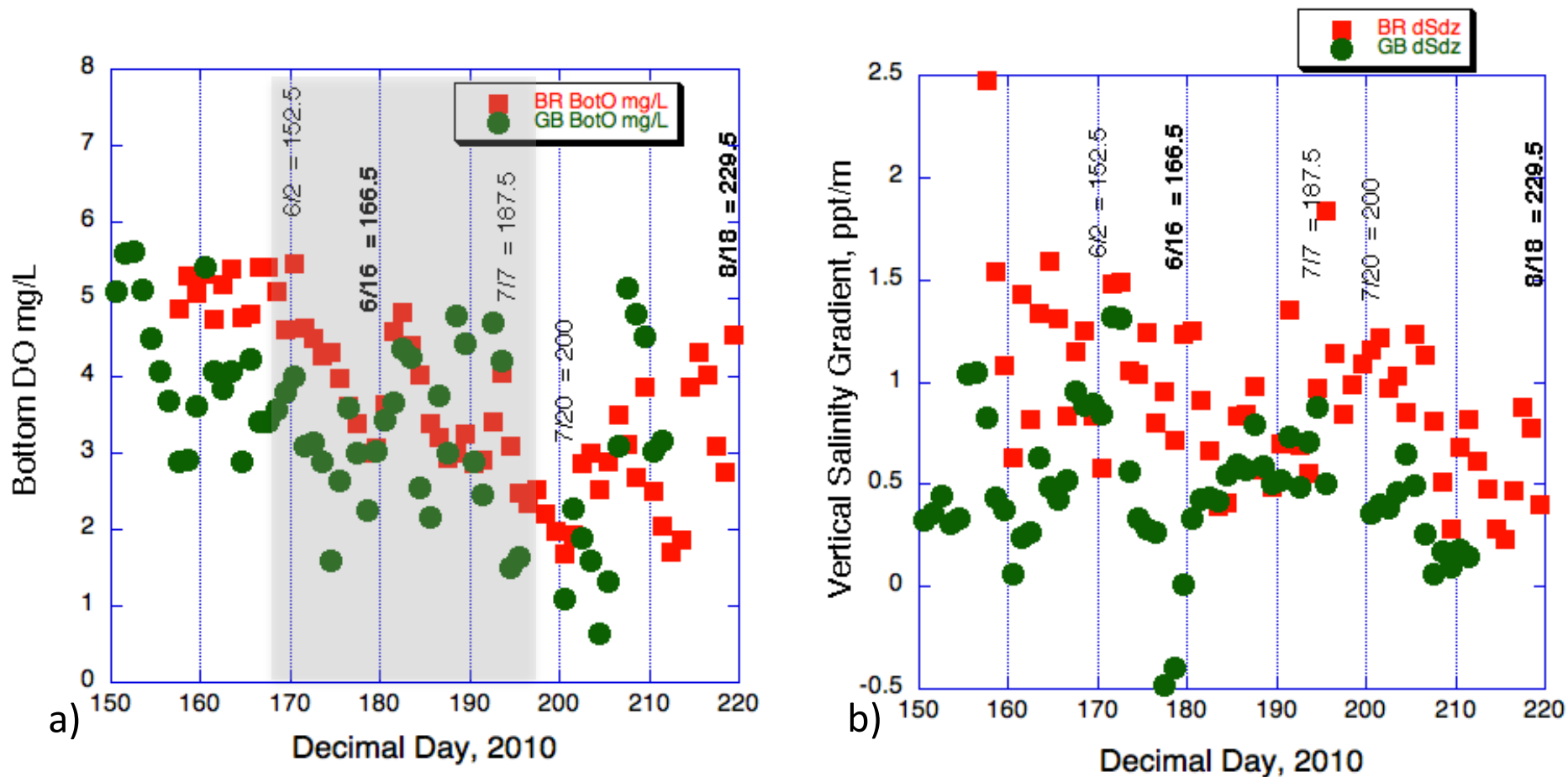


Figure 24. a) Bottom dissolved oxygen (DO) and b) bottom minus surface salinity difference from Narragansett Bay buoy network for stations in the southern Providence River (BR) and Greenwich Bay (GB). Timing of the major summertime blooms are shown in bold for reference (6/16; 8/18). Short-lived periods of slightly higher stratification precede the 6/16/10 production event, but not the 8/18 event. During the June bloom event, bottom oxygen in GB and lower Providence River drops from 5.5 mg/l to 3 mg/l. On days 170-180, stratification reductions in GB and at BR precede a DO recovery on day 182.

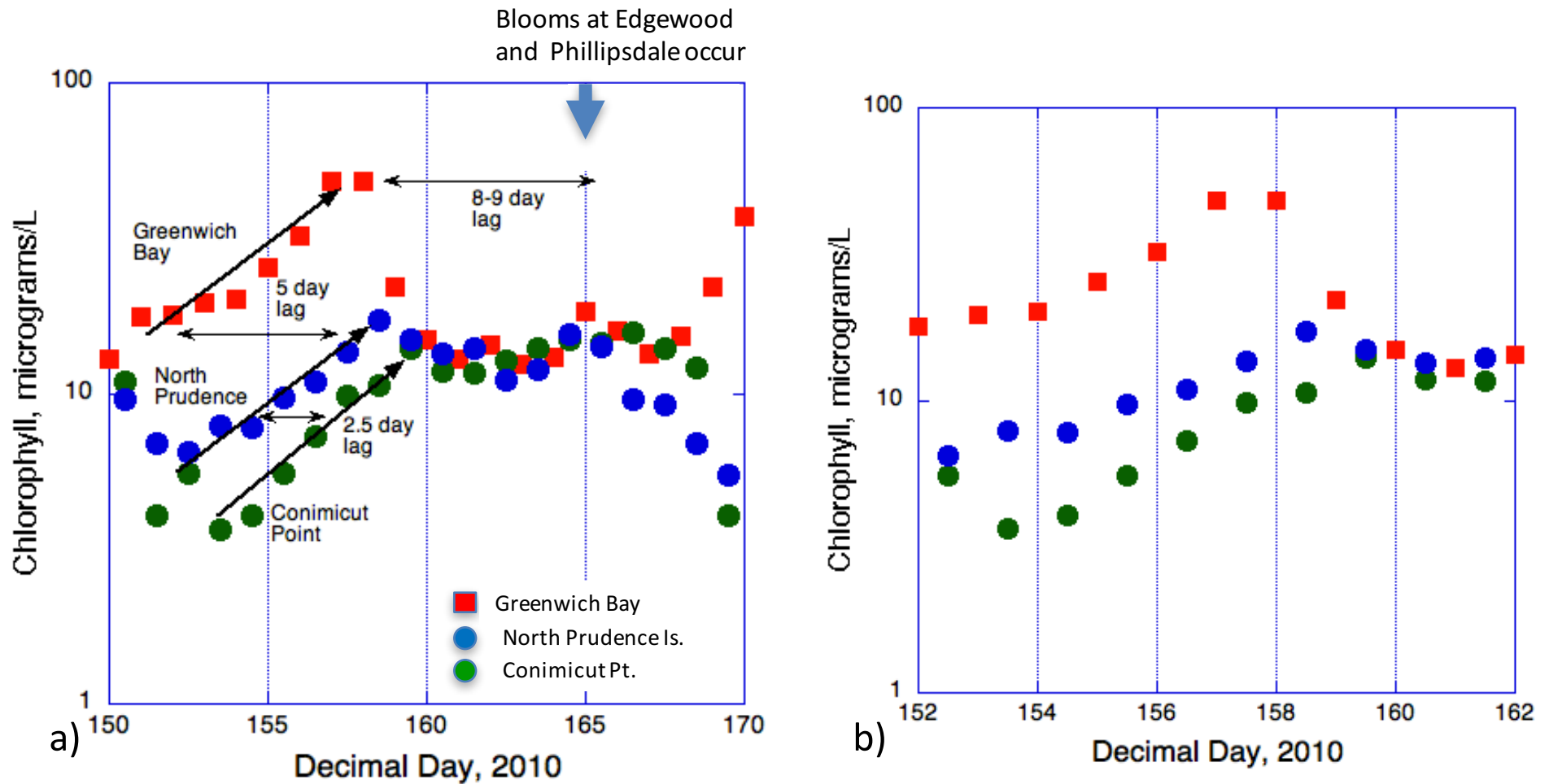


Figure 25. The initial ROMS NPZD model simulations focus on the June 2010 phytoplankton production event and bottom DO depletion event. Model simulations interestingly show that blooms tend to initiate in shallow regions within Greenwich Bay, Ohio Ledge, Mt. Hope Bay and the lower Providence River and progress to Ohio Ledge and northward through the Providence River. Time series plots here show time scales for chlorophyll in Greenwich Bay and at southern and northern boundaries of Ohio Ledge from Bay buoy data. As shown by Bergondo (2001), the event leads in Greenwich Bay. After a 5-6 day lag, a rise in chlorophyll is recorded on Ohio Ledge, followed by a 7-8 day lag to the event recorded in NBC data on Edgewood Shoals and at Phillipsdale. Interestingly Edgewood Shoals values exceed those at Phillipsdale.

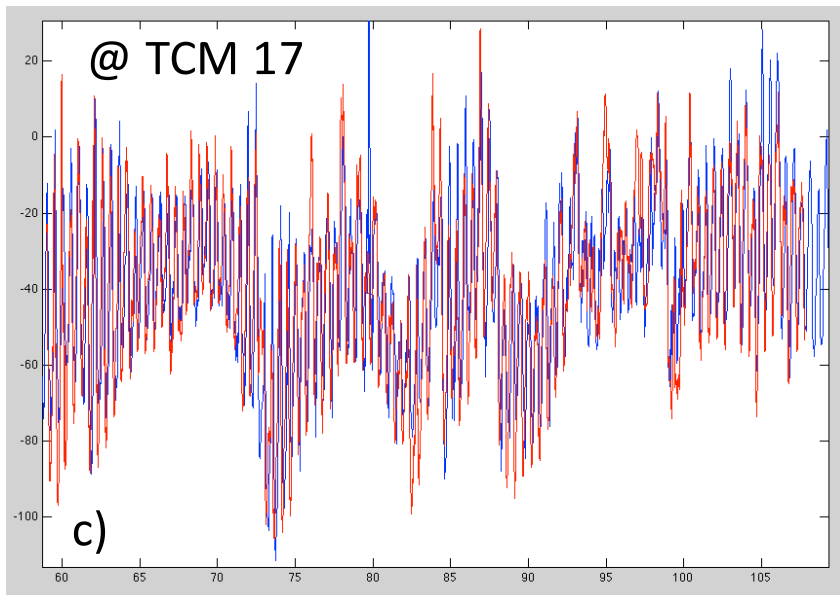
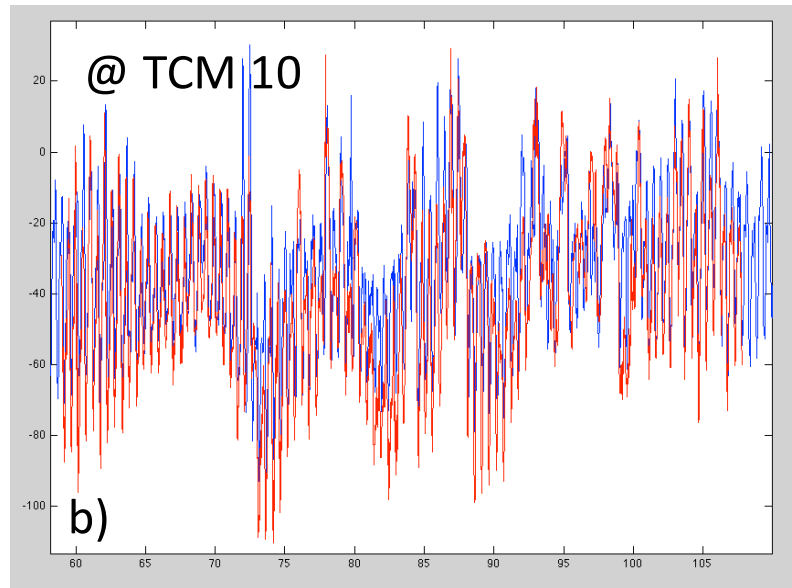
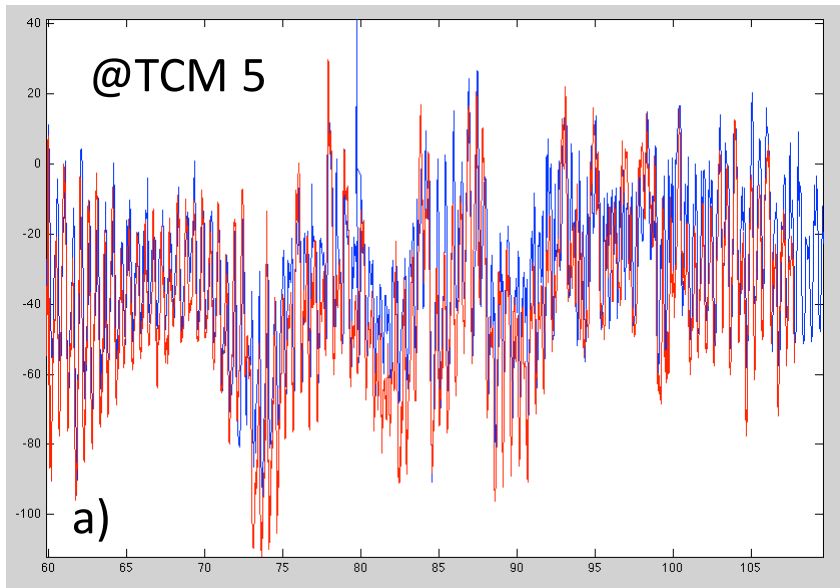


Figure 26. Plots of velocity time series information (northward velocity, cm/s) comparing records between the NB-ROMS (red) and SR-NB-ROMS (blue) at three TCM locations. SR-NB-ROMS matches NB-ROMS records at TCM locations where TCM (data) vs. NB-ROMS (modeled) statistical skill comparisons were strong (Kincaid, 2012).

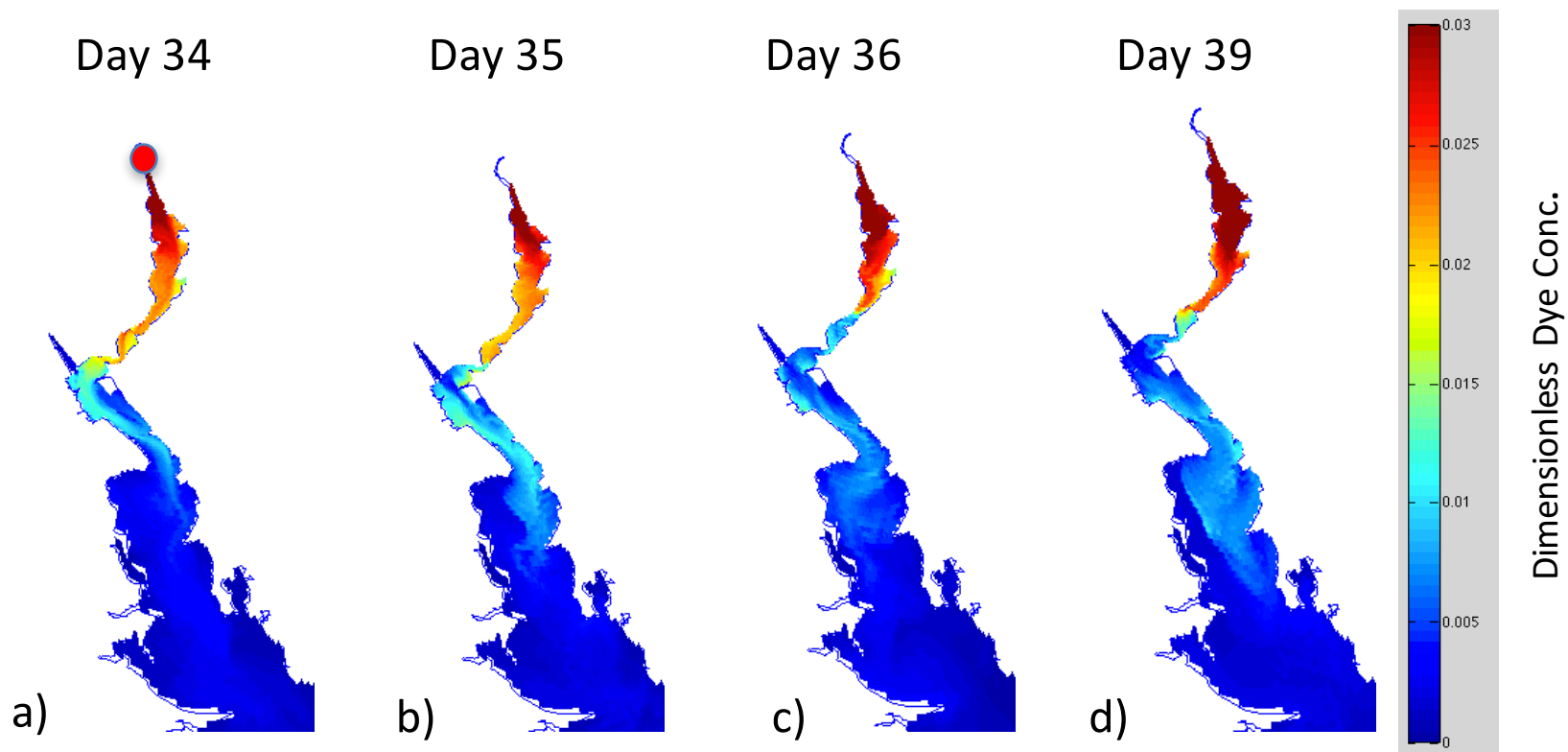


Figure 27. A new ROMS grid has been constructed that includes the Seekonk River. Frames a-d show color contour plots of near-surface transport of dye entering the Blackstone that tracks WWTF inputs determined by the UMass Blackstone TMDL model for 2010. Red color represents a maximum dimensionless concentration of 0.3, which saturates the image in the Seekonk, but allows for imaging the plume further south. Simulations are for year 2010, beginning in January. Shown are dispersion patterns for early February. Results show the thin filament of Blackstone WWTF dye moving and diluting through the Edgewood Shoals section of the Providence River. Red circle indicates dye source location.

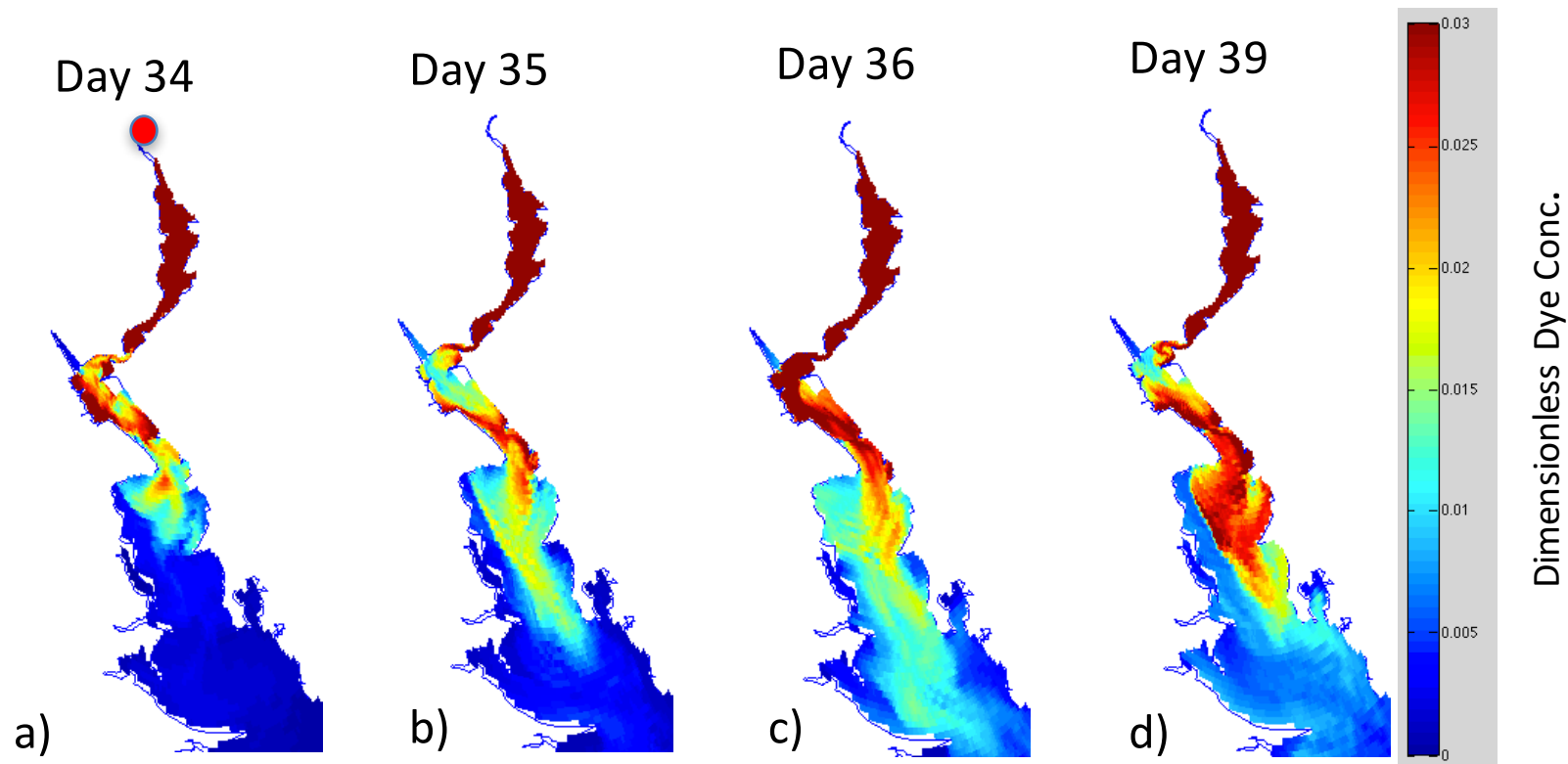


Figure 28 . Frames a-d are similar to previous figure 16, but showing near-surface transport of dye entering the Blackstone that tracks non-point source (NPS) inputs determined by the UMass Blackstone TMDL model for 2010. Colorbar is set such that dimensionless concentrations of ≥ 0.3 are red. Results show a significantly larger plug of NPS dye moving and diluting as far down as the mouth of the Providence River. Results are consistent with current meter data showing a flow separation between channel outflow and the Edgewood Shoals gyre. Red circle shows dye source location.

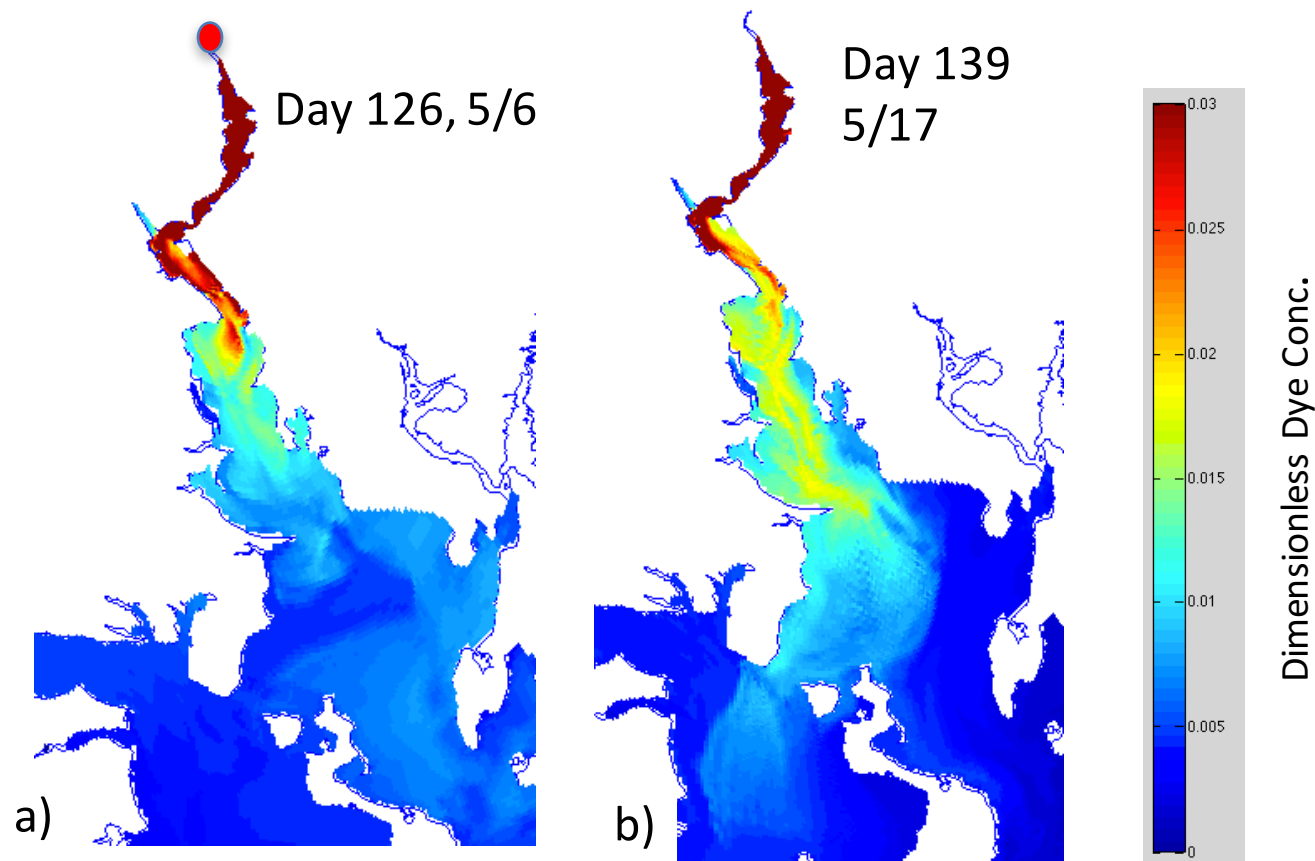


Figure 29. Near-surface transport of dye entering the Blackstone that tracks non-point source (NPS) inputs determined by the UMass Blackstone TMDL model for 2010 for later in the spin-up period for the 2010 SR-ROMS model simulation. Colorbar is set such that dimensionless concentrations of ≥ 0.3 are red. Results show how the NPS dye mass moves and dilutes further down-bay. a) A period when the Blackstone dye field is confined to the eastern side of Ohio Ledge (a key region of the mid-section of Narragansett Bay). b) A second common transport mode for dye from northern sources is along the west shore of Ohio Ledge and into the West Passage. As shown here, conditions are often such that this dye source bypasses Greenwich Bay (Kincaid, 2012). Dye source location shown as red circle.

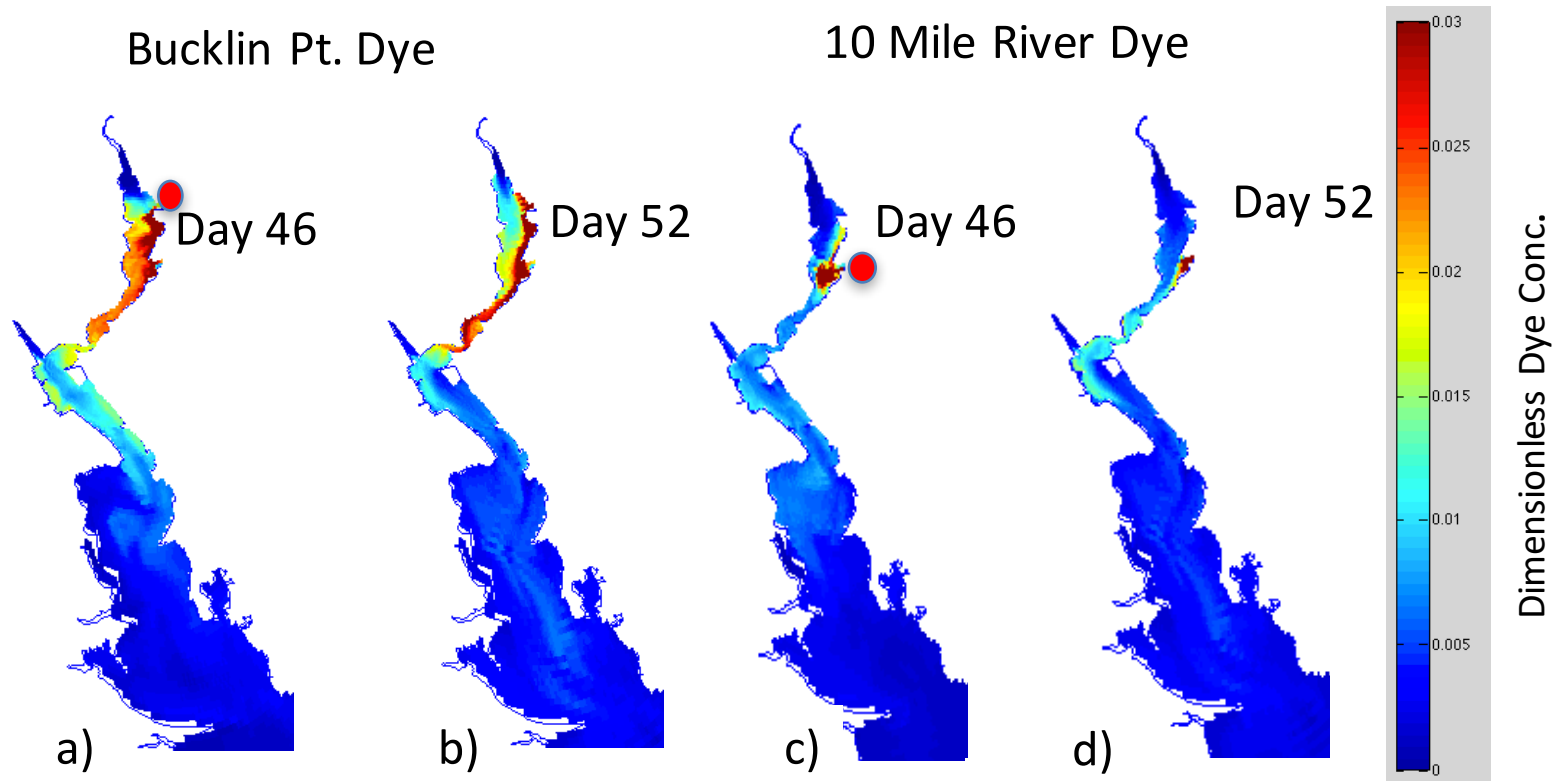


Figure 30. Contours showing near-surface transport of dye entering from Bucklin Point WWTF (a,b) and the 10 Mile River (c,d). Colorbar is set such that dimensionless concentrations of ≥ 0.3 are red. This is done to allow images of the dispersed plume to be seen further to the south. Red circles show dye source location for the two inputs.

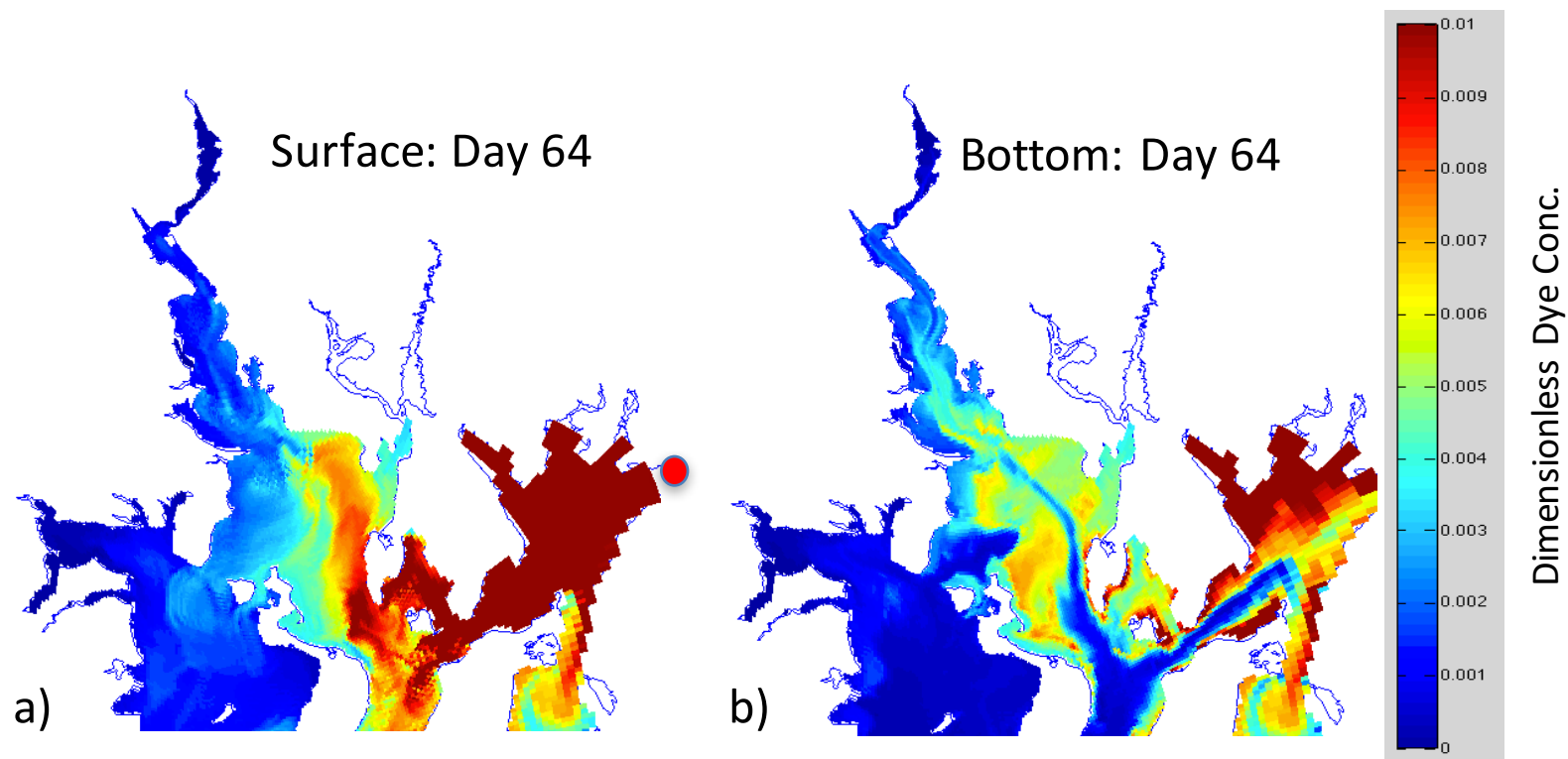


Figure 31 . Color contour plots showing a) near-surface and b) near-bottom dispersion patterns for dye the Taunton River from day 64, or roughly 9 days after the first runoff event of 2010 peaked at day 55 (figure 6). . Near-surface dye disperses more down the East Passage. Deeper dye extends further northward , up to the Port Edgewood channel. Here the colorbar is set such that dimensionless concentrations of ≥ 0.1 are red, saturating the image in Mt. Hope Bay, but showing dispersion paths throughout the Bay. Dye source location shown with red circle.

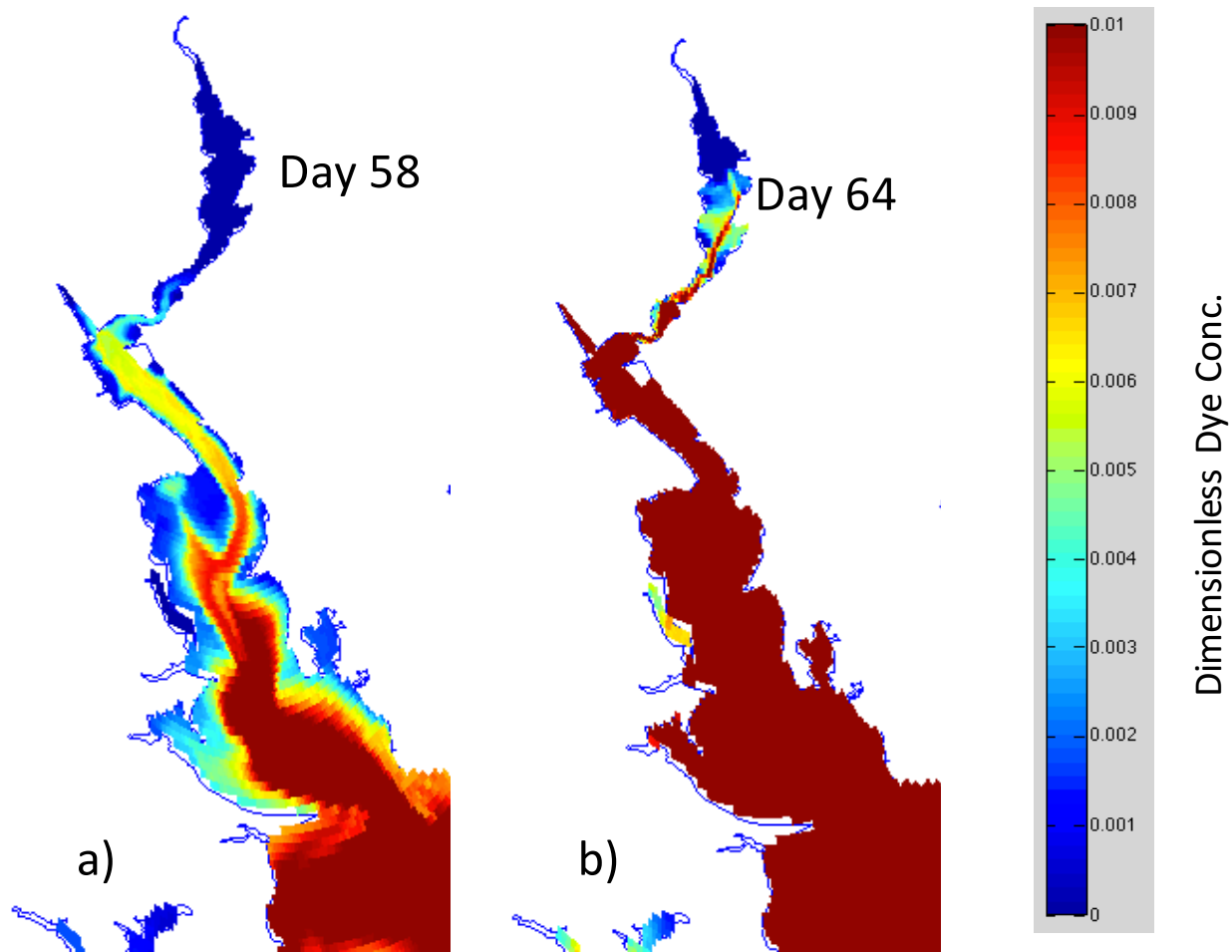


Figure 32. Near-bottom dye from the Taunton River intruding into the Providence and Seekonk Rivers on a) day 58 and b) day 64. The colorbar maximum is reduced to 0.01 to show details in the Seekonk River. Northward entrainment of Taunton River dye occurs despite the runoff event of day 55.

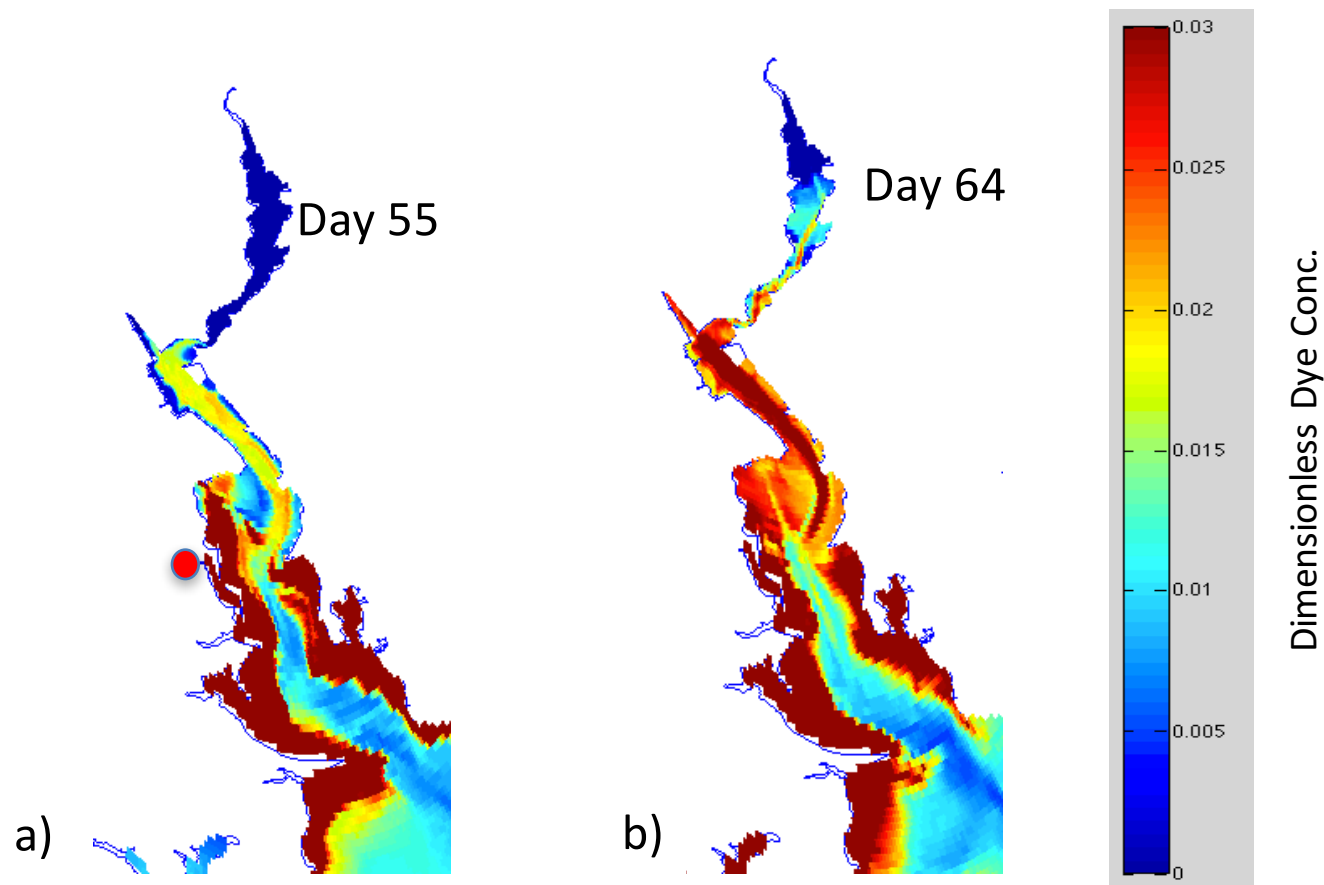


Figure 33. Near-bottom dye from the Pawtuxet River intruding into the Seekonk River on a) day 55 and b) day 64. Deep Pawtuxet dye efficiently moves onto the Edgewood Shoals and all shallow areas throughout the Providence River. It also moves up towards the hurricane barrier and into the Seekonk despite the strong runoff event of Day 55. Dye source location show with red circle.

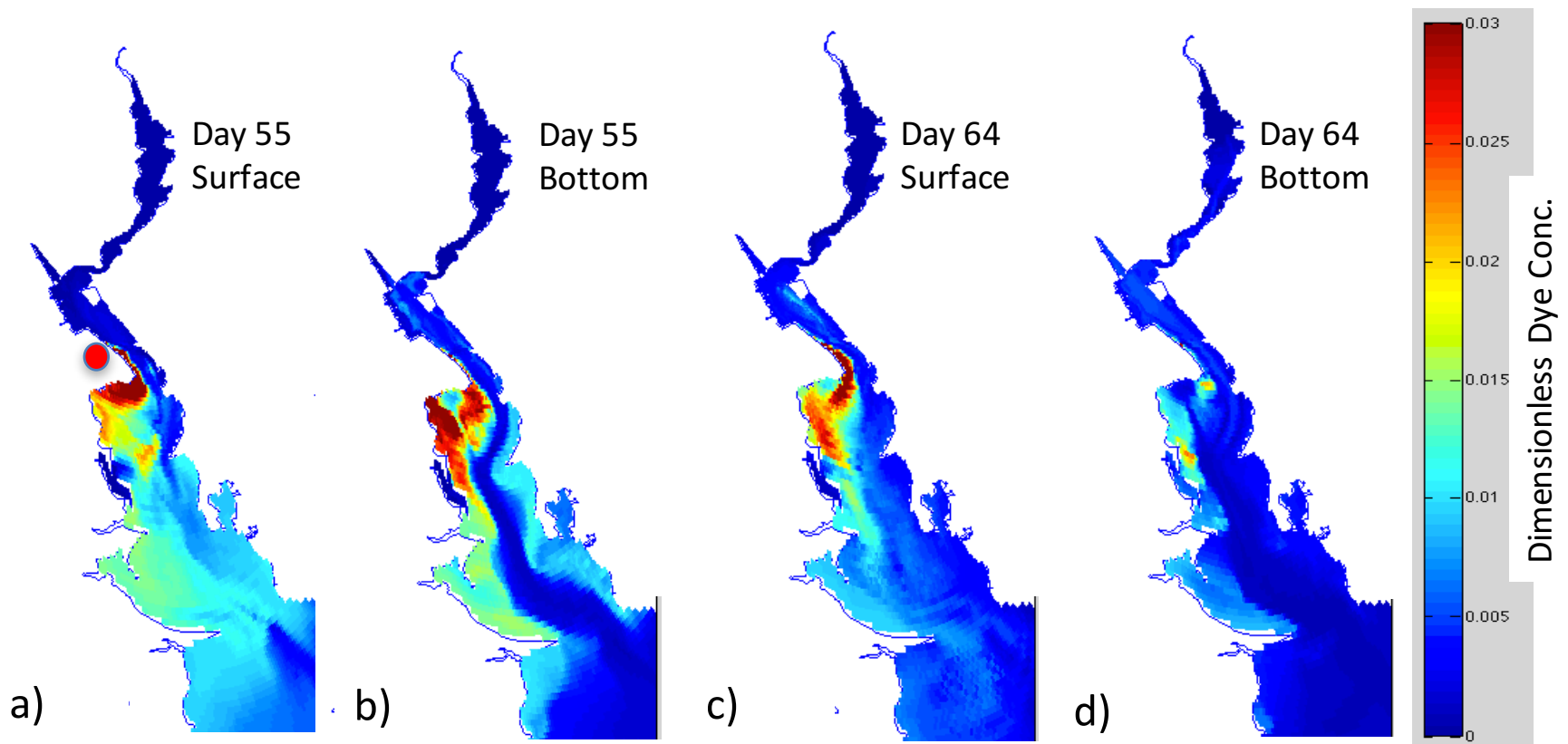


Figure 34. Dispersion patterns for near-surface (a,c) and near-bottom (b,d) dye from the Fields Pt. WWTF for day 55 (a,b) and day 64 (c,d). During the higher runoff period leading up to and after day 55, the Fields Pt. dye plume is efficiently dispersed to the south, onto Edgewood Shoals and along the western coast of the Providence River. Dimensionless dye concentration is shown in color bar, red=0.03. Red circle shows dye source location.

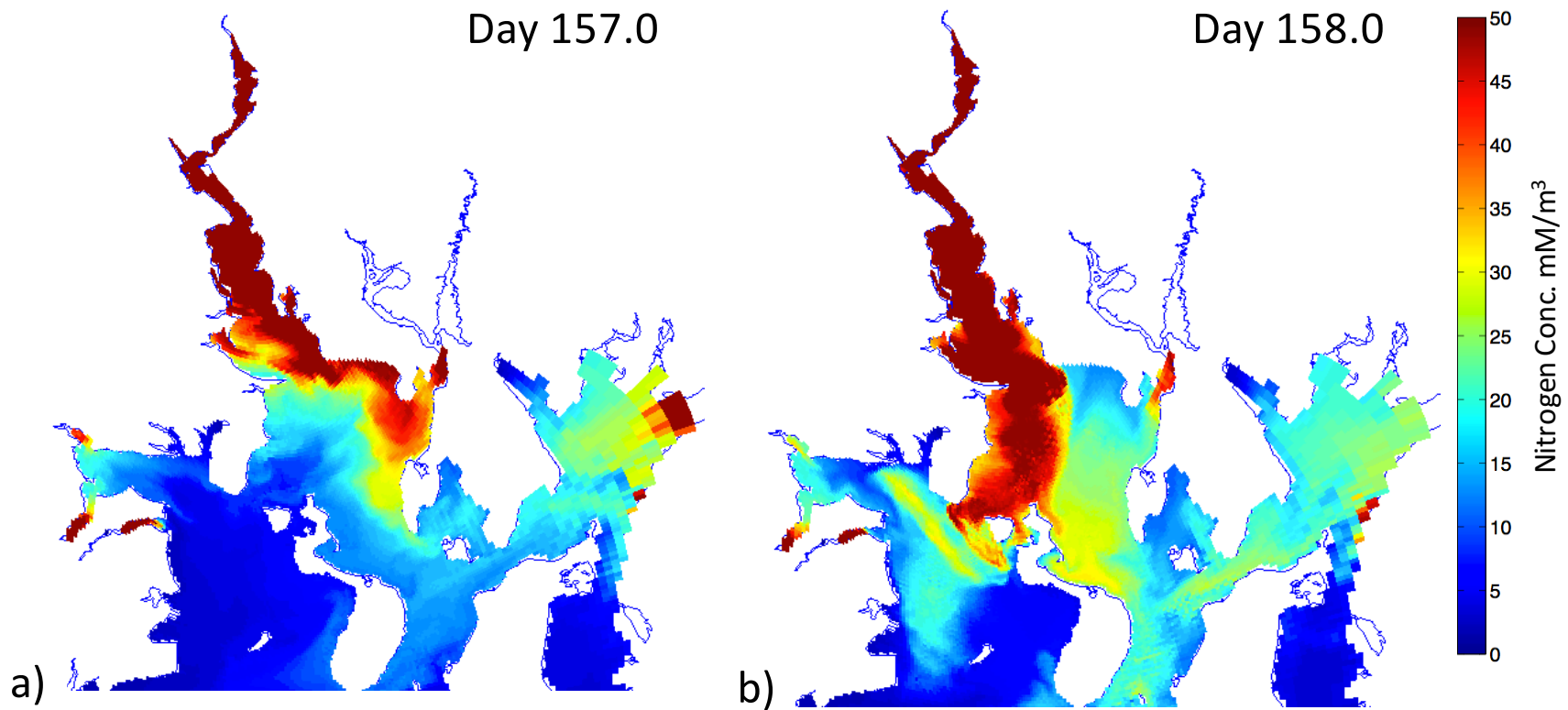


Figure 35. First set of images for simulations running the ROMS-NPZD model instead of just passive dyes. Color contours show surface total nitrogen (N) fields for a case with WWTFs releasing at 1071 mM m^{-3} (15 mg L^{-1}) for a) decimal day 157 when the down-bay plume hugs the northeastern shore of Ohio Ledge, entering the East Passage and b) decimal day 158 when the N-plume enters the upper West Passage. As summarized in Kincaid (2012a), when dye was only a passive tracer, this is a common, representative oscillatory pattern for the N-plume, cycling between different shores of Ohio Ledge. Red colors are 50 mM m^{-3} .

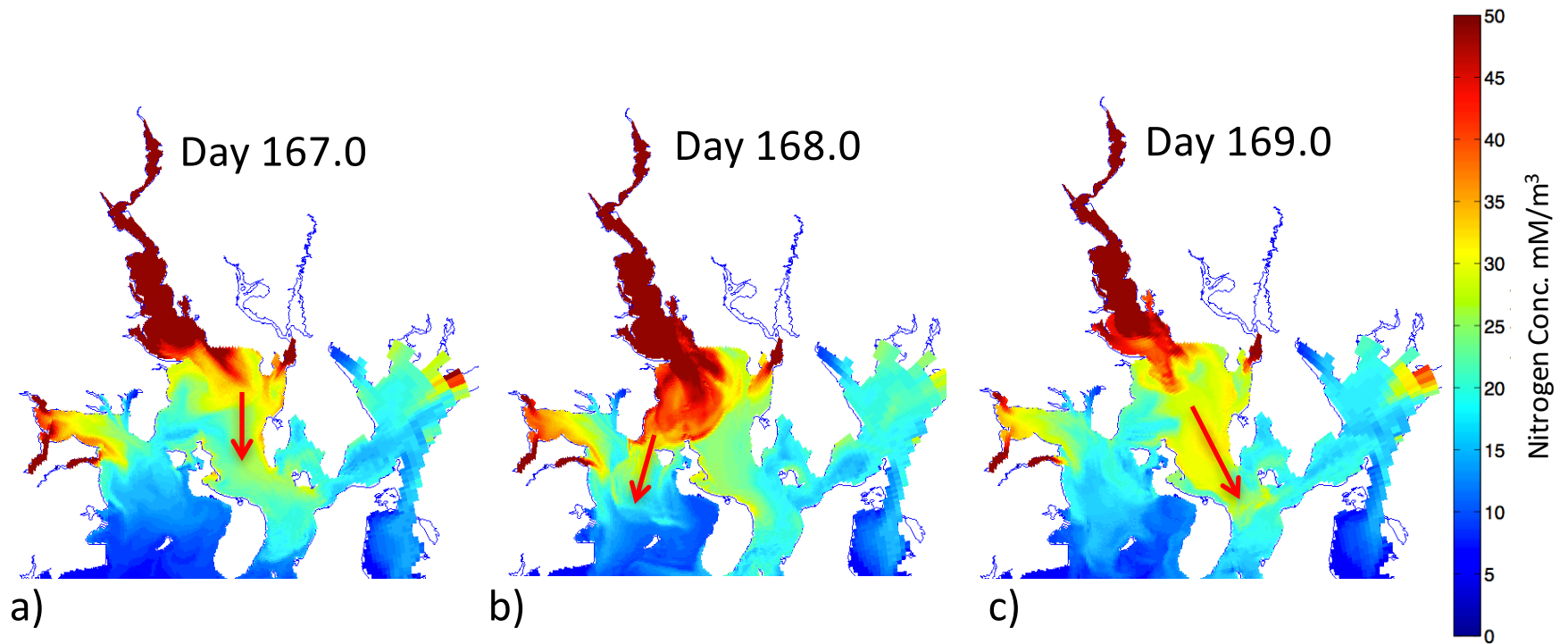


Figure 36. Color contours showing surface N fields for a case where the WWTFs release at nitrogen levels of 355 mM m^{-3} (5 mg L^{-1}). Red colors are 50 mM m^{-3} . Key features are higher N concentrations in the Providence and Seekonk Rivers. Frames show the oscillatory nature of the down-bay N-plume a) decimal day 167 with the N-plume along the northeastern shore of Ohio Ledge, entering the East Passage, b) decimal day 168 when the N-plume enters the upper West Passage and c) day 169 when the N-plume is back favoring the East Passage dispersion pathway. As summarized in Kincaid (2012), when dye was only a passive tracer, this is a common, representative oscillatory pattern for the N-plume, cycling between different shores of Ohio Ledge.

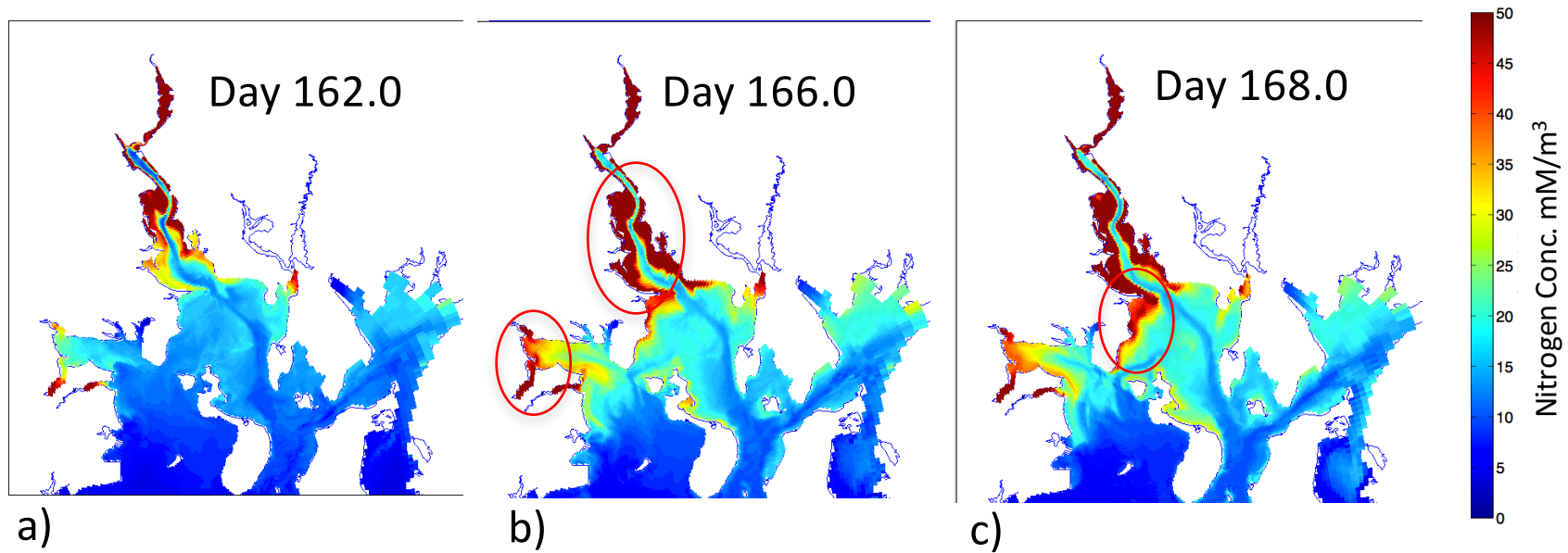


Figure 37. Color contours showing near bottom (sigma layer 5) N fields for 355 mM m^{-3} (5 mg L^{-1}). Red colors are 50 mM m^{-3} . Key, repeatable features are higher bottom N concentrations within the shallow regions of the Providence River, along northwestern shore of Ohio Ledge and inner Greenwich Bay. Frames are a) decimal day 162, b) decimal day 166 and c) day 168.

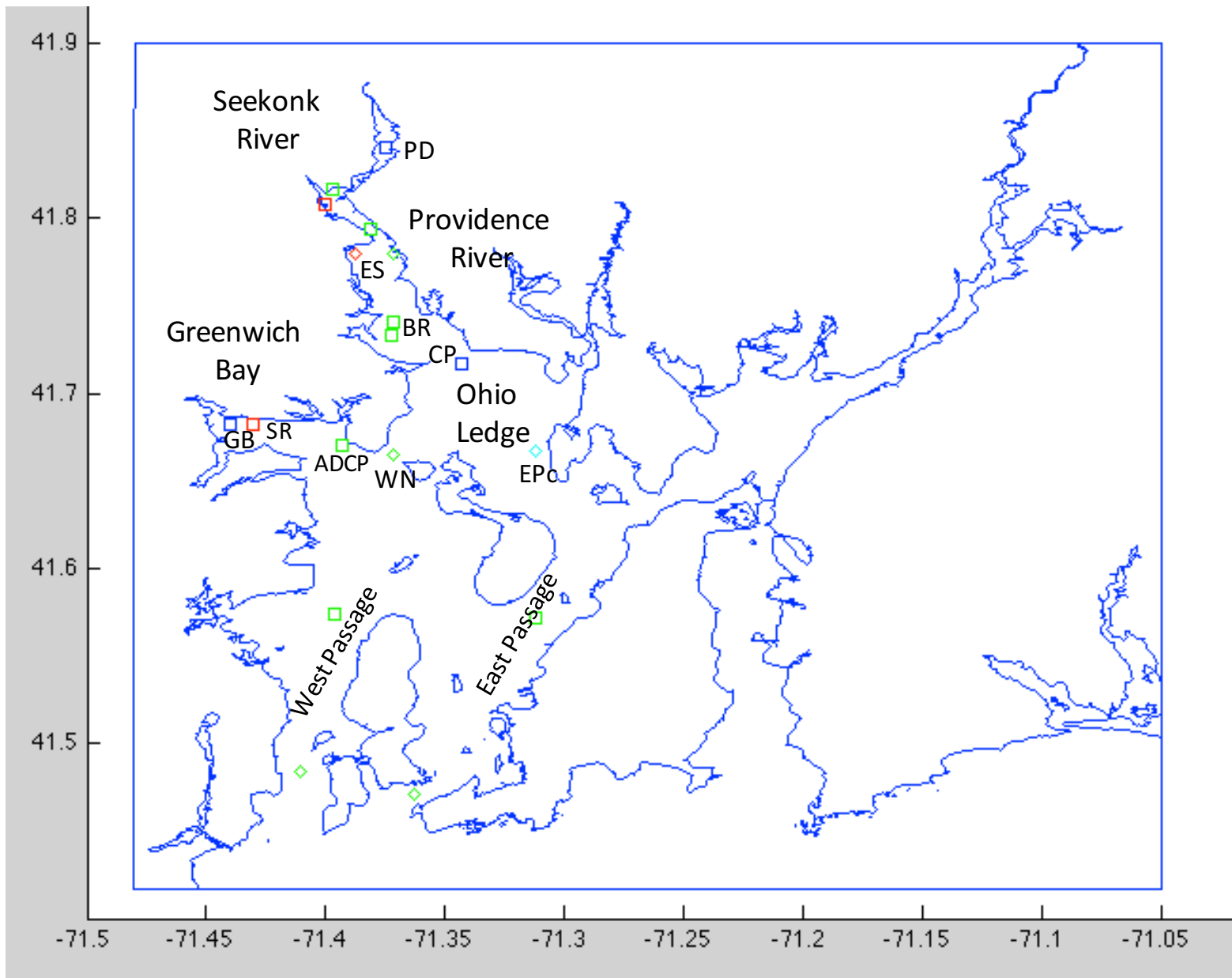


Figure 38. Map of ROMS-NPZD stations used in constructing N,P versus latitude plots and N,P versus time plots. Stations span the Providence River, Greenwich Bay, Ohio Ledge and lower East and West Passages. Symbols are ROMS station outputs: PD=Phillipsdale, ES=Edgewood Shoals, BR=Bullocks Reach, CP=Conimicut Pt., GB=Greenwich Bay, SR=Sally Rock, WN=Warwick Neck, EPC=East Passage channel, ADCP=ADCP site in Greenwich Bay channel.

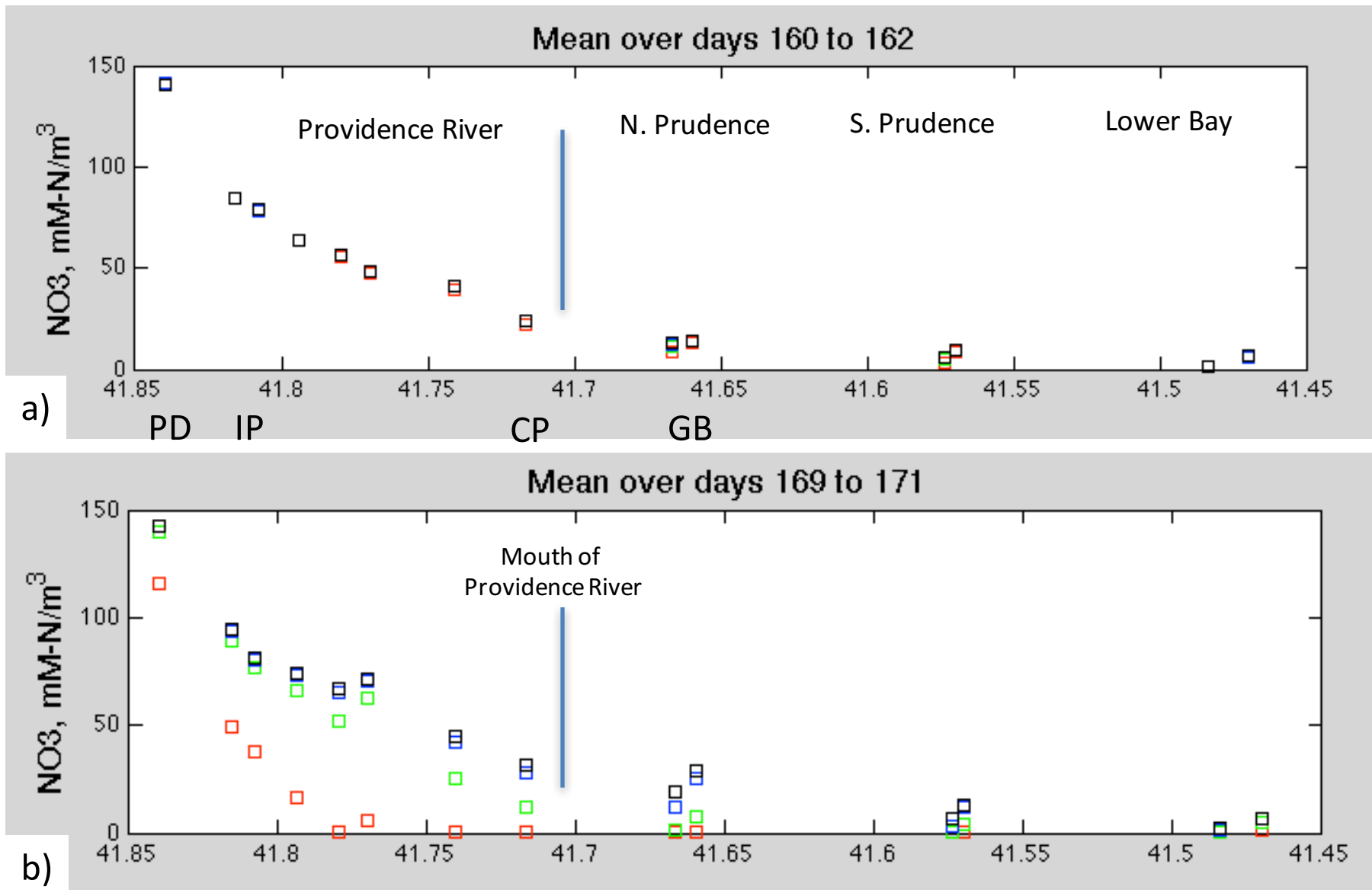


Figure 39. Plots of nitrogen concentration versus latitude for spring-summer ROMS–NPZD simulation for a reference case (no growth-black) and 3 values for phytoplankton uptake (growth) rates (Red: $V_m=2.5 \text{ day}^{-1}$, Green: $V_m=2 \text{ day}^{-1}$ and Blue: $V_m=1.5 \text{ day}^{-1}$). Frames show nutrient distributions before a bloom begins and at a late stage of the bloom. The reference case here is where the nutrient fields are like chemical dyes, advection, diffusion and no biological adjustment. Vertical blue line represents the mouth of the Providence River in all of these latitudinal plots.

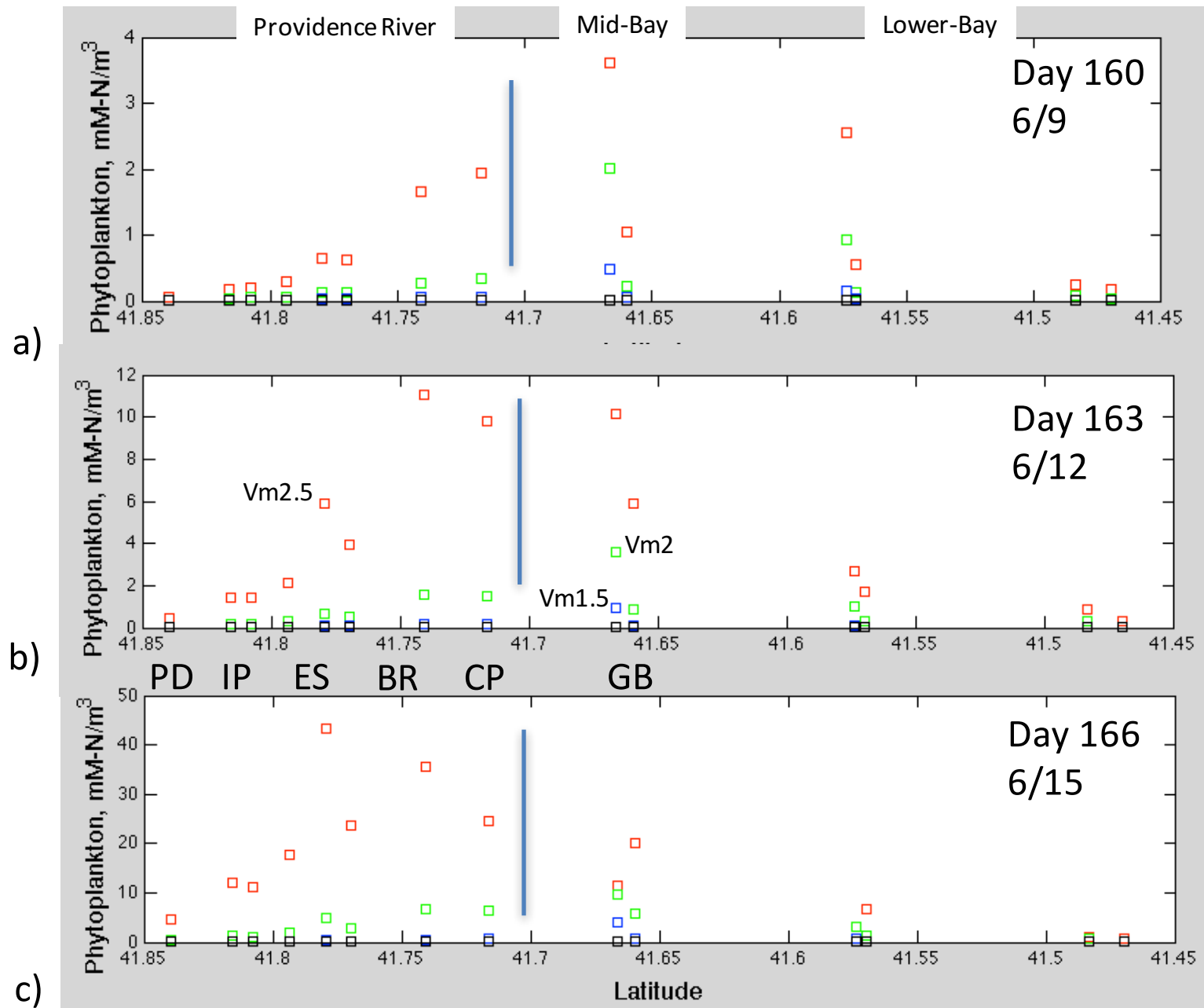


Figure 40. Plots of phytoplankton concentration versus latitude for cases with WWTF levels of 355 mM m⁻³ (5 mg/L) and highlighting the difference between three N uptake rates (R:Vm2.5, G:Vm2, B:Vm1.5). Start of bloom at mid-latitude. CP=Conimicut Pt., BR=Bullocks Reach, ES=Edgewood Shoal, GB=Greenwich Bay, WP=West Passage at Warwick Neck.

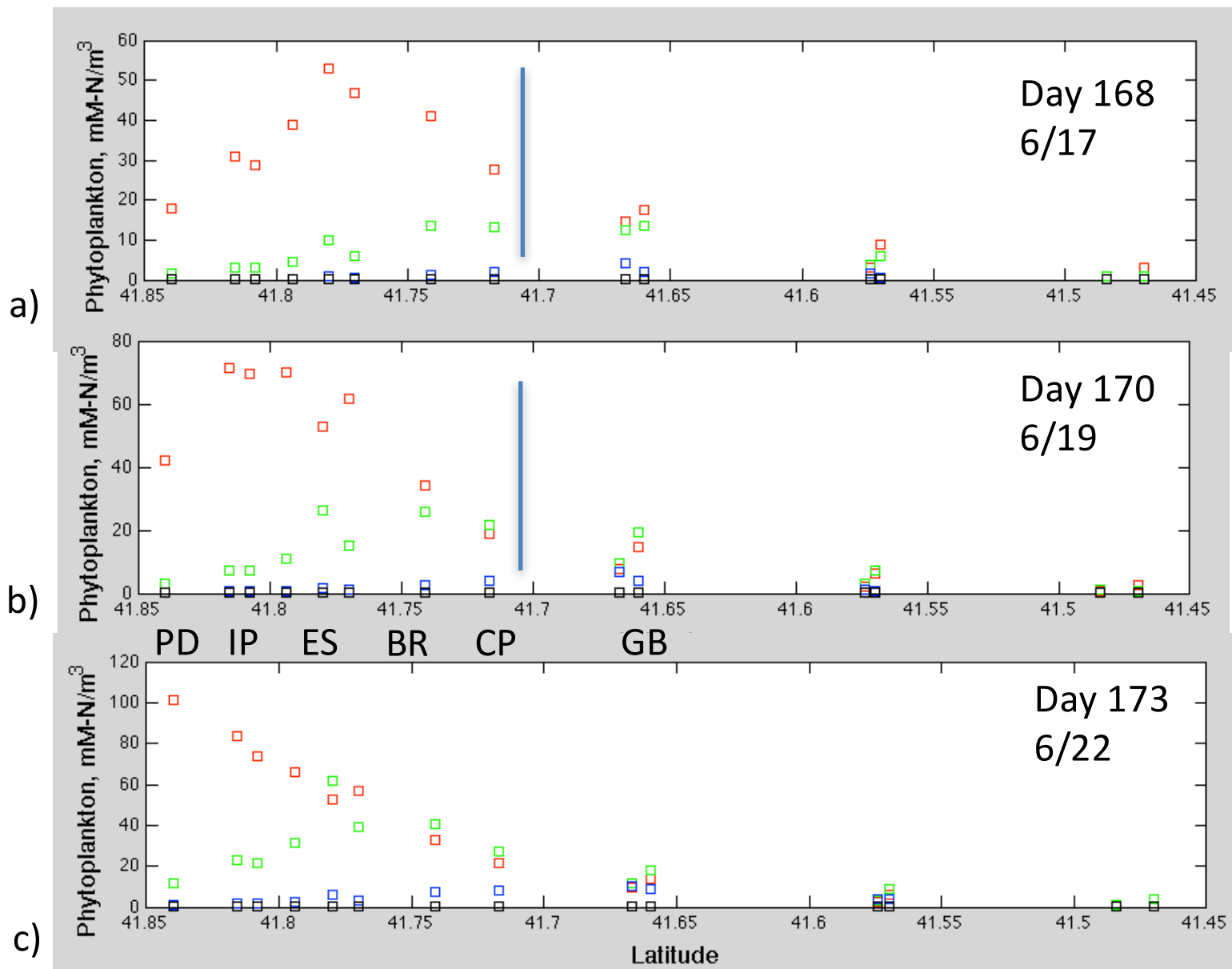


Figure 41. Plots of phytoplankton concentration versus latitude for cases with WWTF levels of 355 mM m⁻³ (5 mg/L) and highlighting the difference between three N uptake rates (R:Vm2.5, G:Vm2, B:Vm1.5). Plots show the progression of the bloom to the north for the Vm2.5 case. A lower amplitude bloom occurs for Vm2 and progresses northward at a slower rate. IP=India Point. PD=Phillipsdale

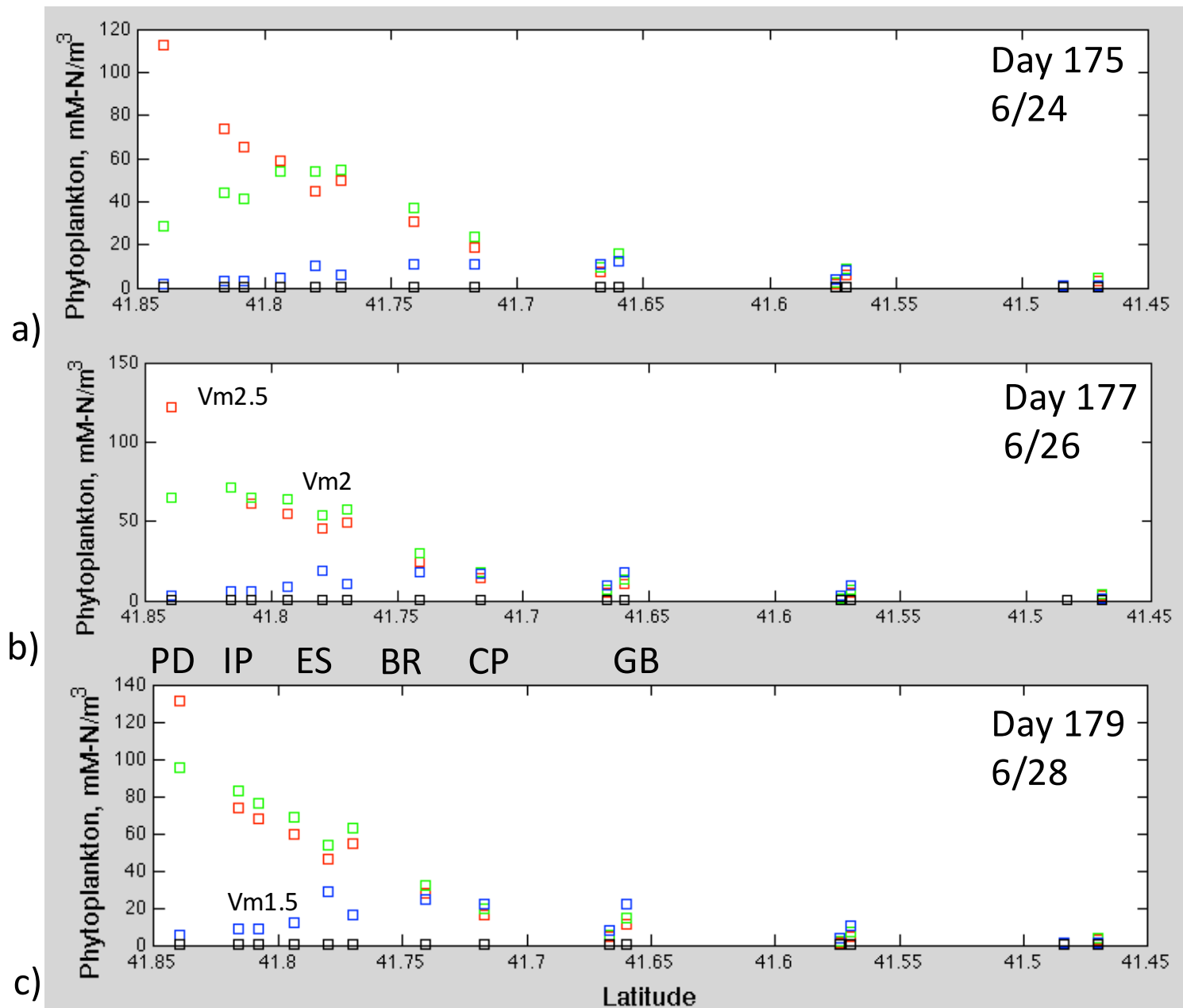


Figure 42. Plots of phytoplankton concentration versus latitude for cases with WWTF levels of 355 mM m⁻³ (5 mg/L) and highlighting the difference between three N uptake rates (R:Vm2.5, G:Vm2, B:Vm1.5). Plots show the late stage progression of the bloom to the northernmost reaches of the Seekonk River for the Vm2 case. A low amplitude bloom is just occurring for the smallest uptake rate of Vm1.5.

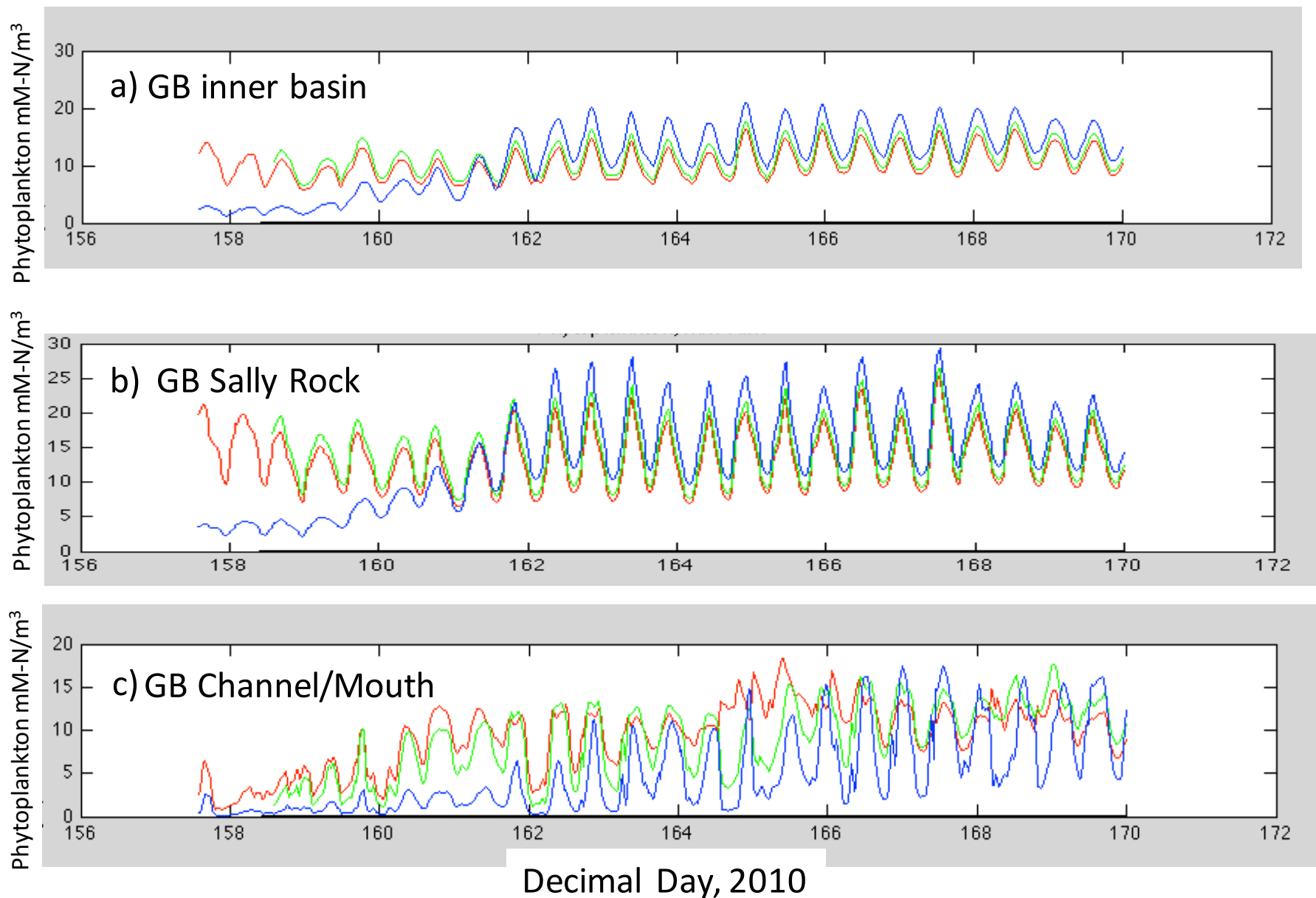


Figure 43. Plots of surface phytoplankton concentration (mM m^{-3}) versus time in Greenwich Bay for cases of all WWTFs releasing at 355 mM/m^{-3} (5 mg/L) and for three different nutrient uptake rates (Red: $V_m = 2.5 \text{ day}^{-1}$, Green: $V_m = 2 \text{ day}^{-1}$ and Blue: $V_m = 1.5 \text{ day}^{-1}$). Plots show that all V_m values result in production (slower with $V_m = 1.5$). The June bloom ($>20 \text{ mM/m}^{-3}$) near Sally Rock occurs at roughly day 162.

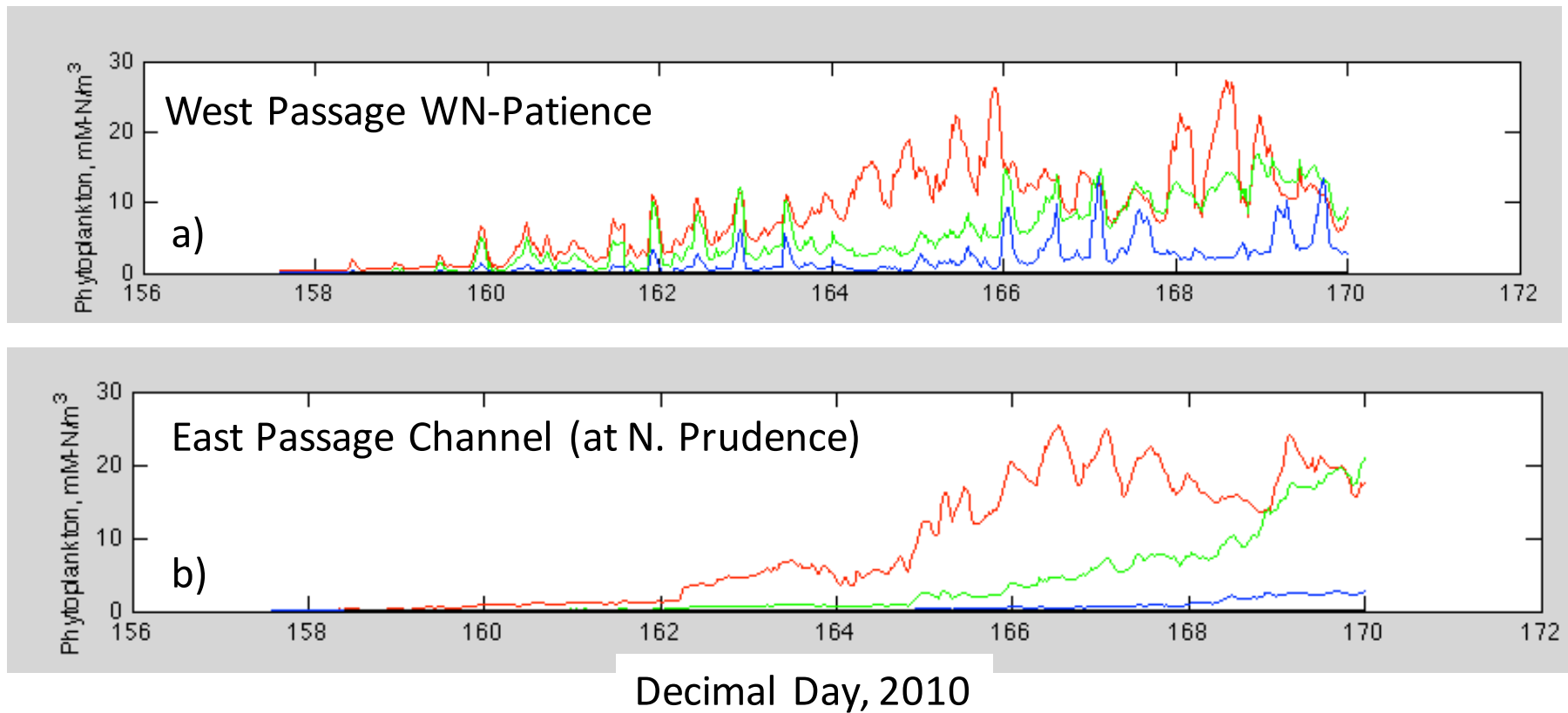


Figure 44. Plots of time series of surface phytoplankton concentration (mM m^{-3}) in the mid-Bay within each channel at latitudes equal to North Prudence Island. Plots are for cases of all WWTFs releasing at 355 mM/m^{-3} (5 mg/L) and for three different nutrient uptake rates (Red: $V_m=2.5 \text{ day}^{-1}$, Green: $V_m=2 \text{ day}^{-1}$ and Blue: $V_m=1.5 \text{ day}^{-1}$). Plots show that uptake rate of $V_m=2.5$ results in a bloom ($>20 \text{ mM m}^{-3}$) first in the West Passage (Warwick Neck) and then the East Passage channel. A smaller uptake rate of 2.0 shows a delayed phytoplankton production, reaching $\sim 20 \text{ (mM m}^{-3})$ at days 169-170, or roughly five days later than the higher $V_m 2.5$ rate. The smallest uptake rate ($V_m=1.5 \text{ day}^{-1}$) produces a small bloom and no bloom during this period in the West and East Passages, respectively.

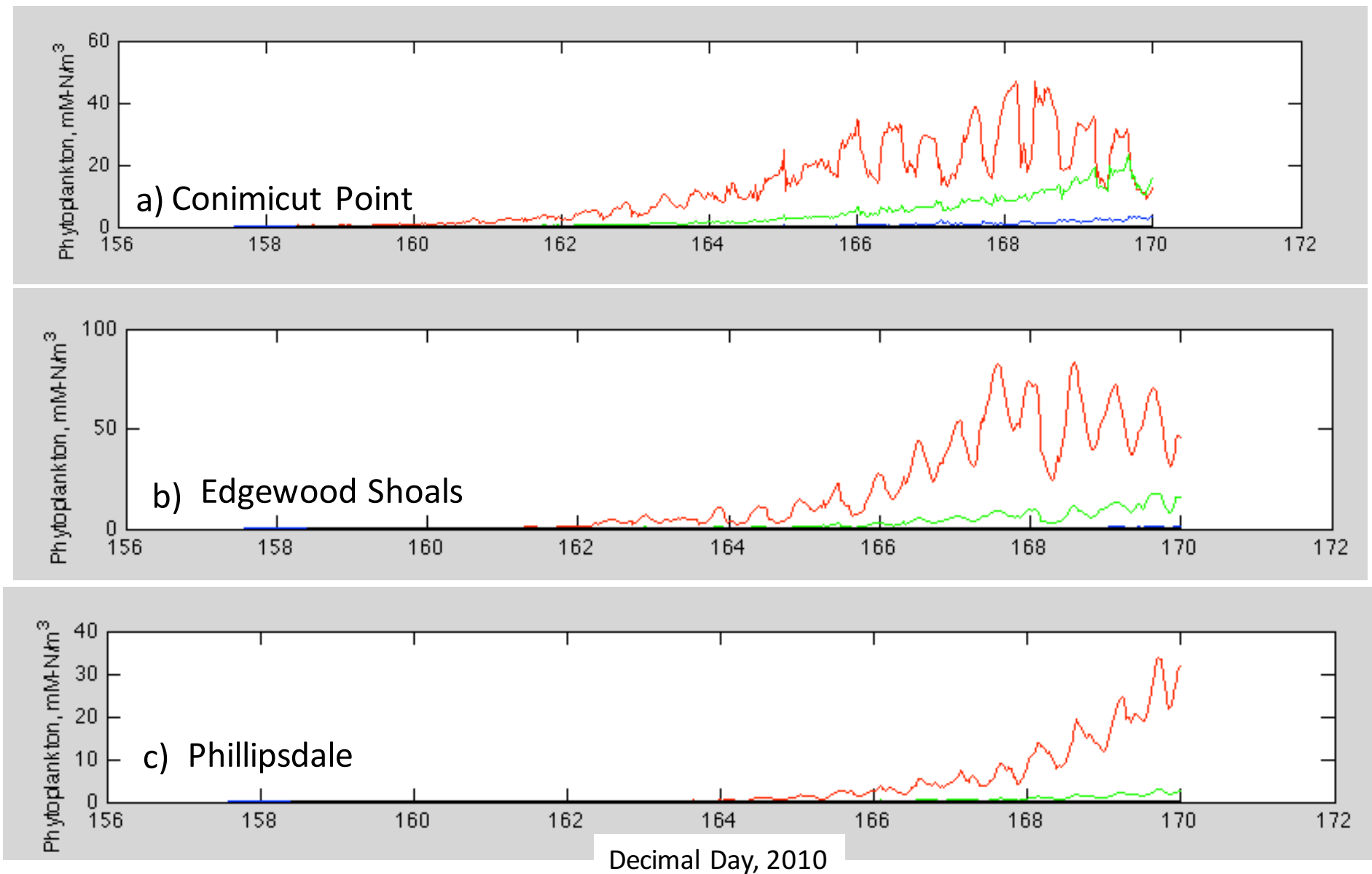
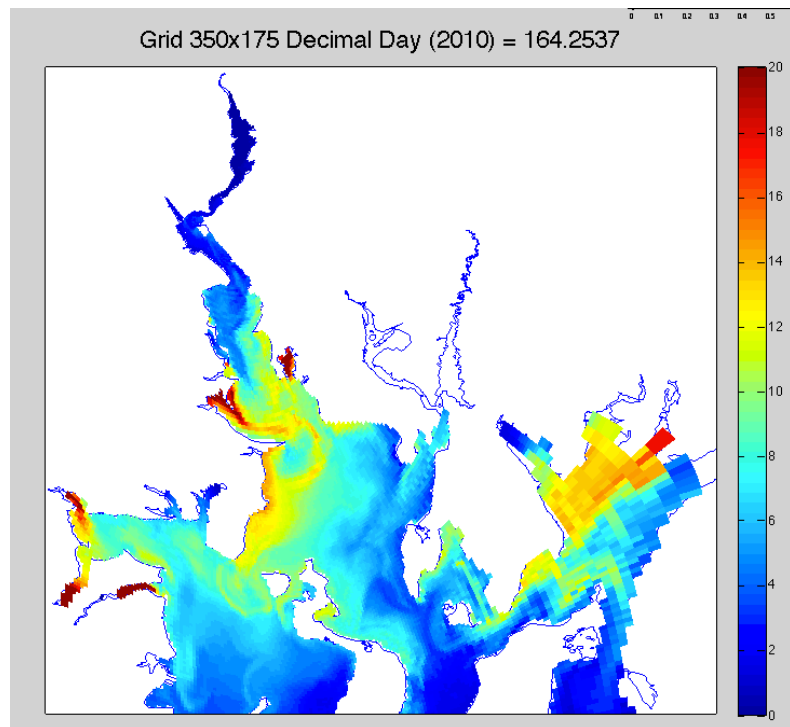
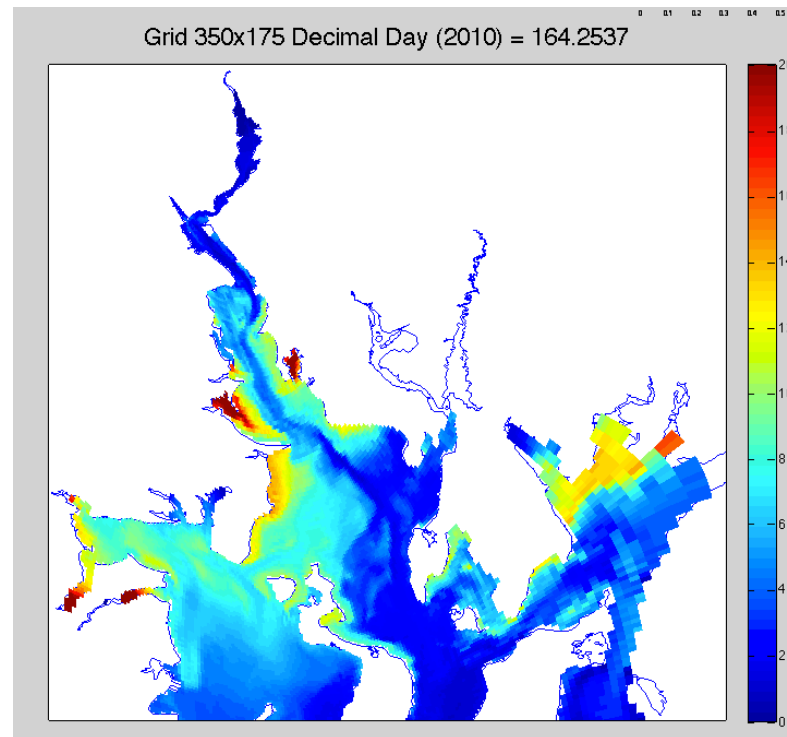


Figure 45. Plots of time series of surface phytoplankton concentration (mM m^{-3}) progressing northward through the Providence and Seekonk Rivers. Plots are for cases of all WWTFs releasing at 355 mM/m^{-3} (5 mg/L) and for three different nutrient uptake rates (Red: $V_m = 2.5 \text{ day}^{-1}$, Green: $V_m = 2 \text{ day}^{-1}$ and Blue: $V_m = 1.5 \text{ day}^{-1}$). Blooms follow a progression in timing from the south to north. In agreement with NBC data collected during this period, the model shows the bloom is strongest in the Pomham Rocks/Edgewood region, with a smaller magnitude near Phillipsdale. In agreement with buoy and NBC data, the phase lag from GB to CP to Edgewood is in the 5-9 day range.



a)



b)

Figure 46. Contour images of near-surface (a) and near-bottom (b) phytoplankton concentrations (red=20 mM m^{-3}) for early to mid progression of June 2010 simulated bloom. This is for a ROMS-NPZD simulation with all WWTFs at 355 mM m^{-3} (5 mg/L) and a phytoplankton nutrient uptake rate of $V_m=2.5 \text{ day}^{-1}$. A pattern that is seen in many simulations of the June 2010 Narragansett Bay high chlorophyll event is that elevated phytoplankton levels tend to initiate within the shallows of Greenwich Bay, Mt. Hope Bay (northern shore), the shallow region off Rocky Pt. and the shallow edges the Providence River (particularly between Gaspee and Conimicut Points).

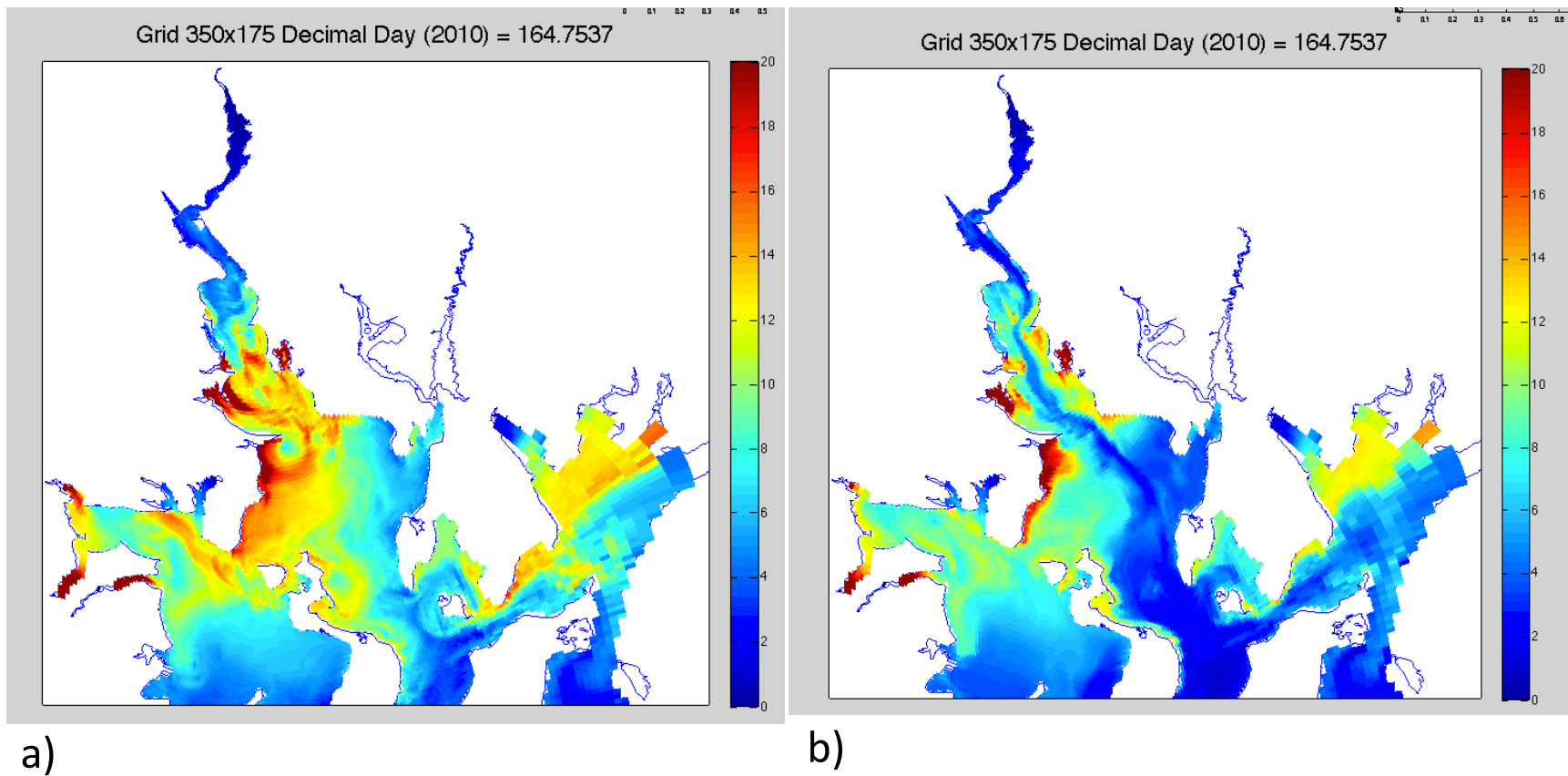
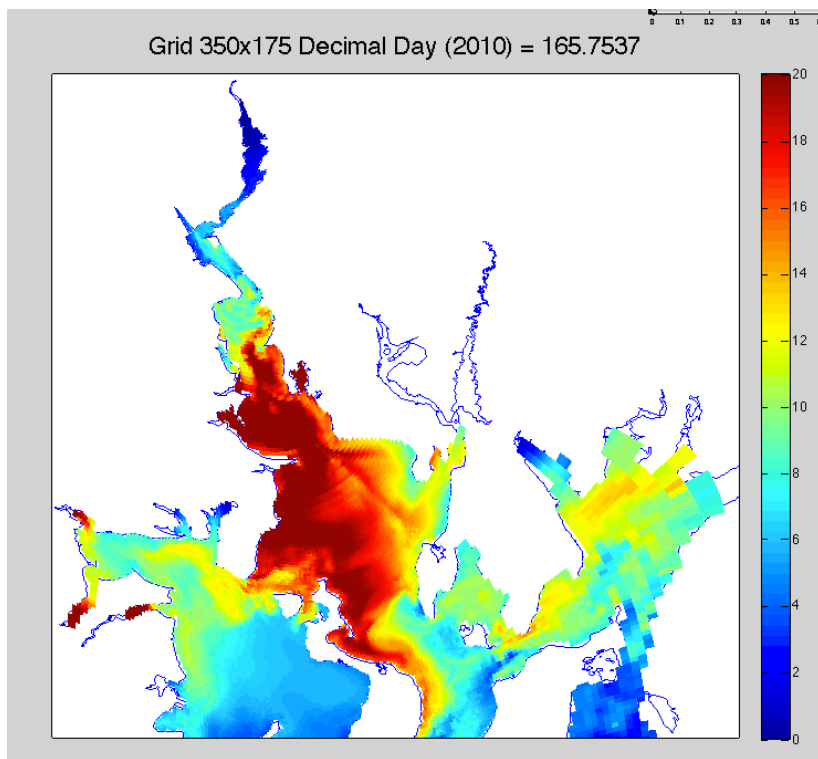
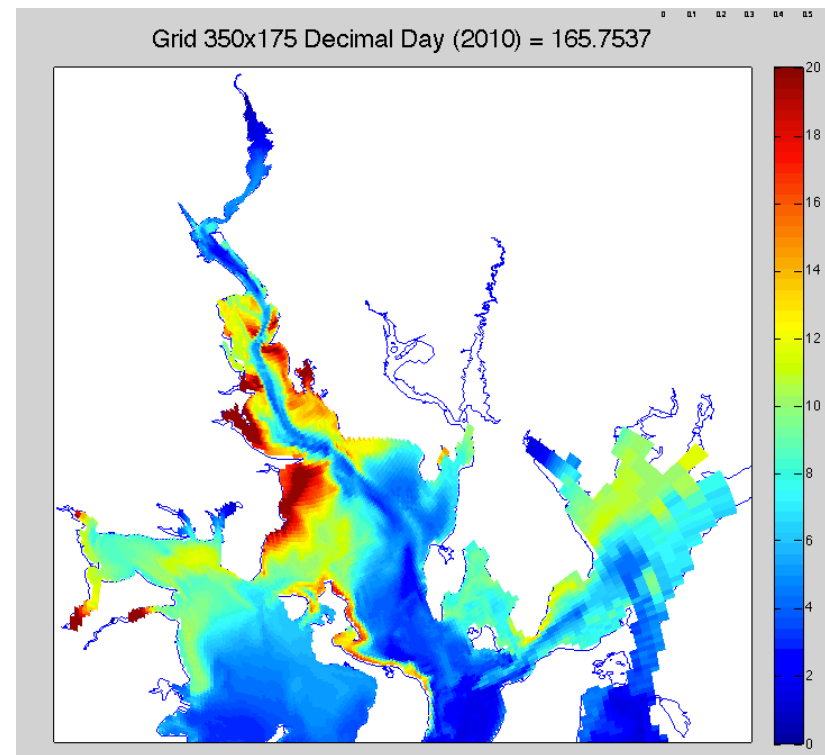


Figure 47. Contour images of near-surface (a) and near-bottom (b) phytoplankton concentrations (red=20 mM m^{-3}) for mid progression of June 2010 simulated bloom (same conditions as previous figure, $\text{WWTF}=355 \text{ mM m}^{-3}$ (5 mg/L) , $V_m=2.5 \text{ day}^{-1}$). The patches of phytoplankton production are growing in strength, particularly within the shallows of the lower Providence River.



a)



b)

Figure 48. Later contour images for the case in Figures 46-47 of near-surface (a) and near-bottom (b) phytoplankton concentrations (red=20 mM m^{-3}) for day 165 (June 14). Parameters are $\text{WWTF}=355 \text{ mM m}^{-3}$ (5 mg/L) , $V_m=2.5 \text{ day}^{-1}$. The bloom has expanded significantly within the surface waters of the mid-Bay region. This feature is exporting phytoplankton (and detritus) northward onto Edgewood Shoals and up the shipping channel towards the Seekonk River. There is also significant phytoplankton transport down the eastern shore of Prudence Island, within the East Passage.

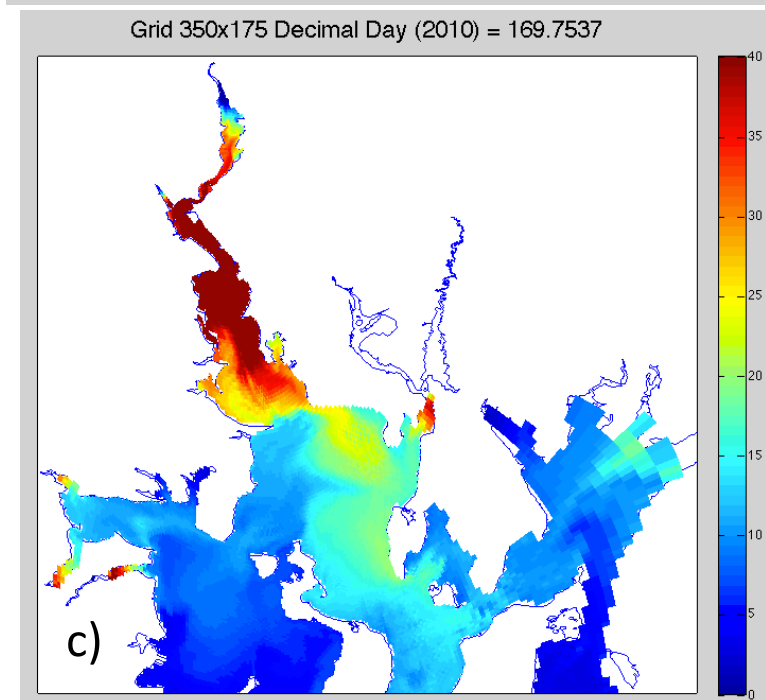
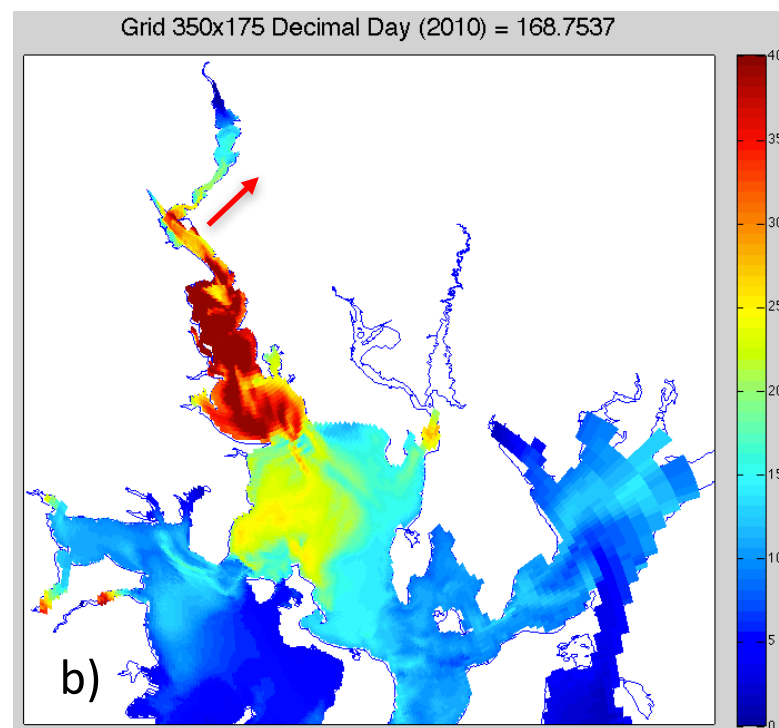
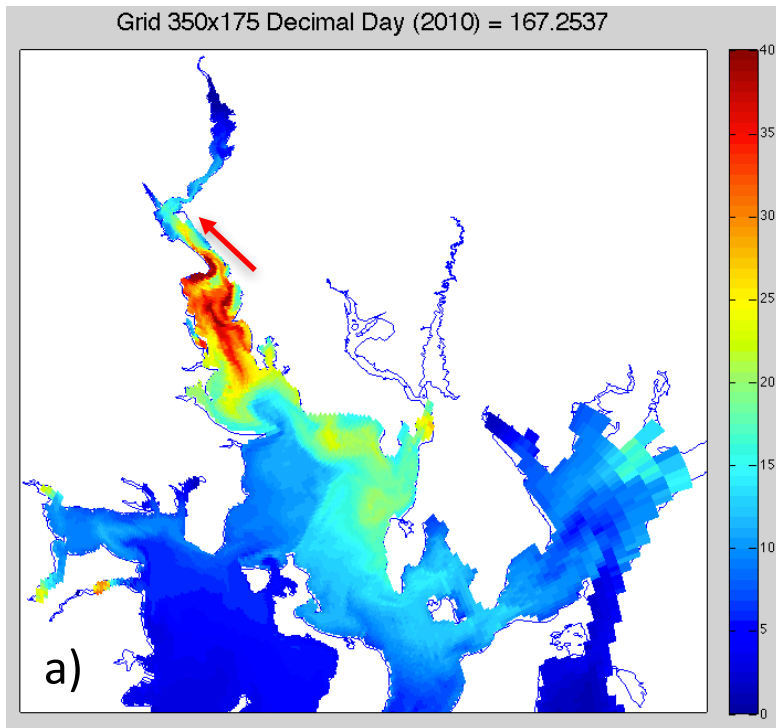


Figure 49. Longer period view of near-surface phytoplankton concentrations for days 167, 168 and 169 for this same case in Figures 46-48 with $WWTF=355 \text{ mM m}^{-3}$ (5 mg/L), $V_m=2.5 \text{ day}^{-1}$. Because the bloom has grown, the colorbar is expanded (red= 40 mM m^{-3}). There is significant phytoplankton growth within the Edgewood Shoals/Pomham Rocks mid-region of Providence River. Subsequent biomass is transported northward into the Seekonk River (c). Viewed as a movie, the tidal pumping and residual transport that carries products of this bloom northward into the Seekonk River is clearly shown to follow a progression of the red arrows.

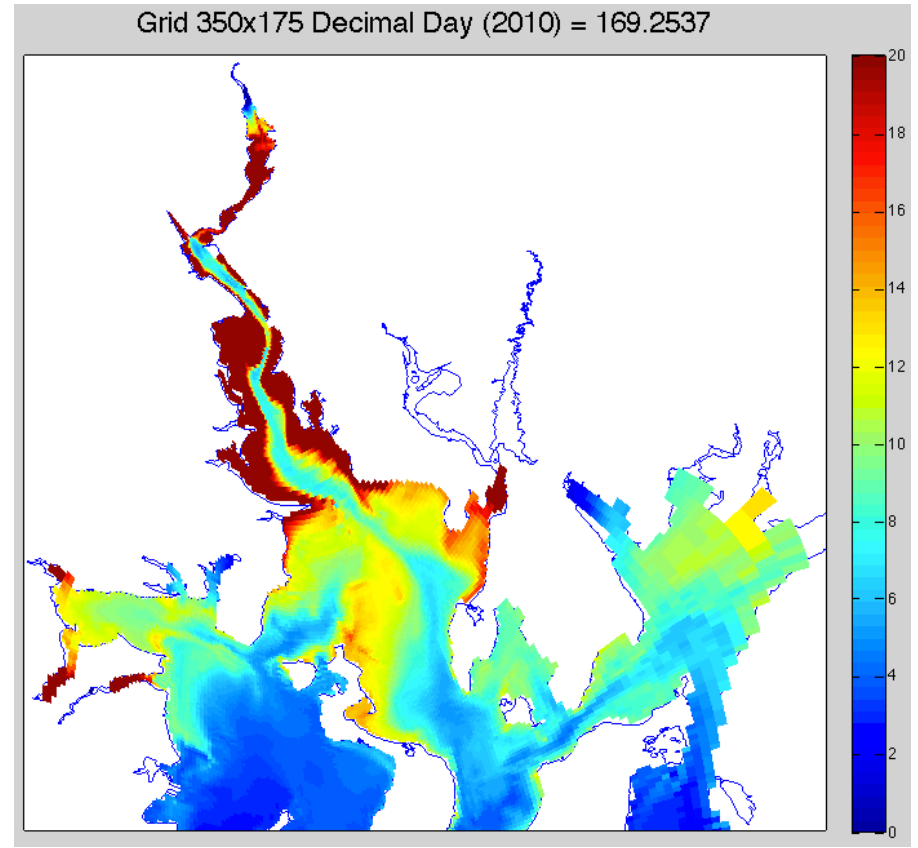
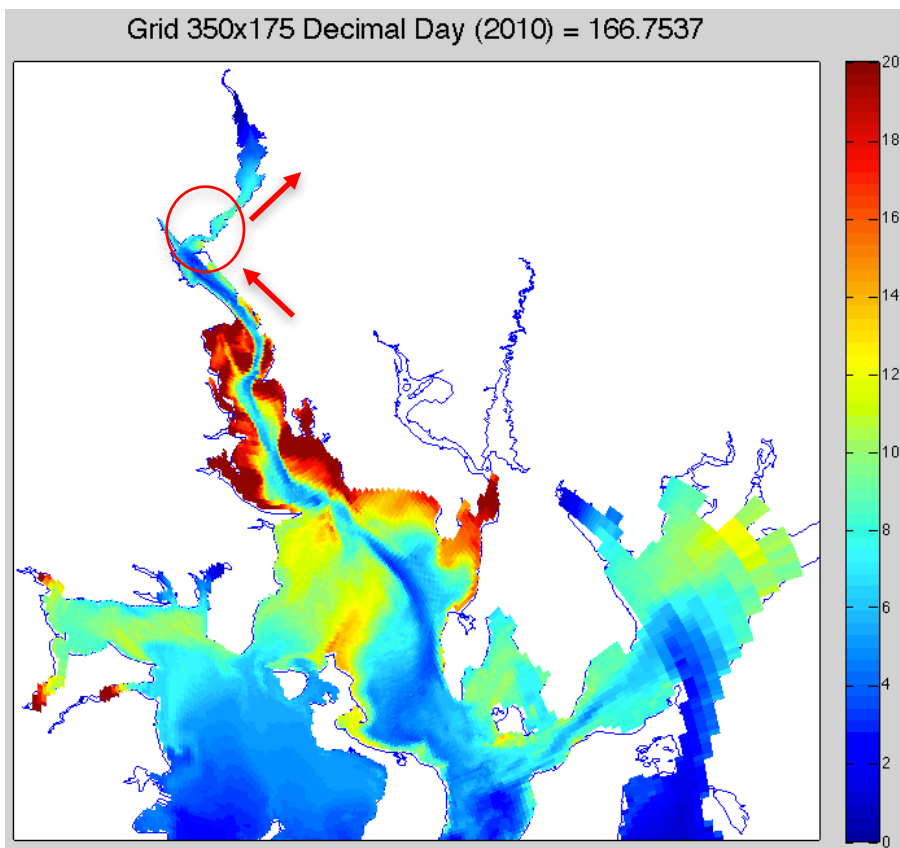
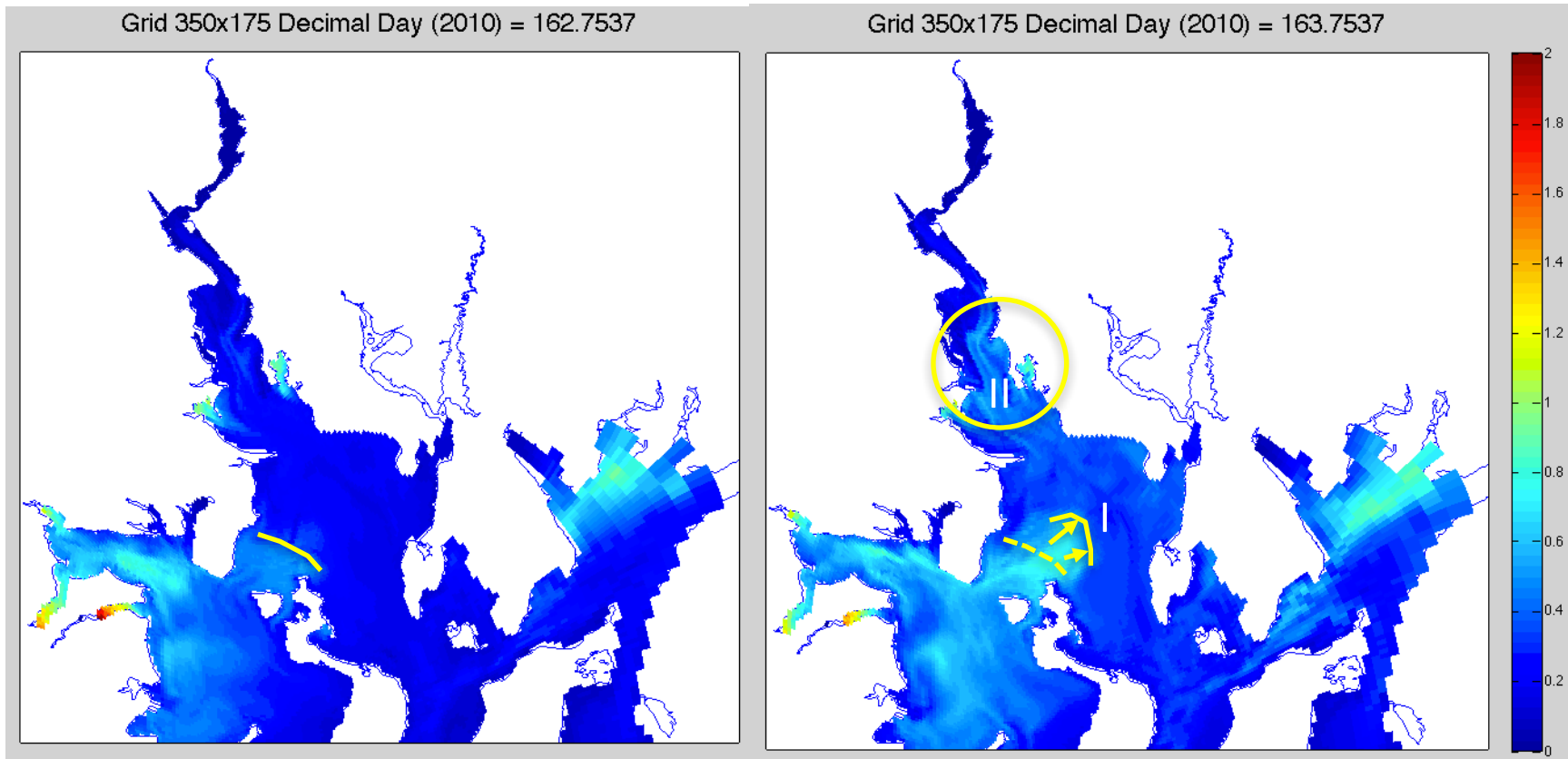


Figure 50. Contour images of near-bottom phytoplankton concentrations (red=20 mM m⁻³) for days 167 and 169. These contours also show there is significant phytoplankton growth within the Edgewood Shoals/Pomham Rocks mid-region of Providence River. Movie image sequences show the tidal pumping and residual transport that carries products of this bloom northward into the Seekonk River. Circle marks constriction at India Point, the interface between the Seekonk and Providence Rivers.



a)

b)

Figure 51. Contour images of near-bottom detritus concentrations (red=2 mM m⁻³) for days 162 and 163 in a case with WWTF=355 mM m⁻³ (5 mg/L) and Vm=2.5 . These contours show the early leaking of Greenwich Bay detrital pool onto Ohio Ledge. The frame sequence (over 24 hours) illustrates changes in detrital levels due to advection (I) and in-situ growth (II). (I) Detritus produced in Greenwich Bay is seen in 6 hour frame increments to advect northeastward across Ohio Ledge at ~2000m/24 hours, a residual flow of ~3 cm/s). (II) Also over this 24 hour period in-situ production of a deep detrital is seen in the central Providence River.

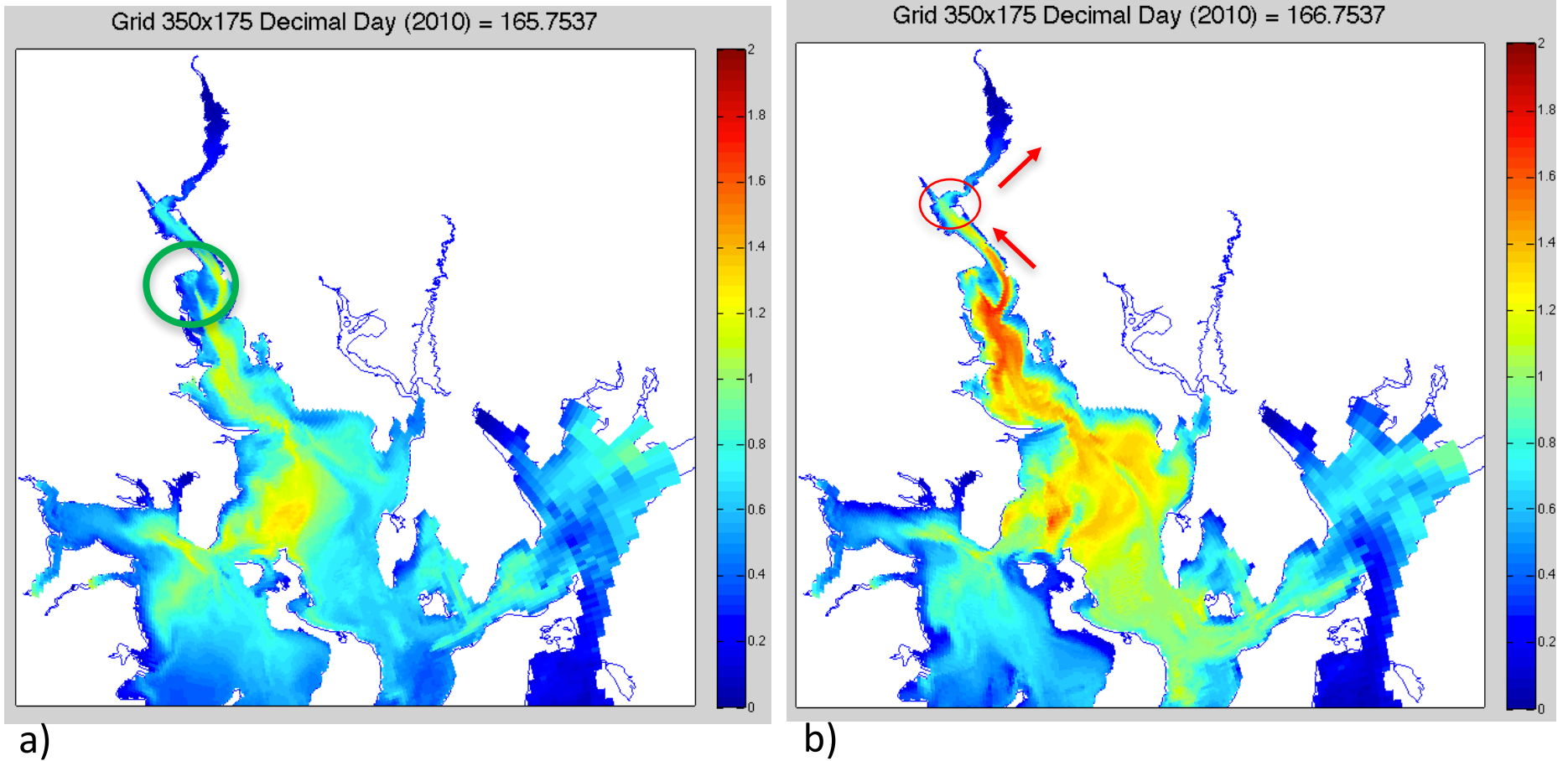


Figure 52. Contour images of near-bottom detritus concentrations ($\text{red}=2 \text{ mM m}^{-3}$) for days 165 and 166 for $\text{WWTF}=355 \text{ mM m}^{-3}$ (5 mg/L) and $\text{Vm}2.5$. Color contours show the detrital products from a bloom on Ohio Ledge where a combination of in-situ production and northward transported material influence the bloom within the Providence River. Annotations of circles and arrows highlight places where up-estuary advection of detritus is occurring in the Port Edgewood Channel and at India Point.

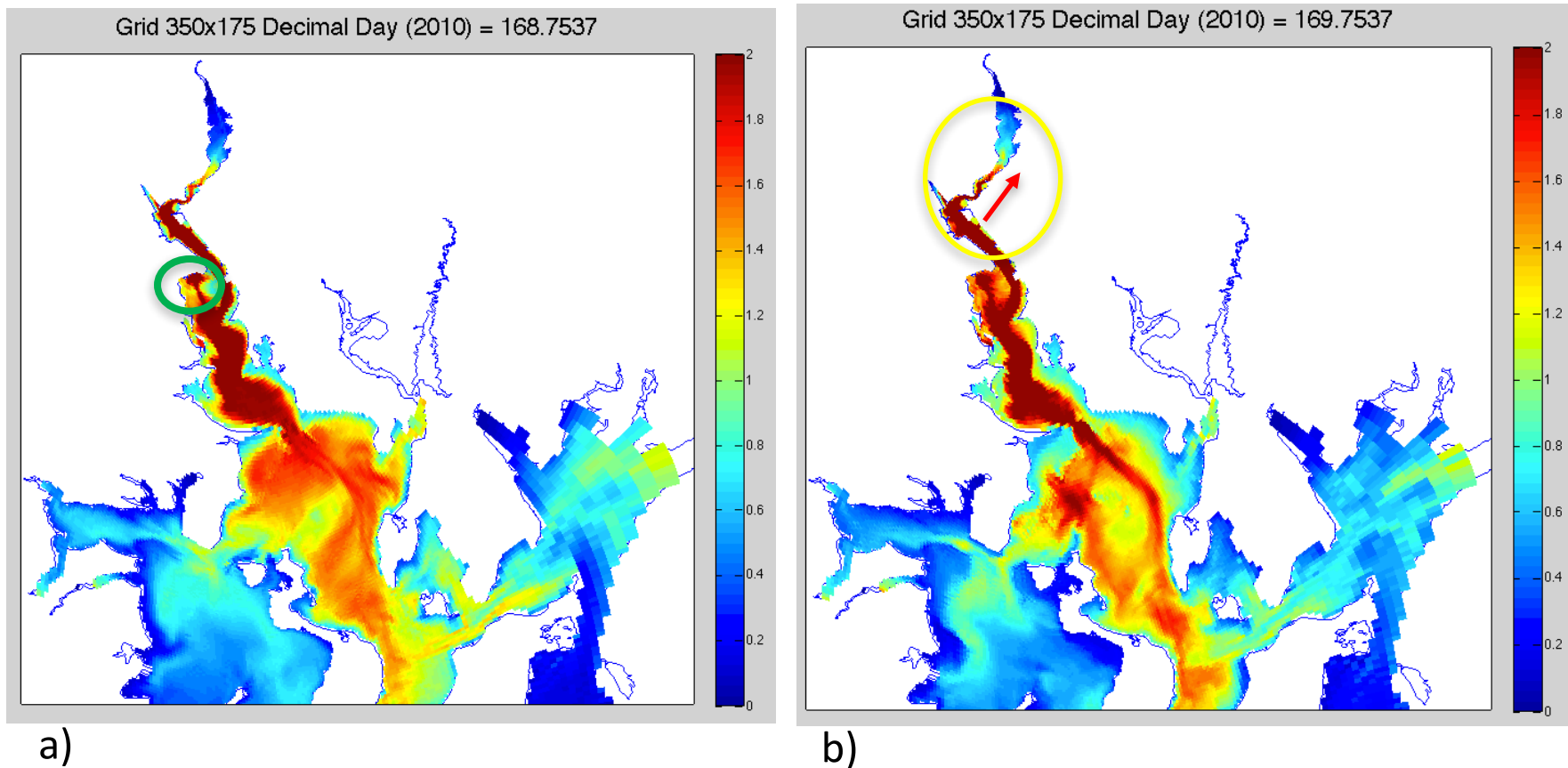


Figure 53. Contour images of near-bottom detritus concentrations (red=2 mM m⁻³) for days 168 and 170 for WWTF=355 mM m⁻³ (5 mg/L) and Vm2.5. This coincides with a period of intense production throughout the Providence River. As in prior two figures, detrital bloom products intensify due to a combination of in-situ production and advective transport of remotely generated products. Highlighted in the yellow circle, detrital products are seen in movies to pump northward past India Pt into the Seekonk River. The high detrital concentration (red) feature (highlighted in green) in (a) is a characteristic, repeatable plume pattern indicative of material rapidly advected up the Port Edgewood channel where it spreads radially within the old boat basin.

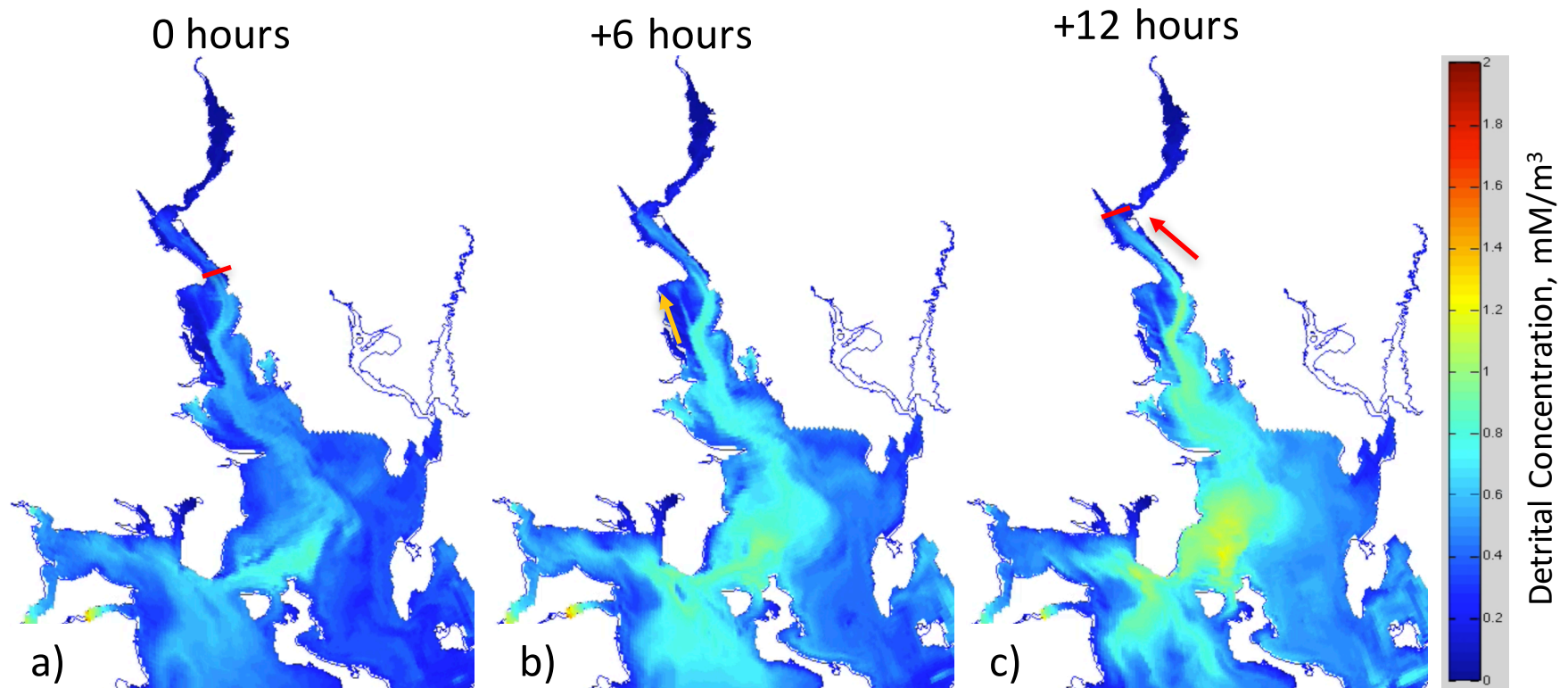


Figure 54. Similar to Figure 52, near-bottom detritus concentrations (red=2 mM m⁻³) are shown over 6 hour increments on day 166 for WWTF=355 mM m⁻³ (5 mg/L) and Vm2.5 to reveal details of the advection of material . Color contours show the detrital concentrations. Over 6-12 hours, the front of elevated detrital concentration is seen in movie output to pump northwestward up the Port Edgewood Channel and northward in the channel from Fields Point to India Point (highlighted by red arrows). Advective transport is 3.6 km in 12 hours, or a residual speed of ~8 cm/s, in line with current meter estimates in this region.

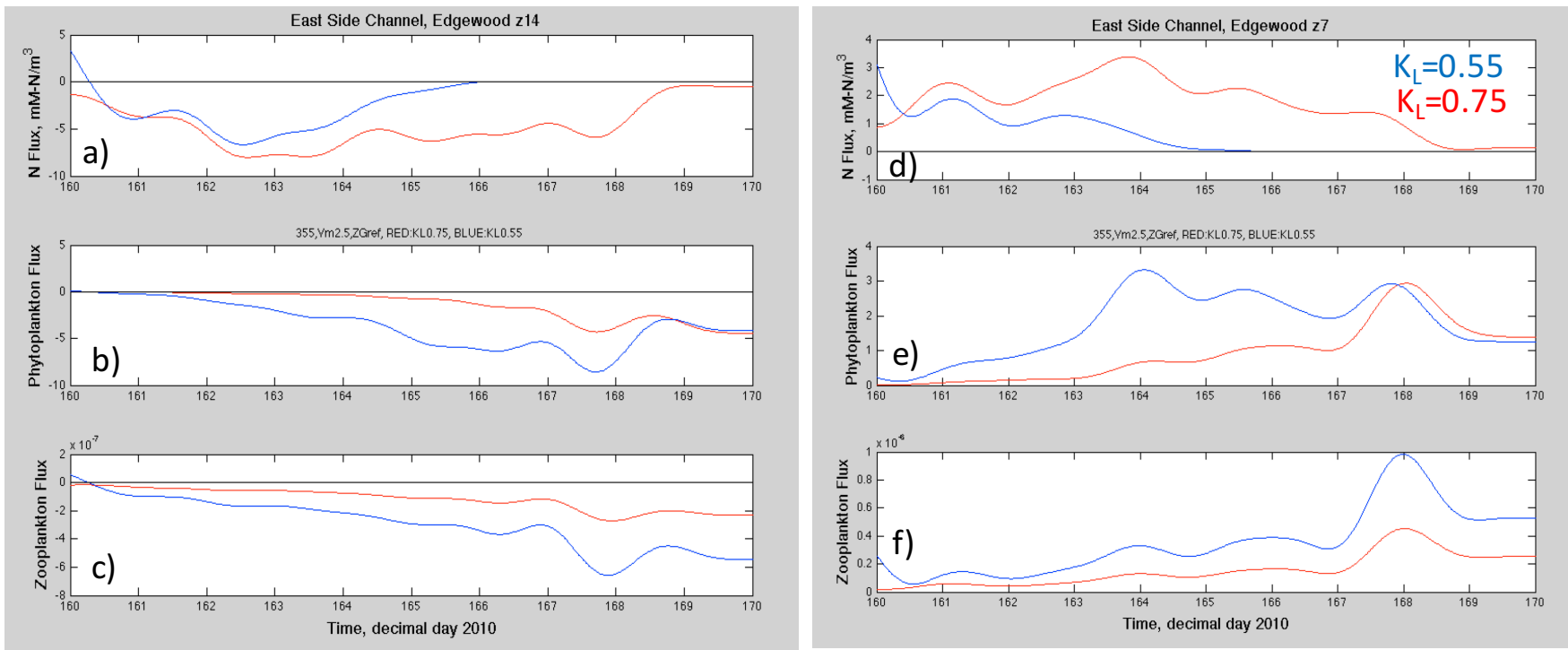


Figure 55. Time series plots of northward (a,c) nitrogen, ((b,e) phytoplankton and (c,f) zooplankton fluxes for ROMS station output in the east side of the shipping channel near Edgewood Shoals. Values are calculated by multiplying residual (de-tided) values for northward velocity with each field. Plots (a-c) show southward fluxes for all three fields in near-surface water. Frames (d-f) show northward fluxes of all fields in the deeper northward residual flow. All bloom products ride this residual current northward from Ohio Ledge to the Seekonk River. Location of the flux calculation station as shown in Figure 3.

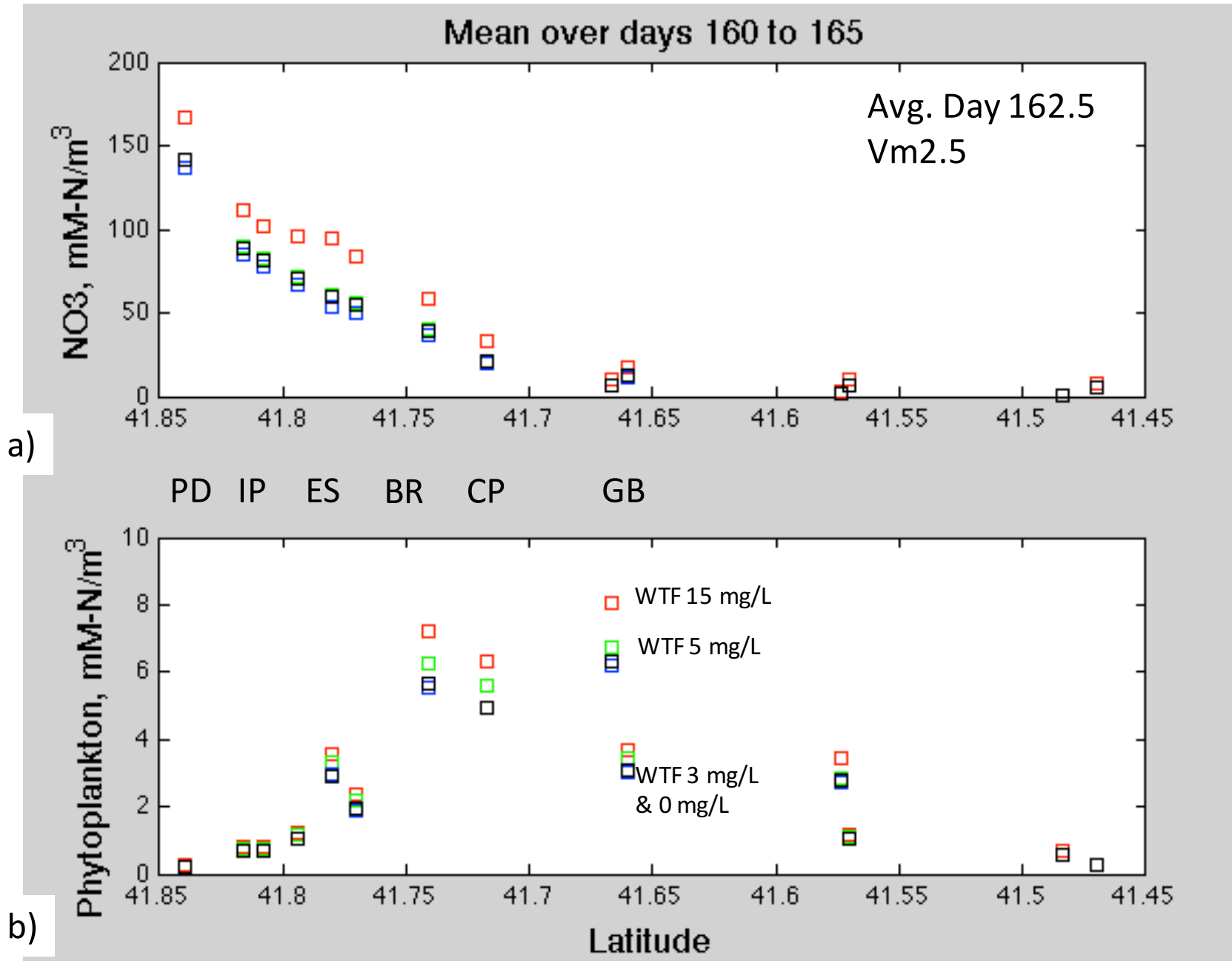


Figure 56. Plots of 6-day time averaged (days 160-165) N and P versus latitude for cases with $V_m=2.5$, comparing impact of different WWTF release strategies (WWTFs releasing at, R:1070 mM m^{-3} (15 mg/L), G:355 mM m^{-3} (5 mg/L), Blue:213 mM m^{-3} (3 mg/L), Black: 0 mM m^{-3} (0 mg/L)). These coincide to values of 15, 5, 3 and 0 mg L^{-1} .

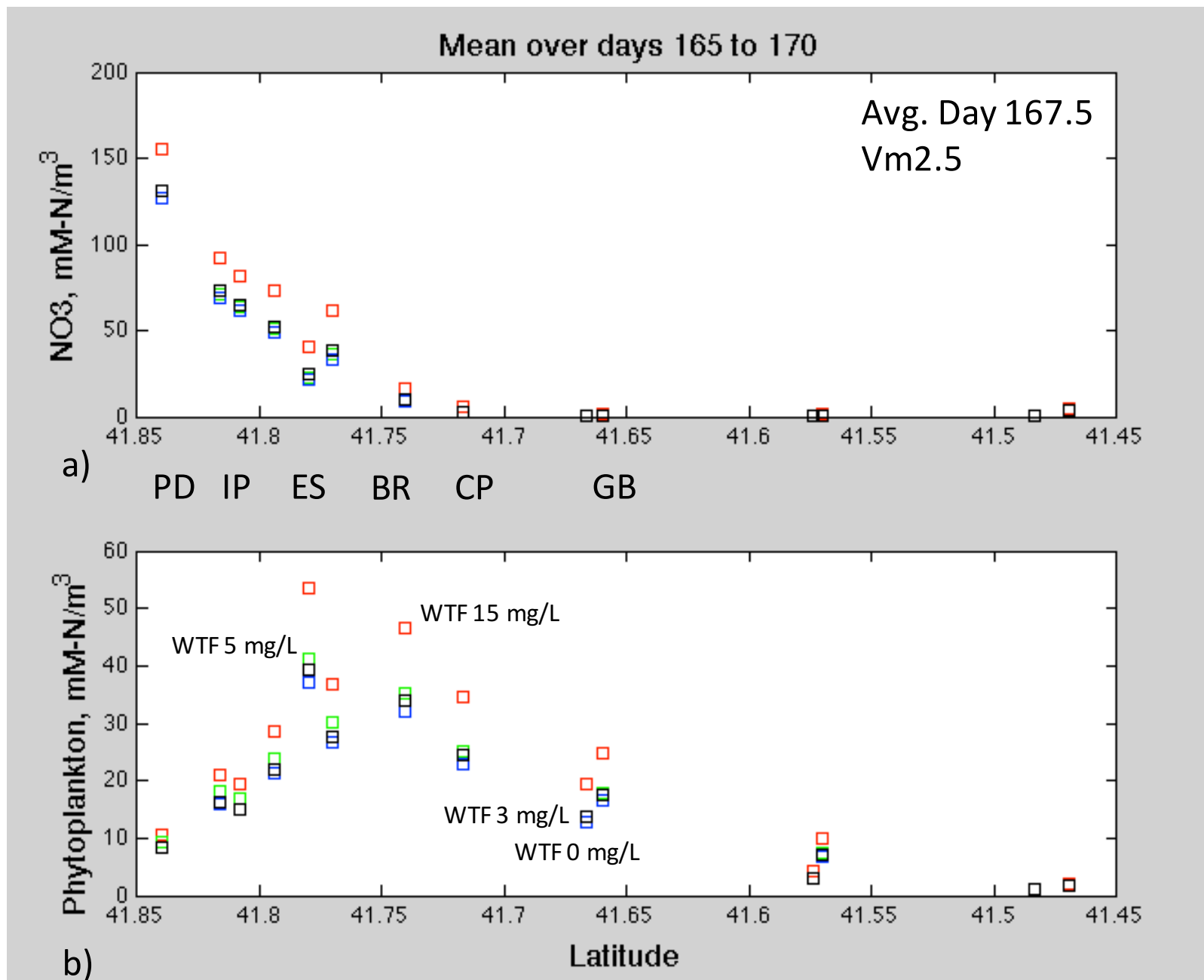


Figure 57. Plots of 6-day time averaged N and P versus latitude for cases with Vm=2.5 for days 165 to 170. Plots with different color squares compare impact of different WWTF release strategies (WWTFs releasing at, R:1070 mM m⁻³ (15 mg/L) G:355 mM m⁻³ (5 mg/L) , Blue:213 mM m⁻³ (3 mg/L), Black: 0 mM m⁻³ (0 mg/L)).

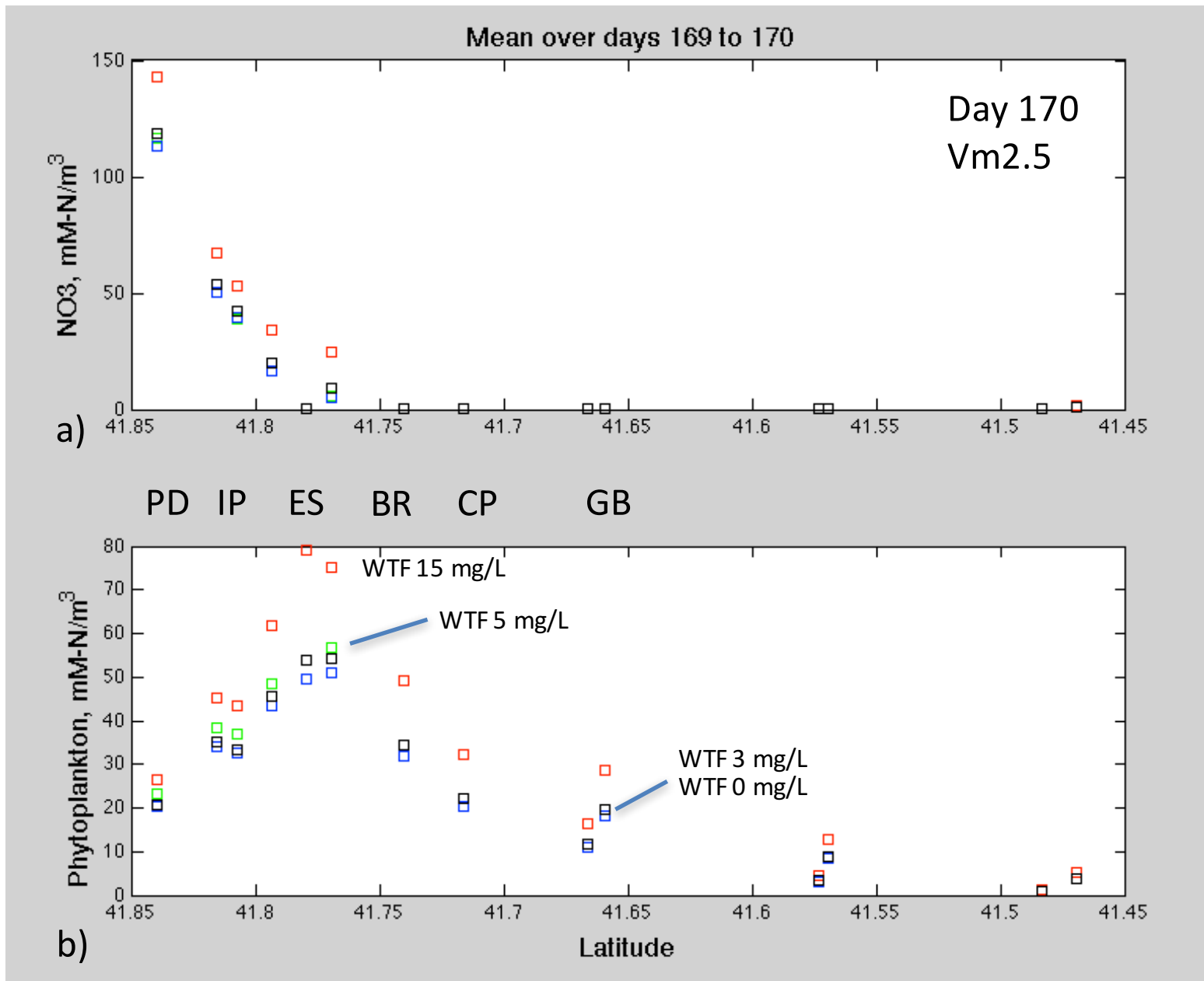


Figure 58. Plots of 2-day time averaged N and P versus latitude for cases with $V_m=2.5$ for day 170. comparing impact of different WWTF release strategies (WWTFs releasing at, R:1070 mM m⁻³ (15 mg/L) , G:355 mM m⁻³ (5 mg/L) , Blue:213 mM m⁻³ (3 mg/L) , Black: 0 mM m⁻³ (0 mg/L)). These coincide to values of 15, 5, 3 and 0 mg L⁻¹.

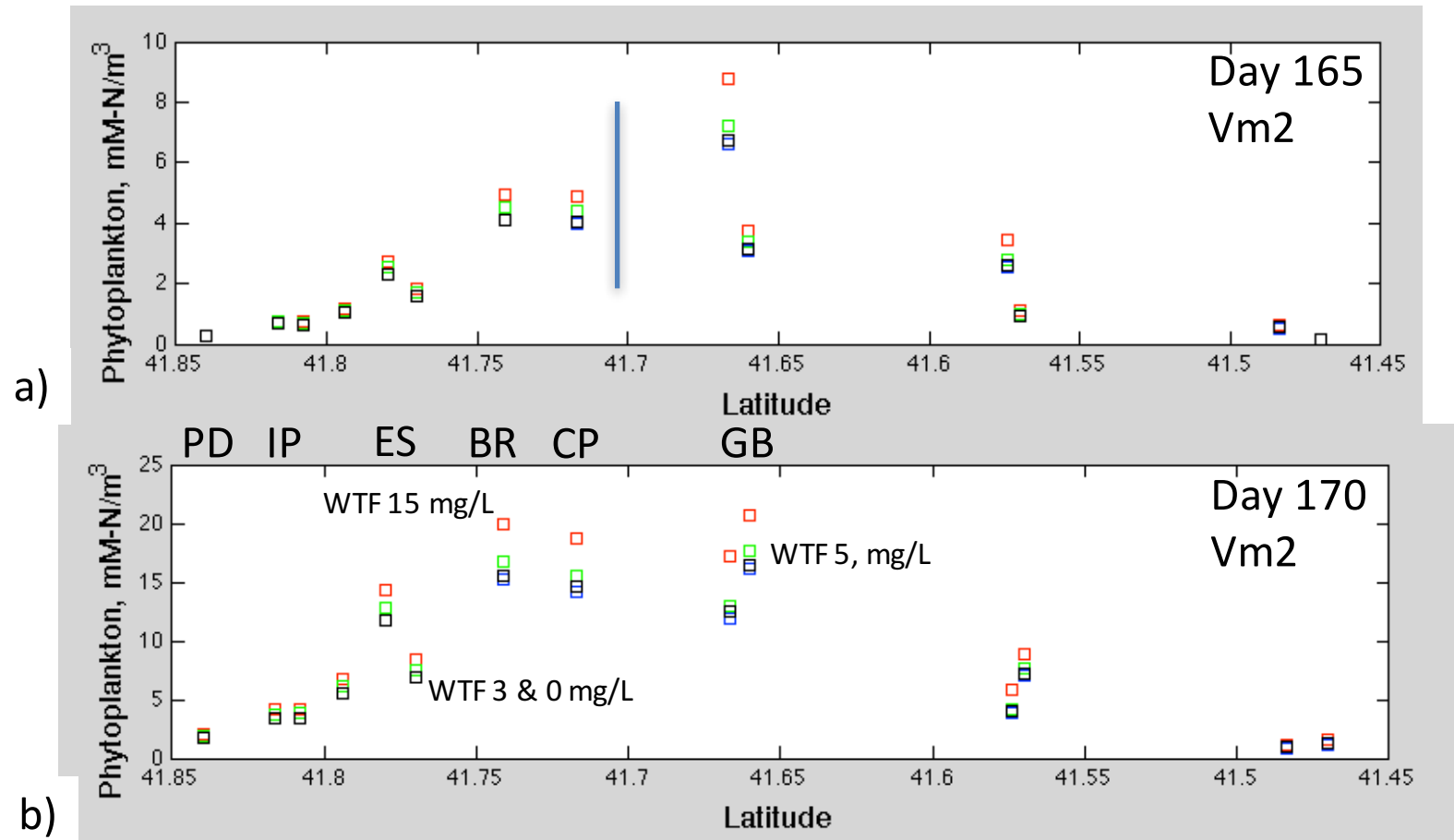


Figure 59. Plots of time averaged (days 165, 170) phytoplankton concentration versus latitude for cases with nutrient uptake rate of $V_m=2.0$. Cases compare impact of different WWTF release strategies (WWTFs releasing at, $R=1070$ (15 mg/L) , $G=355$ (5 mg/L) , Blue= 213 (3 mg/L) , Black= 0 mM m^{-3} (0 mg/L)). The smaller uptake rate produces a similar result as $V_m2.5$, but is significantly delayed (e.g., by 8-9 days).

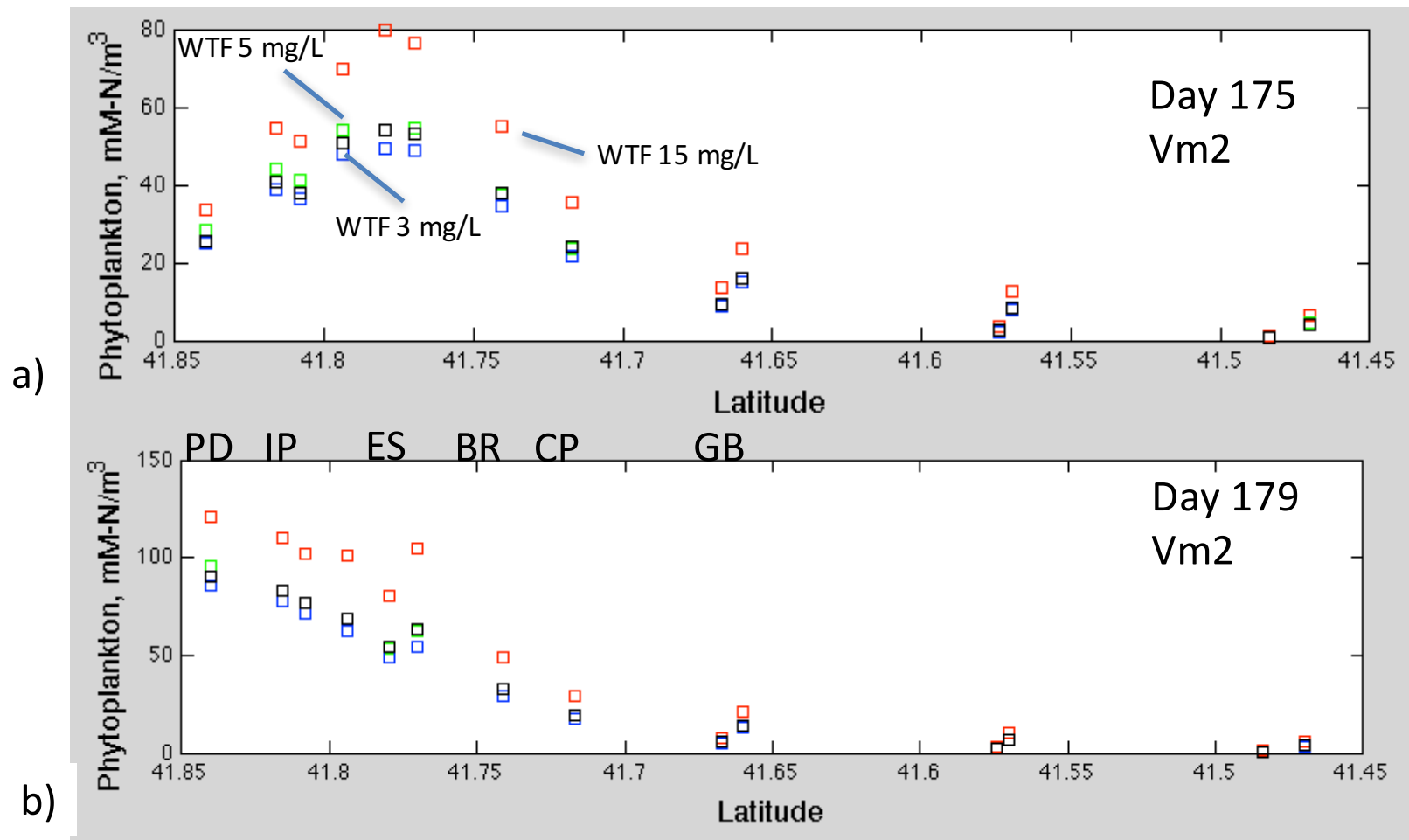


Figure 60. Plots of 2-day time averaged phytoplankton concentration versus latitude for cases with nutrient uptake rate of $V_m=2.0$. Cases compare impact of different WWTF release strategies (WWTFs releasing at, $R=1070$ (15 mg L^{-1}), $G=355$ (5 mg L^{-1}), Blue= 213 (3 mg L^{-1}), Black= 0 mM m^{-3} (0 mg L^{-1})). The smaller uptake rate produces a similar result as $V_m=2.5$, but is significantly delayed (e.g., by 8-9 days). It is interesting that on Edgewood Shoals (ES), the cases with WWTF releases of 5,3 and 0 mg L^{-1} have similar bloom sizes.

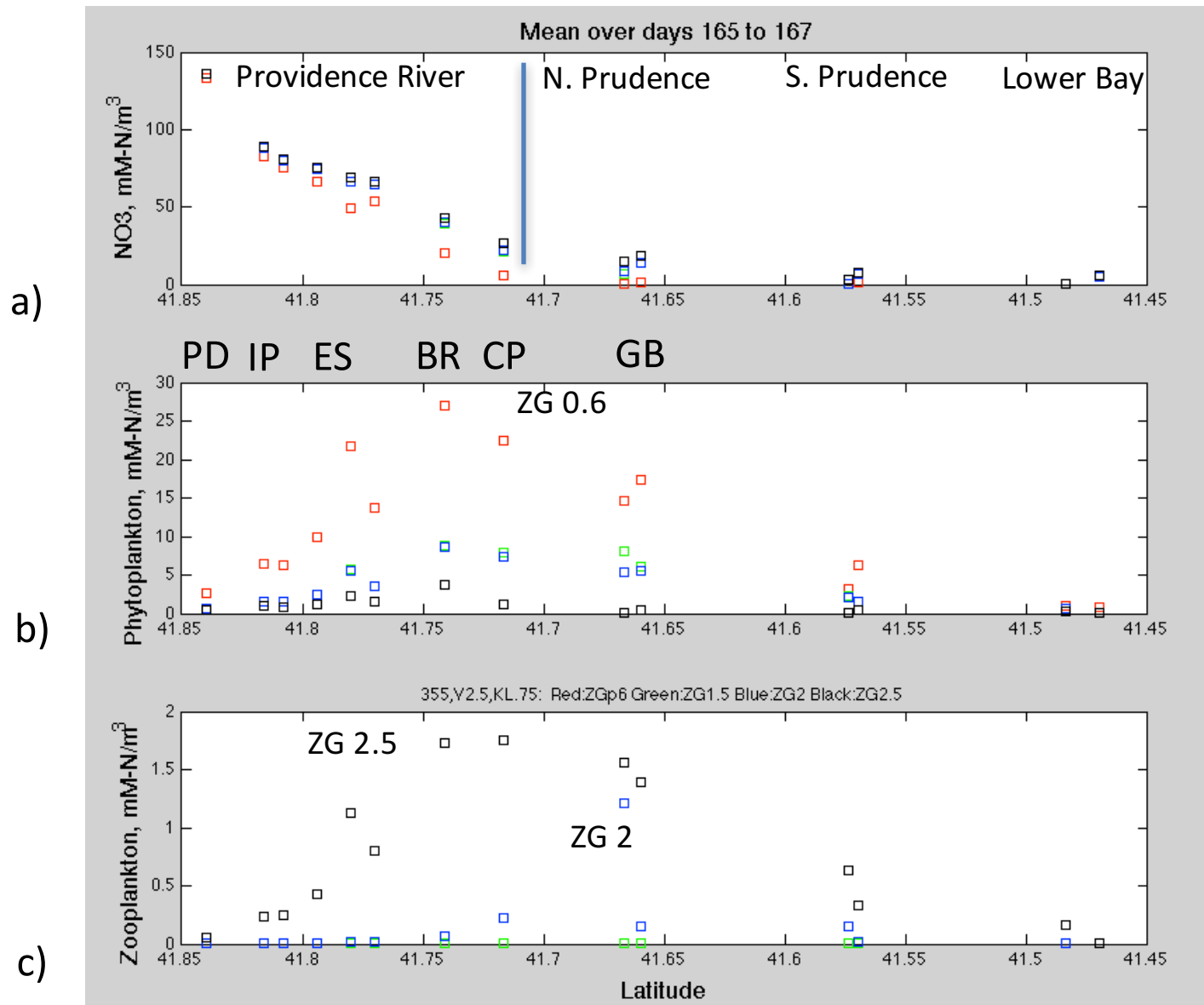


Figure 61. Plots of N, P and Z for a range of zooplankton grazing rates. All cases have WWTFs releasing at 355 mM m^{-3} (5 mg L^{-1}), and uses $\text{KL}=0.75$ and a P uptake rate of 2.5. Cases are for grazing rates of 0.6 (red), 1.5 (green), 2 (blue) and 2.5 (black). Values are plotted versus latitude for 2-day averaging window (d166). Zooplankton concentrations are relatively high (>1 mM-N/ m^3) in the lower Providence River through Ohio Ledge for ZG2.5 at this point. For the lower grazing rate ZG2, values exceed 1 mM-N/ m^3 only within Greenwich Bay.

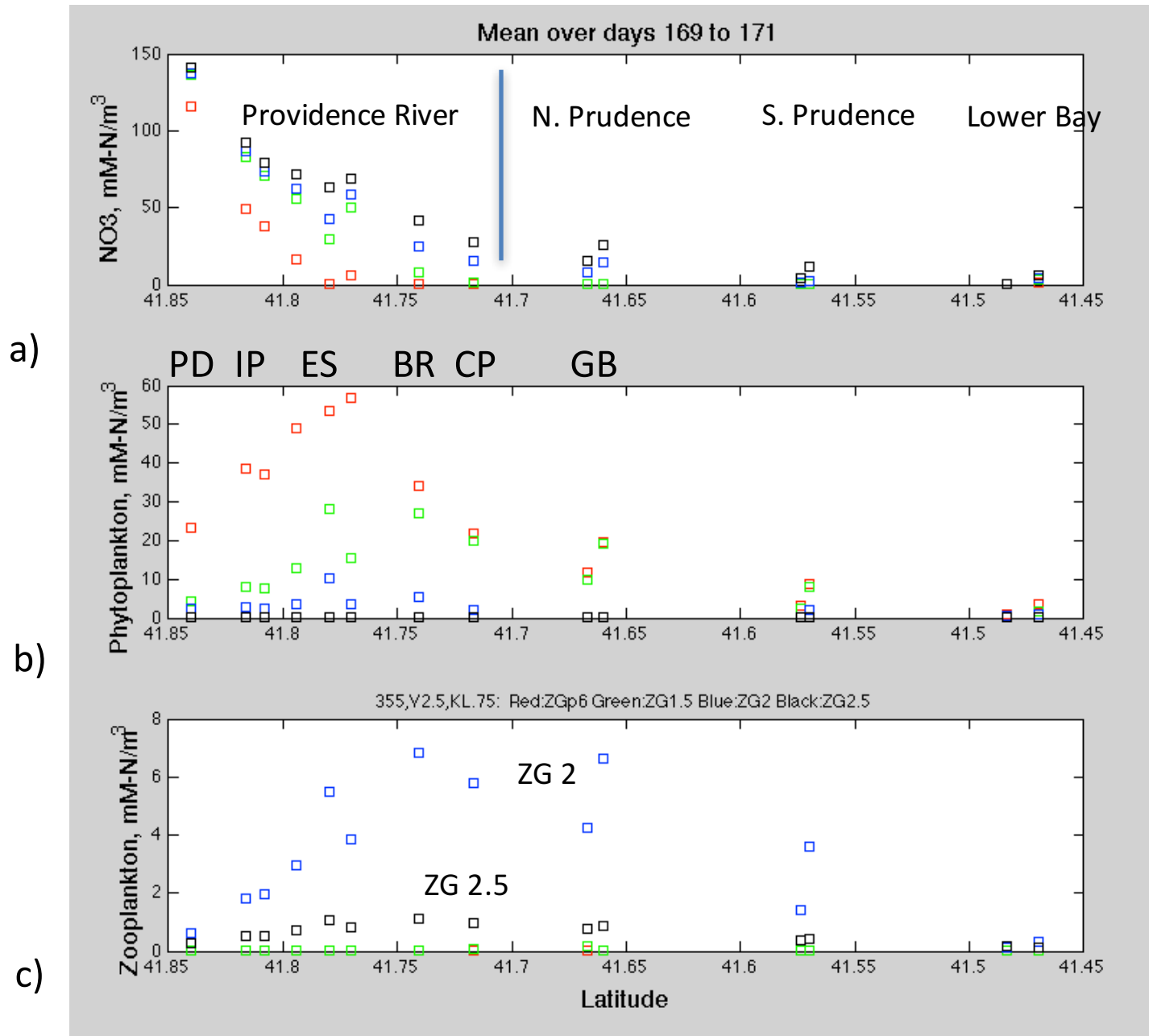


Figure 62. Plots of N, P and Z for a range of zooplankton grazing rates. All cases have WWTFs releasing at 355 mM m⁻³ (5 mg L⁻¹). Here light extinction KL=0.75 and phytoplankton uptake rate is 2.5. Cases are for grazing rates of 0.6 (red), 1.5 (green), 2 (blue) and 2.5 (black). Zooplankton levels similar to Figure 59 for Z_g=2.5, but are elevated (>2 mM-N/m³) in the Providence River and Ohio Ledge for the intermediate grazing rate of Z_g=2 (blue squares). Red squares in (c) plot under the green.

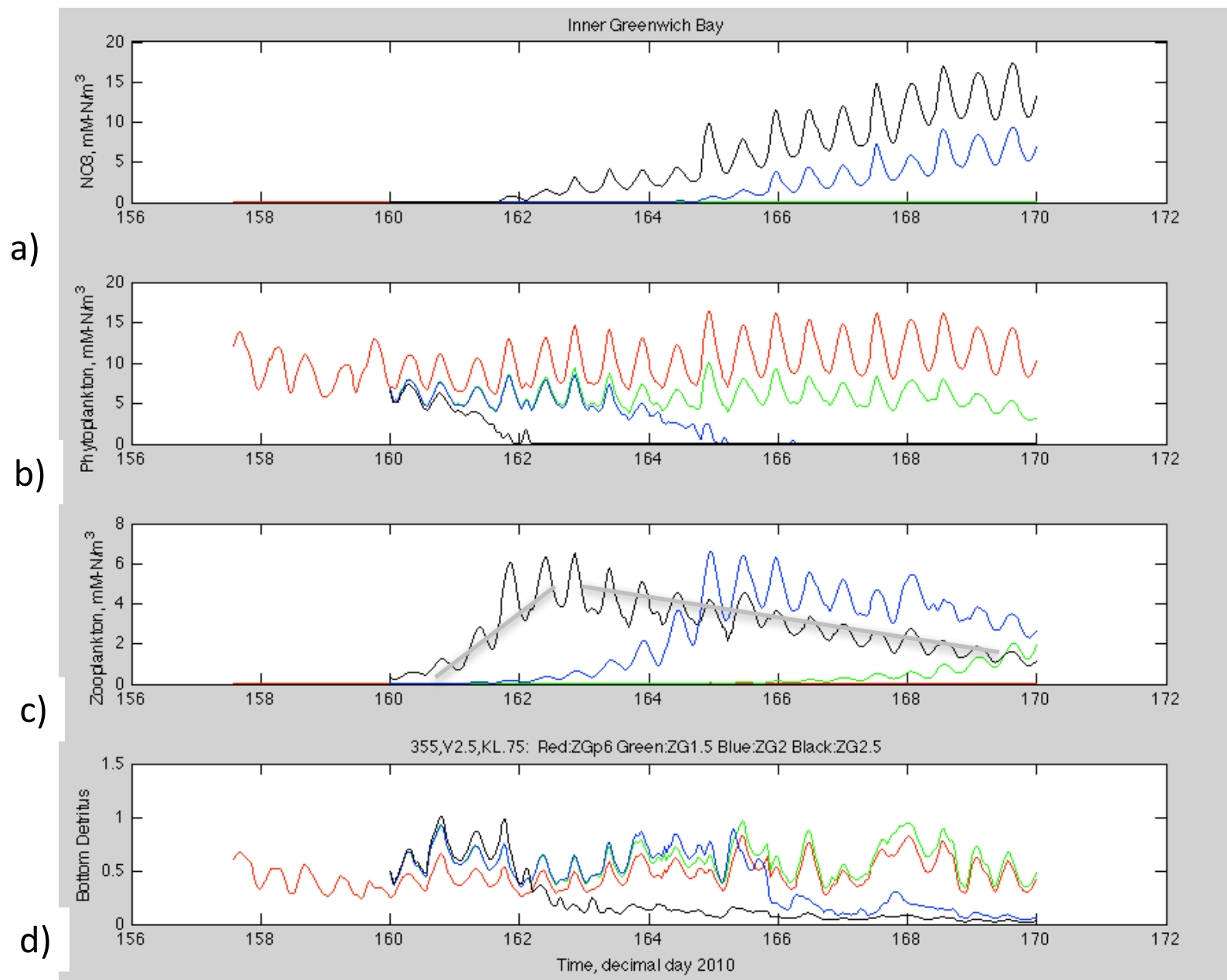


Figure 63. Plots for inner GB of N, P, Z and D versus time for a range of zooplankton grazing rates. All cases have WWTFs releasing at 355 mM m⁻³ (5 mg L⁻¹), and uses $K_l=0.75$ and a P uptake rate of 2.5. Cases are for grazing rates (ZG) of 0.6 (red), 1.5 (green), 2 (blue) and 2.5 (black). Higher ZG rates drive P down (b) allowing N to increase in GB. ZG rates of 0.6 and 1.5 do not produce a zooplankton bloom, or limit P growth. A pulse in D on day 161 fuels resupply of N days 166 to 170.

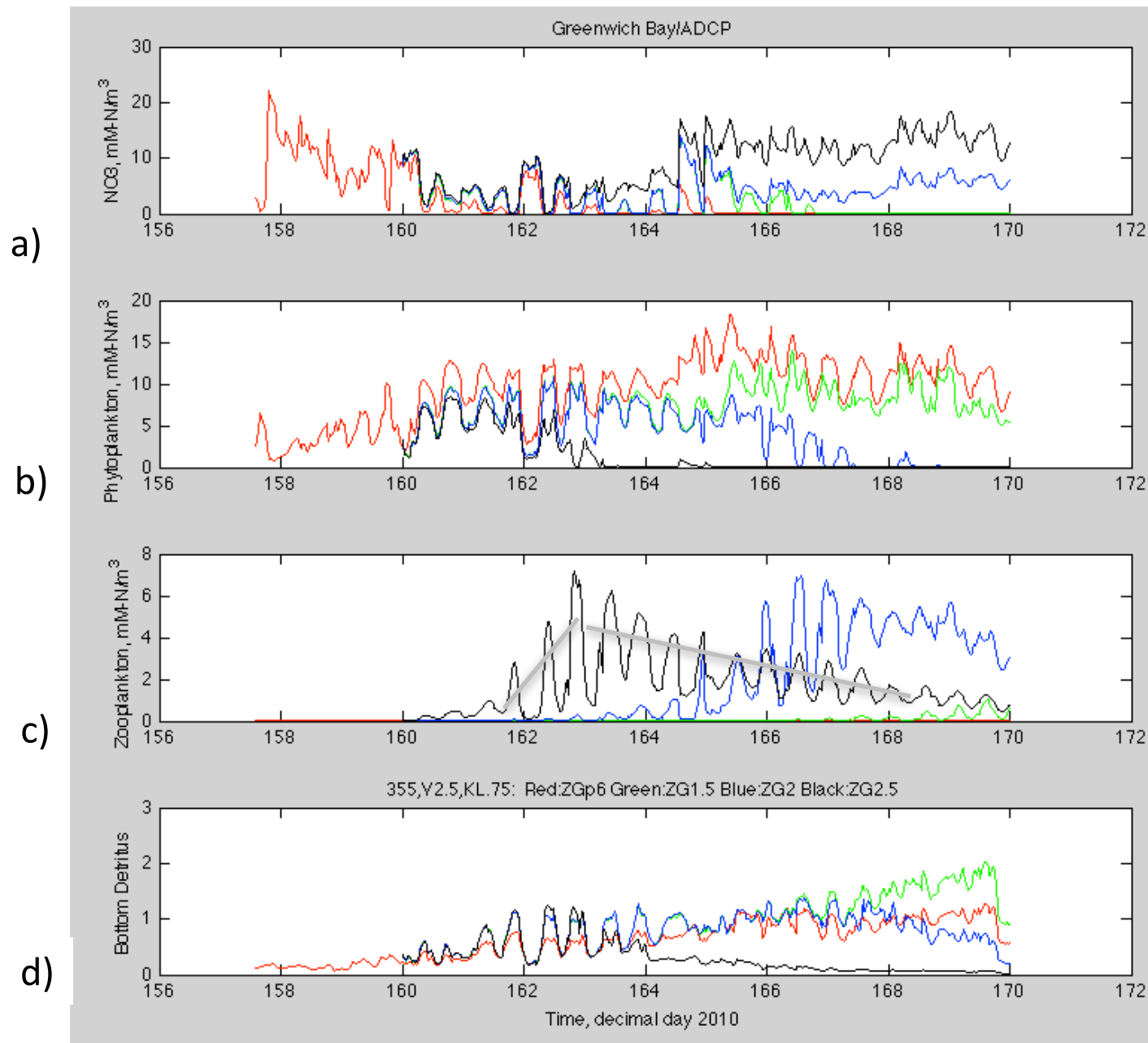


Figure 64. Plots in the channel at the mouth of Greenwich Bay for N, P, Z and D versus time. Results are for a range of zooplankton grazing rates. All cases have WWTFs releasing at 355 mM m^{-3} (5 mg L^{-1}), $K_L=0.75$ and $V_m=2.5$. Cases are for grazing rates (ZG) of 0.6 (red), 1.5 (green), 2 (blue) and 2.5 (black). ZG rates of 2.5 and 2 produce Z blooms separated by 4 days. ZG rates of 0.6 and 1.5 do not limit P levels.

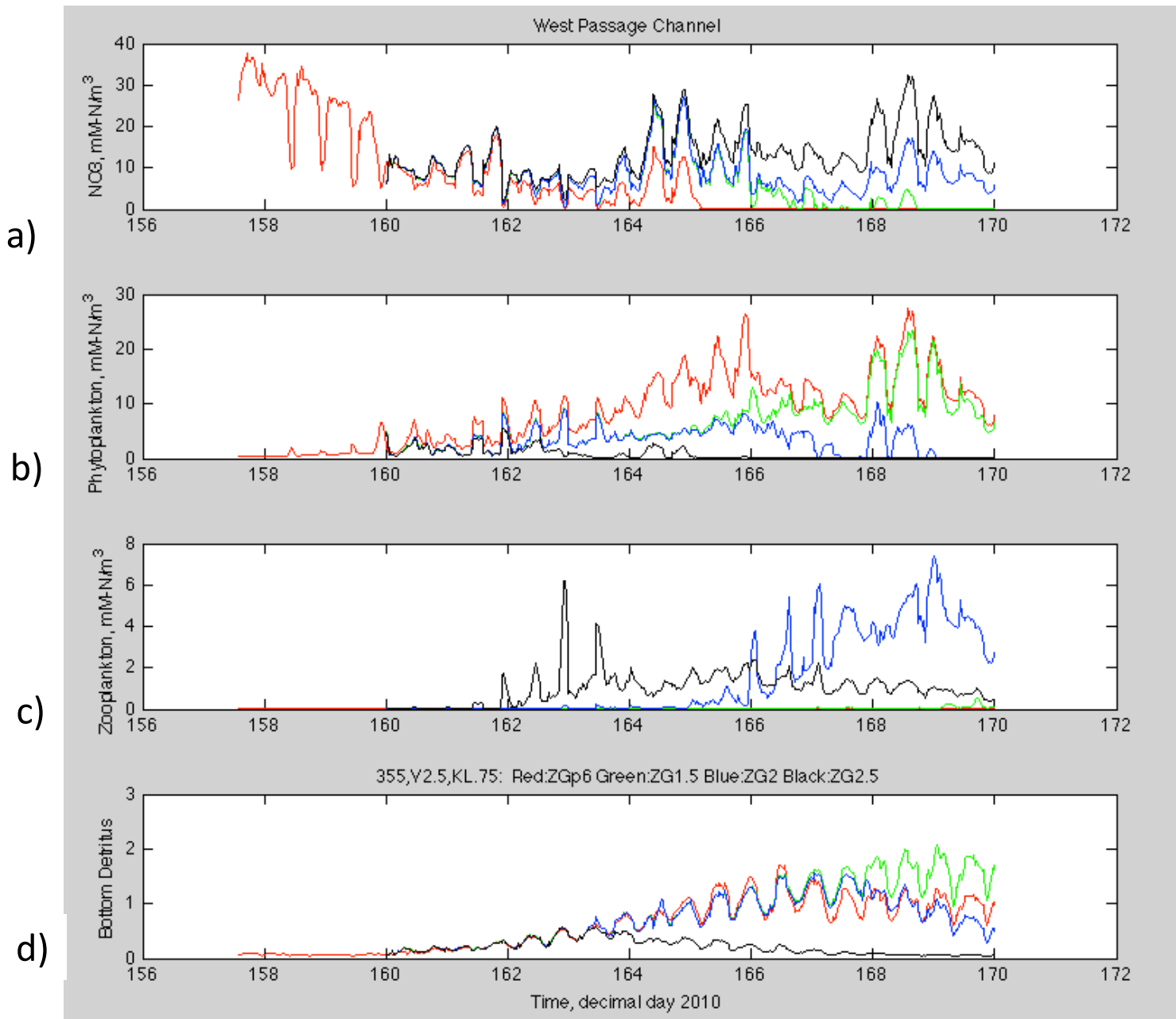


Figure 65. Plots for West Passage channel outside mouth of GB showing N, P, Z and D versus time for a range of zooplankton grazing rates. All cases have WWTFs releasing at 355 mM m^{-3} (5 mg L^{-1}), $K_L=0.75$ and $V_m=2.5$. Cases are for grazing rates (ZG) of 0.6 (red), 1.5 (green), 2 (blue) and 2.5 (black). ZG rates of 2.5 and 2 produce Z blooms separated by ~ 4 days. ZG rates of 0.6 and 1.5 do not limit P levels but higher grazing rates lead to severely limited blooms at this station, located between GB and Ohio Ledge.

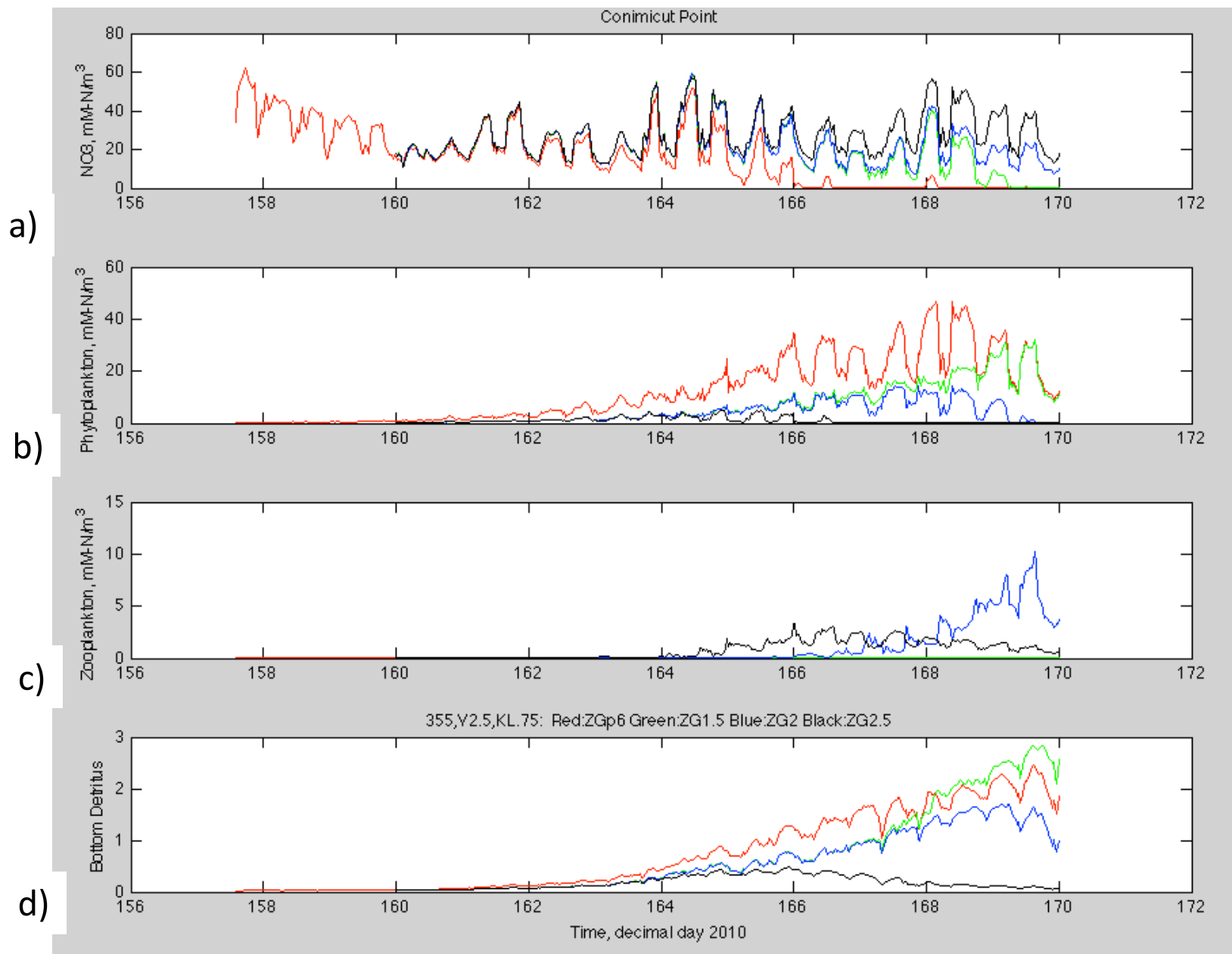


Figure 66. Plots for CP, at the mouth of the Providence River showing N, P, Z and D versus time for a range of zooplankton grazing rates. All cases have WWTFs releasing at 355 mM m⁻³ (5 mg L⁻¹), $K_L=0.75$ and $V_m=2.5$. Cases are for grazing rates (ZG) of 0.6 (red), 1.5 (green), 2 (blue) and 2.5 (black). Interestingly, there is no P bloom in this location for the high ZG rate (black) (frame b).

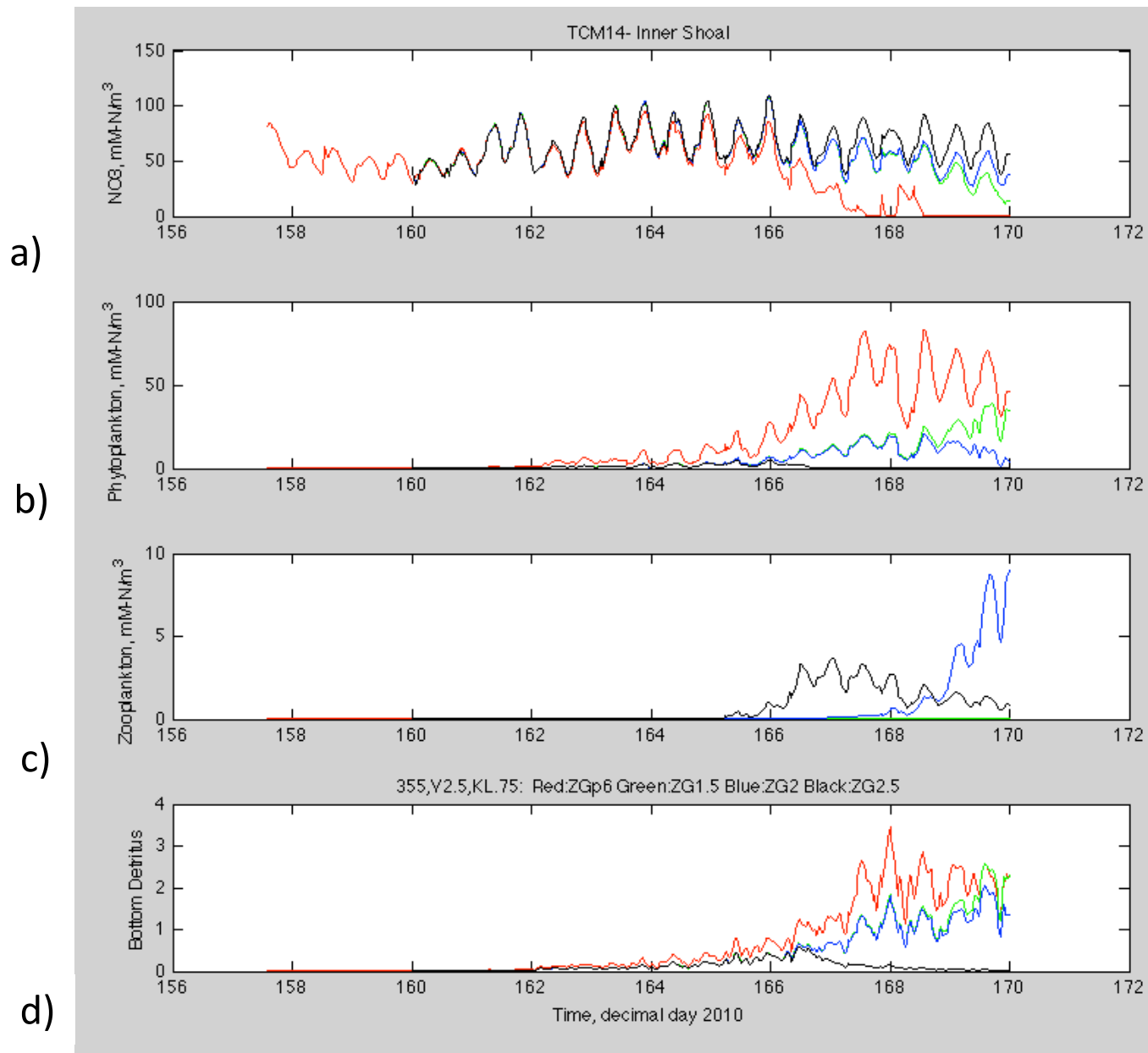


Figure 67. Plots for Edgewood Shoals of the Providence River showing N, P, Z and D versus time for a range of zooplankton grazing rates. All cases have WWTFs releasing at 355 mM m^{-3} (5 mg L^{-1}), $K_L=0.75$ and $V_m=2.5$. Cases are for grazing rates (ZG) of 0.6 (red), 1.5 (green), 2 (blue) and 2.5 (black). Interestingly, there is no P bloom in this location for the high ZG rate (black) (frame b).

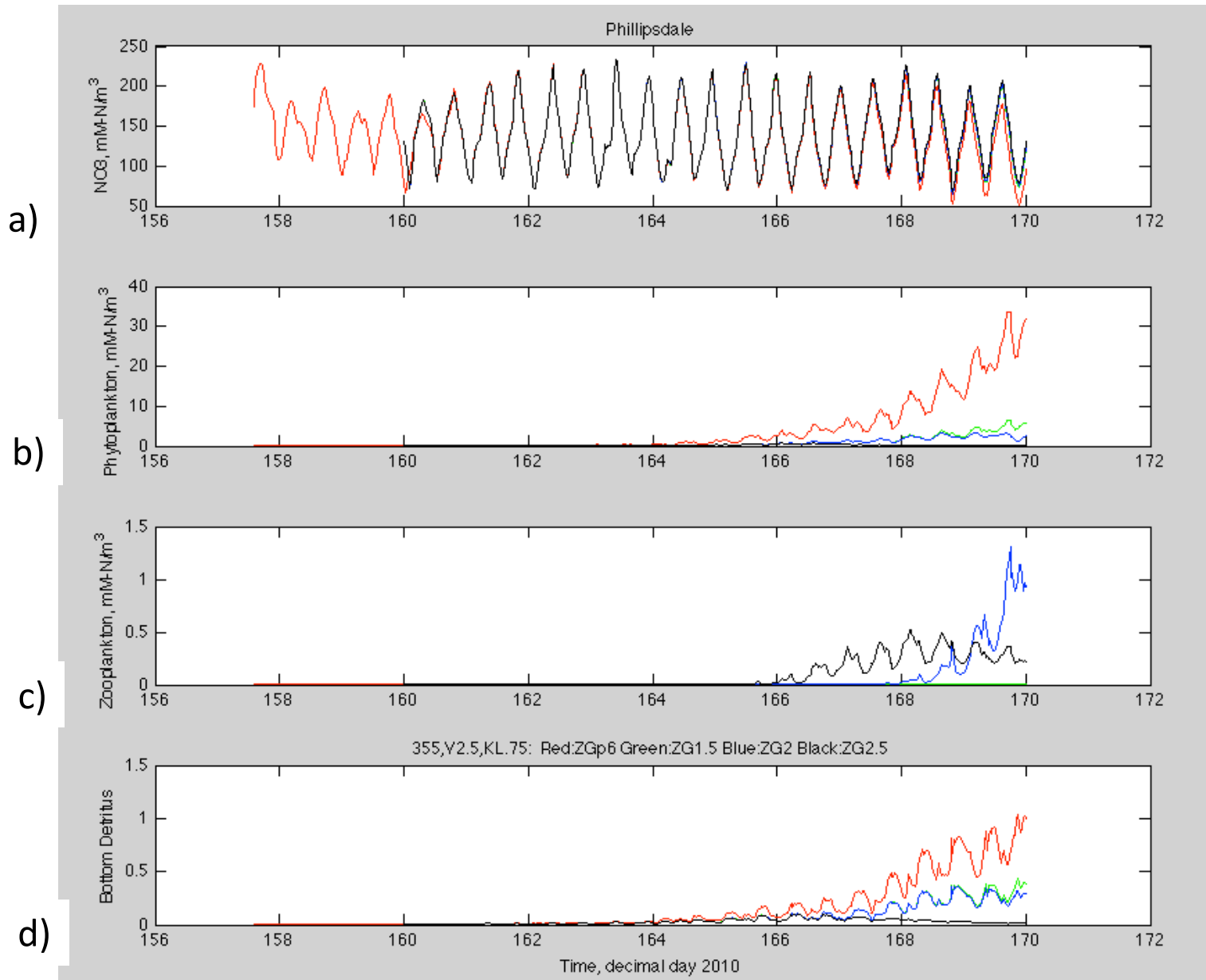


Figure 68. Plots for the Phillipsdale Station of the Seekonk River showing N, P, Z and D versus time for a range of zooplankton grazing rates. All cases have WWTFs releasing at 355 mM m^{-3} (5 mg L^{-1}), $K_L=0.75$ and $V_m=2.5$. Cases are for grazing rates (ZG) of 0.6 (red), 1.5 (green), 2 (blue) and 2.5 (black). The P bloom appears here at day 170 only for the smallest ZG of 0.6.

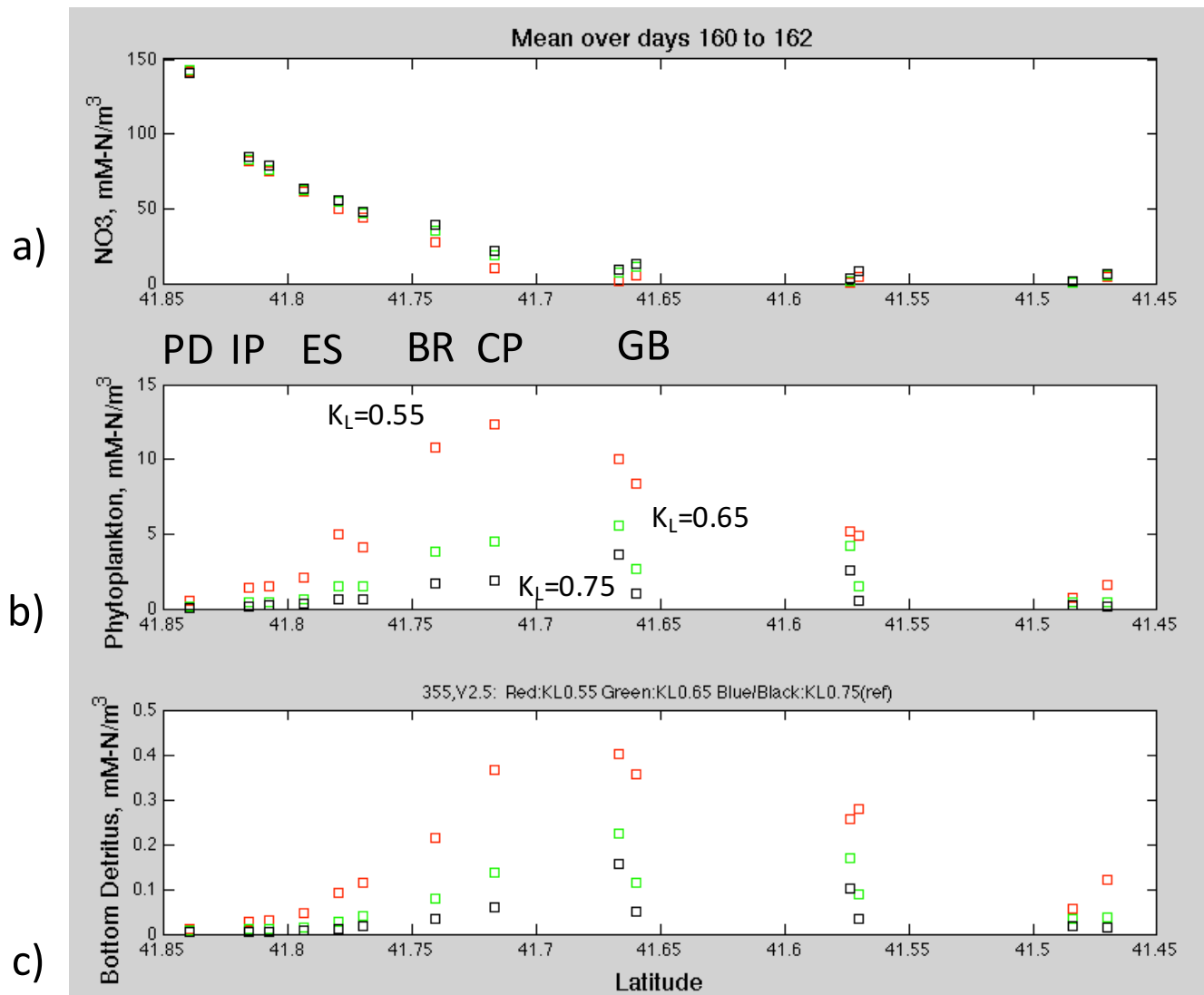


Figure 69. Plots of N, P and Z versus latitude for a range of light extinction coefficients. All cases have WWTFs releasing at 355 mM m^{-3} (5 mg L^{-1}), and uses low zooplankton grazing (0.6 day^{-1}) and $V_m=2.5 \text{ day}^{-1}$. Light extinction values are 0.55 (red), 0.65 (green), and the reference case of 0.75 (black). Values are for 2-day averaging window (day 160-162).

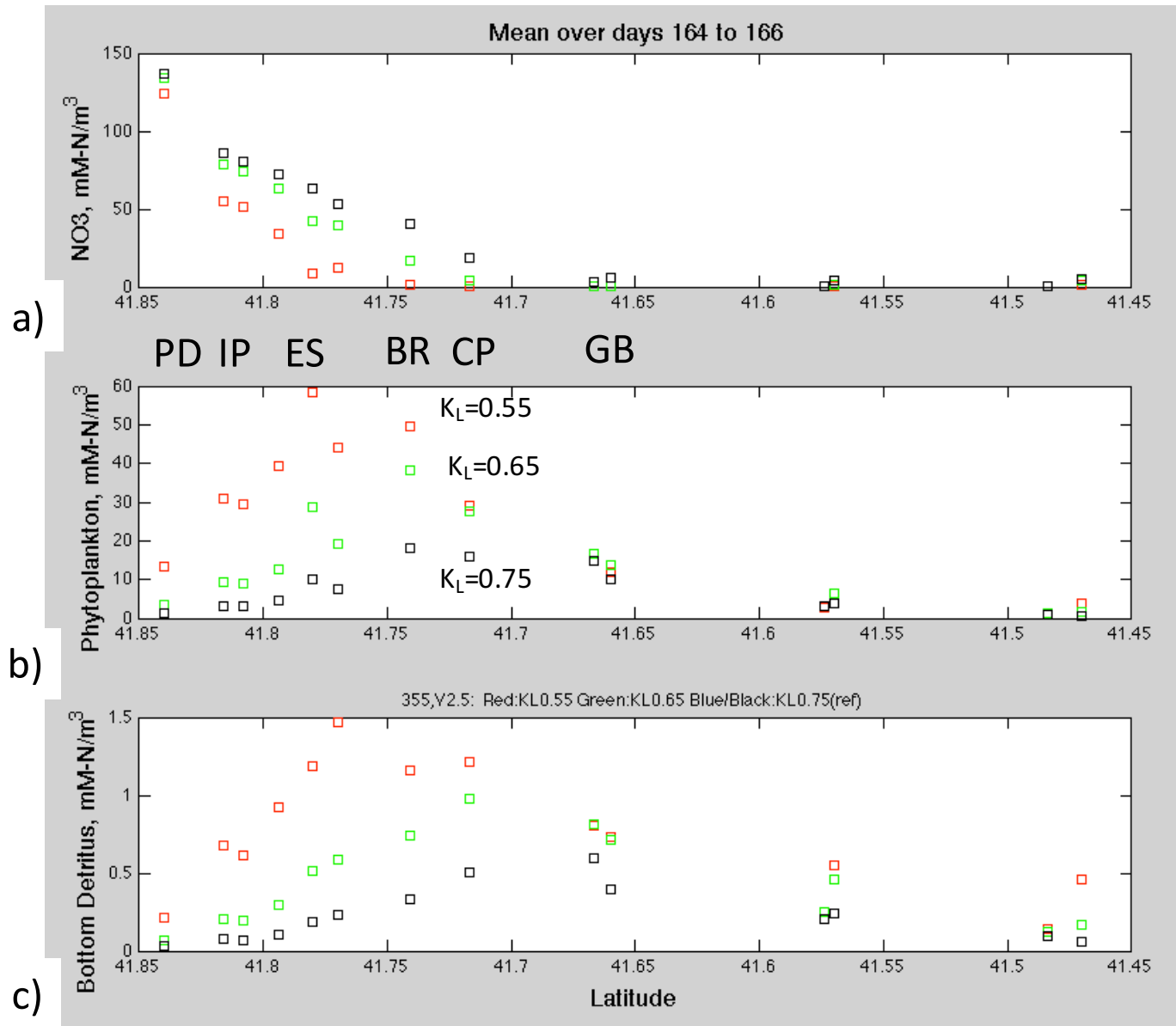


Figure 70. Plots of N, P and Z versus latitude for a range of light extinction coefficients. All cases have WWTFs releasing at 355 mM m^{-3} (5 mg L^{-1}), and uses low zooplankton grazing (0.6 day^{-1}) and $V_m=2.5 \text{ day}^{-1}$. Light extinction values are 0.55 (red), 0.65 (green), and the reference case of 0.75 (black). Values are for 2-day averaging window (day 164-166).

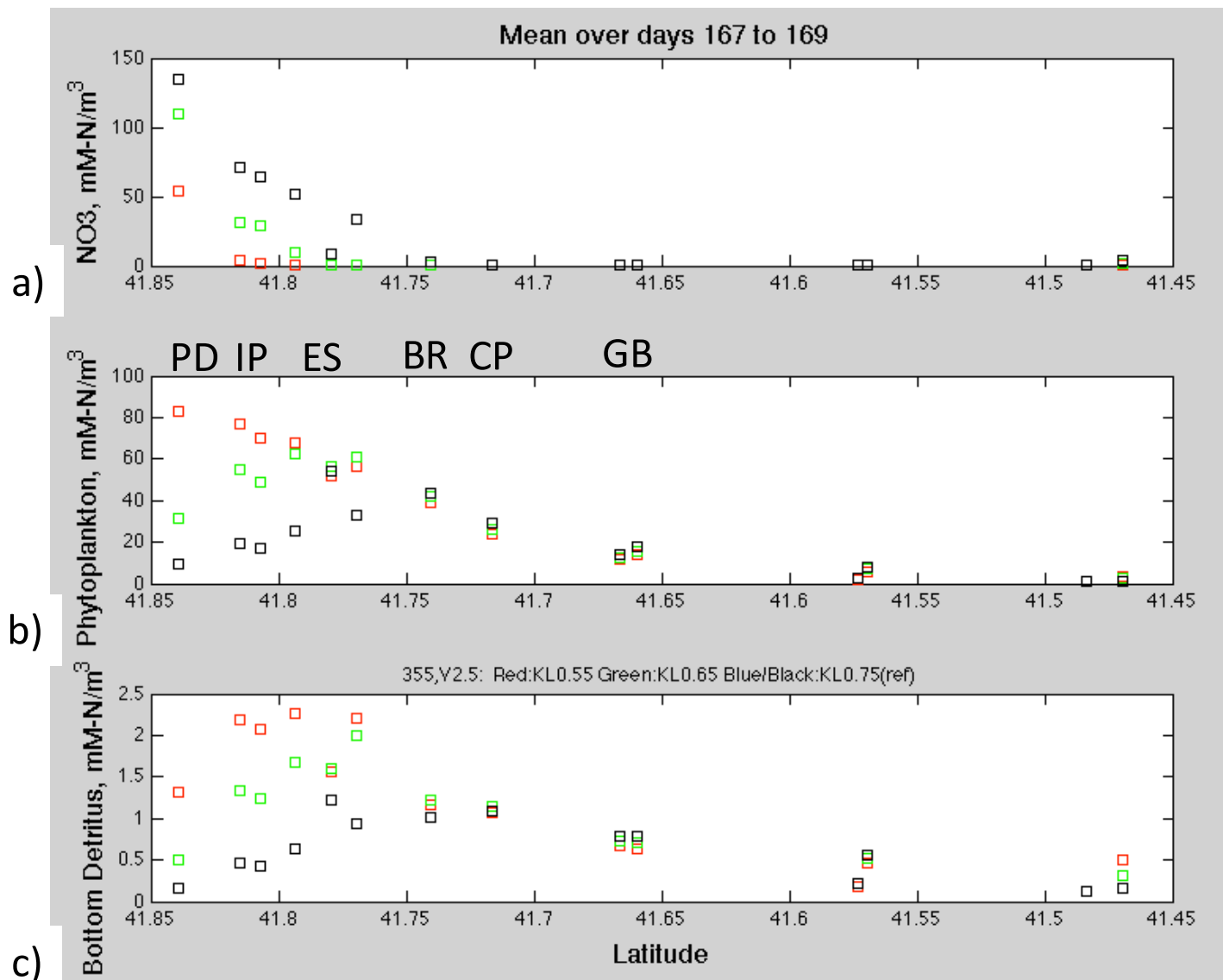


Figure 71. Similar to previous plot, for range in light extinction coefficients, but for averaging window of day 167-169. All cases have WWTFs releasing at 355 mM m^{-3} (5 mg L^{-1}), and uses low zooplankton grazing (0.6 day^{-1}) and $V_m=2.5 \text{ day}^{-1}$. Light extinction values are 0.55 (red), 0.65 (green), and the reference case of 0.75 (black).

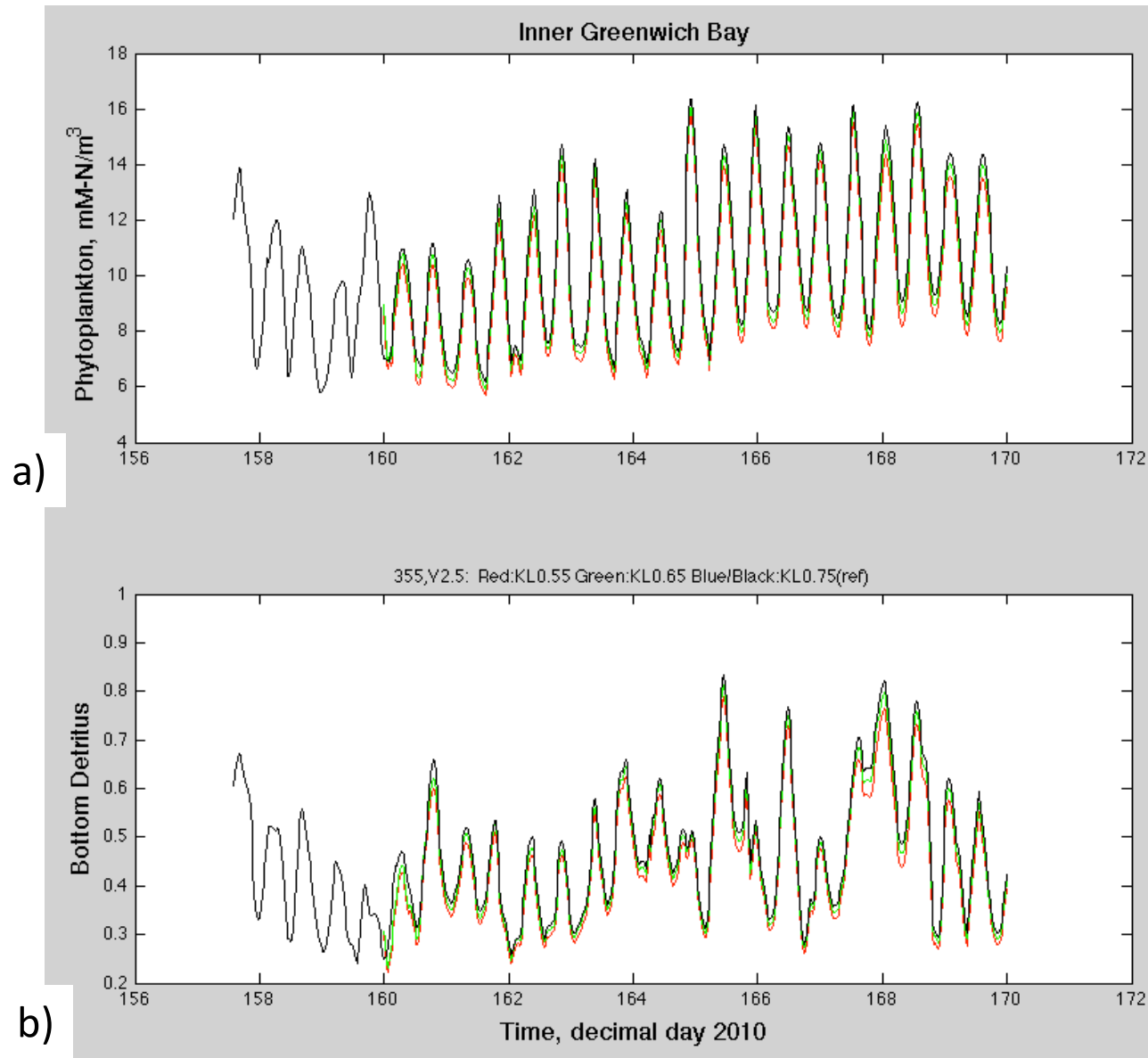


Figure 72. Plots of surface P and bottom D within inner Greenwich Bay versus time for a range of light extinction coefficients. All cases have WWTFs releasing at 355 mM m^{-3} (5 mg L^{-1}), and have low zooplankton grazing (0.6 day^{-1}) and $V_m=2.5 day^{-1}$. Light extinction values are 0.55 (red), 0.65 (green), and the reference case of 0.75 (black). Parameter differences do not change solutions in this region.

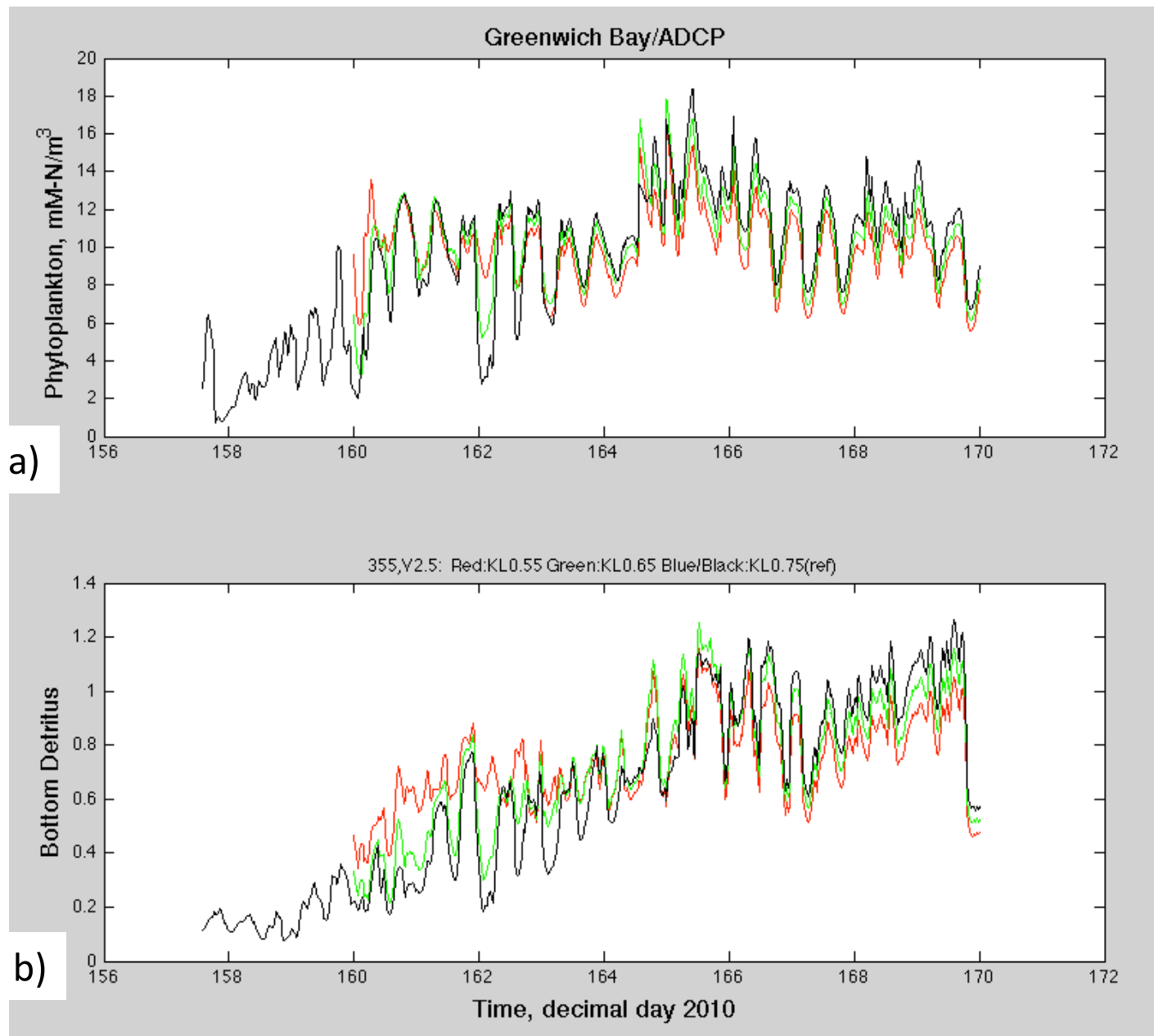


Figure 73. Plots of surface P and bottom D in the channel near the mouth of Greenwich Bay versus time for a range of light extinction coefficients. All cases have WWTFs releasing at 355 mM m⁻³ (5 mg L⁻¹), and have low zooplankton grazing (0.6 day⁻¹) and $V_m=2.5$ day⁻¹. Light extinction values are 0.55 (red), 0.65 (green), and the reference case of 0.75 (black). Parameter differences do not significantly change solutions in this region.

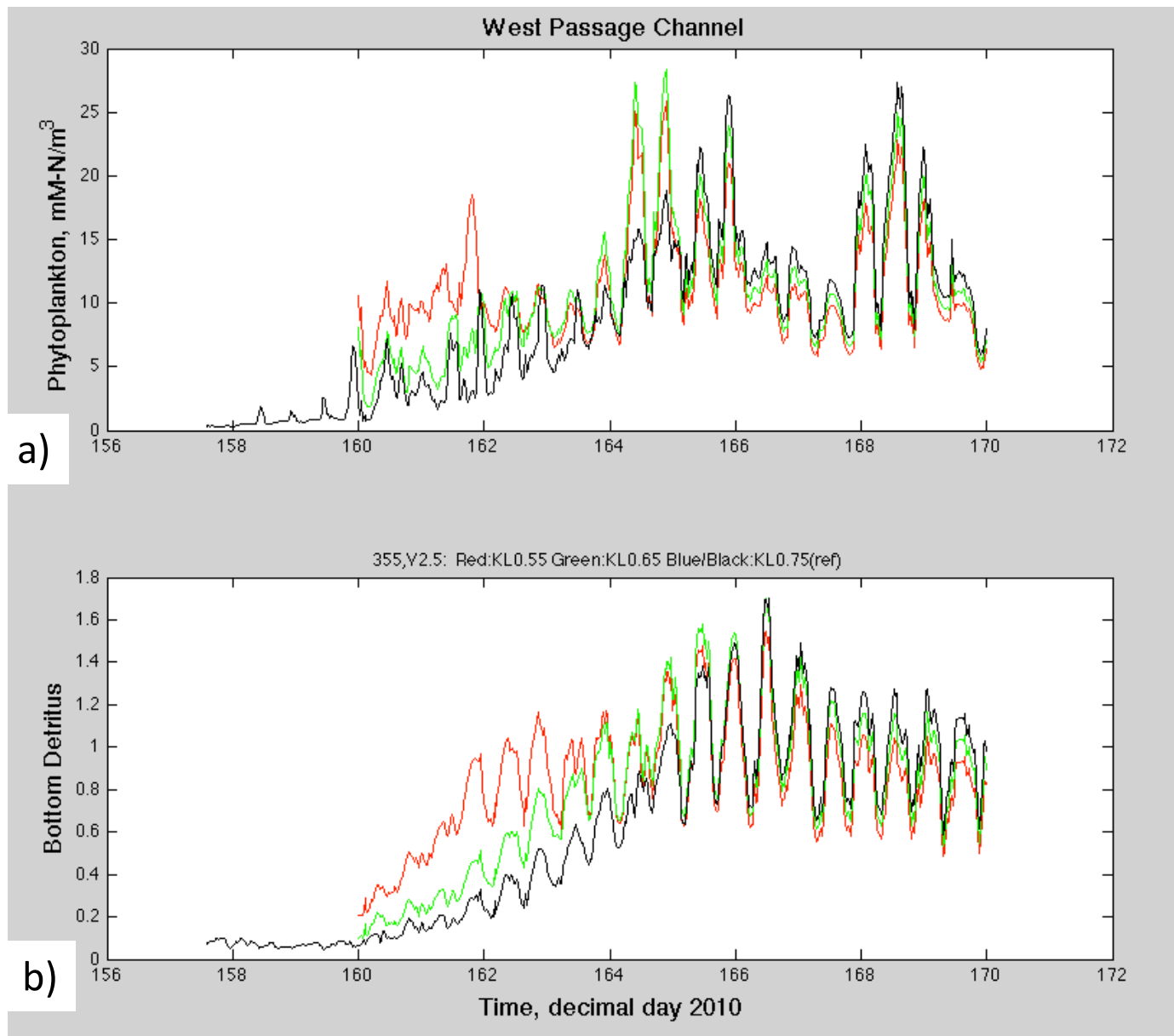


Figure 74. Plots of surface P and bottom D within the West Passage, north of the entrance to Greenwich Bay showing effect of different light extinction coefficients. All cases have WWTFs releasing at 355 mM m⁻³ (5 mg L⁻¹), and have low zooplankton grazing (0.6 day⁻¹) and $V_m=2.5$ day⁻¹. Light extinction values are 0.55 (red), 0.65 (green), and the reference case of 0.75 (black). Parameter differences begin to alter the bloom timing at this location. Detrital fields vary with different K_L values.

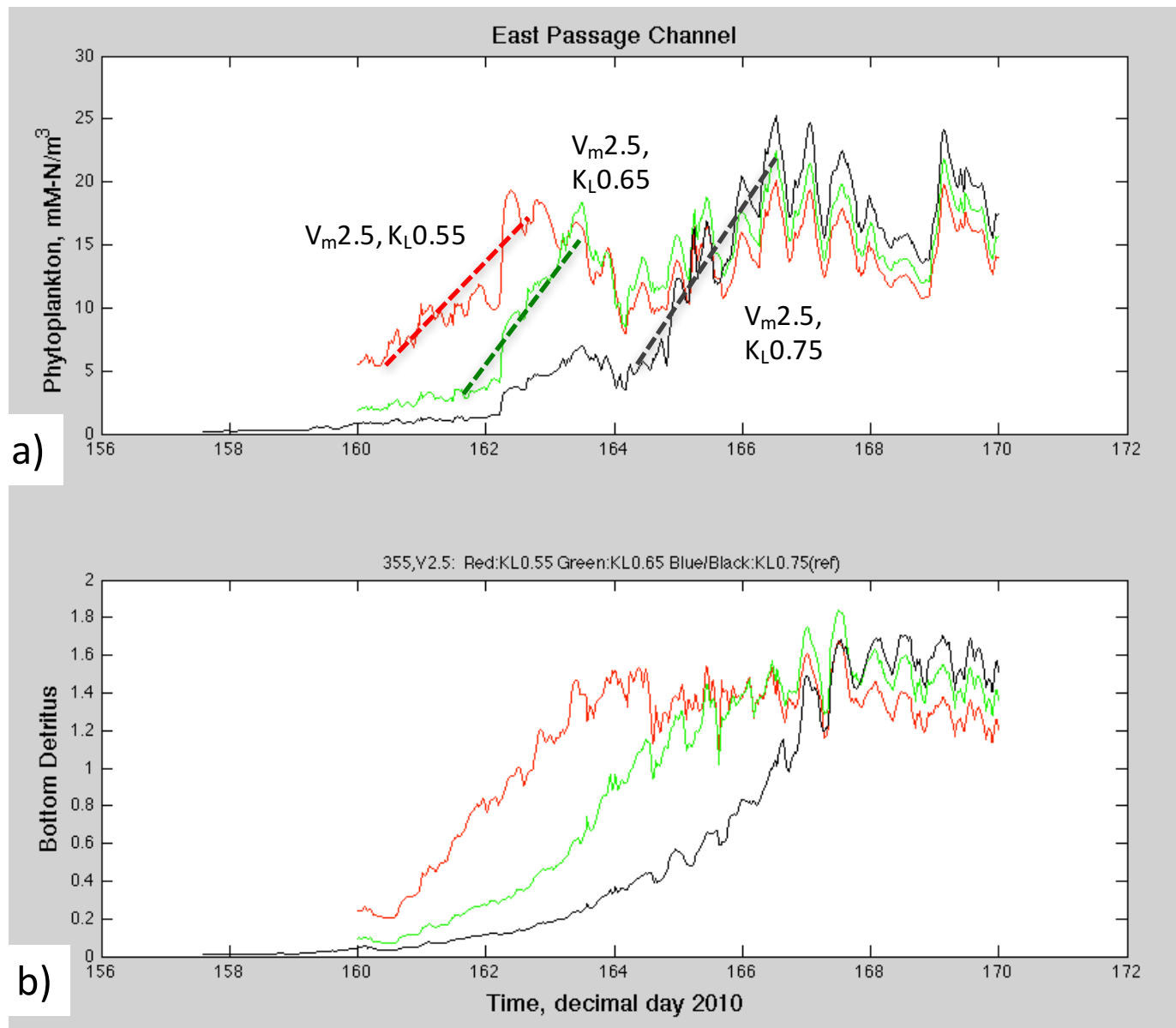


Figure 75. Plots of surface P and bottom D in the East Passage channel, at the southern edge of Ohio Ledge. All cases have WWTFs releasing at 355 mM m⁻³ (5 mg L⁻¹), and have low zooplankton grazing (0.6 day⁻¹) and $V_m=2.5$ day⁻¹. Light extinction values are 0.55 (red), 0.65 (green), and the reference case of 0.75 (black). Higher K_L leads to less light penetration and a delayed bloom. Detrital trends show greater differences, likely reflecting processes occurring away from this site.

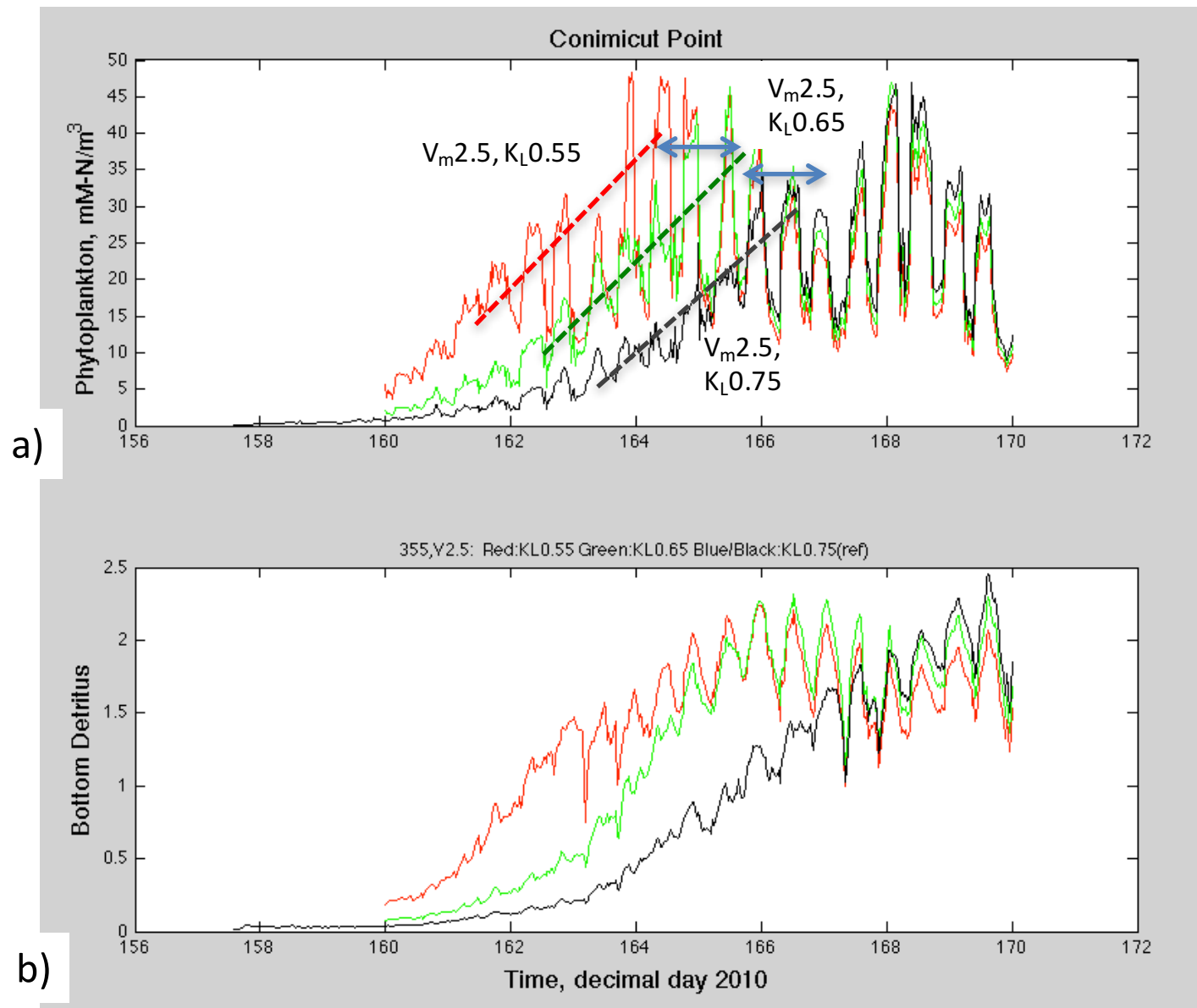


Figure 76. Plots of surface P and bottom D at the mouth of the Providence River (Conimicut Point). All cases have WWTFs releasing at 355 mM m⁻³ (5 mg L⁻¹), and have low zooplankton grazing (0.6 day⁻¹) and $V_m=2.5$ day⁻¹. Light extinction values are 0.55 (red), 0.65 (green), and the reference case of 0.75 (black). Higher K_L leads to less light penetration and a delayed bloom. Delays are roughly 2 to 3 days. Detrital trends show greater differences, likely reflecting processes occurring away from this site.

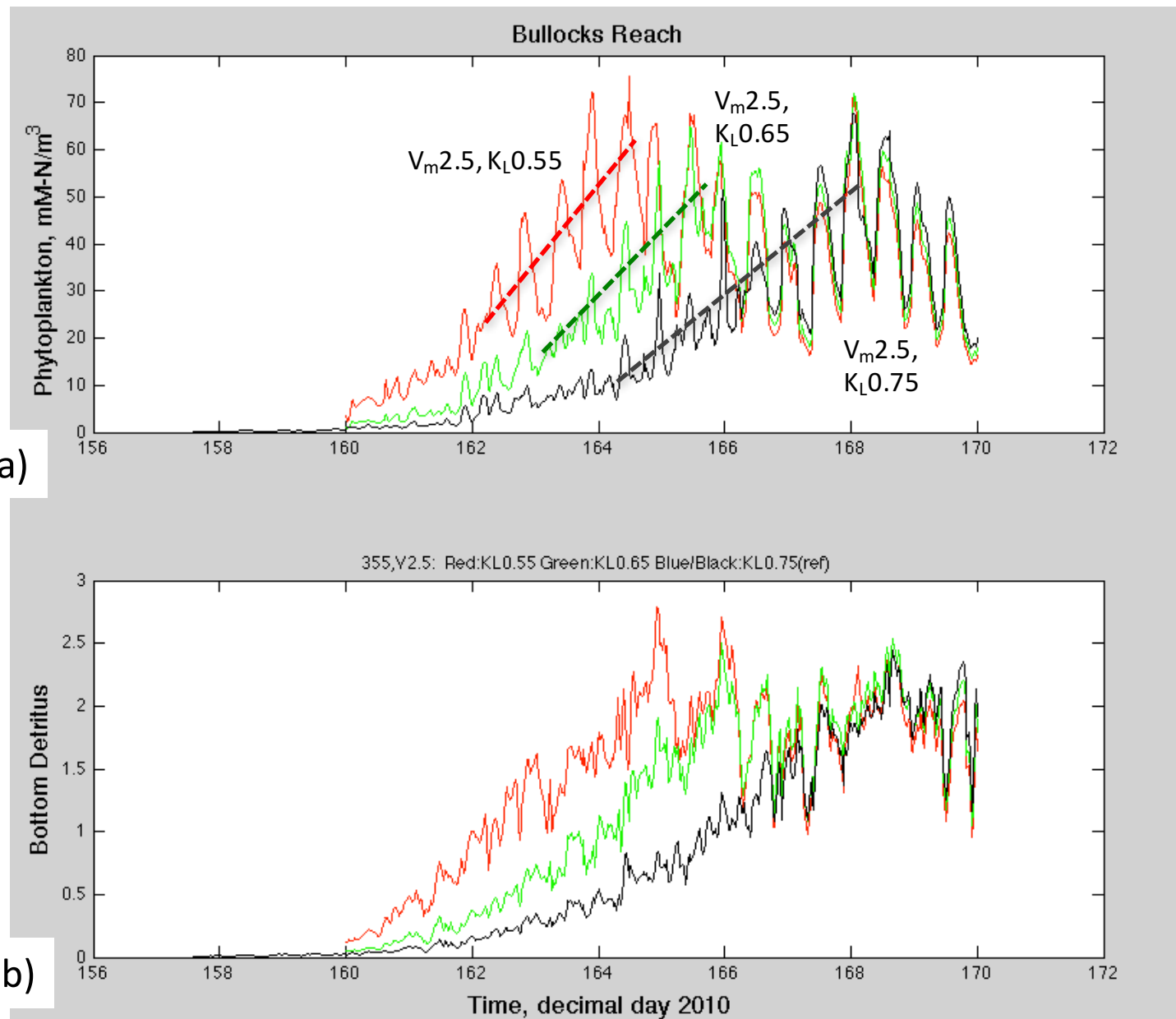


Figure 77. Plots of surface P and bottom D at Bullocks Reach. Different light extinction values are used: 0.55 (red), 0.65 (green), and the reference case of 0.75 (black). Higher K_L leads to less light penetration and a delayed bloom. Detrital trends show greater differences, likely reflecting processes occurring away from this site. Cases have WWTFs releasing at 355 mM m⁻³ (5 mg L⁻¹), and have low zooplankton grazing (0.6 day⁻¹) and $V_m=2.5$ day⁻¹.

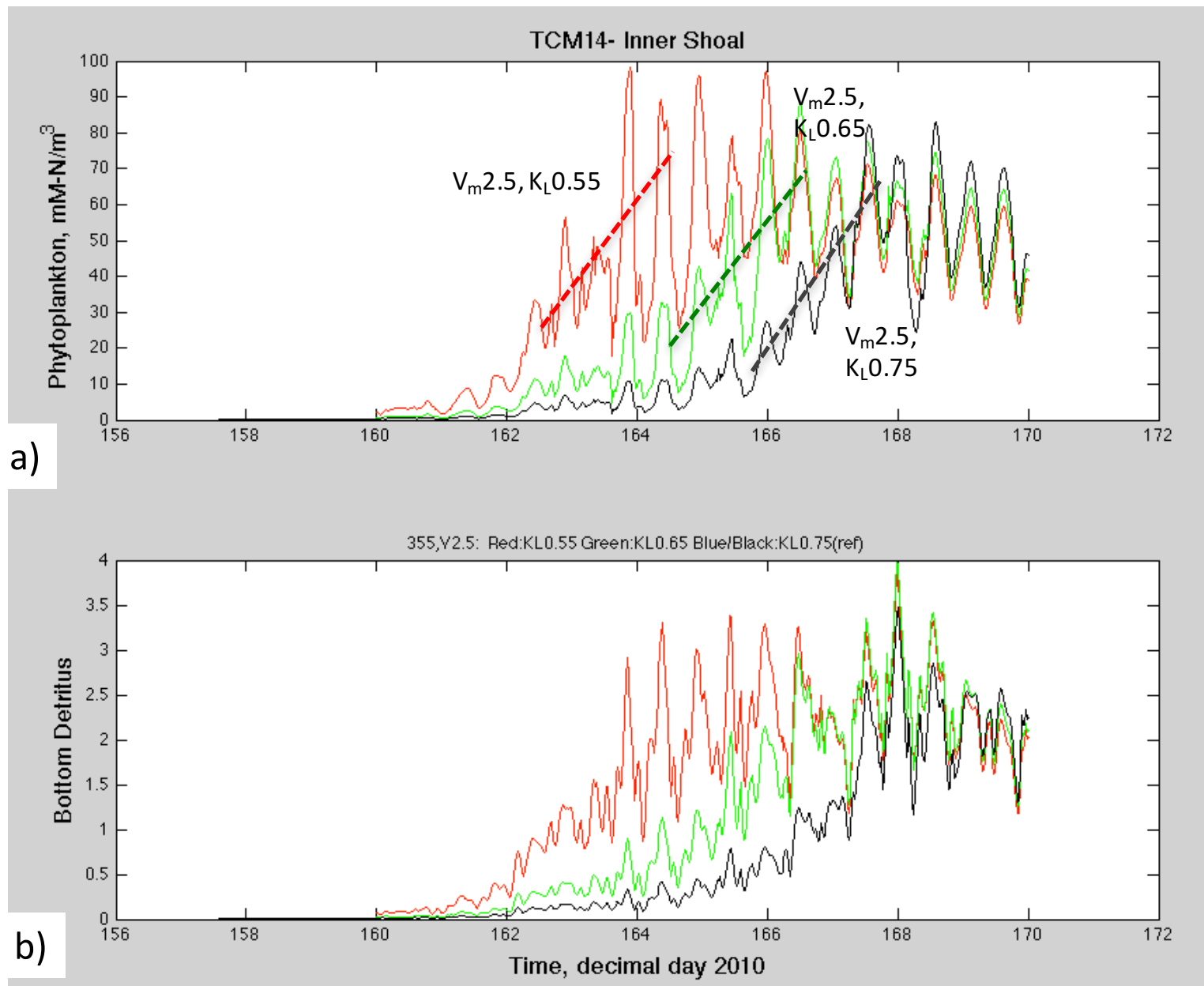


Figure 78. Plots of surface P and bottom D along Edgewood Shoals, south of Fields Point. Different light extinction values are used: 0.55 (red), 0.65 (green), and the reference case of 0.75 (black). Higher K_L leads to less light penetration and a delayed bloom. Cases have WWTFs releasing at 355 mM m⁻³ (5 mg L⁻¹), and have low zooplankton grazing (0.6 day⁻¹) and $V_m = 2.5$ day⁻¹.

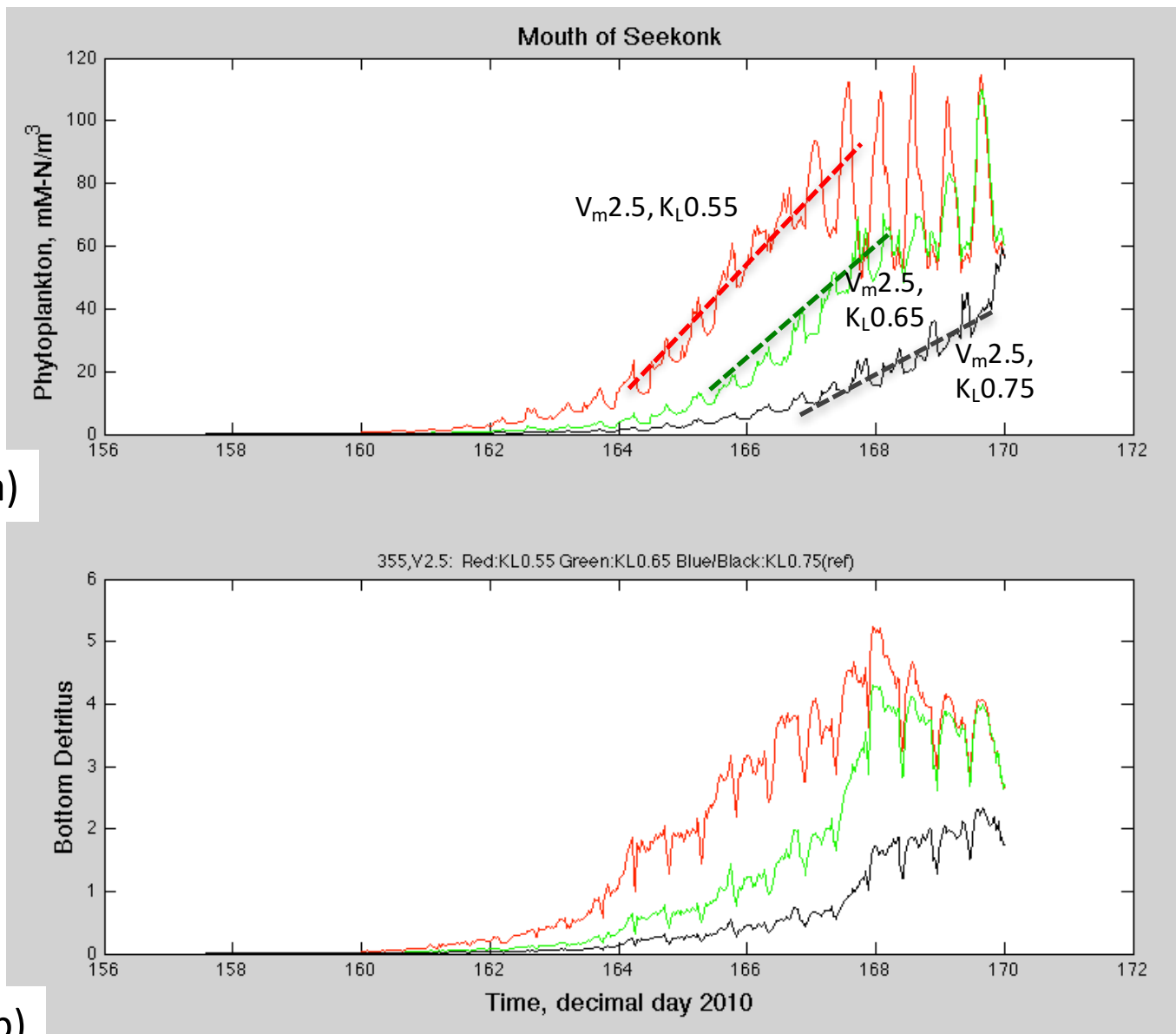


Figure 79. Plots of surface P and bottom D at the mouth of the Seekonk River. Different light extinction values are used: 0.55 (red), 0.65 (green), and the reference case of 0.75 (black). Higher K_L leads to less light penetration and a delayed bloom. Cases have WWTFs releasing at 355 mM m⁻³ (5 mg L⁻¹), and have low zooplankton grazing (0.6 day⁻¹) and $V_m=2.5$ day⁻¹.

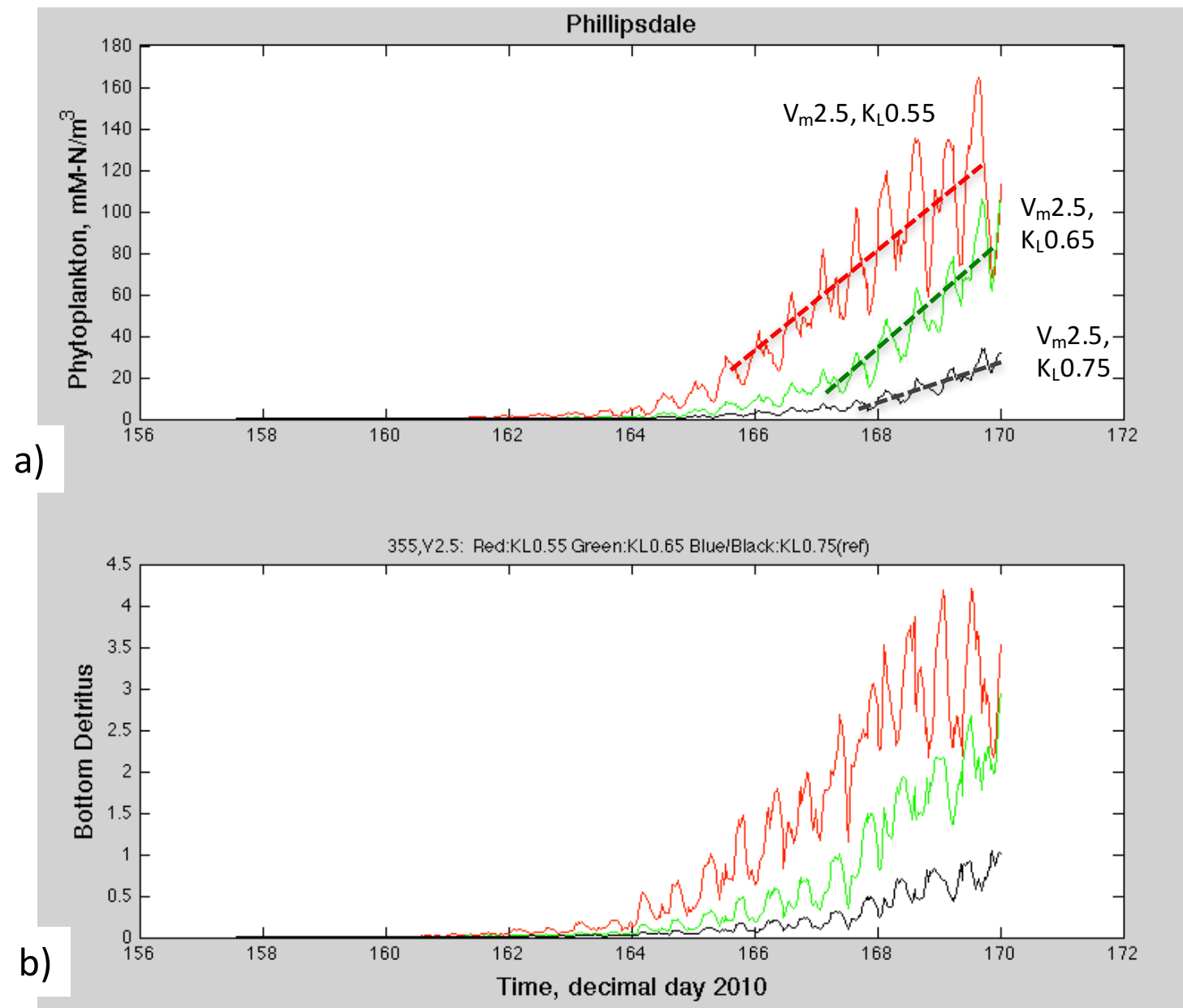


Figure 80. Plots of surface P and bottom D at the northernmost station within the Seekonk River, or Phillipsdale. Different light extinction values are used: 0.55 (red), 0.65 (green), and the reference case of 0.75 (black). Higher K_L leads to less light penetration and a delayed bloom. Cases have WWTFs releasing at 355 mM m^{-3} (5 mg L^{-1}), and have low zooplankton grazing (0.6 day^{-1}) and $V_m=2.5 day^{-1}$.

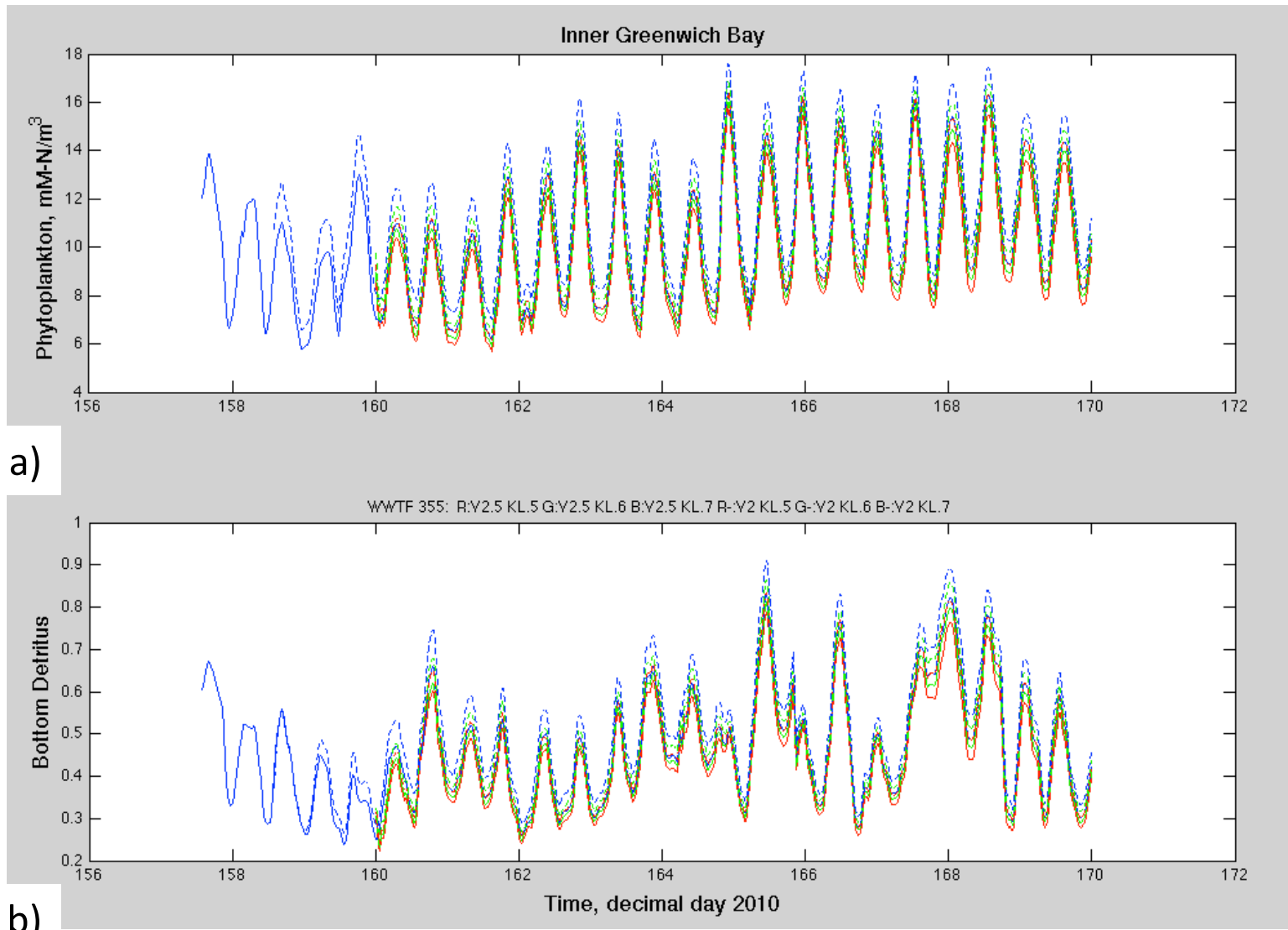


Figure 81. Plots of surface P and bottom D compare different KL and V_m values (red $V_m=2.5$, $K_L=0.55$; red dash $V_m=2$, $K_L=0.55$; green $V_m=2.5$, $K_L=0.65$; green dash $V_m=2$, $K_L=0.65$; blue $V_m=2.5$, $K_L=0.75$; blue dash $V_m=2$, $K_L=0.75$). Cases have WWTFs releasing at 355 mM m^{-3} (5 mg L^{-1}), and have low zooplankton grazing (0.6 day^{-1}). Within inner Greenwich Bay these parameter changes do not influence the solutions.

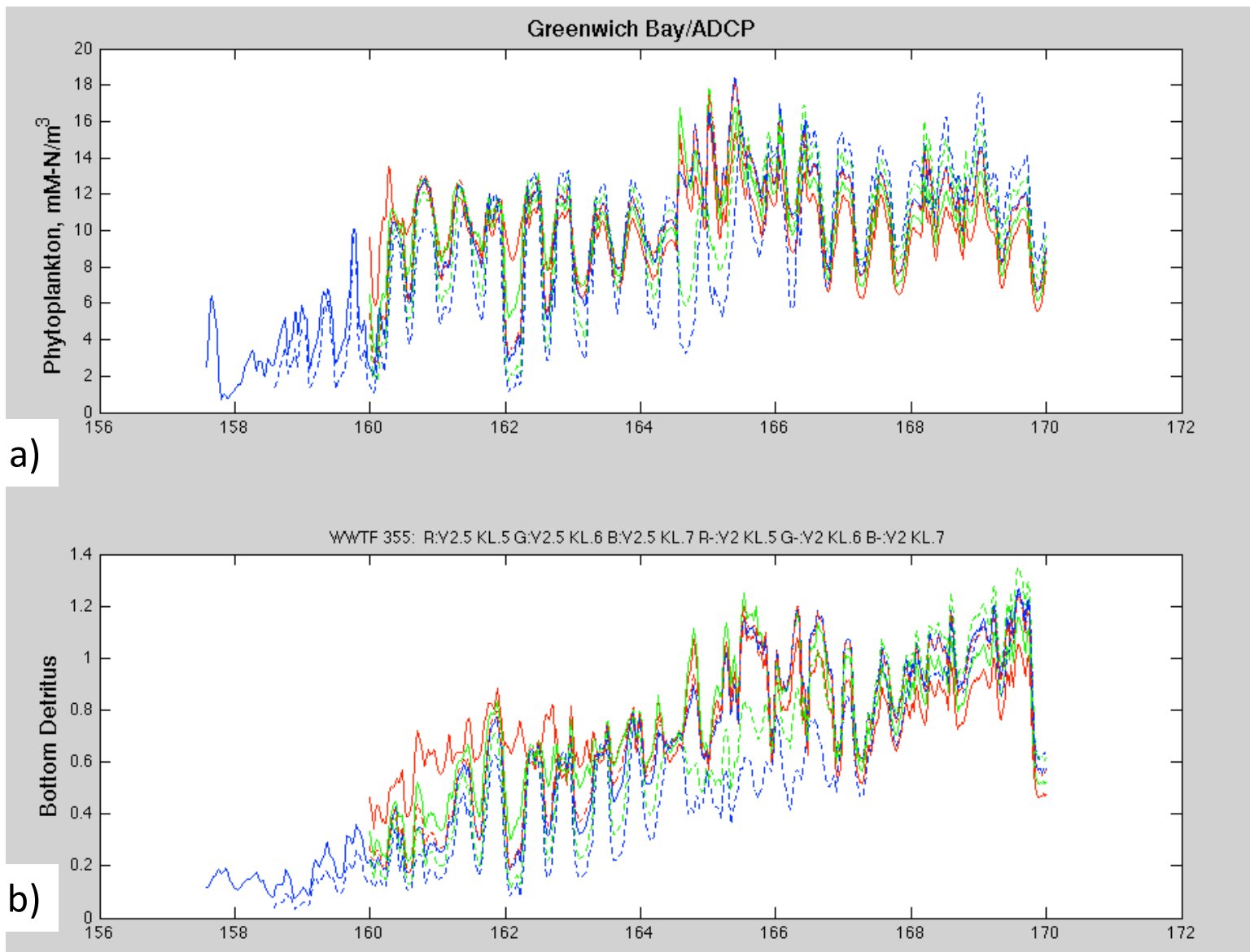


Figure 82. Plots of surface P and bottom D compare different K_L and V_m values (red $V_m=2.5$, $K_L=0.55$; red dash $V_m=2$, $K_L=0.55$; green $V_m=2.5$, $K_L=0.65$; green dash $V_m=2$, $K_L=0.65$; blue $V_m=2.5$, $K_L=0.75$; blue dash $V_m=2$, $K_L=0.75$). Cases have WWTFs releasing at 355 mM m⁻³ (5 mg L⁻¹), and have low zooplankton grazing (0.6 day⁻¹). Plots are from the mouth of Greenwich Bay, in the channel, and show minor differences for this range of parameters.

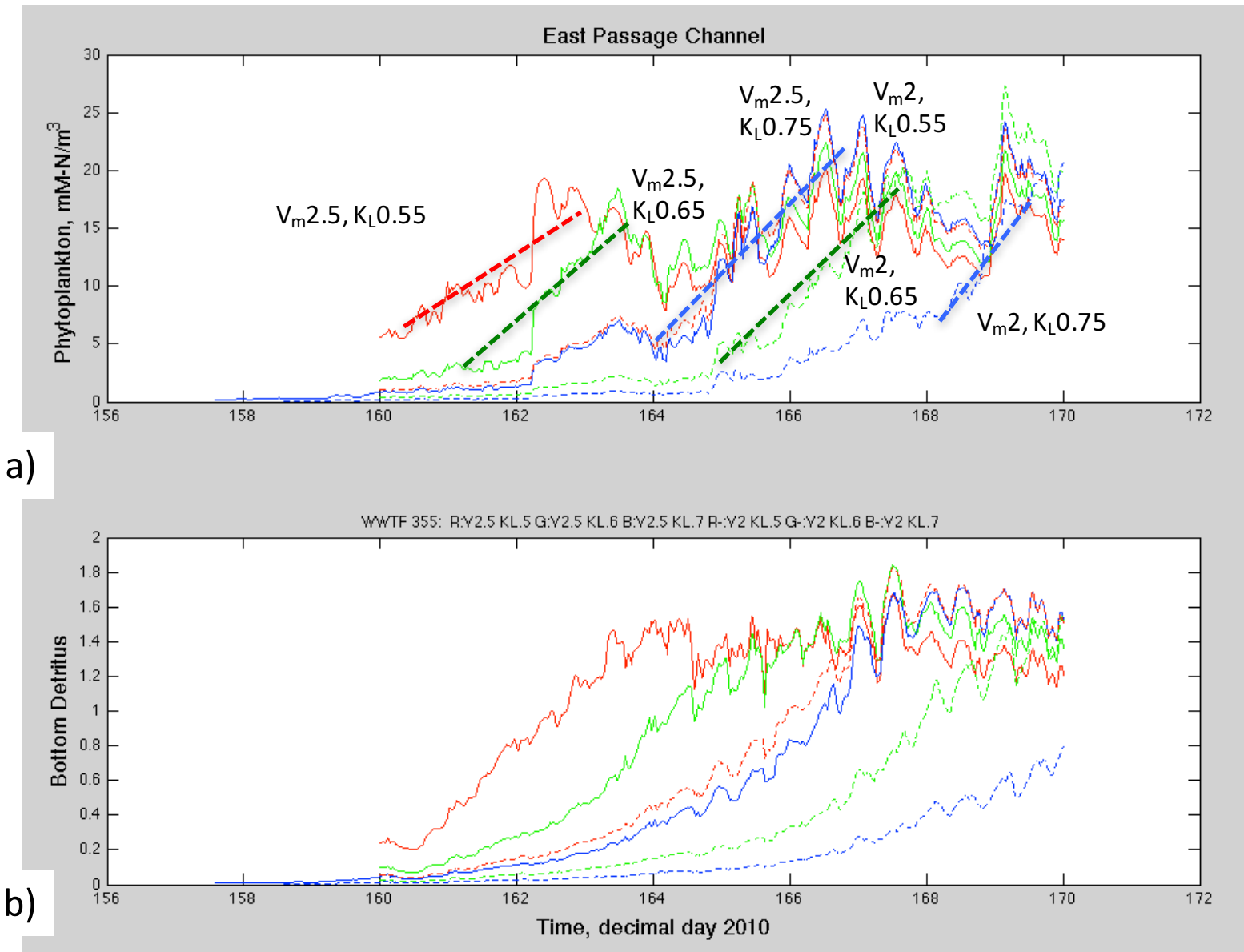


Figure 83. Plots of surface P and bottom D in the East Passage channel at the southern boundary of the Ohio Ledge region. Different K_L and V_m values are: (red $V_m=2.5$, $K_L=0.55$; red dash $V_m=2$, $K_L=0.55$; green $V_m=2.5$, $K_L=0.65$; green dash $V_m=2$, $K_L=0.65$; blue $V_m=2.5$, $K_L=0.75$; blue dash $V_m=2$, $K_L=0.75$). Cases have WWTFs releasing at 355 mM m^{-3} (5 mg L^{-1}), and have low zooplankton grazing (0.6 day^{-1}). Being further from Greenwich Bay, the lower uptake rate $V_m=2$ cases and larger K_L values are now showing more pronounced (2-3 day) delays to the bloom.

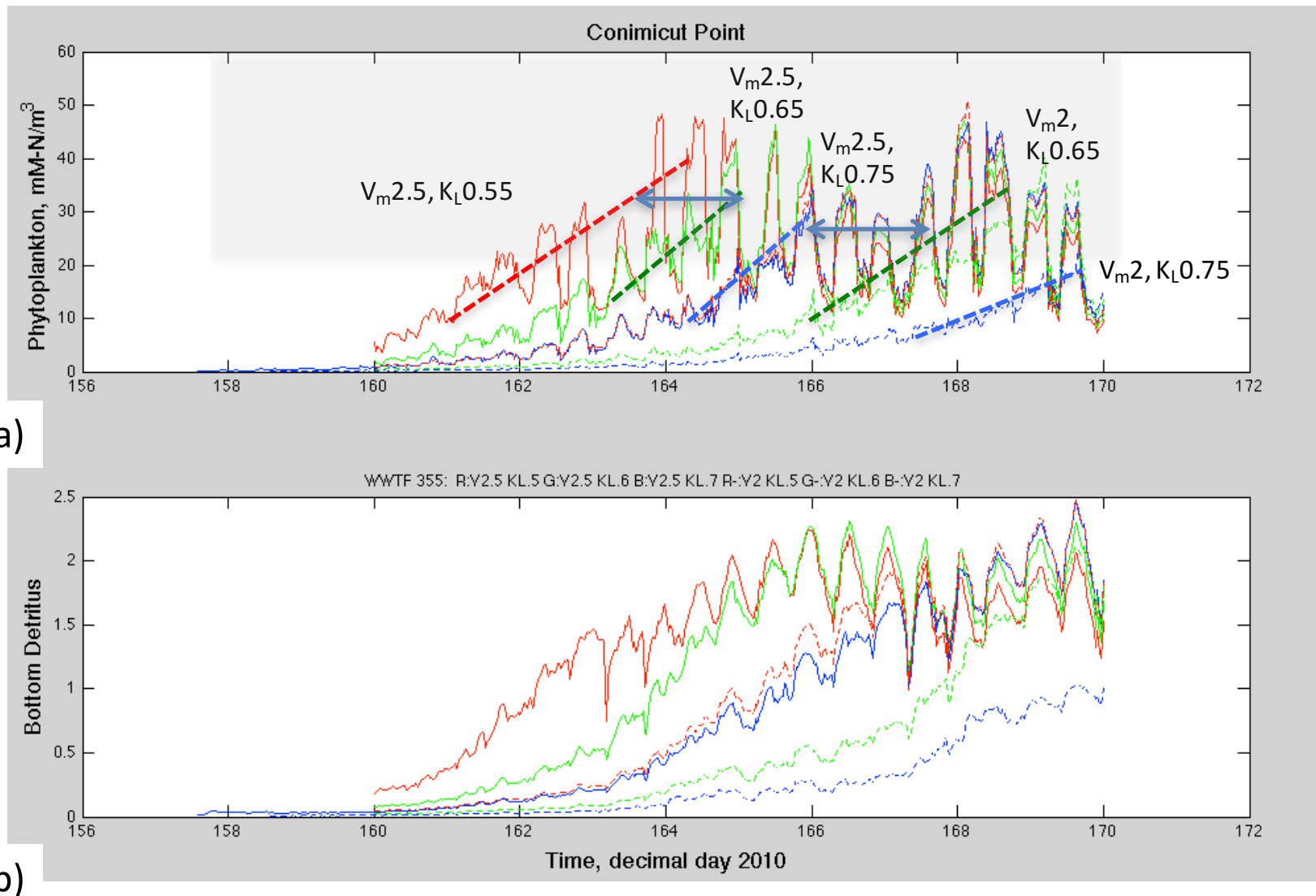


Figure 84. Plots of surface P and bottom D at Conimicut Point, mouth of the Providence River which compare different K_L and V_m values (red $V_m=2.5, K_L=0.55$; red dash $V_m=2, K_L=0.55$; green $V_m=2.5, K_L=0.65$; green dash $V_m=2, K_L=0.65$; blue $V_m=2.5, K_L=0.75$; blue dash $V_m=2, K_L=0.75$). Cases have WWTFs releasing at 355 mM m⁻³ (5 mg L⁻¹), and have low zooplankton grazing (0.6 day⁻¹). The lower uptake rate $V_m=2$ cases and larger K_L values result in regular delays to the bloom. Delays in bloom timing with increasing K_L are ~2 days. Shaded region shows estimate for phytoplankton levels from NBC survey data (Figure 23) providing chlorophyll data during June 2010 bloom (C/chl ratio=20-50; C/N ratio=7).

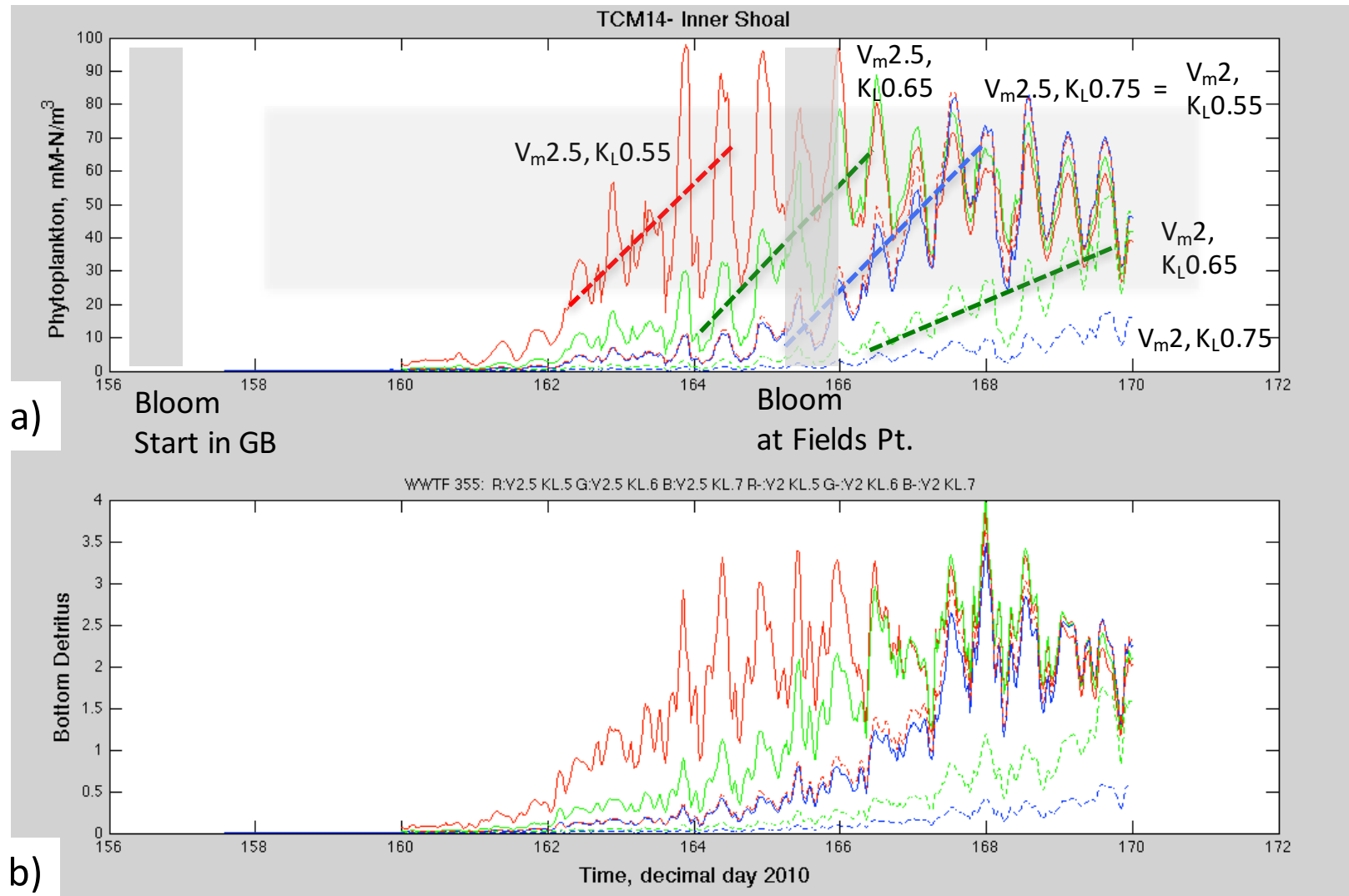


Figure 85. Plots of surface P and bottom D on the Edgewood Shoals comparing different K_L and V_m values (red $V_m=2.5$, $K_L=0.55$; red dash $V_m=2$, $K_L=0.55$; green $V_m=2.5$, $K_L=0.65$; green dash $V_m=2$, $K_L=0.65$; blue $V_m=2.5$, $K_L=0.75$; blue dash $V_m=2$, $K_L=0.75$). Cases have WWTFs releasing at 355 mM m⁻³ (5 mg L⁻¹), and have low zooplankton grazing (0.6 day⁻¹). The lower uptake rate $V_m=2$ cases and larger K_L values result in delays to the bloom. Shaded region shows estimate for phytoplankton levels from NBC survey data (Figure 23) providing chlorophyll data during June 2010 bloom (C/chl ratio=20-50; C/N ratio=7).

Phillipsdale

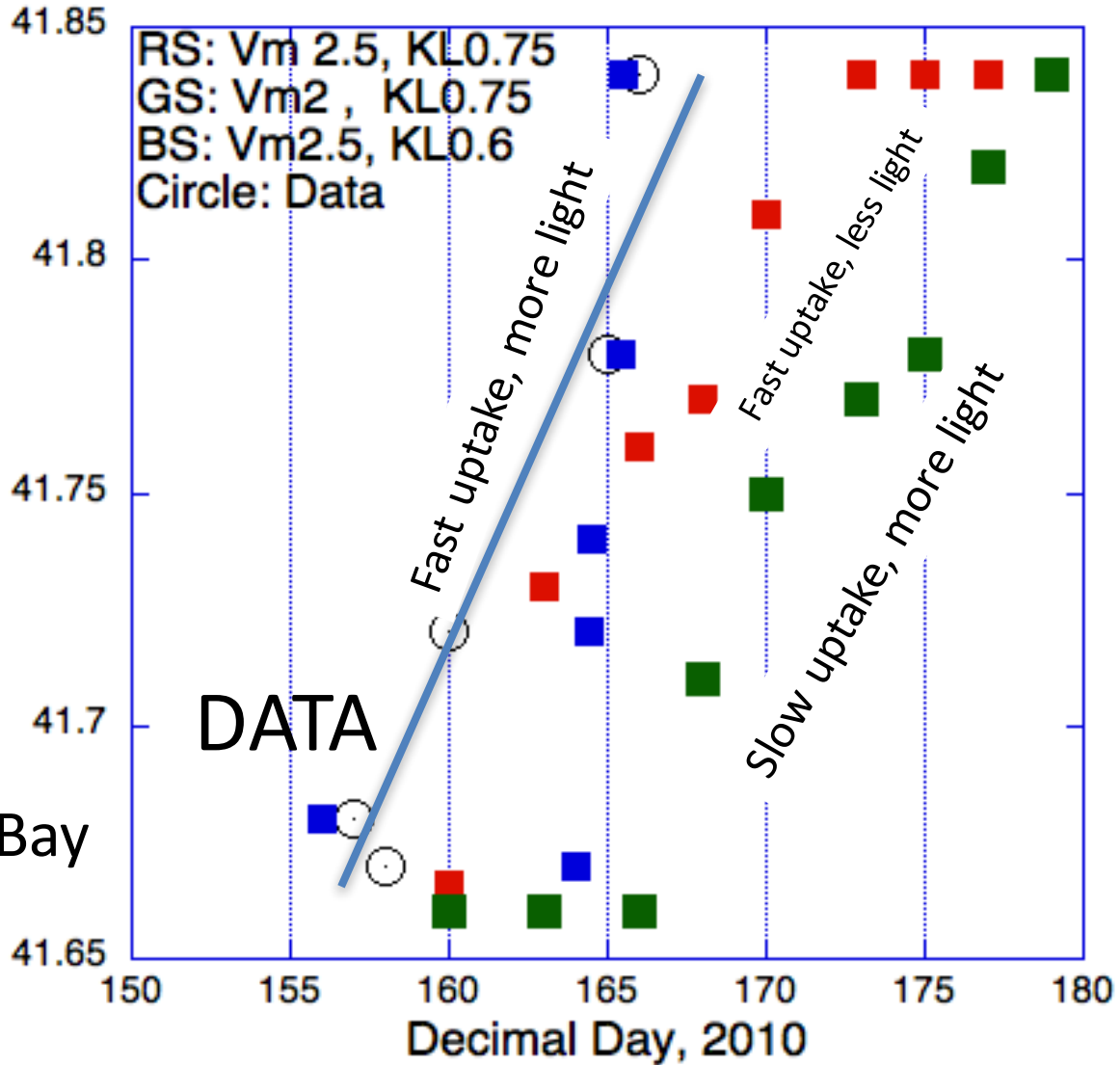


Figure 86. Plot showing the northward progression of the bloom recorded by the location (latitude) of the peak chlorophyll level as a function of decimal day. For the larger Vm2.5 (R) the bloom wave progresses from GB to PD from day 163 to 173, or 10 days. For the uptake of Vm2 the progression from GB to PD begins later on day 167, peaking at PD on day 179 after 13 days.

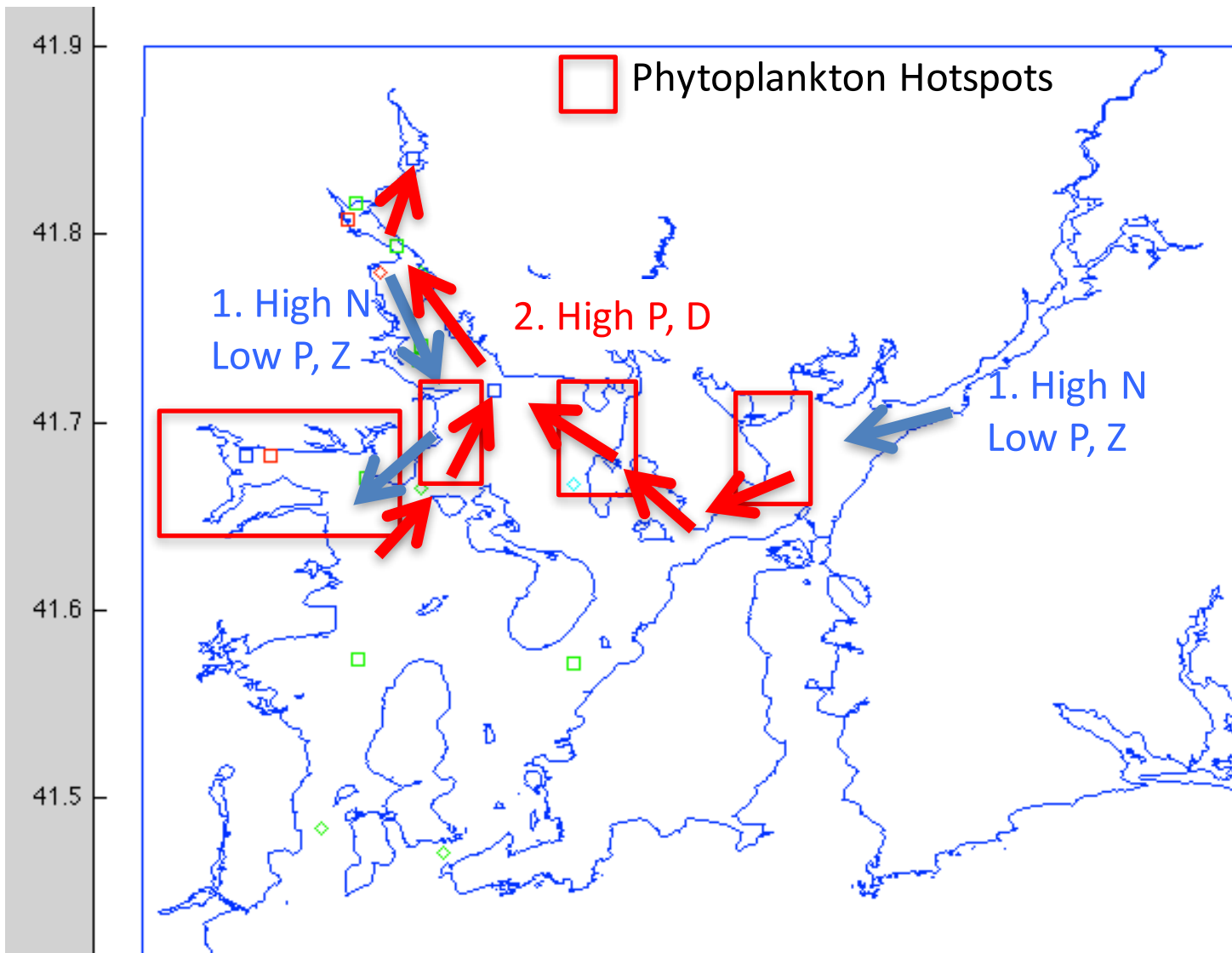


Figure 87. Map of Narragansett Bay showing schematic representation of one style of nutrient/phytoplankton bloom/flow dynamics seen in a number of NPZD-ROMS simulations. Water with very high nutrient and very low phytoplankton concentrations flow from the Providence River to Ohio Ledge. Depending on tide/wind conditions a percentage of the chemical plume diverts either into the East and West Passages. Also, depending on wind/wind conditions, a percentage of the WP plume moves into GB. Phytoplankton growth begins in GB and along the shallow edges of Ohio Ledge. Wind conditions can work to disperse biomass from these regions into long-term, sub-tidal currents that carry mass back northward into the Providence and Seekonk Rivers.

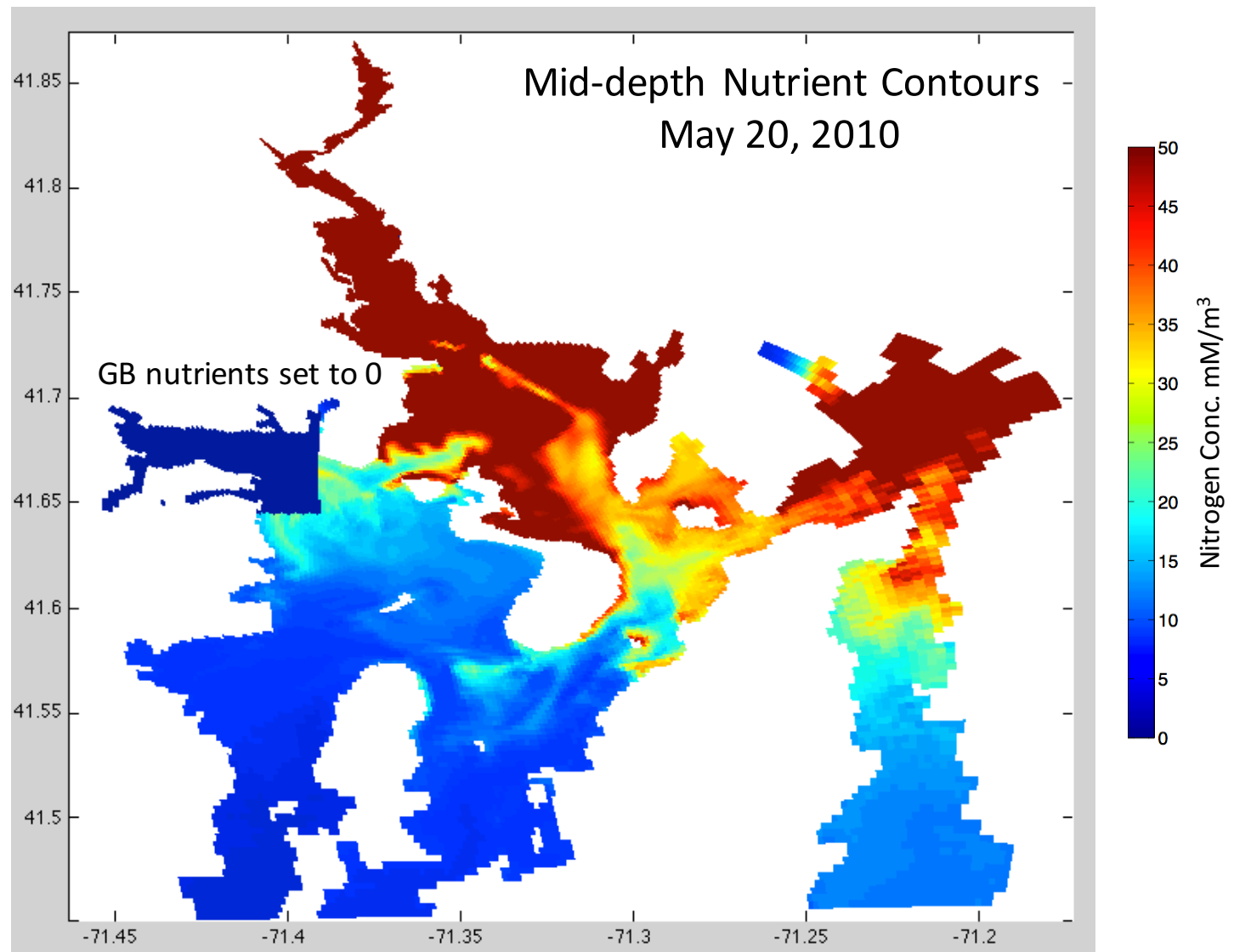
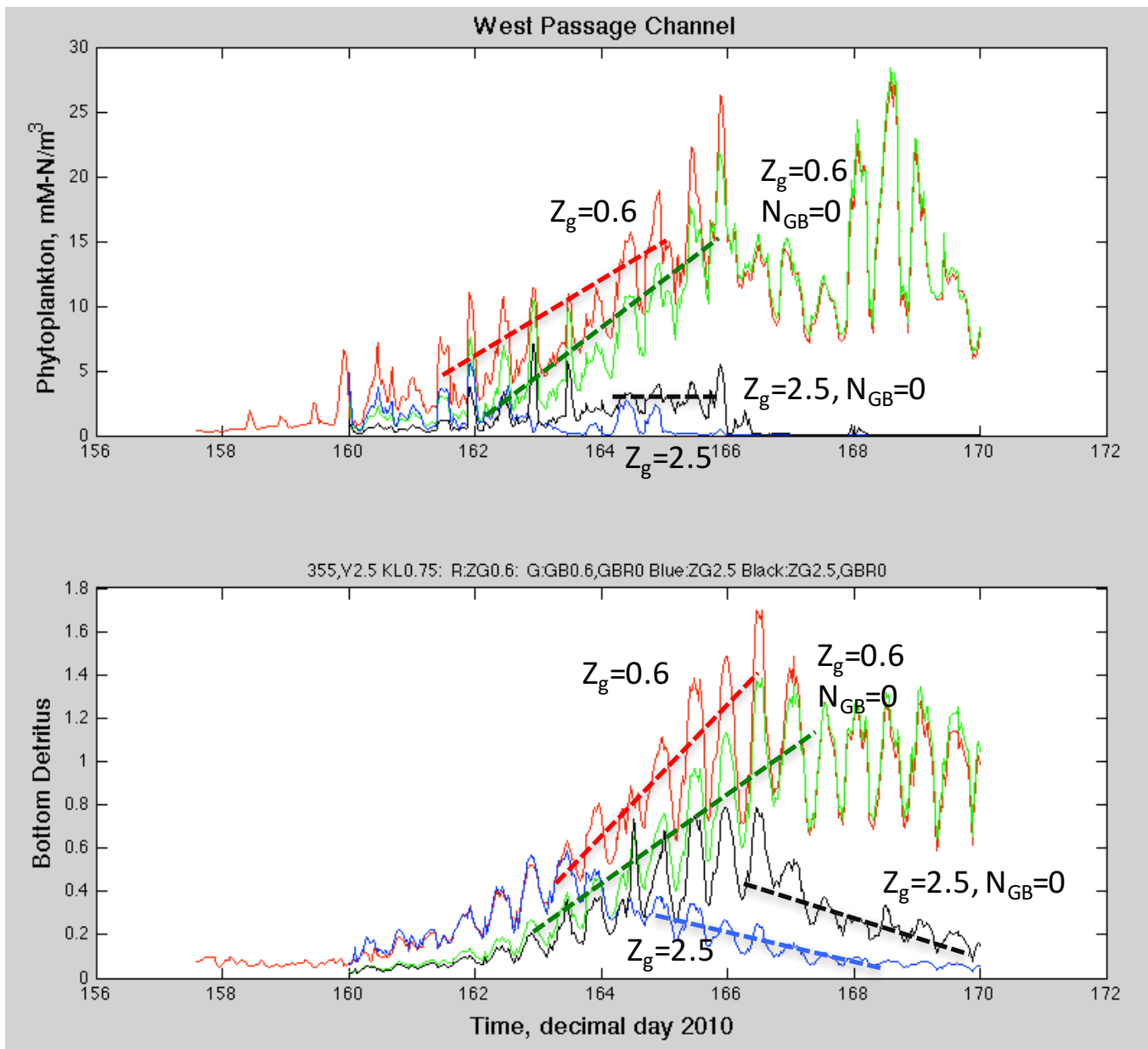


Figure 88. A series of calculations have been run to test the role of Greenwich Bay blooms in influencing more bay-wide processes. These were initiated from May20 output in which Greenwich Bay nutrients were zeroed out to eliminate bloom growth in this area. In addition, the fresh water sources to Greenwich Bay had their nutrient concentrations set to zero.

a)



b)

Figure 89. Plots from the West Passage, north of GB, showing surface P and bottom D for a case where GB nutrients were set to zero. Cases have WWTFs releasing at 355 mM m⁻³ (5 mg L⁻¹), $V_m=2.5$ day⁻¹ and light extinction of 0.75 m⁻¹. Differences are red: $Z_g=0.6$; green: $Z_g=0.6$, GB zeroed; blue: $Z_g=2.5$; black $Z_g=2.5$, GB zeroed.

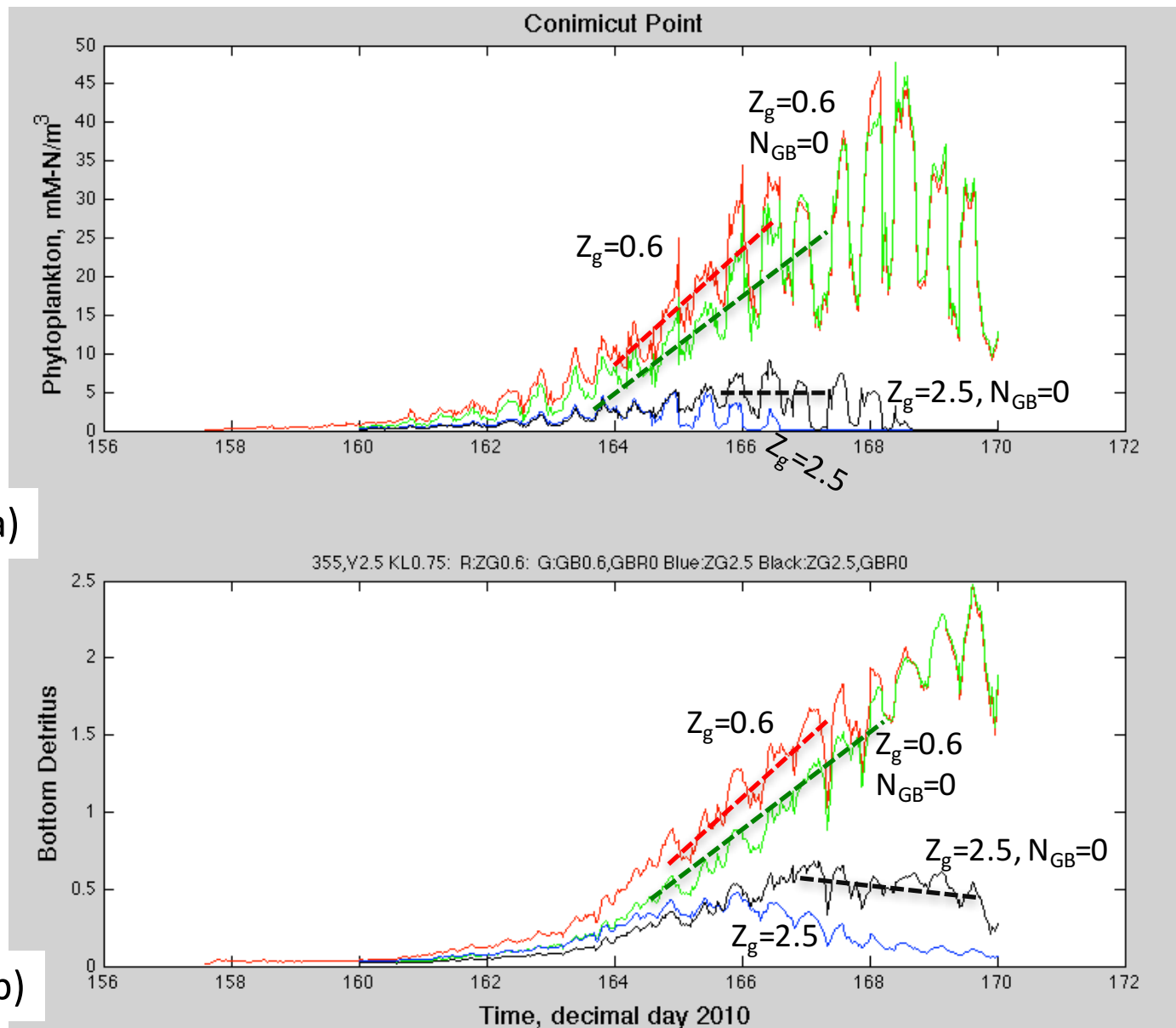


Figure 90. Plots from Conimicut Point, showing surface P and bottom D for a case where GB nutrients were set to zero. Cases have WWTFs releasing at 355 mM m⁻³ (5 mg L⁻¹), $V_m=2.5$ day⁻¹ and light extinction of 0.75 m⁻¹. Differences are red: $Z_g=0.6$; green: $Z_g=0.6$, GB zeroed; blue: $Z_g=2.5$; black $Z_g=2.5$, GB zeroed. For lower grazing cases (R/G) there is little difference between normal and GB-zeroed solutions for P at this site. There are more pronounced differences in the detrital pool. For the high grazing cases (blue/black) the GB-zeroed case results in a stronger bloom and detrital signal at this station.

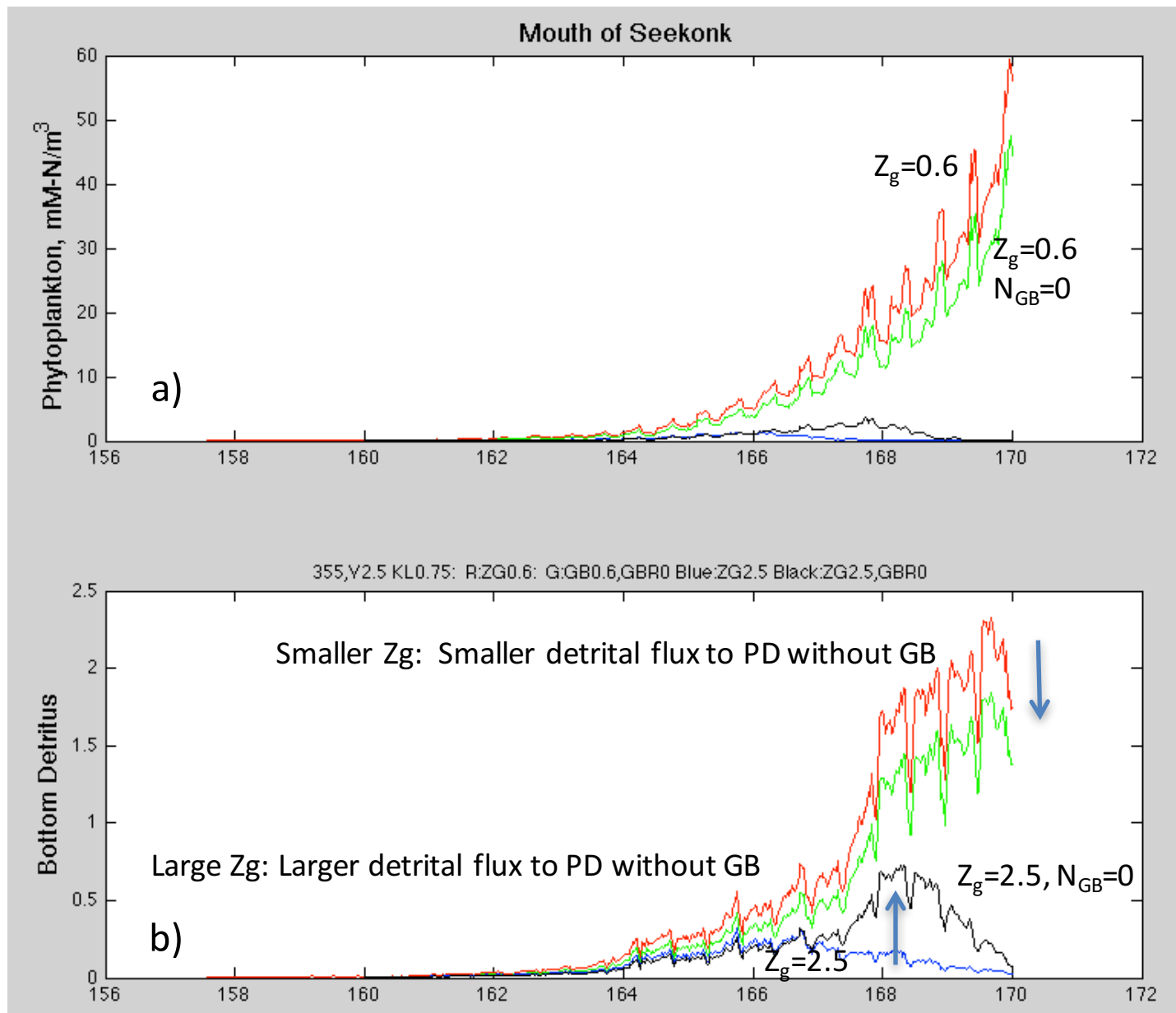


Figure 91. Interestingly, plots from the mouth of the Seekonk River show surface P and bottom D are different for reference and GB-zeroed cases. Here WWTFs released at 355 mM m⁻³ (5 mg L⁻¹). Values were $V_m=2.5 \text{ day}^{-1}$ and light extinction $K_L=0.75 \text{ m}^{-1}$. Differences are red: $Z_g=0.6$; green: $Z_g=0.6$, GB zeroed; blue: $Z_g=2.5$; black $Z_g=2.5$, GB zeroed. For lower grazing cases (R/G) there is little difference between normal and GB-zeroed solutions for P at this site. For the high grazing cases (blue/black) the GB-zeroed case results in a stronger, later pulses in phytoplankton at this station. The differences are more pronounced in the detrital pool.

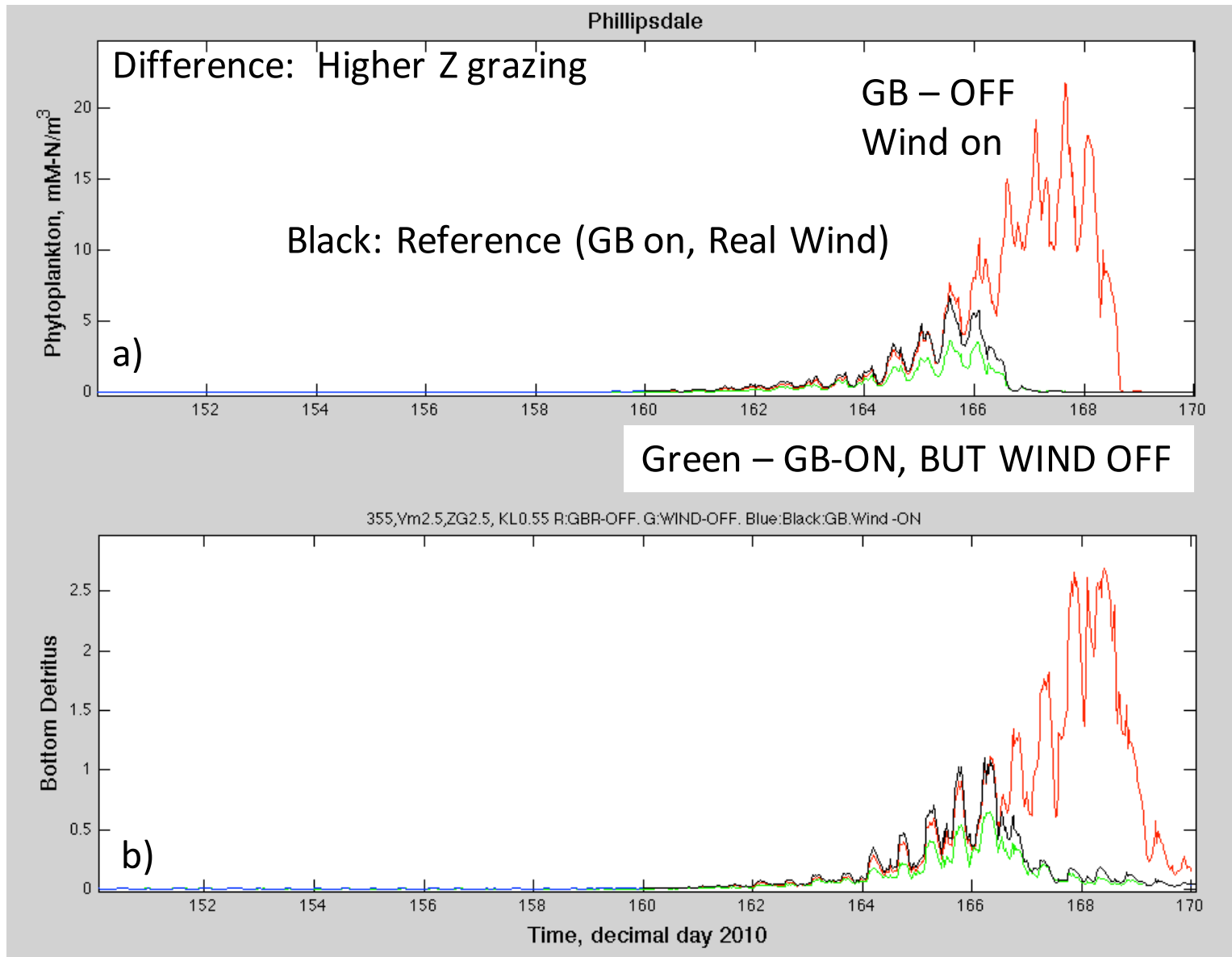


Figure 92. Plots of phytoplankton levels and detritus concentration for Phillipsdale station. Black lines show the reference case, with Greenwich Bay included normally and winds on. Green lines are for same run (with Greenwich Bay in the model) but for WIND OFF. All things being equal, turning off wind leads to a 50% reduction in phytoplankton bloom at Phillipsdale, suggesting northward wind transport preceding the bloom off material from Greenwich Bay is important. The most dramatic effect is shown by the red line, which has winds on, but Greenwich Bay zeroed out. Lower zooplankton levels from having GB-OFF significantly influences the bloom intensity as far north as Phillipsdale. Differences are red: $Z_g=0.6$; green: $Z_g=0.6$, GB zeroed; blue: $Z_g=2.5$; black $Z_g=2.5$, GB zeroed.

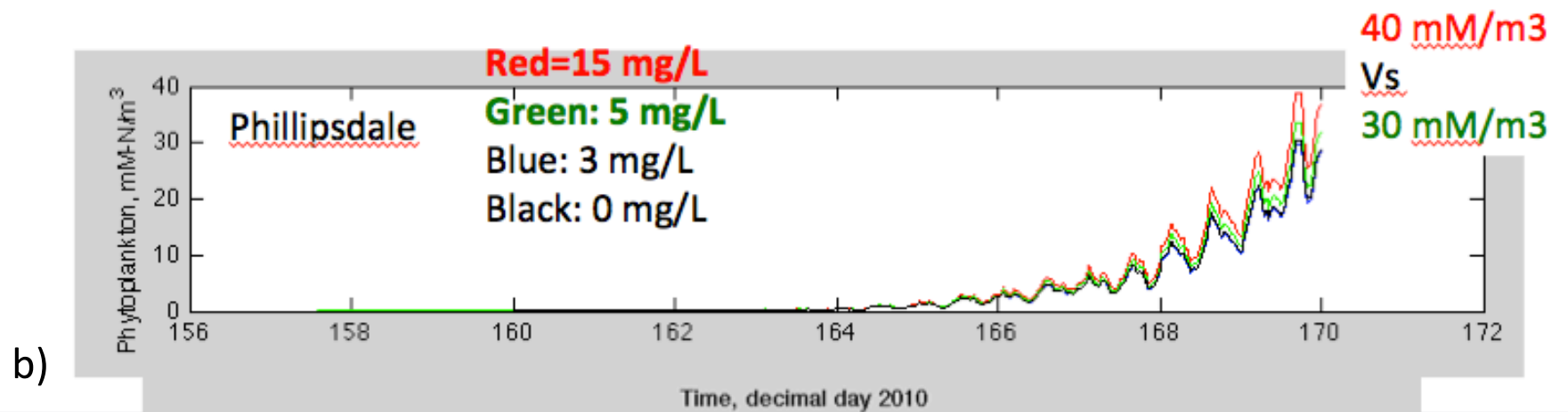
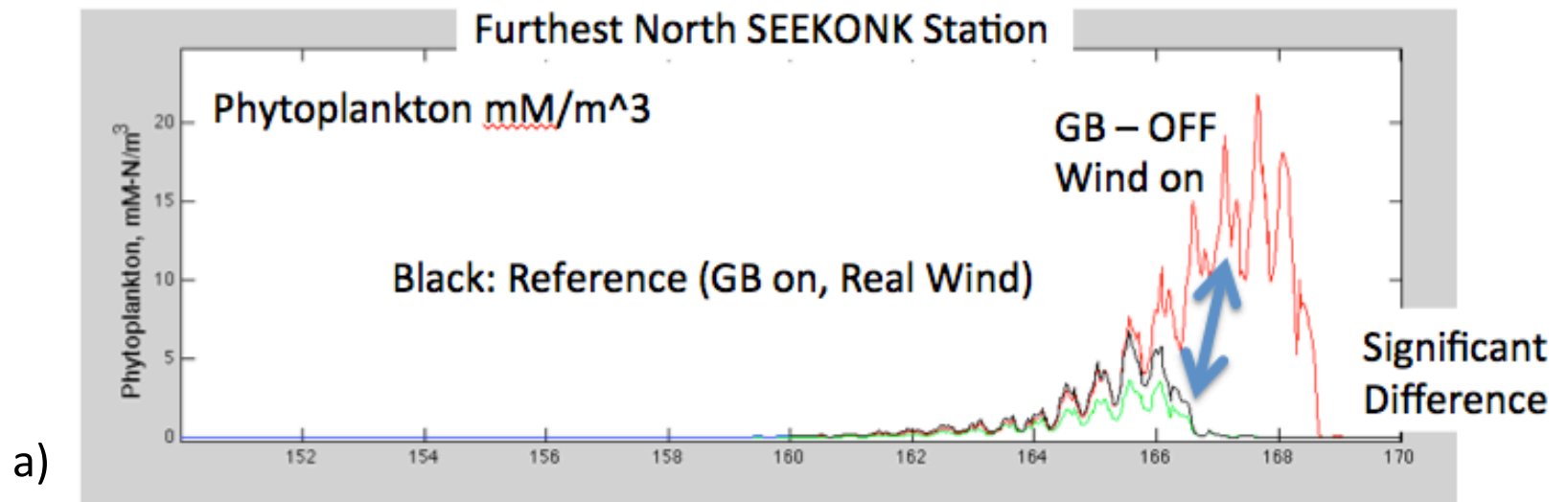


Figure 93. Summary of plots showing phytoplankton bloom intensity for natural parameters (a) winds versus Greenwich Bay effects and (b) managed parameters (WWTF reductions in nitrogen output). These simulations show that Phillipsdale bloom intensity is modulated more strongly by wind and Greenwich Bay impacts than by WWTF reductions. In (a), the green case is where Greenwich Bay is in the model, but the wind forcing is zeroed out.

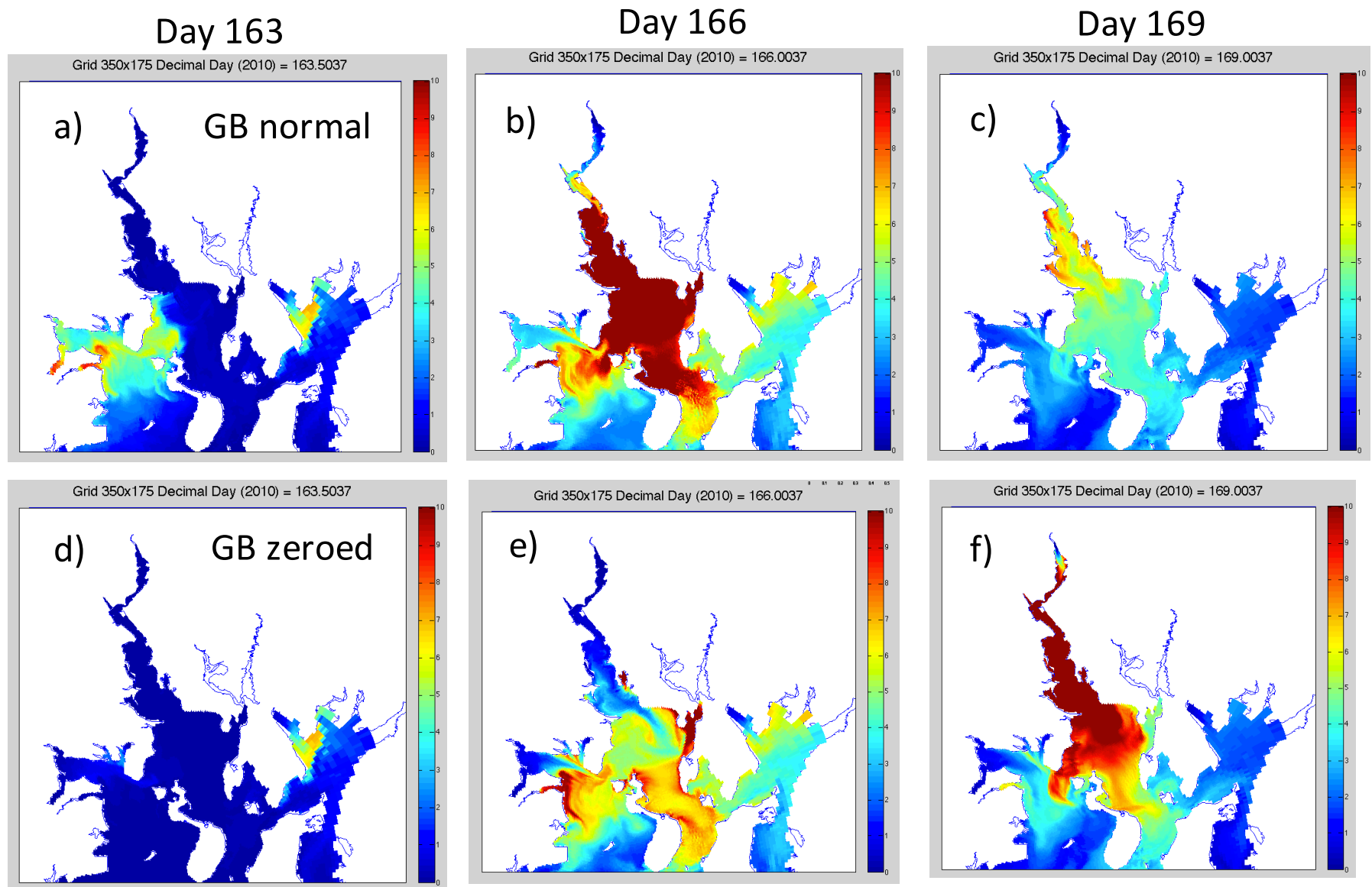


Figure 94. Contours of near surface zooplankton concentration (red = 10 mM/m³) for cases with high phytoplankton uptake ($V_m=2.5$), high zooplankton grazing rate ($Z_g=2.5$) and good light penetration ($k_L=0.55$). Top row shows evolution of a case with Greenwich Bay functioning normally (e.g. initiating a phytoplankton bloom and then a zooplankton bloom) for days a) 163, b) 166 when there is a peak zooplankton bloom mid-bay and c) 169. The bottom row shows same time evolution but for case where all Greenwich Bay nutrients, phytoplankton and zooplankton are zeroed out to start (4/20), including all river inputs to GB. The delayed GB initiated zooplankton bloom (e) allows phytoplankton bloom (Figures 92,93) to grow exceptionally large in the Providence River.

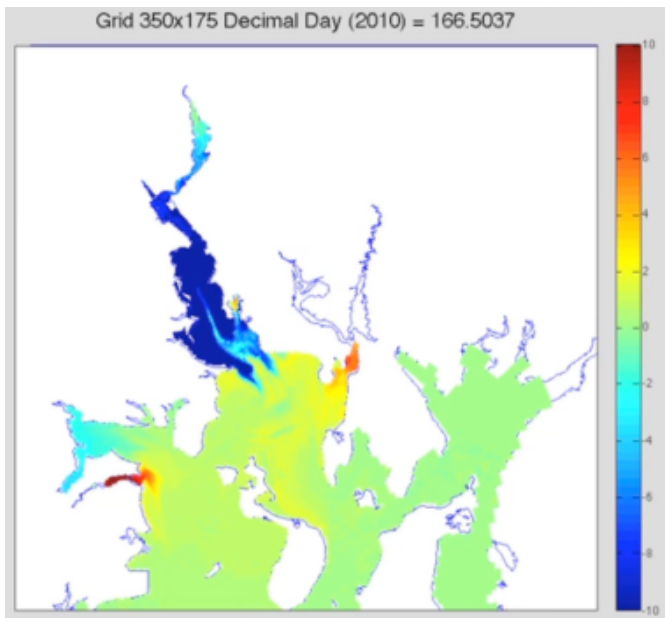
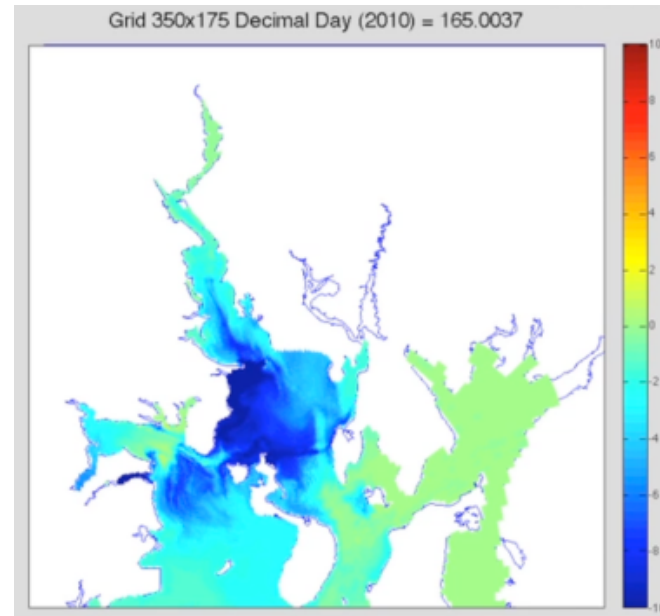
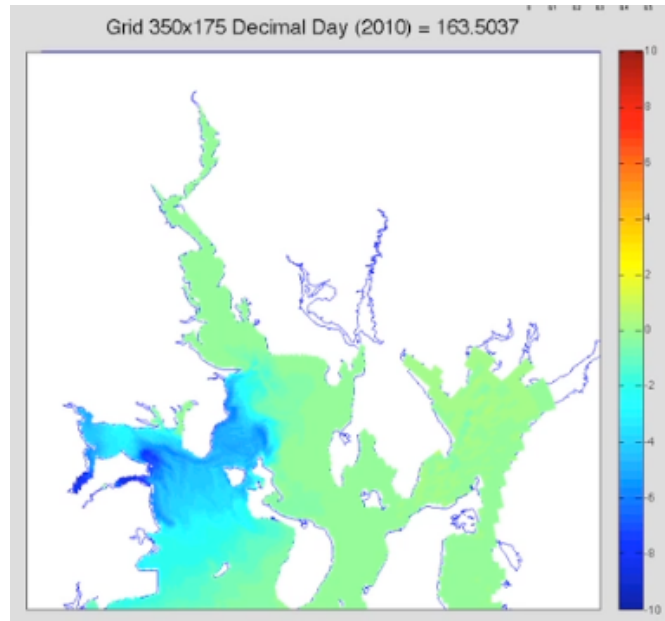


Figure 95. Contours showing the near surface difference in zooplankton concentrations, calculated by subtracting the reference case from the no Greenwich Bay case. Blue colors represent negative zooplankton concentrations due to a deficit in this field in the case where Greenwich Bay has been zeroed out. Frames are for days (a) 163.5, (b) 165 and (c) 166.5 and show that a deficit in zooplankton is initiated in Greenwich Bay and is subsequently seen on Ohio Ledge and up into the Providence and Seekonk Rivers. This leads to unrestricted phytoplankton blooms in the cases where Greenwich Bay has been zeroed out.

Day 154 : 6/2/10

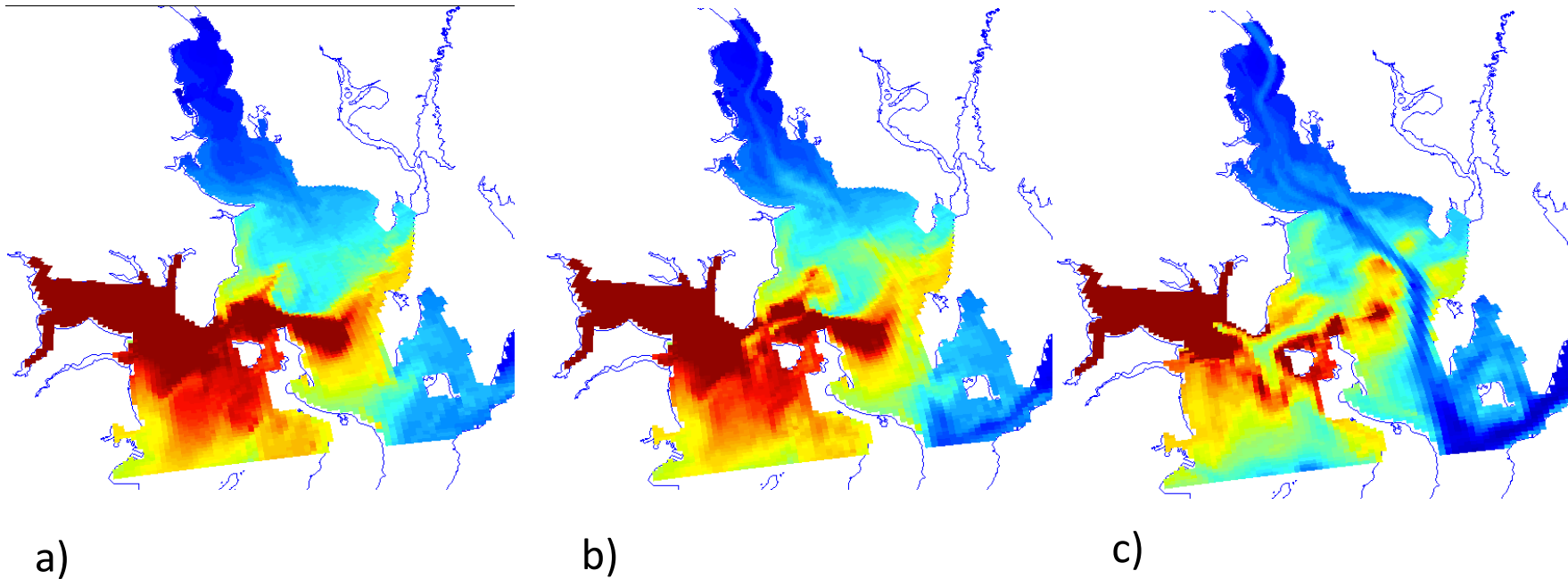


Figure 96 . ROMS NPZD models show that blooms are persistent in Greenwich Bay and that more extensive upper Bay blooms (such as the one in June, 2010) begin in the mid-Bay and progress northwards. Here we show results from the fullbay model simulation for 2010 (Kincaid, 2012a), where distinct dye sources were used to identify and track inputs from all major river and WWTF sources. Color contours here are showing transport of Greenwich Bay dye sources (2 rivers, 1 WWTF) summed together and integrated over a) upper third, b) middle third and c) lower third of the water column. Here red color is dimensionless dye concentration of 0.02. The colorbar is saturated for Greenwich Bay to highlight transport patterns from Greenwich Bay, through northern West Passage entrance (Warwick Neck to Patience Island) and onto Ohio Ledge. Within a day this patch of GB derived mass is dispersed eastward across the entire Ohio Ledge Region. Once on the eastern side of the system, this material is efficiently carried northward, particularly in the waters below the light penetration depth.

Day 160 : 6/8/10

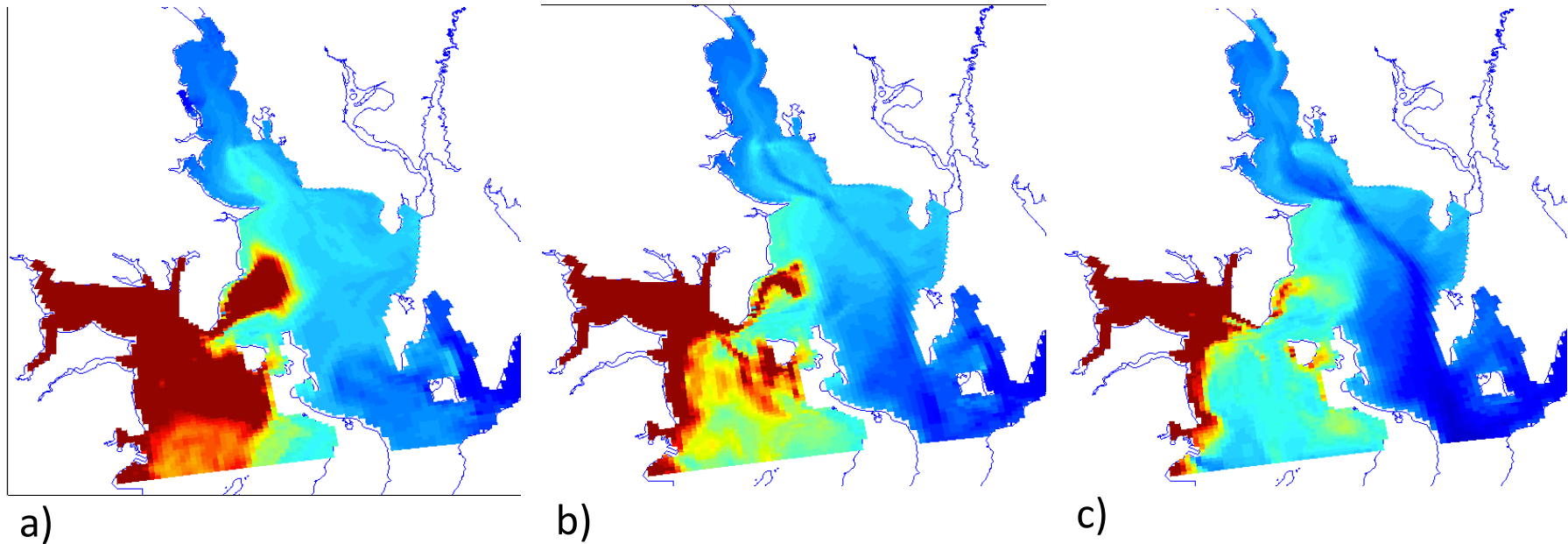


Figure 97. Similar results as in previous figure from the fullbay model simulation for 2010 (Kincaid, 2012a), where distinct dye sources were used to identify and track inputs from all major river and WWTF sources. Color contours show transport of Greenwich Bay dye sources (2 rivers, 1 WWTF) summed together and integrated over a) upper third, b) middle third and c) lower third of the water column. Dimensionless dye concentration is red is $C^*=0.02$. Another patch of GB derived mass pulses onto Ohio Ledge within the upper 2/3 of the water column. Lower concentration ($C^*=0.01$) is carried northward into the Providence River, appearing in both the channel and the shallow shoals regions.

Day 166 : 6/14/10

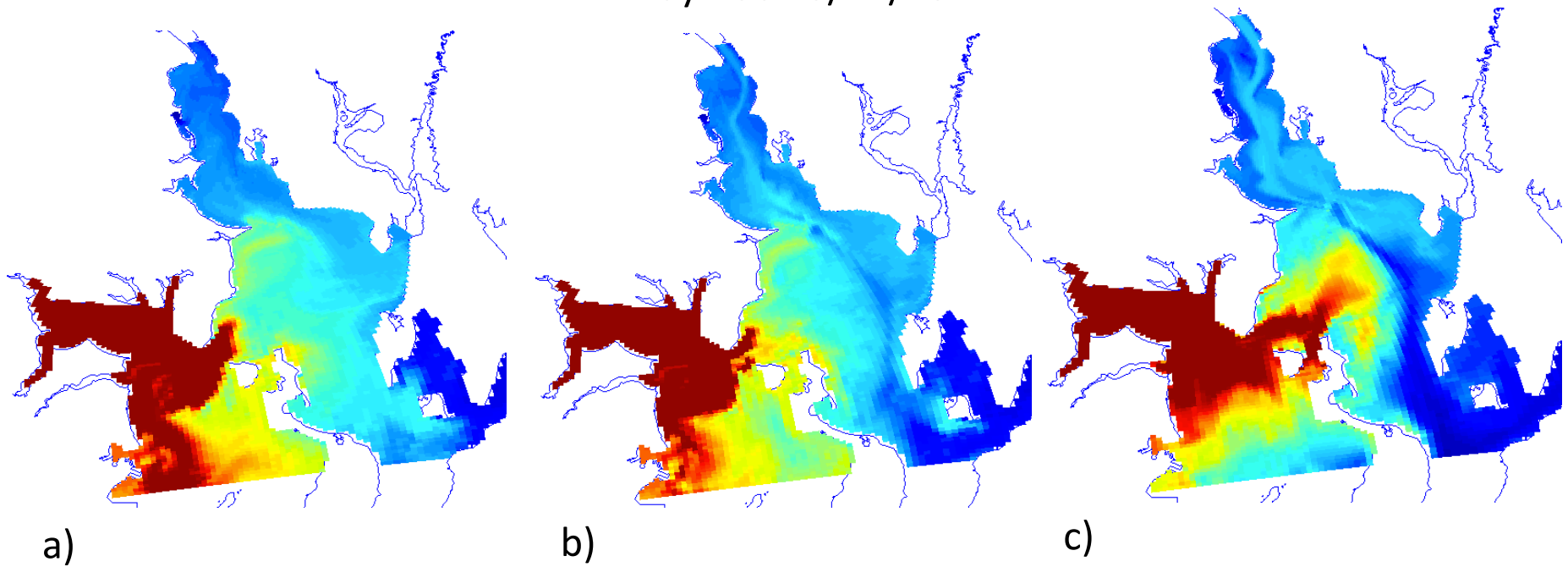
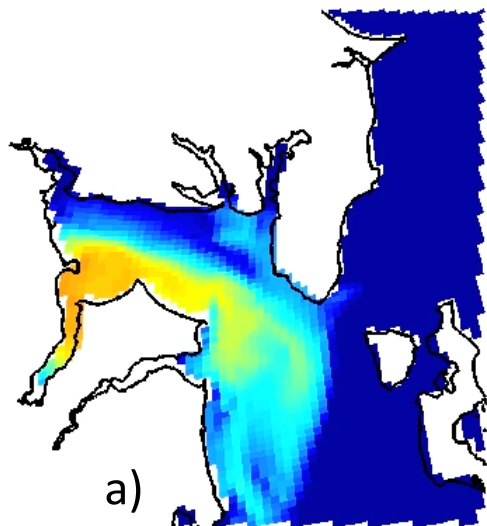


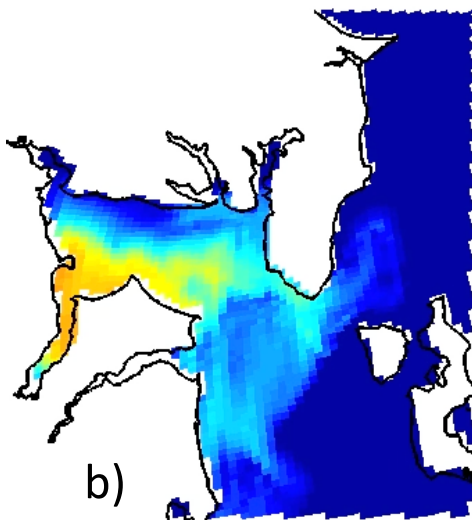
Figure 98. Similar results as in previous figure from the fullbay model simulation for 2010 (Kincaid, 2012a). Color contours show transport of Greenwich Bay dye sources (2 rivers, 1 WWTF) summed together and integrated over a) upper third, b) middle third and c) lower third of the water column. Dimensionless dye concentration is red is $C^*=0.02$. Here a near-bottom plug of GB derived mass moves efficiently eastward across Ohio Ledge. Remnant of previous events are seen in low concentration (light blue shades) within the shipping channel and Port Edgewood Channel of the Edgewood Shoals (c).

194.4133



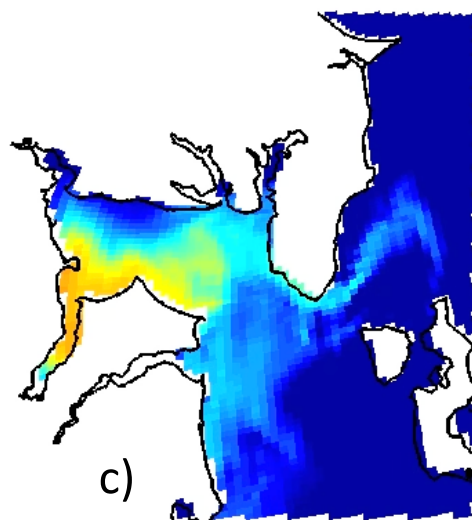
a)

194.5383



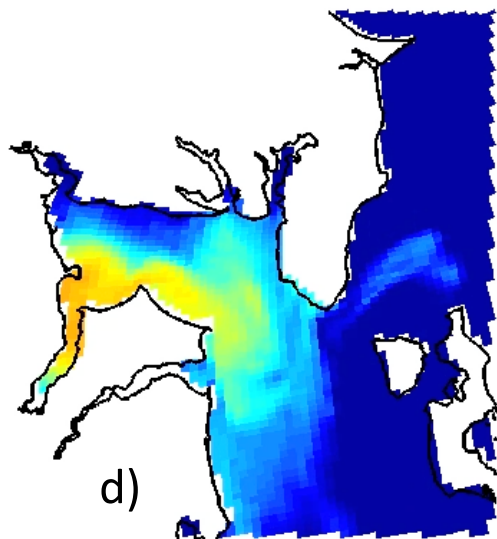
b)

194.6008



c)

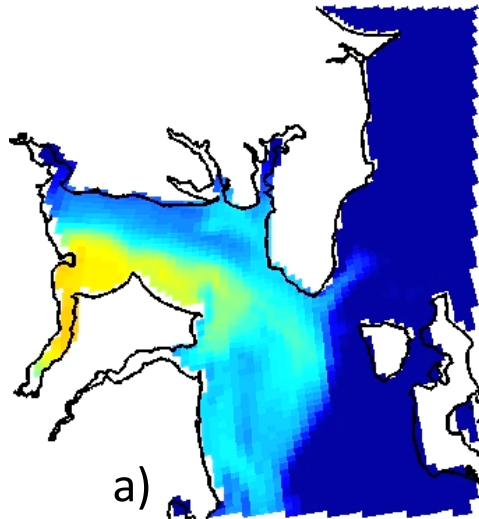
194.705



d)

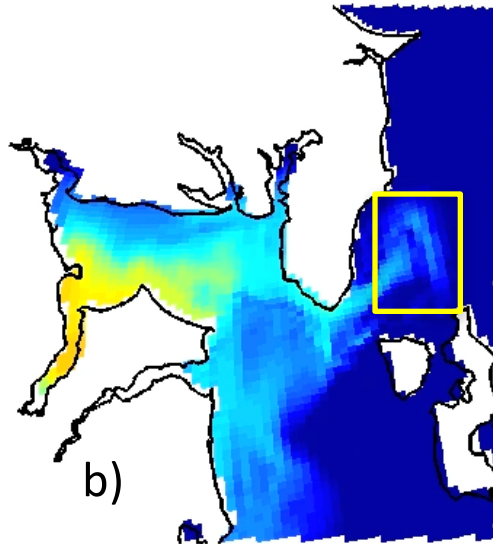
Figure 99. Prior figure summarized a wind driving mechanism for transporting Greenwich Bay biomass onto Ohio Ledge. A second mode of transporting phytoplankton biomass generated in Greenwich Bay onto Ohio Ledge, the primary source region for Providence River northward return flow, is tidal pumping. Frames show transport of a conservative dye in a 2010 NB-ROMS simulation released to inner Greenwich Bay from a) late ebb, b) early flood, c) late flood and d) early ebb tidal stages. Small volumes of dye near the northern mouth of GB is transported northward up onto Ohio Ledge and left there on subsequent ebb.

195.4967



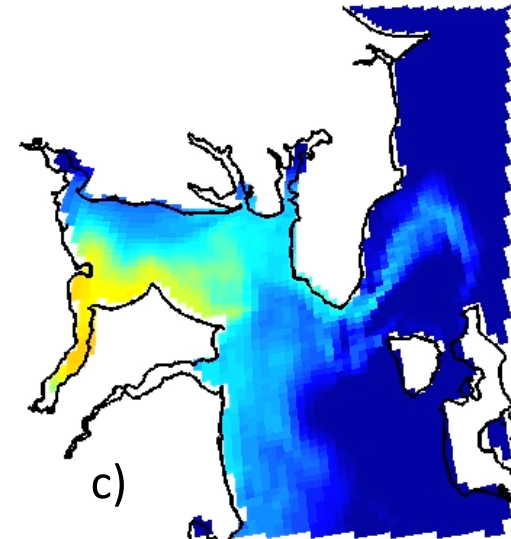
a)

195.6008



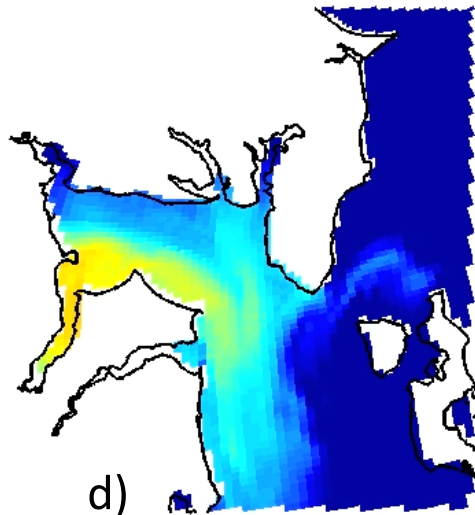
b)

195.6425



c)

195.7883



d)

Figure 100. Similar to prior figure showing a second transport mode for phytoplankton biomass generated in Greenwich Bay onto Ohio Ledge. The mode is tidal pumping, which is smaller volumetrically than wind events, but more regular. Frames show transport of a conservative dye released to inner Greenwich Bay from a) late ebb, b) early flood, c) late flood and d) early ebb tidal stages. Small volumes of dye near the northern mouth of GB is transported northward up onto Ohio Ledge and left there on subsequent ebb.

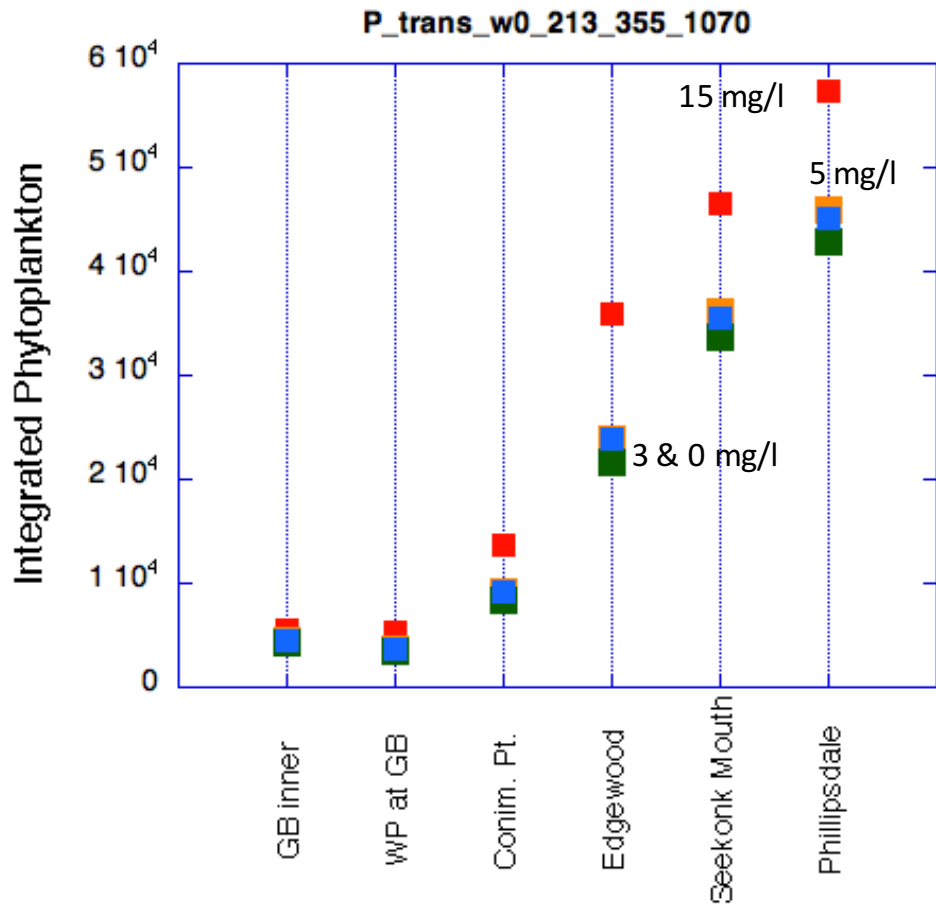


Figure 101. Plots of near surface phytoplankton biomass at key stations from Greenwich Bay to the Seekonk River integrated over a ten day period (days 161 to 170) for the largest growth rate ($V_m=2.5$). Colors correspond to WWTF release concentrations (Red 15 mg/L, Orange 5 mg/L, Green 3 mg/L and Blue 0 mg/L). Here a bloom as initiated in the mid-bay and progressed and intensified to the north. Significant reduction in biomass is predicted for change in WWTF release levels from 15 mg/L to 5 mg/L. Additional modeled reductions do not significantly reduce simulated biomass.

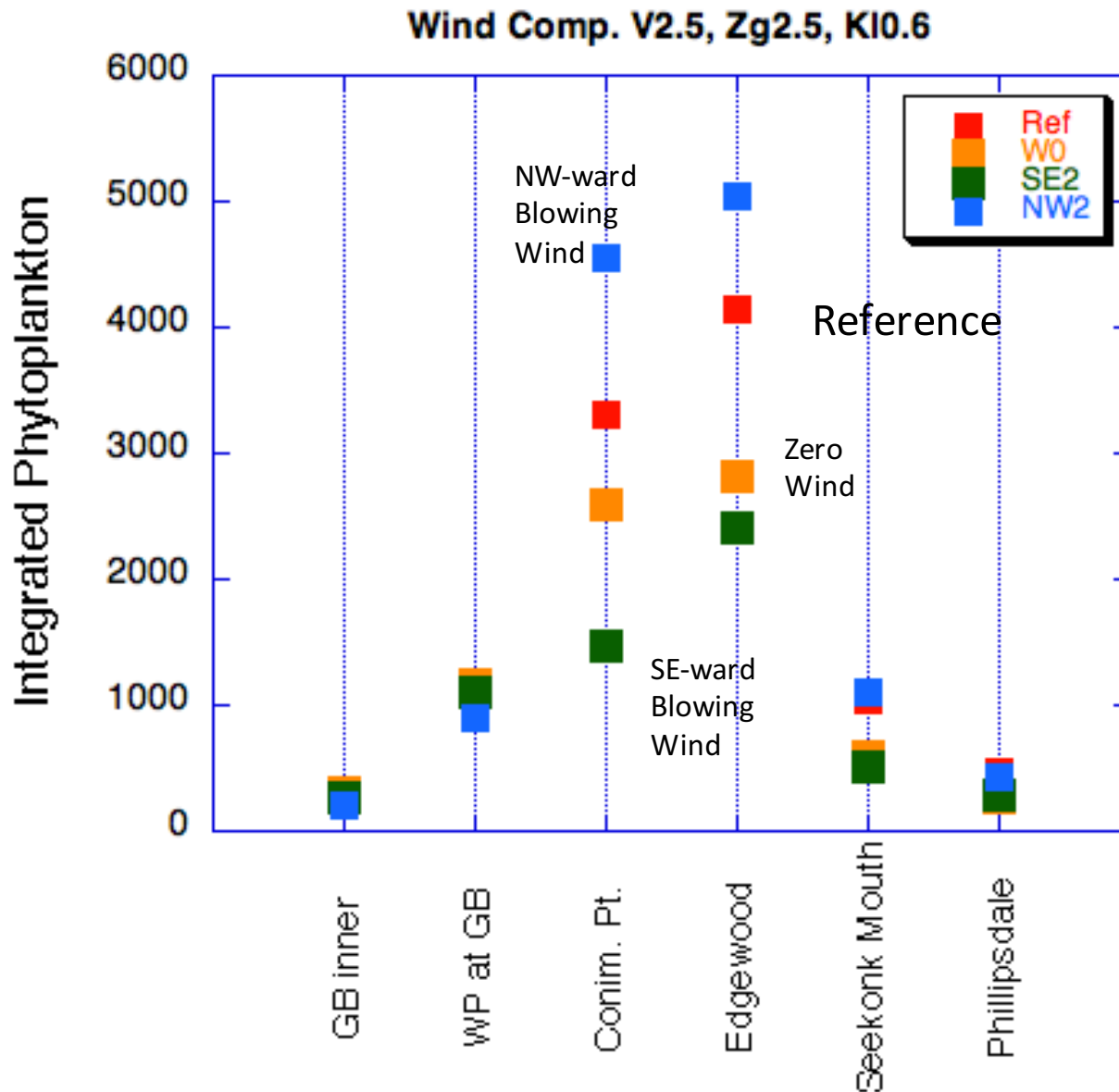


Figure 102. Plot of integrated phytoplankton biomass (mM m^{-3}) (IPB) recorded at distinct stations (x-axis) over 10 day model simulation (days 160-170) showing strong influence of prevailing winds. The reference case has $V_m=2.5$, $Z_g=2.5$ and $K_L=0.6$ and uses actual wind data to force the model. IPB is substantially increased in the Providence River for the simulation with a prevailing northwestward wind. Cases with zeroed out wind, or southeastward blowing wind record reduced IPB levels in the Providence River relative to the reference case.

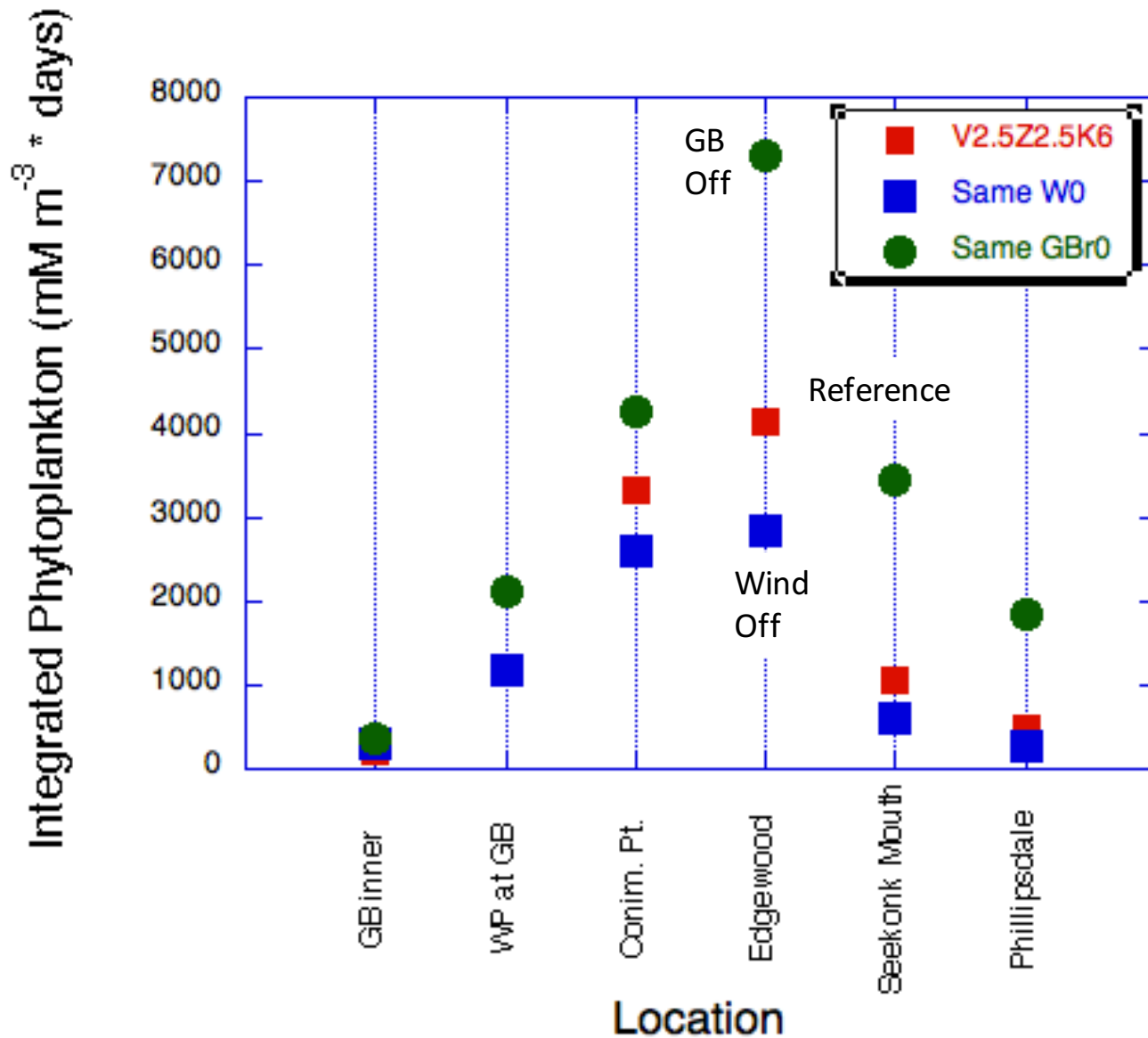


Figure 103. Similar plot to Figures 99,100 of integrated phytoplankton biomass (mM m^{-3}) (IPB) recorded at distinct stations (x-axis) over 10 day model simulation (days 160-170) highlighting the importance of remote forcing. Here GBr0 is an idealized case where Greenwich Bay nutrients/biomass were zeroed out to start, but is otherwise identical to a reference case with $V_m=2.5$, $Z_g=2.5$ and $K_L=0.6$. Interestingly, bloom biomass in the Providence and Seekonk Rivers is substantially increased when all other factors are equal, except that Greenwich Bay is limited. Changes in Greenwich Bay and wind (red squares) can alter biomass in a more significant way than incremental reductions in WWTF outputs.

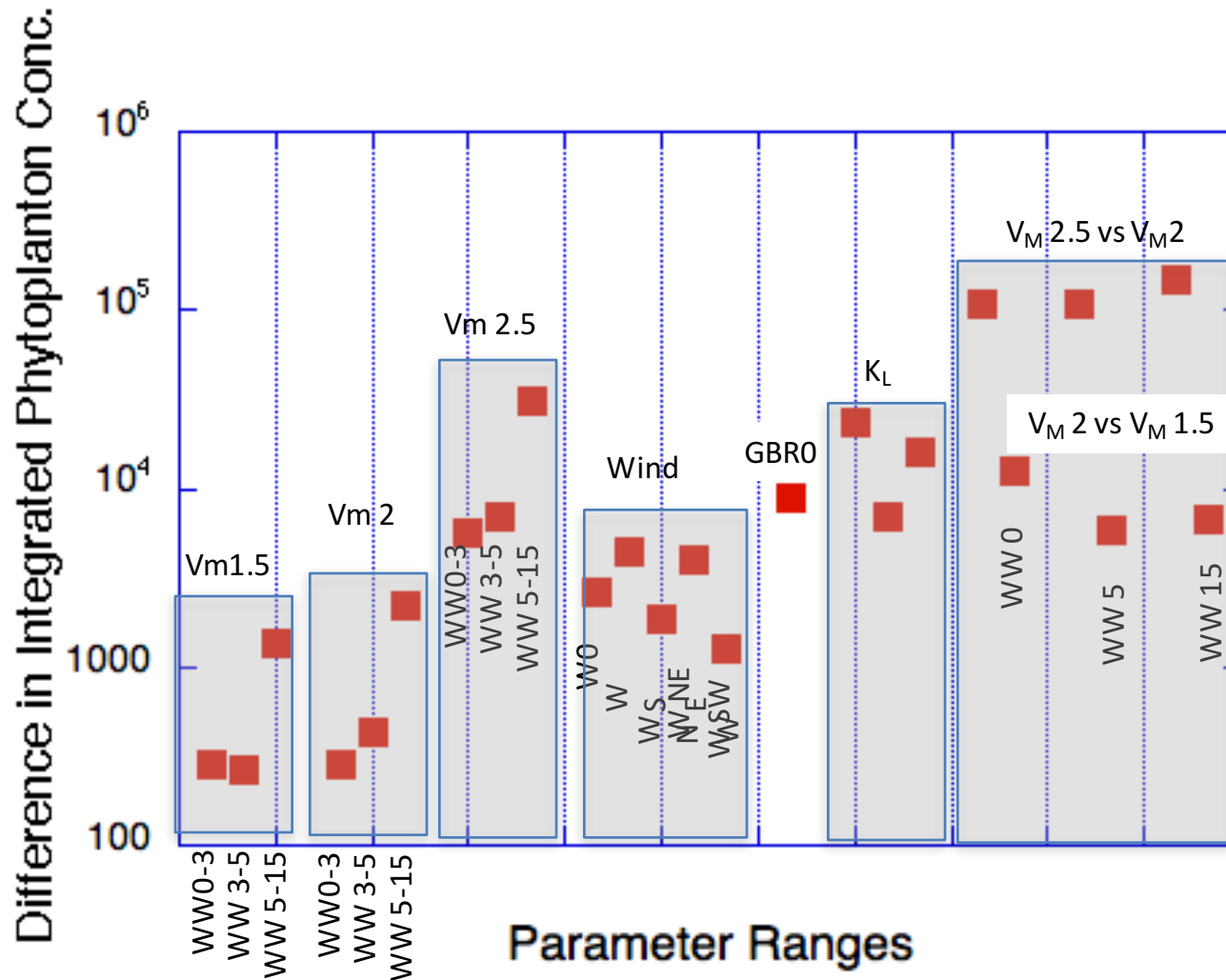


Figure 104. Models allow for gauging the magnitude of baywide changes in biomass during a bloom period brought about by various parameters. This plot show near-surface biomass integrated over 10 days at 6 mid to upper bay stations (used in Figures 99-101) and then differenced between cases with specific parameter choices. WW0-3 means the difference between IPB for WWTF releases of 3 mg/L and 0 mg/L. Only at the highest P growth rate do changes in WWTF release level generate integrated biomass changes equivalent to winds, Greenwich Bay changes, changes in light extinction parameter and P uptake rate.

Table 1. Statistical data-model comparison for sub-tidal or residual flow fields for NBC - supported TCM stations from dye transport study (Kincaid, 2012).

ROMS Station	TCM Station	Wilmont Skill	RMS (cm/s)
18	3	0.78	4.2
16	5	0.88	3.7
14	7	0.82	5.2
12	10	0.89	2.3
8	14	0.82	1.3
3	19	0.8	3.6

Table 2. Listing of various parameters employed in a range of ROMS simulation runs with NPZD model turned on.

Name	Start Date	Length Days	WWTF Conc. mM/m ³	Phyt. Uptake 1/day	Phyt. Mort 1/day	Zoop. Growth 1/day	Light Extinct. 1/m	Inv 1/2 sat. N uptake. (mM_N/m ³) ^{1/2}	GB Status	Wind Real unless noted
srB17x35M20R1ww355b2	5/20	30	355	1.0	0.1	0.6	0.75	0.1		
srB17x35M20R1ww213b2	5/20	30	213	1.0	0.1	0.6	0.75	0.1		
srB17x35M20R1ww54b2rf	5/20	10	54	1.0	0.1	0.6	0.75	0.1		
srB17x35M20R1ww18b2rf	5/20	10	18	1.0	0.1	0.6	0.75	0.1		
srB17x35M30R1ww1071b2	5/20	30	1071	1.0	0.1	0.6	0.75	0.1		
srBM30R1ww355V2	5/20	30	355	2.0	0.2	0.6	0.75	0.1		
srBM30R1ww1070V2	5/20	30	1070	2.0	0.2	0.6	0.75	0.1		
srBM30R1ww213V2	5/20	30	213	2.0	0.2	0.6	0.75	0.1		
srBM30R1ww0V2	5/20	30	0	2.0	0.2	0.6	0.75	0.1		
srBM30R1ww355V2Zg1	5/20	30	355	2.0	0.2	1.0	0.75	0.1		
srBJ8R1ww355V2Zg3	5/20	30	355	2.0	0.2	3.0	0.75	0.1		
srBJ8R1ww355V2Zg2PMp5	5/20	30	355	2.0	0.5	2.0	0.75	0.1		
srBJ8R1ww355V2Zg2MRp2	5/20	30	355	2.0	0.2	2.0	0.75	0.1		
srBM30ww355V1p5Ks1KLp6	5/20	30	355	1.5	0.2	0.6	0.55	1.0		
srBM30ww1070V1p5Ks1	5/20	30	1070	1.5	0.2	0.6	0.75	1.0		
srBM30ww355V1p5Ks1Zg2	5/20	30	355	1.5	0.2	2.0	0.75	1.0		
srBM30ww355V1p7PM25ZG1	5/20	30	355	1.7	0.25	1.0	0.75	1.0		
srBM30ww355V2p5ZG1p5	5/20	30	355	2.5	0.2	1.5	0.75	1.0		
srBM30ww355V2p5ZG2	5/20	30	355	2.5	0.2	2.0	0.75	1.0		
srBM30ww355V2p5ZG2p5	5/20	30	355	2.5	0.2	2.5	0.75	1.0		
srBM30ww355V2p5ZG2p5KL6	5/20	30	355	2.5	0.2	2.5	0.55	1.0		
srBM30ww355V2ZG1p5KL6	5/20	30	355	2.0	0.2	1.5	0.55	1.0		
srBM30ww355V1p5ZG1p5KL6	5/20	30	355	1.5	0.2	1.5	0.55	1.0		
srBM30ww355V2ZG1p5KL7	5/20	30	355	2.0	0.2	1.5	0.65	1.0		
srBM30ww355V2p5KL6	5/20	30	355	2.5	0.2	0.6	0.55	1.0		
srBM30ww355V2p5KL7	5/20	30	355	2.5	0.2	0.6	0.65	1.0		

srBM30ww355V2KL6	5/20	30	355	2.0	0.2	0.6	0.55	1.0	
srBM30ww355V2KL7	5/20	30	355	2.0	0.2	0.6	0.65	1.0	
srBM30GB0ww355V2p5	5/20	30	355	2.5	0.2	0.6	0.75	1.0	zero
srBM30ww355GB0V2p5KL6	5/20	30	355	2.5	0.2	0.6	0.55	1.0	zero
srBM30ww355GB0V2p5ZG2p5KL6	5/20	30	355	2.5	0.2	2.5	0.55	1.0	zero
srBM30ww355GB0V2p5ZG2p5	5/20	30	355	2.5	0.2	2.5	0.75	1.0	zero
srBM30ww355GBR0V2p5ZG2p5	5/20	30	355	2.5	0.2	2.5	0.75	1.0	zero(riv)
srBM30GBR0ww355V2p5	5/20	30	355	2.5	0.2	0.6	0.75	1.0	zero(riv)
srBM30ww355GBR0V2p5ZG2	5/20	30	355	2.5	0.2	2.0	0.75	1.0	zero(riv)
sBM30w355GBR0V2p5Z2p5K6	5/20	30	355	2.5	0.2	2.5	0.55	1.0	zero(riv)
sBM30w355V2p5ZG2p5KL6W0	5/20	30	355	2.5	0.2	2.5	0.55	1.0	wind zero
srBM30w355V2p5W0	5/20	30	355	2.5	0.2	0.6	0.75	1.0	wind zero
sBM30w355GBR0V2p5Z2K6	5/20	30	355	2.5	0.2	2.0	0.55	1.0	zero(riv)
sBM30w355GBR0V2p5Z1p5K6	5/20	30	355	2.5	0.2	1.5	0.55	1.0	zero(riv)
srBM30ww355V2p5ZG2KL6	5/20	30	355	2.5	0.2	2.0	0.55	1.0	
srBM30ww355V2p5Z1p5KL6	5/20	30	355	2.5	0.2	1.5	0.55	1.0	
sBJ8w355V2p5Z2p5K6Wne2	5/20	30	355	2.5	0.2	2.5	0.55	1.0	Wind NE-ward 2 m/s
sBJ8w355V2p5Z2p5K6Wsw2	5/20	30	355	2.5	0.2	2.5	0.55	1.0	Wind SW-ward 2 m/s
sBJ8w355V2p5Z2p5K6Wnw2	5/20	30	355	2.5	0.2	2.5	0.55	1.0	Wind NW-ward 2 m/s
sBJ8w355V2p5Z2p5K6Wse2	5/20	30	355	2.5	0.2	2.5	0.55	1.0	Wind SE-ward 2 m/s

*Other parameters. i) Phy. Mortality, 0.2 (1/day), ii) Zoo. mortality rate, 0.2 (1/day), iii) Zoo. grazing inefficiency, 0.3, iv) Phy. saturation coeff. 0.4 (mM_N/m³), v) Inverse half-saturation for Phy., 0.1 (1/ (mM_N/m³)), vi) Zoo. death bits rate, 0.05 (1/day), vii) Zoo. excreted fraction, 0.15.